UNIVERSITI TEKNOLOGI MARA

STRENGTH AND BONDING PROPERTIES OF RUBBERISED GEOPOLYMER BASED SEMI RIGID REPAIR MATERIAL FOR USE AS SURFACE ROAD REPAIR PAVEMENT

MOHD NAJMUDIN HELMI BIN ABU BAKAR

PhD

August 2026

UNIVERSITI TEKNOLOGI MARA

STRENGTH AND BONDING PROPERTIES OF RUBBERISED GEOPOLYMER BASED SEMI RIGID REPAIR MATERIAL FOR USE AS SURFACE ROAD REPAIR PAVEMENT

MOHD NAJMUDIN HELMI BIN ABU BAKAR

Thesis submitted in fulfilment
of the requirements for the degree of
Doctor of Philosophy
(Civil Engineering)

Faculty of Civil Engineering

August 2026

CONFIRMATION BY PANEL OF EXAMINERS

I certify that a Panel of Examiners has met on 21st May 2026 to conduct the final examination of Mohd Najmudin Helmi bin Abu Bakar on his Doctor of Philosophy thesis entitled "Strength and Bonding Properties of Rubberised Geopolymer Based Semi Rigid Repair Material for Use as Surface Road Repair Pavement" in accordance with Universiti Teknologi MARA Act 1976 (Akta 173). The Panel of Examiners recommends that the student be awarded the relevant degree. The Panel of Examiners was as follows:

Mazidah Mukri, PhD
Associate Professor
Faculty of Civil Engineering
Universiti Teknologi MARA
(Chairman)

Hamidah Mohd Saman, PhD
Professor
Faculty of Civil Engineering
Universiti Teknologi MARA
(Internal Examiner)

Nur Liyana Mohd Kamal, PhD
Senior Lecturer
College of Engineering
Universiti Tenaga Nasional
(External Examiner)

PROFESSOR DR HJH ZURAEDA IBRAHIM
Dean
Institute of Postgraduate Studies
Universiti Teknologi MARA

Date: 14 August 2026

AUTHOR'S DECLARATION

I declare that the work in this thesis was carried out in accordance with the regulations of Universiti Teknologi MARA. It is original and is the results of my own work, unless otherwise indicated or acknowledged as referenced work. This thesis has not been submitted to any other academic institution or non-academic institution for any degree or qualification.

I, hereby, acknowledge that I have been supplied with the Academic Rules and Regulations for Postgraduate, Universiti Teknologi MARA, regulating the conduct of my study and research.

Name of Student	:	Mohd Najmudin Helmi bin Abu Bakar
Student ID. No.	:	2023784416
Programme	:	Doctor of Philosophy (Civil Engineering) – CEEC950
Faculty	:	Civil Engineering
Thesis Title	:	Strength and Bonding Properties of Rubberised Geopolymer Based Semi Rigid Repair Material for Use as Surface Road Repair Pavement
Signature of Student	:	……..
Date	:	: August 2026

ABSTRACT

One-part semi rigid geopolymer is rarely used because of lacking in standardisation testing methods and optimisation for the mix ingredients. Much less one-part geopolymer formulated using industry by product treated crumb rubber (CR) to produce semi rigid geopolymer for road surface repair. The question whether one-part geopolymer incorporating industry by product and treated crumb rubber can achieve mechanical performance and sufficient interfacial bonding as repair material, is becoming a focus of the present work. Therefore, the present study was conducted aimed to produce sustainable semi rigid geopolymer repair material for road surface. This present study developed and evaluated a one-part semi-rigid geopolymer repair material formulated using industrial by-products and CR treated with 5% sodium hydroxide, aiming to enhance mechanical performance and interfacial bonding as a sustainable alternative to conventional repair material. Ground granulated blast furnace slag (GGBS) was used as the primary precursor, while fly ash (FA, Class F) and waste clay tiles (WCT) were incorporated as partial replacements at 10%, 20%, 30%, 40%, and 50%. Precursor-to-solid activator ratios of 90:10 and 80:20 were evaluated to determine the optimum activator content. All specimens were cured under ambient conditions (25 ± 2°C) and tested at 3, 14, and 28 days. Treated CR was used as sand replacement at 5%, 10%, 15%, and 20%. Surface preparation applied to concrete and asphalt substrates included as-cast (AC), wire-brushed (WB), and drilled-hole (DH) methods. Raw materials and binders were characterised using chemical, phase, and microstructural analyses to support interpretation of strength development mechanisms. Fresh and hardened properties were evaluated through workability, setting time, compressive strength, water absorption, abrasion resistance, and bi-surface shear bond strength tests on ordinary portland cement (OPC) concrete and hot mix asphalt (HMA) substrates. Wheel-tracking tests were also conducted to assess rutting resistance on asphalt specimens. The results indicated that one-part geopolymer repair binders incorporating GGBS, FA, and WCT exhibit strong potential for semi-rigid repair applications, achieving great strength development under ambient curing. The optimum mix, comprising 70% GGBS and 30% WCT with a 90:10 solid activator ratio, achieved a compressive strength of 69.16 MPa at 28 days. Incorporation of 15% treated CR resulted in a compressive strength of 52.80 MPa at 28 days, indicating improved deformation tolerance while maintaining adequate strength. The best bonding performance was achieved using the DH surface preparation method, producing bond strengths of 8.69 MPa on concrete and 7.58 MPa on asphalt. Under DH surface preparation, the roughness average (Ra) values were 11.24 μm for concrete and 10.34 μm for asphalt. The developed repair material also demonstrated good rutting resistance, with a rutting depth of only 0.6 mm under wheel-tracking conditions. Overall, the findings confirmed that the proposed one-part semi-rigid geopolymer repair material is suitable for surface road repair applications.

ACKNOWLEDGEMENT

In the name of Allah, the Most Beneficent and the Most Merciful. I am deeply grateful to Allah SWT for His blessings, which enabled me to complete this research and thesis within the planned timeframe. Upon completing this work, I would like to express my sincere appreciation to all those who, in one way or another, contributed to the successful completion of this thesis.

First and foremost, I would like to convey my utmost gratitude to my main supervisor, Ts. Dr. Warid Wazien Ahmad Zailani, and my co-supervisors, Dr. Ni Komang Ayu Agustini (Warmadewa University, Indonesia) and Dr. Suhana Koting (Universiti Malaya), for their continuous guidance, patience, and support throughout this study. The opportunity to work with them in the areas of structural and materials engineering has strengthened my appreciation of the importance of concrete and cement-based research.

Secondly, I would like to express my heartfelt gratitude to my family for their unwavering support, encouragement, and faith in me. I would also like to express my sincere appreciation to my partner, who has always been by my side, encouraging and supporting me through the ups and downs of this journey. Last but not least, I would like to thank my friends and fellow course-mates in the School of Civil Engineering, College of Engineering, Universiti Teknologi MARA (UiTM) Shah Alam, for the assistance and encouragement provided throughout my study.

Special thanks are also extended to all academic, administrative, and technical staff of the School of Civil Engineering, College of Engineering, UiTM Shah Alam, and the Faculty of Engineering, Universiti Malaya, for their valuable input and excellent technical support during my study period.

TABLE OF CONTENTS

		Page
CONFIRMATION BY PANEL OF EXAMINERS		**ii**
AUTHOR'S DECLARATION		**iii**
ABSTRACT		**iv**
ACKNOWLEDGEMENT		**v**
TABLE OF CONTENTS		**ii**
LIST OF TABLES		**ii**
LIST OF FIGURES		**iv**
LIST OF SYMBOLS		**viii**
LIST OF ABBREVIATIONS		**ix**
CHAPTER 1 INTRODUCTION		**1**
1.1	Research Background	1
1.2	Problem Statements	3
1.3	Research Objectives	6
1.4	Scope of Study	6
1.5	Significance of Study	8
1.6	Thesis Outlines	9
CHAPTER 2 LITERATURE REVIEW		**10**
2.1	Introduction	10
2.2	One-Part Geopolymer System	10
	2.2.1 Single Binder	13
	2.2.2 Hybrid Binder	16
2.3	Others Waste Material in One-Part Geopolymer for Pavement Applications	18
2.4	Rubberised Semi Rigid Pavement	20
2.5	Treatments of Crumb Rubber	22
2.6	Reactions and Mechanisms for One-Part Geopolymer	24

2.6.1 One-Part Geopolymer Terminology 25
2.6.2 Mechanism of One-Part Geopolymer 27
2.7 Properties of One-Part Geopolymer for Pavement Applications 29
2.7.1 Setting Time Properties 29
2.7.2 Workability Properties 31
2.7.3 Compressive Strength Properties 34
2.7.4 Water Absorption Properties 38
2.7.5 Abrasive Properties 40
2.7.6 Surface Roughness Evaluation and Bonding Strength 41
2.7.7 Rutting Resistance 44
2.8 Chemical, Phase Composition and Microstructure Analysis for One-Part Geopolymer 46
2.8.1 Chemical Composition Properties 46
2.8.2 Phase Properties 48
2.8.3 Microstructure Properties 51
2.9 Summary and Gap of Research 53

CHAPTER 3 RESEARCH METHODOLOGY 58
3.1 Introduction 58
3.2 Research Framework 58
3.3 Material Preparation & Characterisation 65
3.3.1 Ground Granulated Blast Furnace Slag (GGBS) 66
3.3.2 Fly Ash (FA) 67
3.3.3 Waste Clay Tiles (WCT) 67
3.3.4 Sodium Metasilicate 68
3.3.5 Aggregate 69
3.3.6 Sand 70
3.3.7 Crumb Rubber (CR) 71
3.3.8 Asphalt Binder for Hot Mix Asphalt (HMA) Pavement Substrate 72
3.3.9 Aggregate for Hot Mix Asphalt (HMA) Pavement Substrate 73
3.4 Parameters of Study (Phases 2 to 5) 74
3.4.1 Mix Proportion for One-Part GGBS-FA and GGBS-WCT Geopolymer Binders (Phase 2 and 3) 75

3.4.2 Crumb Rubber as Sand Replacement for One-Part Semi-Rigid Geopolymer Repair Material (Phase 4) 76
3.4.3 Surface Preparation of OPC Concrete and HMA Substrate (Phase 5) 77
3.5 Moulding and Curing 78
3.6 Preparation and Mix Design of Ordinary Portland Cement (OPC) Concrete Substrate 78
3.7 Preparation of Hot Mix Asphalt (HMA) Substrate 79
3.7.1 Sieving and Gradation 80
3.7.2 Aggregate Mixing 81
3.8 Substrate Surface Treatment 82
3.9 Testing of One-Part Geopolymer Repair Binders and One-Part Semi-Rigid Geopolymer Repair Material for Surface Road Repair Pavement (Phase 2 to Phase 5) 83
3.9.1 Workability Test 84
3.9.2 Setting Time Test 84
3.9.3 Compressive Test 85
3.9.4 Chemical Composition Characterisation 86
3.9.5 Phase Characterisation 87
3.9.6 Microstructure Characterisation 88
3.9.7 Water Absorption 89
3.9.8 Abrasion Resistance (AR) 89
3.9.9 Surface Roughness Evaluation 91
3.9.10 Bi-Surface Shear 91
3.9.11 Wheel Tracking Test 92
3.10 Data Collection and Analysis 94
3.11 Summary 95

CHAPTER 4 CHARACTERISTICS OF RAW MATERIALS (PHASE 1), OPTIMISATION OF GGBS–FA AND GGBS–WCT ONE-PART GEOPOLYMER BINDERS (PHASE 2) AND GEOPOLYMERISATION REACTION (PHASE 3) 96
4.1 Introduction 96
4.2 Phase 1: Chemical Composition, Phase and Microstructure Analysis 96
4.2.1 Chemical Composition Analysis 97

4.2.2 Phase Analysis 101
4.2.3 Microstructure Analysis 105
4.3 Phase 2: Optimisation of GGBS Replacement and Solid Precursor to Solid Activator 108
4.3.1 Workability Analysis 109
4.3.2 Setting Time Analysis 111
4.3.3 Compressive Strength Analysis 115
4.4 Phase 3: Geopolymerisation Reaction of GGBS-WCT Based Hybrid One-Part Geopolymer Repair Binders 120
4.4.1 Chemical Composition of GGBS–WCT Based Hybrid One-Part Geopolymer Repair Binders 121
4.4.2 Phase Analysis of GGBS-WCT Based Hybrid One-Part Geopolymer Repair Binders 124
4.4.3 Microstructure Analysis of GGBS-WCT Based Hybrid One-Part Geopolymer Repair Binders 127
4.4.4 Summary 130

CHAPTER 5 OPTIMISATION OF CRUMB RUBBER CONTENT (PHASE 4) AND COMPATIBILITY OF ONE-PART SEMI-RIGID GEOPOLYMER REPAIR MATERIAL WITH ROAD SURFACE LAYERS (PHASE 5) 132
5.1 Introduction 132
5.2 Water Absorption Analysis 132
5.3 Abrasion Resistance Analysis 134
5.4 Compressive Strength Analysis 136
5.5 Phase 5: Compatibility of One-Part Semi-Rigid Geopolymer Repair Material with the Road Surface Layer 138
5.5.1 Surface Roughness Analysis 139
5.5.2 Bonding Strength Analysis 140
5.5.3 Rutting Resistance Analysis 143
5.6 Summary 147

CHAPTER 6 CONCLUSION AND RECOMENDATIONS 149
6.1 General 149
6.2 Recommendations 150

6.3 Recommendation for the Industry 151

REFERENCES **152**

AUTHOR'S PROFILE **172**

LIST OF TABLES

Tables	Title	Page
Table 2.1	Chemical Composition of Various Aluminosilicate Precursors	17
Table 2.2	Chemical Composition of Various Aluminosilicate Precursors	20
Table 2.3	Summary of CR Treatment Methods and Their Effects on Interfacial Bonding and Mechanical Performance of Cementitious Composites	24
Table 2.4	Geopolymer Application Based on Si to Al ratio (Davidovits, 2002)	26
Table 2.5	Summary of Geopolymer Setting Time Studies	31
Table 2.6	Summary of Geopolymer Workability Studies	33
Table 2.7	Summary of Compressive Strength from Different Geopolymer Studies	37
Table 2.8	Water Absorption of Geopolymers with CR Replacement	39
Table 2.9	Summary of Geopolymer Abrasive Resistance Studies	41
Table 2.10	Summary of Surface Preparation and Bond Strength Evaluation Studies	43
Table 2.11	Summary of Rutting Resistance Studies	45
Table 2.12	Chemical Composition of GGBS and CW Aluminosilicate Precursors	47
Table 2.13	Summary of Previous Studies and Research Gap	55
Table 3.1	Summary of Testing Approach, Standardised Methodology, and Number of Specimens	64
Table 3.2	Summary of Overall Materials Used	66
Table 3.3	Specification of Sodium Metasilicate, Anhydrous	69
Table 3.4	Aggregate Proportion for ACW14 Specimen	73
Table 3.5	Parameters of Study	75
Table 3.6	Mix Proportions of Different GGBS Based One-Part Geopolymer Repair Binders	76
Table 3.7	Mix Proportion of One-Part Semi Rigid Geopolymer Repair Material with Various CR Replacement	77

Table 3.8	Mix Proportion and Strength of OPC	79
Table 3.9	Slab weight for Control Mixture	93
Table 4.1	Chemical Composition GGBS	98
Table 4.2	Chemical Composition FA	99
Table 4.3	Chemical Composition WCT	100
Table 5.1	Wheel-Tracking Rutting Depth of HMA and One-Part Semi-Rigid Geopolymer Repair Overlays under Different Surface Preparations	144

LIST OF FIGURES

Figures	Title	Page
Figure 2.1	Schematic Representation of One-Part and Two-Part Geopolymer Preparation Processes (Qin et al., 2022)	12
Figure 2.2	Classification of Aluminosilicate Source Materials (Singh et al., 2015)	14
Figure 2.3	Terminology of Poly(sialate) One-Part Geopolymers (Davidovits, 2002)	26
Figure 2.4	Conceptual Model for Geopolymerisation Processes (Abdila et al., 2022)	27
Figure 2.5	XRD Patterns of Alkali-Activated GGBS Pastes at Different Curing Ages, Showing the Evolution of Crystalline Phases and Reaction Products (Bernal et al., 2013)	49
Figure 2.6	XRD Patterns of FA/GGBS Geopolymers with Different FA-to-GGBS Ratios (Zhang M. et al., 2024)	50
Figure 2.7	XRD Spectra of (a) LCFA-Based Geopolymer, (b) HCFA-Based Geopolymer Prepared at NaOH Concentration of 8 mol/L at Different Curing Ages (Li J. et al., 2024)	51
Figure 2.8	Backscattered Electron (BSE) Images of S10 and S20 Samples at 28 Days (Lee et al., 2014)	52
Figure 2.9	SEM Images of LCFA-Based Geopolymer Gel Curing at 90 days (Li J. et al., 2024)	53
Figure 3.1	Overall Research Framework of the Experimental Programme	59
Figure 3.2	Characterisation Raw Material of One-Part Geopolymer Repair Binders (Precursor) (Phase 1)	60
Figure 3.3	One-Part Geopolymer Repair Binder on Workability, Setting Time and Compressive Strength (Phase 2)	61
Figure 3.4	Geopolymerisation Reaction of One-Part Geopolymer Repair Binder (Phase 3)	62
Figure 3.5	One-Part Semi-Rigid Geopolymer Repair Materials Based on Durability and Mechanical Properties (Phase 4)	63

Figure 3.6	Development and Performance Evaluation of the One-Part Semi-Rigid Geopolymer Repair Material Based on Interfacial Bonding Strength and Rutting Performance (Phase 5)	64
Figure 3.7	Raw GGBS Used as an Aluminosilicate Precursor	66
Figure 3.8	Raw FA Used as an Aluminosilicate Precursor	67
Figure 3.9	Raw WCT Used as an Aluminosilicate Precursor	68
Figure 3.10	Preparation Process of WCT Powder	68
Figure 3.11	Sodium Metasilicate, Anhydrous Used as Solid Activator	69
Figure 3.12	Coarse Aggregates with Particle Size Less than 10 mm	70
Figure 3.13	Natural River Sand with Particle Sizes Ranging from 0.30 mm to 4.75 mm	71
Figure 3.14	CR Used as Flexible Agent / Fine Aggregate Replacement	71
Figure 3.15	Treatment Process of CR with NaOH Solution	72
Figure 3.16	Particle Size Distribution of Aggregate for ACW14 Specimen	74
Figure 3.17	Sieve Shaker Used for Sieving	81
Figure 3.18	Asphalt Slab Compactor	82
Figure 3.19	Surface Preparation Methods Applied to Concrete Substrates: (a) Wire-Brushed and (b) Drilled Holes	83
Figure 3.20	Flow Table Set for Measuring the Diameter of One-Part Geopolymer Repair Binders Spread	84
Figure 3.21	Setting Time Apparatus for Measuring Setting Time of Geopolymer Paste	85
Figure 3.22	Universal Testing Machine (UTM) 1000kN Machine Used to Compress the Geopolymer Specimens	86
Figure 3.23	XRF Spectrometer Used to Determine Chemical Composition	87
Figure 3.24	XRD Diffractometer Used to Determine Phase Characterisation	88
Figure 3.25	SEM Instrument Used to Determine Microstructural Characteristics	88
Figure 3.26	Determination of Specimen Mass for CR Sample	89
Figure 3.27	Surface Abrasion Testing Machine	90
Figure 3.28	Alicona 3D Surface Metrology Instrument	91
Figure 3.29	Composite Specimen for Bi-Surface Shear Test	92
Figure 3.30	Asphalt Rolling Compactor Machine	93

Figure 4.1	X-Ray Diffraction Patterns of GGBS (CS = Calcium Silicate (Ca_3SiO_5: PDF no. 00-031-0301); E = Epidote ($Ca_2Al_2Fe(SiO_4)$ ($Si2O_7$)) : PDF no. 00-017-0514)	101
Figure 4.2	X-Ray Diffraction Patterns of FA (Q = Quartz (SiO_2: PDF no. 01-078-1254); S = Sillimanite ($Al_2(SiO_4)$ O): PDF no. 01-083-1562)	103
Figure 4.3	X-Ray Diffraction Patterns of WCT (Q = Quartz (SiO2: PDF no. 01-078-1254); M = Mullite ($3Al_2O_3 \cdot 2SiO_2$): PDF no. 01-079-1456)	104
Figure 4.4	SEM Micrograph of GGBS Particles at 500× Magnification (BSE mode)	106
Figure 4.5	SEM Micrograph of FA Particles at 500× Magnification (BSE mode)	107
Figure 4.6	SEM Micrograph of WCT Particles at 500× Magnification (BSE mode)	108
Figure 4.7	Workability of GGBS–FA and GGBS–WCT One-Part Geopolymer Repair Binders with 10% Activator Content	110
Figure 4.8	Workability of GGBS–FA and GGBS–WCT One-Part Geopolymer Repair Binders with 20% Activator Content	111
Figure 4.9	Setting Time Development of One-Part Geopolymer Repair Binders with 10% Activator Content: (a) GGBS–FA and (b) GGBS–WCT	113
Figure 4.10	Setting Time Development of One-Part Geopolymer Repair Binders with 20% Activator Content: (a) GGBS–FA and (b) GGBS–WCT	115
Figure 4.11	Compressive Strength Development of One-Part Geopolymer Repair Binders with 10% Activator Content: (a) GGBS–FA and (b) GGBS–WCT	118
Figure 4.12	Compressive Strength Development of One-Part Geopolymer Repair Binders with 20% Activator Content: (a) GGBS–FA and (b) GGBS–WCT	120
Figure 4.13	Chemical Composition of GGBS–WCT One-Part Geopolymer Repair Binders	122

Figure 4.14	Molar Ratio of GGBS–WCT One-Part Geopolymer Repair Binders	124
Figure 4.15	Diffractogram Patterns of Different Specimens, GGBS-WCT (1 = Thomsonite ($NaCa_2Al_5Si_5O_{20}·6H_2O$: PDF no. 01-078-0296); (2 = Laumontite ($CaAl_2Si_4O_{12}·4H_2O$: PDF no. 01-073-0260)	125
Figure 4.16	Micrographs and Corresponding EDX Spectra of GGBS–WCT Hybrid One-Part Geopolymer Repair Binders at 500× Magnification (a) 0% WCT, (b) 10% WCT, (c) 20% WCT, (d) 30% WCT, (e) 40% WCT, and (f) 50% WCT	130
Figure 5.1	Variation of Water Absorption with CR Replacement Level for GGBS–WCT Based Hybrid One-Part Semi-Rigid Geopolymer Repair Material	133
Figure 5.2	Abrasion Resistance of GGBS–WCT Based Hybrid One-Part Semi-Rigid Geopolymer Repair Material with Varying CR	135
Figure 5.3	Compressive Strength of GGBS–WCT-Based Hybrid One-Part Semi-Rigid Geopolymer Repair Material with Varying CR Replacement Levels	137
Figure 5.4	Average Roughness (Ra) of Concrete and Asphalt Substrates under AC, WB and DH Surface Preparations	140
Figure 5.5	Bonding Strength of One-Part Semi-Rigid Geopolymer Repair Material under Different Surface Preparations on Concrete and Asphalt Substrates	141
Figure 5.6	Rutting Depth versus Time for HMA and One-Part Semi-Rigid Geopolymer Repair Overlays under Different Surface Preparations	145
Figure 5.7	Surface Rutting Profiles after Wheel-Tracking under Different Surface Preparations	147

LIST OF SYMBOLS

Symbols

A	Surface Area (millimetre square, mm^2)
AR	Abrasion Resistance, ($mm^2 \cdot hr/g$)
Cs	Compressive strength (MPa)
D	Diameter (mm)
M	Mass of Specimens (g)
P	Maximum Load (N)
S	Bond Strength (MPa)
T	Time (Minutes or Hours)
^oC	Degree Celsius
%	Percentage
±	Plus Minus (eccentricity)
θ	Theta

LIST OF ABBREVIATIONS

Abbreviations

AASHTO	American Association of State & Transportation
AlO_4	Aluminate Tetrahedron
Al	Aluminium
Al_2O_3	Aluminium Oxide
ASTM	American Society for Testing and Material
AC	As-Cast
ACW14	Asphaltic Concrete Wearing Course with 14 mm Nominal Maximum Aggregate Size
BF	Basalt Fibres
BOF	Basic Oxygen Furnace
BS	British Standard
CaO	Calcium Oxide
C–S–H	Calcium Silicate Hydrate
$CaSO_4$	Calcium Sulfate
CW	Ceramic Waste
CWT	Ceramic Waste Tile
CG	Conventionally Activated
CR	Crumb Rubber
DH	Drilled Hole

FA	Fly Ash
GGBS	Ground Granulated Blast Slag
HWT	Hamburg Wheel Tracking
HCFA	High-Calcium Circulating Fluidised Bed Fly Ash
HMA	Hot Mix Asphalt
ITZ	Interfacial Transition Zone
Fe_2O_3	Iron Oxide
L/S	Liquid-to-Solid Ratios
LCFA	Low-Calcium Circulating Fluidised Bed Fly Ash
MgO	Magnesium Oxide
MG	Mechanochemically Activated
MK	Metakaolin
ORGM	One-Part Rubberised Geopolymer Mortar
OPC	Ordinary Portland Cement
PF	Polypropylene Fibre
K_2O	Potassium Oxide
$KMnO_4$	Potassium Permanganate
K_2SiO_3	Potassium Silicate
RHA	Rice Husk Ash
$NaHSO_3$	Saturated Sodium Bisulfide
SEM	Scanning Electron Microscopy
SF	Silica Fume

Si	Silicon
SiO_2	Silicon Dioxide
Si/Al	Silicon to Aluminium
Na_2CO_3	Sodium Carbonate
NaOH	Sodium Hydroxide
SH/SS	Sodium Hydroxide to Sodium Silicate
Na_2O	Sodium Oxide
Na_2SiO_3	Sodium Silicate
SS/SH	Sodium Silicate to Sodium Hydroxide
Na_2SO_4	Sodium Sulfate
S/L	Solid to Liquid
StF	Steel Fibre
H_2SO_4	Sulphuric Acid
SP	Superplasticisers
TiO_2	Titanium Dioxide
TRGM	Two-Part Rubberised Geopolymer Mortar
UGGBS	Ultra-Fine Blast Furnace Slag
WCB	Waste Clay Brick
WCT	Waste Clay Tiles
W/S	Water-to-Solid
WB	Wire Brushed
XRD	X-Ray Diffraction

XRF	X-Ray Fluorescence
EDX	X-Ray Spectroscopy

CHAPTER 1
INTRODUCTION

1.1 Research Background

Asphalt (flexible) and concrete (rigid) pavements are the most widely used pavements globally and have been utilised for several applications such as road, highway, bridge deck top layer, and airport pavements. Although flexible pavement has a short drying period, good point load-bearing capacity, high skid resistance, easy to maintain and repair, it has several significant drawbacks, including surface degradation and rutting caused by repeated concentrated loads (Chen et al., 2021). In contrast, rigid pavements are flexible to traffic loads, have a higher bearing capacity, are long-lasting, resist fatigue and deformation. However, concrete pavements can only be used in certain situations due to their slow construction phase setting time and poor riding quality (noise) primarily brought on by the joints (Mohd Tahir et al., 2022).

Cracking is the initial stage of most surface failures, one of the most common and critical distresses affecting asphalt and rigid pavements. It typically marks the beginning of a progressive chain of damage that, when left unrepaired, cracks can spread into more serious forms of deterioration, such as potholes and delamination, potentially threatening the structural integrity, safety, and serviceability of road networks (Li et al., 2023). Once cracks form, they allow moisture to penetrate through these cracks and damage the pavement base and subgrade, particularly under repeated dynamic vehicular loading (He et al., 2024a; He et al., 2024b). In this way, cracking acts as a gateway mechanism, reducing structural integrity and triggering long-term degradation. Consequently, the timely and durable repair is essential to extending pavement lifespan and reducing long-term maintenance costs.

Among the various types of surface distress, potholes remain a particularly constant, and costly consequence of unresolved cracking on asphalt pavements (Chen L. et al., 2021). Early-stage cracks, when not quickly resolved, tend to widen and deepen under the combined influence of traffic loads and weather conditions, thereby reducing the pavement load-bearing capacity and increasing the risk on the road (Chen L. et al., 2021; Dong et al., 2020; Liu Mengmei et al., 2019). However, existing repair techniques

often fall short when it comes to treating such early-stage cracking. Cold mix asphalt (CMA) patching is widely used because of its ease of application, good storage stability, and cost-effectiveness, making it suitable for rapid, on-demand repairs (Hafezzadeh et al., 2021; Zhao & Tan, 2011). Though these benefits, CMA is usually connected with short service life and inconsistent performance, limiting its effectiveness for long-term crack remediation (Liu M. et al., 2019; Zhang et al., 2022). On the other hand, hot mix asphalt (HMA) offers greater material stability and is supported by established construction practices, yet its application is interfered with complex procedures, high costs, and poor performance during weather conditions particularly for small-scale repairs (Dong et al., 2014; Li et al., 2010; Li et al., 2019; Obaidi et al., 2017).

To overcome the limitations of flexible and rigid pavement, the concept of semi-rigid pavement has been introduced as a hybrid approach. Semi-rigid pavement can be developed using geopolymer concrete incorporating crumb rubber (CR), which has become a focus of this present study. Therefore, this study aims to establish a semi-rigid pavement repair material made from geopolymer concrete using hybrid precursors derived from industrial by-products and waste materials. The semi-rigid pavement, which uses geopolymer as a repair material, is an alternate method for overcoming limits and improving the performance of both flexible and rigid pavements (Zhang & Wu, 2020). A novel classification of geopolymers utilising a one-part mixing technique, "just add water," has been suggested to optimise their benefits by saving the time of dissolution of solid activator solution and eco-friendliness while simultaneously mitigating certain limitations associated with the conventional two-part composition.

Geopolymer concrete, developed through the incorporation of waste rubber as a partial replacement for natural aggregates is commonly referred to as rubberised geopolymer concrete, which the term is also used in the present work. Previous studies have demonstrated advanced performance characteristics of geopolymer incorporating waste rubber as compared to that traditional rubberised concrete made with OPC (Charkhtab Moghaddam et al., 2021; Luhar et al., 2019). The compressive strength of concrete is a key indicator of its microstructure, mechanical integrity, and long-term durability (Neville, 1995). In recent years, rubber particulates obtained from scrap tires have been utilised as a sustainable alternative to natural aggregates in both conventional and geopolymer concrete mixtures (Feng W. et al., 2021; Xie et al., 2019). CR from waste tyres is commonly used as an aggregate replacement to improve the flexibility and toughness of cementitious materials. This green technology addresses the

environmental concerns associated with waste tire accumulation while contributing to the conservation of non-renewable natural resources (Marques et al., 2020; Thakare et al., 2022). It has been reported that rubber content can enhance functional properties of concrete, including crack resistance, and abrasion resistance (Dong et al., 2024). Rubberised geopolymers have gained attention as they combine the advantages of geopolymer binders with those of rubberised aggregates.

Substrate surface roughness significantly influences the bonding efficacy of repair materials. Effectively managing such factors can significantly increase the service life of repaired road segments (Nurdeen Mohamed et al., 2024). Considering these advancements, this study focuses on the development of a one-part geopolymer-based semi-rigid repair material incorporating treated CR for use in surface road repair pavement applications. Treated CR refers to CR that has undergone a pre-treatment process prior to mixing to improve its compatibility and bonding with the geopolymer binder. The high strength and durability of one-part geopolymer binders with the flexibility and abrasion resistance of CR, the research aims to produce a repair material that balances mechanical performance, environmental sustainability, and practical application efficiency. This novel combination offers promising potential for addressing challenges in pavement maintenance and rehabilitation.

1.2 Problem Statements

Geopolymers are synthesised by activating aluminosilicate-rich precursors with alkaline solutions, producing a binder that can replace OPC (El Fadili et al., 2025; Oliveira et al., 2022; Singh & Middendorf, 2020). Their performance is strongly dependent on the characteristics of the raw materials, particularly their chemical composition, phase, and microstructure, as well as the activating solutions (Bahmani & Mostofinejad, 2025; El Alouani et al., 2024; Pundienė et al., 2021). However, for one-part geopolymer repair binders, characterisation of these precursors remains limited, making it difficult to predict geopolymerisation behaviour and optimise mix design for consistent performance. In the one-part geopolymer approach, the alkaline activator is supplied in solid form and mixed with water during preparation, which makes the method more practical, safer, and more suitable for field repair applications compared with conventional two-part geopolymer methods. However, this limitation restricts

increased application in sustainable road repair, especially for semi-rigid pavements where uniform quality and long-term durability are essential. Therefore, characterisation of the raw materials in terms of chemical composition, phase, and microstructure is necessary to support optimal mix design and consistent field performance.

Ground granulated blast slag (GGBS), a commonly used industrial by-product, has long been incorporated into geopolymer formulations as part of a binary or ternary binder (Gopalakrishna & Dinakar, 2024; Rawat & Pasla, 2024; Wang et al., 2024).GGBS possesses its high reactivity can result in short setting time, which reduces workability and makes setting control challenging (Ahmad et al., 2022; Ghostine et al., 2022; Li H. et al., 2024). However, the use of GGBS as the single primary precursor is less common than the use of blended precursors. Use of single GGBS precursor is critical for one-part geopolymer binder used in pavement repair because of early setting time of reaction. Therefore, partial replacement of GGBS with alternative aluminosilicate precursors such as fly ash (FA), metakaolin, rice husk ash, or other suitable by-products is necessary to balance reactivity and optimise the performance of one-part geopolymer binders for pavement repair applications. Waste clay tiles (WCT) and other ceramic wastes have also been investigated as aluminosilicate materials because they contain high amounts of silica and alumina, which can contribute to geopolymerisation and support sustainable waste utilisation (Azevedo et al., 2020; Faldessai et al., 2023). In this present work, waste clay tiles (WCT) were also incorporated to produce sustainable pavement repair materials. Therefore, an important question is whether the combined use of GGBS, FA, and WCT can produce geopolymer materials with sufficient compressive strength for road repair applications.

The performance of one-part geopolymer binders composed of hybrid precursors can be inconsistent because of variations in geopolymerisation reactions and the resulting reaction products (Zhao Q. et al., 2023). In particular, the relationships between chemical composition, phase development, and microstructural evolution, and their effects on strength development and durability performance in one-part geopolymer repair binders, remain insufficiently characterised. Therefore, investigating geopolymerisation reactions through chemical composition, phase, and microstructure analyses is essential to establish structure property relationships and to support the development of consistent, high performing repair materials.

Geopolymer concrete exhibits limited tensile and flexural deformability because of its brittle failure behaviour (Shao et al., 2025). Incorporating crumb rubber (CR) as a partial replacement for fine aggregate (sand) has been reported to improve flexibility and abrasion resistance, and alkaline activators may enhance interfacial bonding and compatibility between the geopolymer matrix and rubber particles (Dong et al., 2021; Elzeadani et al., 2021). In this study, rubberised geopolymer refers to a geopolymer repair material incorporating alkaline-treated CR as partial sand replacement. The treatment improves the rubber surface and bonding compatibility with the geopolymer matrix, thereby enhancing deformability, energy absorption, and resistance to surface wear. In this study, CR was treated by immersion in 5% NaOH solution to improve its surface condition and bonding compatibility with the geopolymer matrix. It is the question whether the treated using 5% NaOH is effective for CR incorporating in geopolymer. For one-part semi-rigid geopolymer repair materials used in pavement applications, the optimum CR content that balances durability and mechanical performance remain insufficiently established. Therefore, optimisation of CR as sand replacement is required to achieve consistent, high-performing one-part semi-rigid geopolymer repair materials while supporting waste tyre utilisation (Xiao et al., 2022).

Under Budget 2026, the Malaysian government allocated RM2.5 billion for the maintenance of federal roads, including pothole resurfacing and the replacement of damaged road furniture (New Straits, 2025). Surface deterioration is typically caused by repetitive vehicular loads and the infiltration of moisture through cracks. When water penetrates the pavement layers, it weakens bonding between the asphalt and underlying layers, leading to delamination, slippage, cracking, and pothole formation (Chen & Wang, 2024). In practice, weak bonding between the overlay and the existing surface often limits the formation of a continuous layered structure, meaning overlay performance cannot be assumed to match that of newly constructed pavements (Bae et al., 2026). In this study, substrate surface treatment was carried out using three preparation methods, namely as-cast, wire-brushed, and drilled holes, to evaluate how different levels of surface roughness influence interfacial bonding and rutting resistance. Therefore, an important question is whether substrate surface treatment can improve bonding strength for road repair applications. This issue is directly related to pavement repair performance, as weak bonding between the repair layer and the existing concrete or asphalt substrate can cause premature repair failure, even when the repair material itself has developed good mechanical performance.

Although one-part geopolymer binders and treated CR can enhance sustainability, flexibility, and abrasion resistance, repair performance in the field is often control by interfacial bonding to existing concrete and asphalt substrates. At present, the formulation criteria that ensure both strong mechanical properties and good interface performance for semi-rigid geopolymer repairs are not yet well defined. Hence, an integrated development and evaluation of one-part semi-rigid geopolymer repair materials is required to deliver durable, sustainable, and practical surface road repairs.

1.3 Research Objectives

The objectives of the study are as follows:

a) To characterise the raw materials for one-part geopolymer repair binders with respect to its chemical composition, phase and microstructure analysis.
b) To determine the optimum GGBS replacement (10%, 20%, 30%, 40% and 50% of fly ash (FA) and waste clay tiles (WCT) and optimum ratio of solid precursor to solid activator (10% and 20%) in one-part geopolymer repair binders in terms of fresh, and mechanical properties.
c) To determine the geopolymerisation reaction (chemical composition, phase, and microstructure analysis) of one-part geopolymer repair binders.
d) To determine the optimum crumb rubber (CR) as sand replacement (5%, 10%, 15%, and 20%) in the one-part semi-rigid geopolymer repair materials based on durability, and mechanical properties.
e) To investigate the effect of substrate surface roughness on interfacial bonding performance concrete/asphalt substrates and rutting resistance of asphalt repaired using one-part semi-rigid geopolymer materials.

1.4 Scope of Study

The scope of this study was established to achieve the objective above mentioned and focused mainly on experimental work. The testing methods and work procedures were specified according to British Standard (BS), American Society for Testing and Material (ASTM), and other recommended test procedures proposed by

previous researchers. The research is structured in five (5) Phases. Phase 1 involved characterise of raw materials namely GGBS, fly ash (FA), waste clay tiles (WCT), using various analysis. X-Ray Fluorescence (XRF) for chemical composition, X-Ray Diffraction (XRD) for phase composition, and Scanning Electron Microscopy (SEM) was employed to observe the microstructure of the raw material. Phase 2 focused on preparing one-part geopolymer repair binder specimens to determine the optimum replacement of GGBS with FA and WCT. Five (5) series of mix proportion were produced with replacement levels of 10%, 20%, 30%, 40%, and 50%. The effect of the solid precursor-to-solid activator ratio was evaluated using ratios of 90:10 and 80:20 (equivalent to activator contents of 10% and 20% by the total binder). Fresh and hardened properties were assessed through workability using the flow table method in accordance with ASTM C1437 (ASTM-C1437, 2020), setting time (initial and final) in accordance with ASTM C191 (ASTM-C191, 2007), compressive strength in accordance with ASTM C109 (ASTM-C109, 2020).

Phase 3 further characterised the GGBS-WCT based one-part geopolymer repair binder specimen. The hardened binder was analysed using XRF, XRD, and SEM to determine geopolymerisation reaction in chemical composition, phase, and microstructure, and to relate these characteristics to strength and durability performance. Phase 4 involved the investigation using crumb rubber (CR), treated by immersion in 5% sodium hydroxide (NaOH), as sand replacement in the one-part semi-rigid geopolymer repair materials at replacement levels of 5%, 10%, 15%, and 20%. The hardened properties were assessed using water absorption ASTM C642 (ASTM-C642, 2022), abrasion resistance BS 812-113:1990 (BS-812-113, 1990), compressive strength ASTM C109 (ASTM-C109, 2020) tests. Phase 5 involved evaluation the bonding performance between the geopolymer repair material and conventional substrates, concrete and asphalt, representing rigid and flexible pavements. Substrate surface conditions were prepared using as-cast (AC), wire-brushed (WB), and drilled-hole (DH) treatments to generate different surface roughness levels and to examine their influence on the interfacial bonding. The substrate bonding was tested using bi-surface shear tests ASTM C882/C882M (ASTM-C882, 2020) on the surface substrate. In addition, rutting resistance was assessed using wheel-tracking tests BS 598-110 (BS-598-110, 1998), on hot mix asphalt (HMA) substrates before and after overlay application.

1.5 Significance of Study

This study contributes to the development of a sustainable and high-performance repair material for surface road pavement applications by advancing one-part geopolymer-based semi-rigid repair. The research provides scientific and practical significance by addressing key limitations in conventional pavement repair, particularly deterioration, and inadequate interfacial bonding with existing concrete and asphalt substrates. From a scientific perspective, the study establishes a clearer understanding of structure property relationships one-part geopolymer repair binders. Characterisation of GGBS, FA, and WCT, together with geopolymerisation reaction, offers insights into chemical composition, phase, and microstructure development influence strength and durability under ambient curing conditions. This supports the production of more consistent geopolymer binders and improves confidence in mix design selection for repair applications.

From an engineering performance perspective, the study identifies suitable mix design ranges for one-part geopolymer repair materials and evaluates the influence of treated CR on mechanical and functional performance. The inclusion of CR promotes improved flexibility and abrasion resistance, which are desirable for surface repairs subjected to repeated traffic loading, while also supporting sustainable waste tyre utilisation and reduced dependence on natural aggregates. Importantly, this study highlights the critical role of substrate surface roughness in controlling interfacial bonding performance. By assessing bonding behaviour between geopolymer repair materials and both concrete and asphalt substrates under different surface preparation conditions, the research provides practical guidance for surface preparation to minimise debonding and enhance repair durability. In addition, the evaluation of rutting resistance on repaired asphalt surfaces supports the relevance of the developed material for real pavement conditions. Overall, the outcomes of this study support the adoption of low-carbon, durable, and practical repair materials for pavement maintenance. The findings provide value to researchers, road authorities, and industry by offering an evidence-based approach for designing geopolymer-based semi-rigid repair materials with reliable strength, durability, and interfacial performance for surface road repair applications.

1.6 Thesis Outlines

This thesis comprises six (6) chapters. A brief layout of each chapter is summarised in this section. Chapter 1 presents the background of the study, problem statement, research aim, research objectives, research questions, scope of work, significance of the study, and overall structure of the thesis.

Chapter 2 reviews the relevant literature related to geopolymer materials, one-part geopolymer binders, rubberised geopolymer concrete, and road repair materials. This chapter also discusses the use of industrial by-products, such as ground granulated blast furnace slag (GGBS), fly ash (FA), and waste clay tile (WCT), in geopolymer binder. In addition, previous studies on crumb rubber, surface preparation methods, bonding performance, and compatibility between repair materials and road surface layers are reviewed. The research gaps are also identified in this chapter.

Chapter 3 describes the research methodology adopted to achieve the research aim and objectives. This chapter explains the experimental programme, materials used, mix design procedures, specimen preparation, curing conditions, and testing methods. The procedures for evaluating fresh properties, mechanical performance, durability-related properties, microstructural characteristics, bond strength, rutting resistance, and permeability are also presented.

Chapter 4 presents the characteristics of the raw materials and the optimisation of GGBS–FA and GGBS–WCT one-part geopolymer binders. This chapter also discusses the geopolymerisation reaction based on the chemical, phase, and microstructural analyses. The optimum binder composition for developing the one-part semi-rigid geopolymer repair material is identified in this chapter.

Chapter 5 focuses on the optimisation of crumb rubber content and the compatibility of the developed one-part semi-rigid geopolymer repair material with road surface layers. This chapter evaluates the effect of treated crumb rubber as a sand replacement on the properties of the repair material. It also discusses the bonding performance between the repair material and concrete and asphalt substrates using different surface preparation methods.

Chapter 6 presents the conclusions and recommendations of the study. This chapter summarises the main findings based on the research objectives and highlights the contributions of the research. Recommendations for future studies are also provided.

CHAPTER 2
LITERATURE REVIEW

2.1 Introduction

This chapter reviews the literature related to the development of one-part geopolymer semi-rigid repair materials for pavement applications. The review focuses on the use of one-part geopolymer systems, precursor materials, crumb rubber as sand replacement, material properties, bonding behaviour, rutting resistance, and microstructural development. These aspects are important because pavement repair materials must provide suitable workability, strength, durability, surface wear resistance, and strong bonding with existing pavement substrates. The chapter first discusses one-part geopolymer systems, including single binder and hybrid binder approaches. It then reviews the use of waste materials in geopolymer binders, followed by rubberised semi-rigid pavement and crumb rubber treatment. The reaction mechanisms of one-part geopolymer are also discussed precursor dissolution, gel formation, and matrix development influence material performance. This is followed by a review of fresh, hardened, durability, bonding, and rutting resistance properties relevant to pavement repair applications. Finally, chemical composition, phase properties, and microstructure analysis are reviewed to support the understanding of geopolymer reaction products and matrix formation. Overall, this chapter provides the theoretical basis for developing a one-part geopolymer semi-rigid repair material with strength, durability, bonding, and pavement performance. Therefore, the following section discusses the one-part geopolymer system, focusing on its binder concept, material components, and suitability for practical pavement repair applications.

2.2 One-Part Geopolymer System

Geopolymers are produced through the activation of aluminosilicate raw materials using alkaline activators. These aluminosilicate materials may come from natural sources or industrial by-products containing significant amounts of silica and alumina. According to Cong and Cheng (2021), geopolymer production normally

involves the use of alkaline activators under moderate temperature conditions. The formation of geopolymer binders occurs through a series of chemical reactions, including dissolution, dispersion, polycondensation, and subsequent hardening (Oliveira et al., 2022). During this process, the alkaline activator promotes the dissolution of silica and alumina from the precursor materials, followed by the formation of binding gels that contribute to strength development and matrix densification. Geopolymer technology has received significant attention since it was introduced by Davidovits in the late 1970s. Since then, extensive studies have been conducted on geopolymer synthesis, physical properties, mechanical performance, microstructural development, and durability characteristics. In civil engineering applications, geopolymer binders are commonly considered as alternative binders to ordinary portland cement because they can utilise aluminosilicate by-products and waste materials. However, the performance of geopolymer binders depends strongly on the type of precursor, activator composition, curing condition, and mixing method.

In general, two main method are used for geopolymer synthesis, namely the two-part system and the one-part system (Ren et al., 2021). The conventional two-part geopolymer system is commonly produced by mixing solid aluminosilicate precursors with liquid alkaline activators. Geopolymers are formed through the reaction between an alkaline activator and a solid aluminosilicate precursor, commonly involving alkali hydroxide, silicate, carbonate, or sulphate solutions in a two-part system with the addition of water (Luukkonen et al., 2018). Although this approach is widely used and can produce good mechanical performance, it also has several practical limitations. Liquid alkaline activators are often corrosive, viscous, and heat-generating, which may difficulties in preparation, transportation, storage, and handling. These issues can make the conventional two-part geopolymer system less practical for large-scale applications.

To overcome these limitations, the one-part geopolymer system, also known as the “just add water” system, has been developed. In this system, the aluminosilicate precursor and solid alkaline activator are dry mixed, and water is added during mixing to initiate the reaction. Therefore, the use of liquid alkaline activator solutions is reduced. This approach makes one-part geopolymer more similar to OPC-based materials in terms of handling and application because only water is required at the site (Santos et al., 2023). As a result, one-part geopolymer systems offer better practicality, safer handling, easier transportation, and improved suitability for cast-in-situ applications compared with two-part geopolymer systems. The development of one-

part geopolymer represents an important step in improving the field applicability of geopolymer binders. In one-part mixtures, the final binder is produced by combining dry precursor materials, solid alkaline activators, and water, as shown in Figure 2.1. The use of solid alkaline activators reduces the challenges associated with liquid activators and improves the potential use of geopolymer materials in the construction industry. However, some studies have reported that one-part geopolymer systems may show lower mechanical performance compared with conventional two-part systems, depending on the precursor type, activator dosage, and curing condition (Ren et al., 2021). Therefore, further optimisation is required to ensure that one-part geopolymer binders can achieve suitable workability, setting time, strength, and durability.

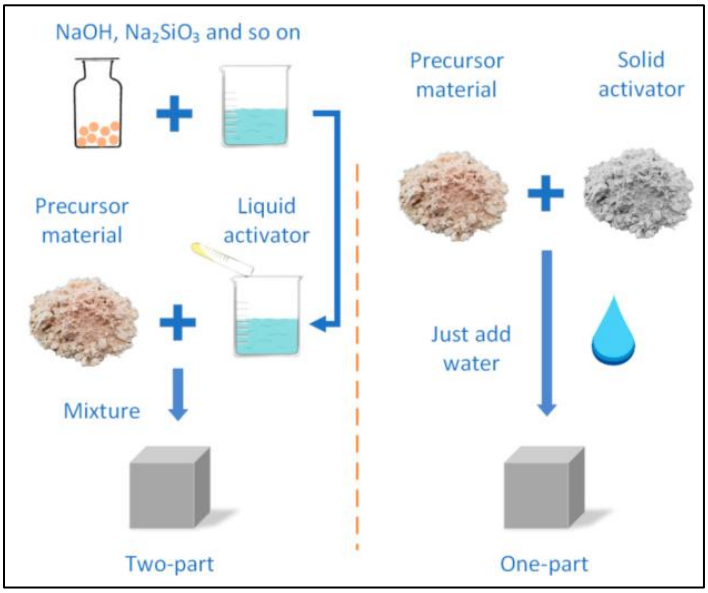


Figure 2.1 Schematic Representation of One-Part and Two-Part Geopolymer Preparation Processes (Qin et al., 2022)

Generally, the aluminosilicate precursors in the synthesis of one-part geopolymers are the ones that have been used in the production of conventional geopolymer binders. Fly ash (FA) and ground granulated blast slag (GGBS) are the most common solid precursors used. Other materials, such as clay minerals or hydrous aluminosilicates, red mud, and natural aluminosilicates such as shale, clays and zeolite are other materials that can be used as precursors materials (Luukkonen et al., 2018). In one-part geopolymer mixtures, the activator can be any solid substance that supplies alkali cations, increases the pH of the reaction mixture, and facilitates the dissolution of aluminosilicate species. Activators employed in one-part geopolymer mixes include

solid sodium hydroxide (NaOH), sodium metasilicate (Na_2SiO_3), sodium metasilicate pentahydrate ($Na_2SiO_3 \cdot 5H_2O$), sodium carbonate (Na_2CO_3), sodium aluminate ($NaAlO_2$), calcium sulphate ($CaSO_4$), sodium sulphate (Na_2SO_4), potassium hydroxide (KOH) are among the activators that have been used in various studies over the years (Opiso et al., 2021). The modulus silicon dioxide/sodium oxide (SiO_2/Na_2O molar ratio) of commercial solid sodium silicates has varied between 0.93 and 3.32 in the published one-part geopolymer studies (Luukkonen et al., 2018).

Among these activators, anhydrous sodium metasilicate (Na_2SiO_3, modulus 0.93) resulted in higher compressive strength and better workability than sodium silicate pentahydrate ($Na_2SiO_3 \cdot 5H_2O$, modulus 1.00) or unspecified hydrous sodium silicate ($Na_2SiO_3 \cdot nH_2O$, modulus 2.06) when activating FA and GGBS with or without hydrated lime in one-part geopolymer systems. The usage of solid activators in past research shows an outperformance compared with alkaline solutions. Sodium metasilicate anhydrous dissolution of aluminosilicate compounds with the greatest ability to create an alkaline environment and led to the highest mechanical properties (Ma et al., 2018; Yousefi Oderji et al., 2019). The major difference between two-part and one-part geopolymers was the reactive rate and the availability of Si, Al, and Ca in source materials, which influenced the strength and microstructure development of geopolymers. Hence, the solid Al-Si materials were usually adopted in one-part geopolymers. In one-part geopolymer systems, the selection of binder composition is important because it influences workability, setting time, strength development, and microstructural formation. The following subsections therefore examine single binder and hybrid binder systems as the main approaches used to develop one-part geopolymer repair materials.

2.2.1 Single Binder

A single binder system in one-part geopolymer refers to the use of one main precursor material, such as FA, GGBS, or metakaolin, activated by a solid alkaline activator. This system is commonly used to evaluate the individual behaviour of each precursor in terms of workability, setting time, strength development, and microstructural formation. However, its performance depends strongly on the chemical composition, fineness, and reactivity of the selected precursor. Aluminosilicate

precursors are main source materials in geopolymer synthesis. A various range of aluminosilicate precursors, including both industrial by-products and naturally occurring raw materials, have been identified as viable sources of aluminosilicate raw materials, as shown in Figure 2.2. The worldwide availability of various aluminosilicate source materials such as FA (which is generated from burning of coal in thermal power stations), GGBS (which is the waste from iron extraction process from raw ore), MK (which is produced by calcining kaolinite clay at 750 °C for several hours) and other abundantly accessible natural or industrial wastes such as tungsten mine waste mud, Lumpur Sidoarjo (LUSI) mud, and palm oil fuel ash (POFA) has increased the research and development in this field. Those precursors were used with the intention of high alumina and silica content, coupled with lower costs because some of them were from industrial waste products and this is one of the reasons for this growing interest in geopolymer (Davidovits, 1994).

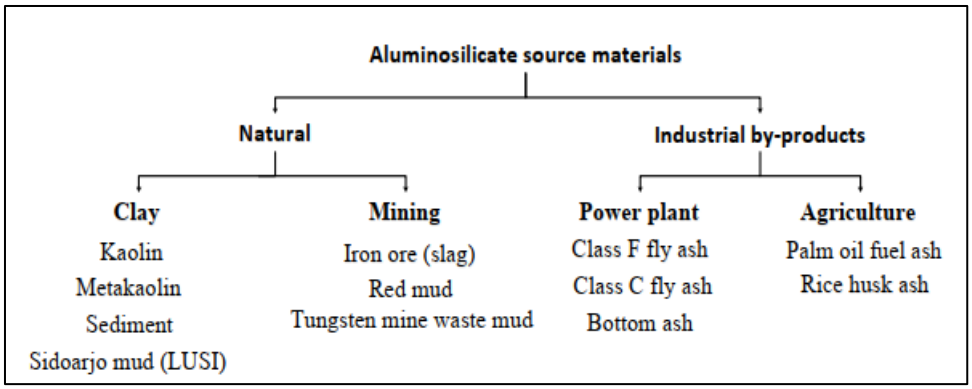


Figure 2.2 Classification of Aluminosilicate Source Materials (Singh et al., 2015)

GGBS is widely recognised as a suitable aluminosilicate precursor for geopolymer binder formulations due to its huge availability, high reactivity, and good chemical composition. GGBS is a secondary material derived from the blast furnace process in the metallurgical industry. This material is formed during the reduction of iron ore to iron, producing a molten slag rich in silicates and calcium oxide. The molten slag, which floats on top of the molten iron due to its lower density, is quickly cooled with water to form a glassy, amorphous structure. Chemically, GGBS typically contains about 40% calcium oxide (CaO), 30–40% silicon dioxide (SiO_2), and 10–20% aluminium oxide (Al_2O_3), which makes its chemical structure comparable to OPC (Almutairi et al., 2021). This similarity enables GGBS to partially or fully replace OPC in binder systems. Moreover, the use of GGBS contributes to sustainable construction

by reducing the need for limestone quarrying and decreasing carbon dioxide emissions associated with cement production.

FA is a widely used aluminosilicate precursor in geopolymer synthesis due to its pozzolanic reactivity, fine particle size, and chemical composition. It is a by-product of coal combustion in coal-fired power plants. During combustion, fine particles are expelled from the boiler and flue gases and collected using electrostatic precipitators or bag filters. In the academic literature, this by-product is commonly referred to as "pulverised fuel ash." FA is classified into Class F and Class C, with Class F being low in calcium oxide and particularly suitable for geopolymer formulations. Its chemical composition, dominated by silica (SiO_2), alumina (Al_2O_3), and smaller amounts of calcium oxide (CaO), makes it ideal as a partial replacement for Portland cement in concrete systems. The pozzolanic activity of FA enhances the mechanical strength, densifies the microstructure, and improves the durability of geopolymer binders (Akmalaiuly et al., 2023).

Ceramic Waste Tile (CWT) is an aluminosilicate precursor obtained as a by-product from the ceramic tile industry. During the dressing and polishing of ceramic products, large quantities of ceramic dust are generated, much of which is discarded as waste (Luhar et al., 2021). CWT is often disposed of on-site in excavation pits, yet its potential as a precursor for geopolymerisation has gained interest due to its high silica content and pozzolanic properties. The global ceramic industry generates substantial waste, with an estimated 12.6 billion m² of ceramic tile production in 2019, increasing to 18.2 billion m² by 2021 (Pompo, 2021). It is projected that approximately 30% of all ceramic production becomes waste, which is non-biodegradable and requires significant landfill space for disposal. Incorporating CWT into geopolymer binders promotes sustainable construction by reducing natural resource consumption and decreased landfill pressure. According to Araújo et al. (2019), ceramic wastes display pozzolanic and filler characteristics, making them suitable for both precursor and aggregate use in geopolymer formulations.

Overall, single binder systems help explain the individual roles of aluminosilicate precursors in one-part geopolymer synthesis. GGBS, FA, and WCT contain silica, alumina, and calcium compounds that contribute to geopolymerisation, strength development, and microstructural formation. However, their performance depends on chemical composition and reactivity, optimisation is often required to achieve suitable properties for one-part geopolymer repair materials. Therefore, the next

subsection discusses hybrid binder systems, where two or more precursors are combined to improve overall binder performance.

2.2.2 Hybrid Binder

A hybrid binder system in one-part geopolymer uses two or more precursor materials activated by a solid alkaline activator. This approach is used to balance the limitations of single binders and improve overall performance. By combining different precursor materials, the binder can achieve a more balanced chemical composition and mechanical properties. Therefore, hybrid binders are important for achieving suitable workability, setting time, strength development, and microstructural formation in one-part geopolymer repair materials.

Migunthanna et al. (2021) studied one-part geopolymer binders made with waste clay brick (WCB) under ambient curing, using solid sodium metasilicate as the only activator. WCB was blended with FA Class F or GGBS at 20–80% replacement, and activator contents of 10% and 20% (by total binder) were evaluated. The results showed that WCB alone gave low compressive strength, while adding GGBS produced much higher strength than adding FA. Overall, WCB can be used as a geopolymer precursor, but better performance is achieved when it is combined with GGBS.

Faraji et al. (2026) developed one-part geopolymer foam concrete using GGBS, waste concrete sludge (WCS), and waste bamboo powder (WBP), activated with sodium metasilicate. The optimum mix containing 5% WBP and no WCS achieved the highest 28-day compressive strength of 11.4 MPa and flexural strength of 1.2 MPa. The improvement was attributed to pore refinement and crack-bridging effects from WBP, which also reduced water absorption and drying shrinkage. However, higher WCS content reduced strength and transport performance due to increased heterogeneity and macro-void connectivity.

Narasimhamurthy et al. (2026) developed and characterised an optimum one-part geopolymer concrete using GGBS and fly ash (FA) as precursors under ambient curing. The study used anhydrous sodium metasilicate as a solid activator at dosages of 6–16%, with GGBS ratios of 50:50, 60:40, and 70:30. The results showed that the optimum mix was achieved at a GGBS ratio of 60:40 with 14% activator, producing the highest 28-day compressive strength of 54.36 MPa and split tensile strength of 4.15

MPa. This mix also achieved about 15–20% higher compressive strength than conventional concrete, although the split tensile strength was slightly lower. Microstructural analysis showed the formation of N-A-S-H and C-A-S-H gels, which contributed to strength development and matrix densification.

Zhao et al. (2026) investigated the effect of precursor composition and solid activator on the fresh, mechanical, and microstructural properties of FA-GGBS-based one-part geopolymer paste. The study used low fly ash (LFA), high fly ash (HFA), GGBS, and solid sodium metasilicate anhydrous (Na_2SiO_3), with different silicon dioxide to aluminium oxide (SiO_2/Al_2O_3) and calcium oxide to silicon dioxide (CaO/SiO_2) ratios. The results showed that higher SiO_2/Al_2O_3 and CaO/SiO_2 ratios improved compressive strength and produced a denser microstructure, although workability and setting time were reduced. Na_2SiO_3 with a modulus of 1.0 and 8% alkali content was identified as the optimum activator condition.

Overall, previous studies show that hybrid binders are more effective than single binders in one-part geopolymer systems because they can balance chemical composition and improve binder performance. As shown in Table 2.1, GGBS provides high CaO for early strength development, while FA, LFA, WCB, and other waste materials supply SiO_2 and Al_2O_3 for geopolymerisation and microstructural formation. However, hybrid binder performance depends on precursor ratio, activator dosage, and material reactivity. Excessive replacement with less reactive waste materials may reduce workability, strength, and density. Therefore, optimisation is necessary to achieve suitable workability, setting time, compressive strength, and microstructural development for one-part geopolymer repair materials.

Table 2.1
Chemical Composition of Various Aluminosilicate Precursors

Reference	**aluminosilicate precursors**	**Chemical composition of aluminosilicate precursors (%)**							
		SiO_2	**Al_2O_3**	**Fe_2O_3**	**TiO_2**	**CaO**	**MgO**	**Na_2O**	**Loss on ignition**
(Migunthanna et al., 2021)	WCB	68.97	3.35	12.07	1.68	3.35	-	-	-
	GGBS	27.54	61.13	0.76	1.05	61.13	-	-	-
	FA	57.13	8.67	12.79	2.74	8.67	-	-	-
(Faraji et al., 2026)	GGBS	37.6	8.2	1.3	-	38.4	12.7	0.3	0.5
	WCS	10.9	3.4	2.3	-	47.1	2.1	0.3	32.8
(Narasimhamurthy et al., 2026)	FA	46.04	25.31	9.9	1.46	12.25	1.14	0.32	-
	GGBS	32.92	13.8	0.58	0.57	42.13	5.76	0.2	-

Table 2.1
Chemical Composition of Various Aluminosilicate Precursors (Cont'd)

Reference	aluminosilicate precursors	Chemical composition of aluminosilicate precursors (%)							
		SiO_2	Al_2O_3	Fe_2O_3	TiO_2	CaO	MgO	Na_2O	Loss on ignition
(Zhao et al., 2026)	GGBS	31.45	16.85	0.36	1.23	45.65	-	-	-
	LFA	54.45	31.85	4.92	1.32	3.56	-	-	-
	HFA	36.98	25.45	5.23	1.39	28.70	-	-	-

Note: SiO_2 -Silica Dioxide, Al_2O_3 - Alumina oxide, Fe_2O_3 - Iron oxide, TiO_2 – Titanium dioxide, CaO – Calcium oxide, MgO - Magnesium oxide, Na_2O - Sodium oxide, WCB - waste clay brick, FA - Fly Ash, GGBS - Ground Granulated Blast-Furnace Slag, WCS - Waste Concrete Sludge, LFA – Low Fly Ash, HFA - High Fly Ash

2.3 Others Waste Material in One-Part Geopolymer for Pavement Applications

One-part geopolymer systems have been less explored than conventional two-part geopolymer systems in pavement engineering research. Previous studies have mainly focused on two-part geopolymer binders as sustainable alternatives to Ordinary Portland Cement (OPC) because of their mechanical strength, durability, and reduced environmental impact. In pavement applications, geopolymer binders have been investigated for rigid pavement, semi-rigid pavement, and repair works, where resistance to repeated traffic loading, cracking, rutting, abrasion, and environmental degradation is important. However, the use of one-part geopolymer systems for pavement repair remains limited, especially in terms of waste material utilisation and field practicality.

Abbass and Singh (2021) examined Rice husk ash (RHA) as source material and Basalt Fibres (B.F.) as fiber reinforcement in geopolymer concrete for rigid pavement application. It can consume the impendency to increased rigid pavement flexibility, elasticity and fabricate supplementary sustainable road surface elucidations. The ratio replacement of RHA with B.F. (1, 5, 10, 15, 20, and 25%) in mixes. From the ratio, 10% B.F. is the optimum replacement that is a better alternative for cement rigid pavements for multilane roads with minimum slab thickness, and infinite loading cycles.

Eisa et al. (2021) conducted a study on the influence of metakaolin (MK) on the length of rigid pavement slabs made of geopolymer concrete in recent years. This study was carried out because one of the issues that portland cement concrete encounters is the allowed spacing for transverse joints in rigid pavements plain concrete slabs. The

recommended length of slabs is 4.5-5 feet, as indicated by several standards and design guidelines. The narrow-permitted transverse joint spacing in rigid pavement slows installation and raises costs. Because MK-based geopolymer concrete obtains 100% of the requisite strength at 7 days, it is more effective in rigid pavement slabs implementation rate than Portland cement concrete.

Wang et al. (2021) investigated the bond interface failure patterns and the microstructure and chemical interactions between various geopolymer repair mortars and concrete substrates at the interfacial transition zone (ITZ). Because of their better endurance and mechanical performance, ITZs between regular OPC and geopolymer mortars have great promise in rehabilitating existing concrete structures. According to the findings, GGBS-based geopolymers had superior bonding strength and mechanical performance than those with low calcium concentrations. Furthermore, the width of ITZs generated in high-calcium geopolymer repair binders was greater than that in low-calcium geopolymer repair binders, resulting in a smoother transition between the repair and substrate materials.

Chen J. et al. (2021) investigated MK-based geopolymer mortar cured at ambient conditions for pavement repair by adding GGBS at replacement ratios ranging from 0% to 40%. The results showed that the early addition of GGBS can considerably boost the strength of MK mortar. At 28 days, compressive and flexural strengths of four mortar series increased by 39%-66% and 29%-54%, respectively, compared to alkali-activated pure-MK mortar. The bond strength and dry shrinkage of the mortar with 30% GGBS replacement were higher than in many other pavement repair products.

Asayesh et al. (2021) used GGBS-based geopolymer concretes with partial dosages of pumice and silica fume (SF) as restorative solutions for degraded concrete pavements. GGBS-based geopolymer concrete replaces slag with 0%, 5%, 10%, and 15% pumice and silica fume replacements by total binder weight. Including pumice and silica fume increased fresh concrete setting time and workability, decreased the compressive, tensile, and flexural strength, and had no influence on the bond strength. It also raised the coefficient of thermal expansion and shrinkage. Furthermore, water absorption and porosity increased as the amount of pumice and SF usually decreases workability and reduce porous because of its fineness and high pozzolanic reaction, likely due to the porous nature of pumice and the finer particle size of silica fume, both of which contributed to a less dense and more porous geopolymer matrix.

As shown in Table 2.2, the different SiO_2, Al_2O_3, and CaO contents of these precursors influence binder reactivity and strength development. High-calcium materials such as GGBS promote faster strength gain and are suitable for pavement repair, while low-calcium materials such as FA, MK, RHA, and WCB usually require mix optimisation to good performance. Therefore, blended systems such as GGBS–FA or GGBS–WCB are commonly used to improve workability, strength, and durability under ambient curing. The next subsection discusses rubberised semi-rigid pavement and the role of crumb rubber as a flexible modifier to balance strength and flexibility.

Table 2.2
Chemical Composition of Various Aluminosilicate Precursors

Reference	aluminosilicate precursors	Chemical composition of aluminosilicate precursors (%)							
		SiO_2	Al_2O_3	Fe_2O_3	TiO_2	CaO	MgO	Na_2O	Loss on ignition
(Abbass & Singh, 2021)	RHA	91.5	0.15	0.06	-	0.48	-	0.27	3.1
	B.F.	54.93	16.62	9.16	1.39	6.83	4.65	5.71	-
(Eisa et al., 2021)	MK	57.81	34.97	1.72	-	0.05	0.54	-	1.88
(Wang et al., 2021)	FA	47.8	33.3	6	0.8	6.2	1.8	0.9	6.5
	GGBS	31.4	16.7	0.3	0.7	39.9	7.4		0.26
	OPC	19	4.8	3.1	0.6	65.7	1.4	0.5	1.38
(Chen J. et al., 2021)	MK	53.65	43.12	0.76	0.24	0.17	0.06	0.06	1.27
	GGBS	31.57	15.27	0.23	0.74	43.18	6.68	0.21	1.44
	OPC	19.08	5.26	2.86	0.29	64.12	1.04	0.17	2.99
(Asayesh et al., 2021)	GGBS	37.22	9.02	0.69	2.73	36.03	7.57	1.47	-
	Pumice	58.58	14.3	3.72	0.62	11.12	1.66	5.91	1.89
	SF	91.64	0.5	0.81	-	0.66	0.71	2.52	1.95
	OPC	20.74	4.9	3.5	-	62.95	1.2	-	2.3

Note: SiO_2 -Silica Dioxide, Al_2O_3 - Alumina oxide, Fe_2O_3 - Iron oxide, TiO_2 – Titanium dioxide, CaO – Calcium oxide, MgO - Magnesium oxide, Na_2O - Sodium oxide, B.F. - Basalt Fibres, FA - Fly Ash, OPC – Ordinary Portland Cement, SF - Silica Fume

2.4 Rubberised Semi Rigid Pavement

Rubberised semi-rigid pavement refers to a pavement or repair material that combines the strength of a rigid binder with the flexibility provided by rubber particles. In general, semi-rigid pavement is to overcome the limitations of gap between flexible asphalt pavement and rigid pavement. Flexible pavement can provide good riding quality and flexibility, but it is more prone to rutting and permanent deformation. Rigid pavement has higher stiffness and load-bearing capacity, but it may be prone to

brittleness, cracking, and longer repair time. Therefore, semi-rigid pavement is introduced to provide a balance between strength, stiffness, and deformation resistance.

In semi-rigid pavement materials, the binder phase is usually responsible for strength and stiffness, while the flexible component helps reduce brittleness and improve deformation tolerance. Conventional semi-rigid pavement commonly uses cementitious grout to fill the voids in porous asphalt. However, cementitious materials may still be prone to cracking under repeated traffic loading, shrinkage, and temperature variation. This limitation may lead to cracking, debonding, and reduced long-term repair performance. Therefore, flexible modifiers such as polymer (Luo et al., 2020), emulsified asphalt (Xu et al., 2020), rubber powder (Chen Z. et al., 2023), and crumb rubber (Zhao J. et al., 2023) have been investigated to improve the flexibility and crack resistance of semi-rigid pavement materials.

Crumb rubber (CR) has gained attention as a flexible modifier because it is produced from waste tyres and can improve the functional behaviour of pavement materials. In recent years, rubber particles from scrap tyres have been increasingly used as partial replacement for natural aggregates in normal concrete and geopolymer concrete (Feng W. et al., 2021; Xie et al., 2019). This approach is considered a sustainable method for reducing waste tyre disposal problems while conserving natural aggregate resources (Marques et al., 2020; Thakare et al., 2022). The incorporation of CR can reduce brittleness, enhance deformation tolerance, improve energy absorption, and increase resistance to surface wear. These characteristics are important for pavement repair because the repair layer must resist traffic loading while accommodating small movements from the existing pavement substrate.

Overall, rubberised semi-rigid pavement aims to balance the flexibility of asphalt pavement with the strength of rigid cementitious pavement. CR is a suitable flexible modifier because it can improve deformation resistance, energy absorption, and surface wear resistance while supporting waste tyre recycling and natural aggregate conservation. However, its effectiveness depends on the bonding between CR particles and the binder matrix. Therefore, the following section discusses the treatment of crumb rubber to improve its surface properties and bonding performance within the binder matrix.

2.5 Treatments of Crumb Rubber

Crumb rubber (CR) treatment is important to improve the bonding between rubber particles and the binder matrix. Untreated CR usually has a hydrophobic surface, which can weaken interfacial bonding, increase porosity, and reduce mechanical strength. Therefore, surface treatments such as NaOH treatment, oxidation treatment, or cement coating are used to improve CR surface roughness, and compatibility with cementitious or geopolymer binders.

CR is a ductile material, with rubber constituting more than 50% of its composition. The CR particles are angular in shape with a smooth surface texture and specific gravity of 1.10 ± 0.05. These particles are highly hydrophobic, as indicated by their water contact angle of 95–122°, where a contact angle greater than 90° shows that the surface repels water (Assaggaf et al., 2021). The degradation of the properties of crumb rubber concrete , in comparison with the properties of normal concrete, is attributed to the weaker bond between the cement matrix and CR particles at the interfacial transition zone (ITZ) due to: (i) the high hydrophobicity of CR, (ii) the low workability and tendency of segregation in crumb rubber concrete and (iii) entrapped air and suspended impurities in the crumb rubber concrete (Mohammadi et al., 2014).

Recently, few researchers investigated the possibility of overcoming the degradation in the mechanical properties by treating CR particles, using chemical techniques in Table 2.3. Thameem Ansari et al. (2021) investigated the use of chemically treated CR as a partial replacement for natural sand in M30 concrete to produce eco-friendly concrete. The CR was treated using NaOH and $KMnO_4$ solution to enhance surface polarity and promote chemical bonding with the cement matrix. The results showed that treated CR improved interfacial adhesion, enabling the concrete to retain a significant amount of its mechanical performance, with optimal strength observed at low replacement levels 2.5–5%, while higher CR contents led to increased permeability and water absorption.

Assaggaf et al. (2022) investigated the effect of CR pre-treatment using NaOH, $KMnO_4$, and cement coating on the performance and sustainability of crumb rubber concrete, where CR replaced 2–40% of sand (by weight) at a constant w/c of 0.4. The findings showed that treatment enhanced the CR–cement interfacial properties and improved mechanical performance, with $KMnO_4$ and treated CR with coating with

cement providing greater strength enhancement than NaOH, while also improving abrasion resistance. The study further reported that CR concrete mixtures contributed to reduced energy use and CO_2 emissions compared to conventional concrete, supporting the sustainability potential of treated with $NaOH^-$, $KMnO^{4-}$, and cement-treated CR crumb rubber concrete.

Rajagopal et al. (2024) investigated the effectiveness of NaOH pre-treatment and micro-silica in improving the mechanical and environmental performance of crumb rubber concrete. The CR was pre-treated by soaking in 5 Molar NaOH for 20 min, followed by washing and air-drying for 24 hours, before being used as a partial replacement of fine aggregate. The findings showed that NaOH pre-treatment improved the rubber cement interfacial bonding, contributing to strength recovery compared to untreated CR concrete, while micro-silica further enhanced strength performance, with the best results generally observed at low CR replacement levels 5%.

Shah et al. (2024) examined the influence of chemical treatment of CR on the performance of lightweight cement composites. The CR (1–4 mm) was treated using sulphuric acid (H_2SO_4) and potassium permanganate ($KMnO_4$) to improve surface characteristics and bonding with the cement paste. The results showed that treated CR enhanced water absorption and interfacial, leading to higher compressive strength and lower water absorption, with H_2SO_4 treatment giving the most significant improvement, particularly when combined with the replaced aggregate.

Overall, Table 2.3 shows that NaOH pre-treatment is practical and cost-effective for improving CR surface properties, while $KMnO_4$, H_2SO_4, cement slurry coating, and micro-silica coating generally provide good interfacial enhancement and better mechanical and durability performance. However, previous studies commonly reported that the optimum CR replacement level remains low, around 2.5–5%, because higher CR content may reduce strength and increase porosity, permeability, and water absorption. These limitations highlight the need to improve CR treatment for semi-rigid repair materials where strong interfacial bonding is required. Therefore, the following section discusses the reactions and mechanisms of one-part geopolymer, focusing on chemical reaction, gel formation, and their contribution to mechanical performance.

Table 2.3
Summary of CR Treatment Methods and Their Effects on Interfacial Bonding and Mechanical Performance of Cementitious Composites

Researcher	Treatment	Treatment Ratio Used	Findings
(Thameem Ansari et al., 2021)	-Sodium Hydroxide (NaOH) -Potassium Permanganate ($KMnO_4$) -Saturated Sodium Bisulfide ($NaHSO_3$)	-5% NaOH solution and washed with clear water -5% $KMnO_4$ solution and adding sulphuric acid - $NaHSO_3$ solution	$KMnO_4$ and cement coating improved bonding, strength, and abrasion resistance more than NaOH.
(Assaggaf et al., 2022)	-Sodium Hydroxide (NaOH) -Potassium Permanganate (KMnO4) -Cement (OPC)	-5% NaOH solution and washed with clear water -5% KMnO4 solution and washed with clear water -Cement slurry with a w/c ratio of 0.4	$KMnO_4$ and cement coating improved bonding, strength, and abrasion resistance more than NaOH.
(Rajagopal et al., 2024)	-Sodium Hydroxide (NaOH) - Micro Silica	- NaOH: 5 M (20 min soaking), wash, air-dried 24 hours -Micro-silica: 10% cement replacement	5 M NaOH improved rubber and cement bonding also improved strength.
(Shah et al., 2024)	-Potassium Permanganate ($KMnO_4$) -Sulphuric Acid(H_2SO_4)	-5% $KMnO_4$ soaked in the solution for 2 hr followed by washing with water and dried for 24 hr -10 wt% H_2SO_4	H_2SO_4 performed better than $KMnO_4$, improving bonding, strength, and water absorption.

2.6 Reactions and Mechanisms for One-Part Geopolymer

Geopolymer is a binder material produced from aluminosilicate source materials containing high amounts of silica and alumina, which react with alkaline activators to form hardened binding products. Aluminosilicate raw materials are widely used in geopolymer formulation because their chemical composition, fineness, and reactivity strongly influence the properties and performance of the resulting binder. The performance of geopolymer binders is mainly influenced by the type of precursor material, the alkaline activator, and the reaction products formed during geopolymerisation.

In conventional two-part geopolymer systems, alkaline activator solutions are commonly used to activate the precursor materials. However, in one-part geopolymer systems, the alkaline activator is used in solid form, and water is added to initiate the reaction. Therefore, the main constituents of one-part geopolymer binders are aluminosilicate precursor materials, solid alkaline activators, and water. These components work together to promote dissolution, gel formation, polycondensation, and hardening.

This section presents the key terminology commonly used in geopolymer systems, followed by a discussion of the geopolymerisation mechanism, focusing on dissolution, polycondensation, and network formation. These aspects provide the theoretical foundation for understanding the behaviour of one-part geopolymer binders and explaining the influence of material composition and processing conditions on their performance.

2.6.1 One-Part Geopolymer Terminology

Generally, one-part geopolymer structures consist of silicate tetrahedron (SiO_4) and aluminate tetrahedron (AlO_4) tetrahedral connected alternatively by sharing all oxygen atoms. Hence, the connectivity leaves negative charges in the IV-fold coordinated Al, which is the positive ions such as (Na^+, K^+, H_3O^+, $Ba_2{}^+$, $Ca_2{}^+$, and $NH_4{}^+$) balanced the free charge. Since the aluminium is IV-folded, these cations must exist to sustain the structure neutrality. However, it is still unclear how the role play of these cations occur, either by charge balancing or are actively bonded into the geopolymer matrix (Elgarahy et al., 2023). Nevertheless, the main inclusion of cations into geopolymer matrix influences the leaching characteristic and the final structure stability. Geopolymer consists of the following empirical formula:

$$M_n\,(-(SiO_2)_z\text{-}AlO_2)_n,\ wH_2O \qquad (2.1)$$

where in M is monovalent cation (K^+, Na^+, or Ca^{2+}); z is 1, 2, 3 or higher, n is a degree of polycondensation and w is the amount of binding water (Davidovits, 1991). One-part geopolymer can be designed in three sialate structures as shown in Figure 2.3 (Davidovits, 2002). One-part geopolymer involves at least four elementary units depending on the Si:Al atomic ratio.

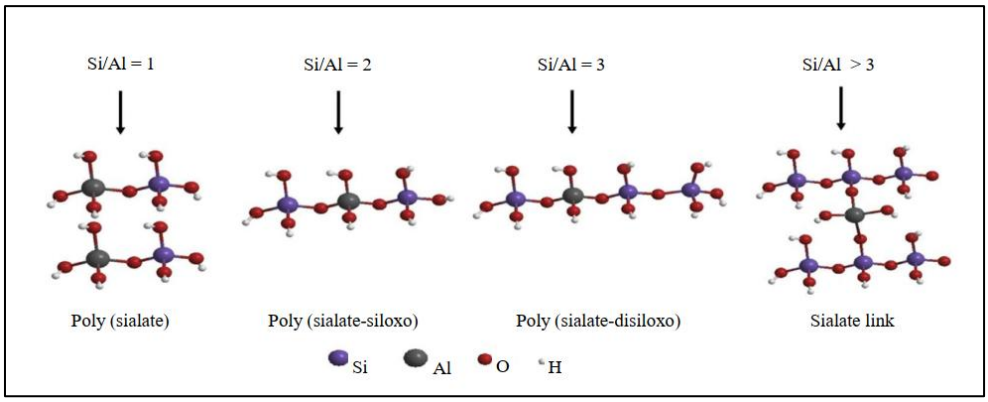


Figure 2.3 Terminology of Poly(sialate) One-Part Geopolymers (Davidovits, 2002)

Furthermore, sialate is the term for silicon-oxo-aluminate. To form a one-part geopolymer structure, polysialate can be formed into a chain or ring polymer with Si^{4+} and Al^{3+} in IV-fold coordination connecting with oxygen and ranging from amorphous to semi-crystalline (Davidovits, 2005). In addition, the application fields for one-part geopolymer for use as repair materials can generally refer to the atomic ratio silicon to aluminium (Si/Al) as shown in Table 2.4. From the table, it suggests that the one-part geopolymer reaction required more Si than Al for high durability applications (Davidovits, 2002). The Si/Al ratio 2 of the geopolymer is sufficient for cement and concrete application. Thus, the performance of geopolymers as repair materials can be highlighted by their chemical structures based on Si to Al ratio. The following subsection discusses the mechanism of one-part geopolymer formation, including dissolution, gel formation, polycondensation, and hardening.

Table 2.4
Geopolymer Application Based on Si to Al ratio (Davidovits, 2002)

Si/Al	Application
1	Bricks, ceramics, fire protection
2	Low CO_2 cements, concrete, radioactive and toxic waste encapsulation
3	Heat resistance composites, foundry equipment, fibre glass composites
< 3	Sealants or coating for industry
Between 20 and 35	Fire resistance and heat resistance fibre composites

2.6.2 Mechanism of One-Part Geopolymer

The process of one-part geopolymer formation exhibits distinct differences when compared to OPC. While OPC achieves hardening primarily through hydration, geopolymerisation serves as the principal mechanism for hardening and strength development in geopolymers. The hydration process of OPC necessitates the presence of water as a catalyst, and implementing water curing is crucial for achieving optimal strength enhancement. However, utilising alkali solutions is imperative for activating aluminosilicate source materials in the context of geopolymerisation. It is remarkable that the occurrence of geopolymerisation can take place under ambient conditions, subject to various influencing factors.

The geological polymerisation mechanism comprises three primary stages, which are as follows: (1) The dissolution of oxide minerals, specifically alumina and silica, from source materials occur under highly alkaline conditions. (2) Following the dissolution, the dissolved oxide minerals orientation occurs, followed by the subsequent processes of coagulation and gelation. (3) Finally, polycondensation forms a three-dimensional network characterized by an aluminosilicate structure. The geological aggregation process encompasses a series of sequential steps outlined in the conceptual model, as depicted in Figure 2.4.

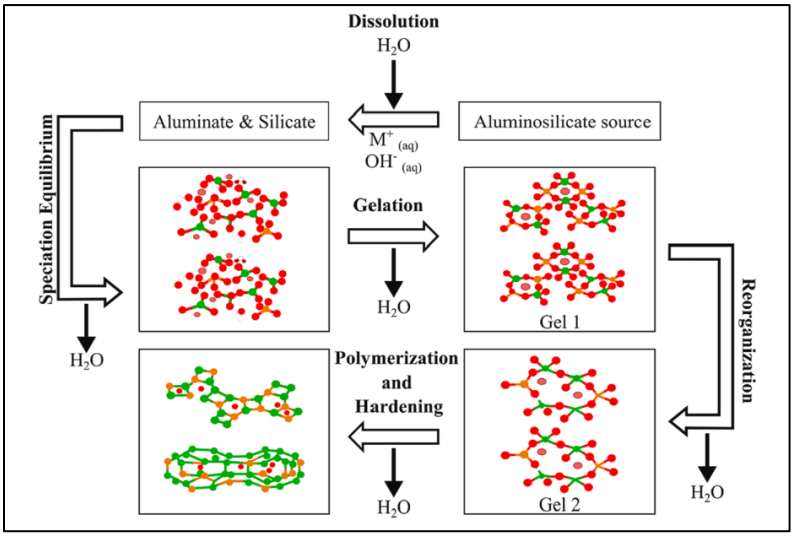


Figure 2.4 Conceptual Model for Geopolymerisation Processes (Abdila et al., 2022)

The present model states that the geopolymerisation process begins with the dissolution of the source materials through the action of the alkaline solution. This

dissolution event disrupts the aluminosilicate bond, resulting in the silica and alumina, which are mainly present within the source materials. The dissolved substances undergo a chemical reaction leading to the formation of sialic acid chains, the extent of which is dependent on the Si/Al ratio, as previously indicated. The electronegative charge produce within the aluminosilicate chain is effectively counterbalanced by the presence of alkali metal cations, namely potassium, sodium, or calcium. Hence, the concentration of silica and alumina within the source material plays a significant role in apply control over the various properties exhibited by the geopolymer.

Moreover, it is worth noting that a direct correlation exists between the increase in alkalinity of the solution and the corresponding rise in the dissolution rate. The parameter controls the time required for saturation, where the aluminosilicate solution transforms into a condition of supersaturation (Duxson et al., 2005). Subsequently, the primary condensation phase occurs, causing the aluminosilicate gel to undergo oligomerisation and precipitate, resulting in large and heightened networks with higher stability. The initial polymer, herein referred to as Gel 1, is synthesised through a solution of elevated silicon (Si) and aluminium (Al) species.

As the chemical reaction progresses, an increasing quantity of silicon is introduced into the solution, forming a gel with elevated Si content (referred to as Gel 2). The start of the initial phase occurs when the rate of condensation of aluminosilicate species surpasses the dissolution rate. Polycondensation and rearrangement processes persist in their effort to generate an collection of interconnected three-dimensional networks, thereby leading to forming the ultimate geopolymer matrix (Abdila et al., 2022). The formation of this geopolymer matrix is directly related to the mechanical properties of one-part geopolymer binders. A denser and well-connected gel network can improve strength, stiffness, durability, and resistance to deformation. These properties are important for pavement applications because the repair material must withstand traffic loading, surface wear, moisture exposure, and interface stress. Therefore, the following section discusses the properties of one-part geopolymer for pavement applications, including fresh, mechanical, durability, and performance-related characteristics.

2.7 Properties of One-Part Geopolymer for Pavement Applications

The properties of one-part geopolymer materials are important for evaluating their suitability as pavement repair materials. These properties include fresh, hardened, durability, bonding, and performance behaviour, which influence placement, early hardening, strength, surface durability, and resistance to traffic loading. The following subsections discuss setting time, workability, compressive strength, water absorption, abrasion resistance, surface roughness and bond strength, and rutting resistance. These properties are important to ensure that one-part geopolymer repair materials can achieve balanced workability, strength, durability, bonding performance, and deformation resistance for semi-rigid pavement repair applications.

2.7.1 Setting Time Properties

Setting time is an important fresh property of one-part geopolymer materials because it determines the working time for mixing, placing, and finishing before hardening begins. Although two-part geopolymer systems have been widely studied, research on one-part geopolymer for pavement repair applications is still limited. For pavement repair, setting time must be properly controlled to ensure workability, early strength development, and timely reopening to traffic. It is mainly influenced by precursor composition, activator concentration, calcium content, and water demand.

Asayesh et al. (2021), said that geopolymer combinations build up faster than cement mixtures. It found that geopolymers set faster than cement. For example, the cement mixture took 167 minutes to start setting and 254 minutes to fully set. In comparison, the 100% GGBS based geopolymer started setting at 74 minutes and finished at 105 minutes. When GGBS was partly replaced with pumice and silica fume (SF), the setting time increased. This may be attributed to the reduced amount of highly reactive GGBS in the mixture, which slowed the early reaction process. Using 5% pumice made the mix set in about 108 to 123 minutes, while 15% pumice increased it to 124 to 135 minutes. For SF, 5% gave a setting time of 123 to 143 minutes, and 15% increased it to 140 to 167 minutes. This means that adding more pumice and SF increases the setting time of the geopolymer. In addition, pumice and SF may increase water demand and reduce the rate of binder dissolution, resulting in slower gel

formation and longer hardening time. Geopolymers with only GGBS set faster, while those with additives like pumice or SF take more time to harden.

Patel et al. (2022) investigated the initial and final setting times of geopolymer concrete and at the ambient temperature. Based on penetration resistance measurements, the geopolymer concrete exhibited values of 3.43 MPa at 210 minutes and 26.67 MPa at 330 minutes, corresponding to the initial and final setting times, respectively. For the geopolymer binder, Vicat needle penetration decreased from 33 mm at 110 minutes to 0 mm, with the final setting time identified at 570 minutes, when no visible surface impression was observed.

Liu et al. (2022) study implemented on setting times, as well as ultra-early-stage (4, 8, 12, 16, 20, and 24 hours(h)) mechanical strength. The proper setting time indicates the binder pumpability and timeliness, and the right gap between the initial setting time and the final setting time is also beneficial to the following construction process. As can be seen, the initial setting time from 35 to 62 minutes, the final setting time ranges from 46 to 72 minutes, and the period between the two ranges from 6 to 15 minutes.

Hamid Abed et al. (2022) examined the effect of NaOH molarity on the setting behaviour of mechanochemically activated (MG) and conventionally activated (CG) geopolymer grouts. Increasing NaOH concentration from 1.25 M to 2.5 M extend the setting process, where the initial setting time increased by 35% (MG) and 29% (CG), while the final setting time increased by 31% (MG) and 29% (CG). This delay may be attributed to the higher alkalinity and concentration, which can increase mixture viscosity and reduce the dissolved aluminosilicate species, slowing early gel formation. However, a further increase to 3.75 M reduced the setting time, indicating that above an optimum alkalinity, the reaction becomes sufficiently rapid to accelerate hardening.

Osman and Irshidat (2023) investigated the influence of the SS/SH ratio on the setting time of geopolymer mortar. They reported that increasing the SS/SH ratio initially delayed setting; for mixes with 25% GGBS, the setting time increased from 24 to 30 minutes. However, further increases in the ratio shortened the setting time markedly, where raising SS/SH from 0.75 to 1.5 reduced the setting time from 30 minutes to 6 minutes. This trend suggests that excessive activator content can accelerate reaction kinetics and early gel formation, resulting in rapid stiffening.

Overall, previous studies show that geopolymer setting time is mainly influenced by precursor composition, calcium content, activator concentration, and mineral additives. GGBS mixtures generally set faster, while pumice or silica fume may

delay setting by reducing reactive GGBS content and increasing water demand. For pavement repair, setting time must be optimised to provide enough working time during placement and early hardening for traffic reopening. The setting time response to key parameters is summarised in Table 2.5.

Table 2.5
Summary of Geopolymer Setting Time Studies

Reference	Varius parameter	Result	Finding
(Asayesh et al., 2021)	Replacements of pumice and silica fume (SF) at 0%, 5%, 10%, and 15%	Initial setting time 34-140 minutes Final setting time 18-167 minutes	The addition of pumice and SF increased setting time due to lower GGBS reactivity and slower gel formation
(Patel et al., 2022)	Replacements of sand, Intermediate aggregate and coarse aggregate	Initial setting time 210 minutes Final setting time 330 minutes	Penetration resistance was 3.43 MPa at 210 minutes and 26.67 MPa at 330 minutes as initial and final setting times
(Liu et al., 2022)	- Replacements of GGBS of 25%, 35%, and 45% -Molar ratio of silicone dioxide/sodium oxide 1.3,1.4 and 1.5 -Mass ratio of activator solution to solid 1.4, 1.5, and 1.6	Initial setting time 46-59 minutes Final setting time 54-66 minutes	Interval between the initial setting time and the final setting time ranges from 6 minutes to 15 minutes
(Hamid Abed et al., 2022)	- Replacement GGBS and FA 25% ,50% and 75% - NaOH molar 1.25, 2.5, and 3.75	Initial Setting time 8-38 minutes Final setting time 9-35 minutes	Optimum molar concentration of NaOH was 1.25 the initial setting time of both MG and CG grouts increased by 35%
(Osman & Irshidat, 2023)	- Replacements of GGBS of 0%, 25%, 50%, 75% and 100% - SS/SH 1.5, 1.25, 1.0, 0.75, and 0.5	Setting time 11-2 minutes	Optimum sodium silicate to sodium hydroxide ratio 1.5 setting time 6 minutes

2.7.2 Workability Properties

Workability is an important fresh property of one-part geopolymer materials because it determines the ease of mixing, placing, spreading, and compacting before setting begins. While two-part geopolymer systems have been widely studied, studies on one-part geopolymer for pavement repair applications remain limited. For pavement repair, suitable workability is required to ensure proper filling of damaged areas, good contact with the existing substrate, and uniform compaction of the repair material. Poor workability may lead to void formation, weak bonding, and reduced mechanical

performance. Therefore, understanding workability behaviour is important for developing one-part geopolymer repair materials that are practical for field application.

Laskar and Talukdar (2017) investigated geopolymer concrete incorporating ultra-fine blast furnace slag (UGGBS) and FA as binders, with slump measured at different time intervals. All mixtures exceeded the minimum slump requirement of 15 mm (lower limit), whereas only a small number reached 25 mm (desired limit), and none exceeded 35 mm (upper limit), consistent with pavement quality concrete slump guidelines. Increasing the UGGBS content and NaOH molarity reduced workability, producing harder mixes with faster setting behaviour. Mixtures G50M12, G75M12, and G100M12 (where G represents UGGBS content and M12 denotes 12 M NaOH) showed noticeably lower slump. In contrast, partial replacement with FA improved flowability, resulting in a gradual increase in slump and better overall workability.

Asayesh et al. (2021) investigated the workability of Portland cement and geopolymer mixtures. Ordinary Portland cement (OPC) showed a slump value of about 5 cm, which was lower than the geopolymer mixtures. The 100% ground granulated blast-furnace slag (GGBS)-based geopolymer mixture achieved a slump of 15 cm. When GGBS was partially replaced with pumice, the slump value increased further, indicating improved workability. For example, the mixture containing 15% pumice showed a higher slump than the 10% pumice mixture. The increase in slump may be attributed to the lower particle interlocking and improved particle movement within the mixture. In addition, the incorporation of silica fume (SF) also increased the slump value, particularly in GGBS–pumice mixtures. This improvement may be related to the fine particle size and filler effect of SF, which can improve particle packing and reduce internal friction, thereby enhancing the workability of the geopolymer mixture.

Girish et al. (2022) evaluated the workability of geopolymer mixtures using the slump test by examining the combined influence of GGBS content and NaOH molarity. The results showed that the workability was affected by both precursor composition and activator concentration. Increasing the GGBS content increased the availability of calcium, which promoted faster geopolymer reaction and early formation of calcium aluminosilicate hydrate gel. This rapid reaction may increase mixture stiffness and reduce the time available for handling. Meanwhile, NaOH molarity influenced the dissolution of silica and alumina from the precursor materials, rather than directly supplying SiO_2 and Al_2O_3. At higher NaOH molarity, the reaction became faster, causing the mixtures to become more rigid and more difficult to work with. Overall, the

study showed that GGBS content and NaOH molarity must be properly controlled to achieve suitable workability and setting behaviour in geopolymer mixtures.

Prasad et al. (2023) evaluated the workability of geopolymer concrete (GPC) using the slump test under 8 M and 10 M sodium hydroxide (NaOH) solutions. Overall, increasing NaOH molarity from 8 M to 10 M reduced the slump value, indicating lower workability. For fibre-reinforced mixes, the slump also decreased as the fibre dosage increased. The fibres used were basalt fibre (BF), steel fibre (StF), and polypropylene fibre (PPF). The slump of geopolymer concrete reinforced with BF mixtures decreased from 165 to 113 mm at 8 M and from 160 to 109 mm at 10 M when BF content increased from 0.10% to 0.35%. For geopolymer concrete reinforced with StF mixtures, the slump decreased from 165 to 129 mm at 8 M and from 160 to 120 mm at 10 M when StF content increased from 0.40% to 0.60%. Meanwhile, geopolymer concrete reinforced with PPF mixtures showed a reduction in slump from 165 to 105 mm at 8 M and from 160 to 96 mm at 10 M when PPF content increased from 0.05% to 0.30%. This reduction in workability may be attributed to increased fibre contact, interlocking, and yield stress within the fresh mixture as fibre content increased.

Overall, workability of geopolymer mixtures is mainly influenced by precursor composition, NaOH molarity, mineral additives, and fibre content. Higher GGBS content, NaOH molarity, and fibre dosage generally reduce slump due to faster reaction, increased stiffness, and fibre interlocking. For pavement repair, workability must be optimised to ensure proper placement, compaction, and bonding with the existing substrate. A summary of workability results is presented in Table 2.6.

Table 2.6
Summary of Geopolymer Workability Studies

Reference	Varius parameter	Result	Finding
(Laskar & Talukdar, 2017)	- FA of amounts of 20, 30, 40 and 50% -Addition of superplasticizer of amounts of 0.5, 1.5 and 3% - NaOH concentrations of 8, 10, 12 and 14M	-5 min(22-200)mm -15 min (22-180) mm -30 min (10-150) mm	-GGBS content and NaOH molar concentration increased, more difficult to work, and more quickly set
(Asayesh et al., 2021)	Replacements of pumice and SF at 0%, 5%, 10%, and 15%	5-25 cm	- Partial replacement with pumice and SF increased slump and workability

Table 2.6
Summary of Geopolymer Workability Studies (Cont'd)

Reference	Varius parameter	Result	Finding
(Girish et al., 2022)	-Replacements of FA at 25%, 50%, 75%, and 100% -NaOH solutions of 8, 10, and 12 M	20-28mm	- Higher GGBS content and NaOH molarity reduced workability by increasing mixture stiffness
(Prasad et al., 2023)	- BF dosages 0.1-0.35% -StF dosages 0.4-0.6% -PF dosages 0.05-0.25%	-165 and 113 mm at 8 M -160 to 109 mm at 10 M	-Increase in BF, StF, and PF content; the slump value gradually decreases for both 8 M and 10 M of NaOH concentration

2.7.3 Compressive Strength Properties

Compressive strength is one of the main hardened properties used to evaluate the load-bearing capacity of geopolymer materials. For pavement repair applications, adequate compressive strength is required to resist traffic loading, surface pressure, and early damage after repair. Although two-part geopolymer binders have been widely studied, the compressive strength performance of one-part geopolymer and rubberised geopolymer concrete for pavement repair is still limited. The strength development is mainly influenced by precursor composition, activator type, activator concentration, curing condition, crumb rubber (CR) content, and gel formation. Therefore, understanding compressive strength behaviour is important to assess the suitability of geopolymer-based materials as semi-rigid pavement repair materials.

Azmi et al. (2016) investigated FA based geopolymer concrete with 0 to 20% fine aggregate replacement by CR and observed a progressive strength reduction with increasing CR content. At 28 days, compressive strength decreased from about 65 MPa (0% CR) to 15.8 MPa (20% CR), with a reduction of approximately 60% at 15% CR replacement. The strength loss was attributed to the hydrophobic nature of rubber particles, weak interfacial bonding between CR and the geopolymer matrix, and increased internal voids, which act as stress concentration points. Despite this reduction, rubberised geopolymer concrete demonstrated acceptable strength for non-structural and pavement-related applications, particularly where impact resistance, durability, and sustainability are prioritised over high load-bearing capacity.

Laskar and Talukdar (2017) investigated the effect of NaOH molarity (8, 10, 12, and 14 M) on the compressive strength development of GGBS–FA based geopolymer concrete. The highest compressive strength was achieved at 10 M NaOH, with a 28-day

compressive strength of 51.89 MPa, while lower strength was observed at 8 M and reduced strength was reported at higher molarities of 12 M and 14 M due to excessive alkalinity. The results indicate that 10 M NaOH is the optimum molarity for achieving maximum compressive strength.

Tahir et al. (2019) examined the effect of the SS/SH ratio and solid-to-liquid ratio on geopolymer strength. The maximum compressive strength of 65.09 MPa was achieved at a SS/SH ratio of 2.5, while higher or lower ratios reduced strength. Similarly, increasing the solid-to-liquid ratio improved strength up to a point, with 3.0 achieving 62.28 MPa. However, excessive solid content left unreacted material, reducing workability and strength. Overall, a SS/SH ratio of 2.5 and solid-to-liquid ratio of 2.0 were identified as the optimum mix parameters.

Migunthanna et al. (2021) studied the compressive strength of geopolymers incorporating waste clay brick (WCB) and found that strength was highly dependent on precursor type and activator content. WCB alone with 10% activator showed low strength of 14.9 MPa, but blending with GGBS significantly improved performance, reaching 38.3 MPa at 28 days. Increasing activator content from 10% to 20% lead to a strength decrease, especially in WCB–GGBS mixes. The study highlighted that WCB alone is insufficient for structural use, but in combination with high-calcium precursors, it can produce sustainable and effective geopolymer binders.

According to Tahir et al. (2022), NaOH molarity significantly affects the compressive strength of FA-based geopolymer. The strength increased with molarity, reaching 15.57 MPa at 8 M and peaking at 31.48 MPa at 10 M. However, further increase to 12 M reduced the strength to 18.59 MPa. This behaviour is attributed to excessive hydroxide concentration causing premature aluminosilicate gel precipitation and ion release. Therefore, 10 M NaOH was identified as the optimum concentration for maximum compressive strength development.

Girish et al. (2022) reported that FA–GGBS geopolymer concrete achieved more than 50% of its 28-day strength after just 7 days of ambient curing. The 28-day compressive strength reached 40 MPa, about 1.5 times the 7-day strength. Further curing to 56 days increased strength by only 3.53%, indicating most gains occur early. Increasing NaOH molarity from 8 M to 12 M enhanced strength by up to 22%, as higher molarity promoted greater aluminosilicate dissolution and denser microstructure formation.

Orhan et al. (2023), produced slag-based geopolymer concrete activated with 12 M KOH and replaced fine aggregate with crumb rubber (CR) at 0 to 15% (by volume). The 28-day compressive strength ranged from 38.17 MPa (0% CR) to 25.95 MPa (15% CR), showing a clear strength reduction as CR increased. The reported reductions were 16.51% (5% CR), 23.76% (10% CR), and 32.01% (15% CR). This decrease was mainly linked to the weaker rubber paste interfacial bonding and the lower stiffness of rubber compared to natural sand, which promotes microcracking and earlier failure under compression.

Zhao J. et al. (2023) compared two-part rubberised geopolymer mortar (TRGM) with one-part rubberised geopolymer mortar (ORGM) and found that compressive strength decreased as CR replacement increased (5 to 15%). For TRGM, the 28-day strength dropped from 64.27 MPa (0% CR) to 50.48 MPa (5% CR), 41.78 MPa (10% CR), and 35.24 MPa (15% CR). For ORGM activated by anhydrous Na_2SiO_3 (ORGM-NS), the 28-day strength reduced from 63.29 MPa (0% CR) to 47.47 MPa (5% CR), 40.73 MPa (10% CR), and 35.10 MPa (15% CR). The reduction was mainly linked to weaker rubber–paste bonding (weak ITZ) and higher entrapped air or porosity in mixes with higher CR.

Raut et al. (2024) investigated steel slag–based geopolymer composites incorporating CR as a partial replacement of crusher dust at 0 to 30% by volume, activated using a combination of 12 M NaOH and Na_2SiO_3. The 28-day compressive strength of the control geopolymer reached approximately 58.67 MPa, while mixtures containing CR exhibited a reduction in strength with increasing CR content. At 10%, 20%, and 30% CR replacement, the compressive strength reductions were reported to be approximately 12 to 16%, 22 to 25%, and 34 to 41%, respectively, depending on the rubber particle size. Despite this reduction, all CR-modified geopolymer blocks maintained compressive strengths exceeding 12 MPa, satisfying the requirement for first-class bricks. The strength loss was primarily attributed to the lower elastic modulus of CR, weaker rubber geopolymer interfacial bonding, and the formation of rubber induced macro porosity, which promoted microcracking and earlier failure under compressive loading.

Overall, compressive strength is mainly influenced by precursor type, activator condition, curing age, and CR content. GGBS supports early strength development, while FA and other supplementary materials can improve binder optimisation and geopolymerisation. However, excessive activator content and high CR replacement

may reduce strength due to weak bonding, higher porosity, and microcrack formation. Therefore, binder formulation and CR content must be optimised for semi-rigid pavement repair applications. Table 2.7 summarises compressive strength results from previous geopolymer studies.

Table 2.7
Summary of Compressive Strength from Different Geopolymer Studies

Reference	Molarity (M)	Various parameter	Compressive strength				Finding
			3day (MPa)	7day (MPa)	14day (MPa)	28day (MPa)	
(Azmi et al., 2016)	-	CR content (0%, 5%, 10%, 15%, 20%)	-	8.5 to 24	-	65 to 15.4	Compressive strength decreased as CR content increased
(Laskar & Talukdar, 2017)	8, 10, 12 and 14 M	- FA of amounts of 20, 30, 40 and 50% -Addition of SP of amounts of 0.5, 1.5 and 3%	40.44	-	-	51.89	-10 M NaOH optimal
(Tahir et al., 2019)	12M	-SS/SH ratio 1.5,2.0,2.5 and 3.0	-	43.83 to 65.09	-	-	-SS/SH 2.0 optimum
(Migunthanna et al., 2021)	-	-Replacement FA and GGBS 20%, 40%, 60% and 80%	-	2.5 to 68	4 to 80	5 to 83	-WCB and GGBS, with an activator content of 10% from the total binder
(Tahir et al., 2022)	8M,10M,12M	-FA to alkaline activator 1.5:1-3:1 - SS to SH ratio 1.5:1-3:1	-	15.57 to 31.48	-	-	-10M NaOH optimal
(Girish et al., 2022)	8M,10M,12M	-Replacement GGBS 25%-100%	-	19 to 41	-	60 to 121	-12 M NaOH optimal
(Orhan et al., 2023)	-	CR content (0%, 5%, 10%, 15%)	-	-	-	25.95 to 38.17	Higher CR content reduced compressive strength due to weak CR interfacial bonding

Table 2.7
Summary of compressive strength from different geopolymer studies (Cont'd)

Reference	Molarity (M)	Various parameter	Compressive strength				Finding
			3day (MPa)	7day (MPa)	14day (MPa)	28day (MPa)	
(Zhao J. et al., 2023)	-	-Activator (NaOH powder and Na_2SiO_3 powder) -CR content (0%, 5%, 10%, 15%)	-	ORGM-NS: 27.04 to 49.78 ORGM-NH: 10.44 to 13.74	-	-	One-part typically exhibited decreased compressive strength relative to two-part systems
(Raut et al., 2024)	-	CR content (0%, 10%, 20%, 30%)	-	54.6 to 38.4	-	57.2 to 42.7	The addition of CR typically results in a decrease in compressive strength

2.7.4 Water Absorption Properties

Water absorption is an important durability property because it indicates the ability of geopolymer materials to resist water penetration. For pavement repair, low water absorption is needed to reduce moisture ingress, pore connectivity, and long-term deterioration. Although two-part geopolymers have been widely studied, water absorption in one-part and rubberised geopolymer repair materials remains limited. This property is influenced by precursor composition, activator condition, curing age, pore structure, and crumb rubber (CR) content. Therefore, understanding water absorption is important for evaluating the durability of geopolymer-based semi-rigid pavement repair materials.

Wongsa et al. (2018) expressed the water absorption of lightweight geopolymer mortar utilising 100% CR as a substitute for fine aggregate is substantially higher than that of traditional mortars. The numerical results indicate that the water absorption values for CR geopolymer mortar mixtures vary from 7.8% to 17.1%, influenced by the alkaline solution-to-FA ratio and curing conditions. The control geopolymer mortar with river sand revealed a water absorption value of only 1.6%. The significant rise is due to the porosity of CR and the voids in the rubber binder contact. Increased curing temperatures, such as 90°C, result in increased absorption of water, reaching a maximum of 17.1%, whilst ambient curing conditions yield lower values of approximately 7.8%.

Orhan et al. (2023), the addition of CR markedly declines the water absorption of geopolymer concrete. In this investigation, water absorption percentages dropped as CR content rose, with reductions of 5.3%, 9.85%, and 11.82% noted for 5%, 10%, and 15% CR substitution, respectively. The decreased water absorption results from the hydrophobic characteristics of CR, which simultaneously decreases the permeability of the concrete. This attribute improves the material durability against freeze-thaw cycles and sulfate conditions. Geopolymer concretes with 15% CR absorbed about three times less water when subjected to sulfate exposure than conventional geopolymer concretes. The rise in water absorption characteristics enhances the material overall durability.

Zakeremamreza et al. (2023) revealed that the incorporation of CR in alkali-activated mortar significantly impacts water absorption. The hydrophobic nature of the rubber particles minimises the general water absorption of the mortar. The data indicated that the water absorption capacity of the rubberised mortar was around 6.5%, which is lower than that found in conventional repair mortars. The decrease in water absorption contributes to the enhanced strength of the repaired structures.

Overall, water absorption of rubberised geopolymer materials depends on CR content, curing condition, pore structure, and rubber bonding. CR may either increase absorption due to higher porosity and weak bonding or reduce absorption due to its hydrophobic nature. Therefore, mix design and curing conditions must be properly controlled to minimise moisture ingress and improve durability. Table 2.8 summarises the water absorption results reported in various geopolymer studies incorporating different levels of CR replacement.

Table 2.8
Water Absorption of Geopolymers with CR Replacement

Reference	Varius parameter	Result	Finding
(Wongsa et al., 2018)	100% CR substitution	7.8% to 17.1%	Higher water absorption due to porosity of CR and voids in rubber-binder contact
(Orhan et al., 2023)	CR content (5%, 10%, 15%)	5.3%, 9.85%, 11.82% reduction	Decreased water absorption due to hydrophobic characteristics of CR, improving durability
(Zakeremamreza et al., 2023)	CR in alkali-activated mortar	6.5%	Lower water absorption due to hydrophobic nature of CR, enhancing strength of repaired structures

2.7.5 Abrasive Properties

Abrasion resistance is an important surface durability property that reflects the ability of geopolymer-based pavement repair materials to resist wear from traffic loading, tyre friction, and abrasive action. Although two-part geopolymer systems have been widely studied, abrasion resistance in one-part and rubberised geopolymer repair materials remains limited. This property is influenced by binder strength, pore structure, crumb rubber (CR) content, rubber particle size, and rubber–matrix bonding. Therefore, understanding abrasion resistance is important for evaluating the long-term surface performance of rubberised geopolymer semi-rigid repair materials.

Thomas et al. (2016) reported that replacing fine aggregate with CR up to 20% reduced abrasion depth, showing improved wear resistance in line with BS EN 1338 (BS-EN-1338, 2003). This improvement is linked to the elastic rubber particles that absorb grinding and reduce direct damage to the binder surface, even though rubber matrix bonding is weaker than natural aggregates. Fine CR is typically more effective than larger rubber chips because it disperses more uniformly and dissipates surface stresses better; therefore, despite possible reductions in compressive strength due to interfacial voids, rubberised geopolymer composites remain attractive for pavements and surface repair where wear resistance is critical.

Bisht and Ramana (2017) reported that increasing CR replacement (0–5.5% as fine aggregate replacement) slightly reduced abrasion resistance, shown by a higher depth of wear. The depth of wear increased to about 0.93 mm at 5.5% CR, which was 0.14 mm higher than the control mix. This increase was attributed to the lower density of rubber particles and weaker interfacial bonding between the rubber and cement matrix, allowing easier particle movement under abrasive action. Despite this increase, the measured wear values remained within the permissible limits specified by IS-1237 (IS-1237, 2012), indicating that rubberised concrete maintains acceptable abrasion resistance and is suitable for applications such as pavements and concrete tiles where surface durability is required.

Feng L.-Y. et al. (2021) reported that incorporating waste tire rubber particles as partial sand replacement significantly increased the abrasion resistance of rubberised concrete, with abrasion resistance rising as rubber content increased (10–20% by volume), while compressive strength decreased with higher rubber dosages. The

improvement was attributed to the rubber particles high deformability and energy absorption, which form an elastic protective layer that reduces grinding damage and produces a smoother surface that is less prone to erosion under abrasive action.

Overall, CR affects abrasion resistance depending on its content, particle size, bonding condition, and test method. Rubber particles can improve abrasion resistance by absorbing abrasive energy and reducing surface damage, but weak bonding may increase wear depth. Therefore, CR content must be optimised to balance abrasion resistance, compressive strength, and surface durability. Table 2.9 summarises abrasion resistance results from previous geopolymer studies with different CR replacement levels.

Table 2.9
Summary of Geopolymer Abrasive Resistance Studies

Reference	Varius parameter	Result	Finding
(Thomas et al., 2016)	CR content (2.5%, 5%, 7.5% by volume of fine aggregate)	Abrasion depth decreased with increasing CR content	CR improved abrasion resistance by absorbing abrasive action but reduced mechanical strength due to weak rubber bonding
(Bisht & Ramana, 2017)	CR content 4%, 4.5%, 5%, 5.5% by volume of fine aggregate)	Depth of wear increased with CR content; maximum 0.93 mm at 5.5% CR	CR slightly reduced abrasion resistance due to weak bonding and particle movement, but the wear depth remained within IS 1237:2012 limits
(Feng L.-Y. et al., 2021)	- CR Content: 10%, 15%, 20% - CR Size: 1–3 mm & 3–5 mm - CR Pretreatment: Tap Water (Rinsed), NaOH, NaOH + KH570	15% CR: 16.96 $h \cdot m^2 \cdot kg^{-1}$ 20% CR: 28.26 $h \cdot m^2 \cdot kg^{-1}$ NaOH+KH570: 20.02 $h \cdot m^2 \cdot kg^{-1}$	- Higher CR content, larger particle size, and NaOH + KH570 treatment improved abrasion resistance, although compressive strength decreased

Note: For Feng L.-Y. et al. (2021), $h \cdot m^2 \cdot kg^{-1}$ represents the abrasion resistance index, where h refers to hour, m^2 refers to the abrasion area, and kg refers to mass loss.

2.7.6 Surface Roughness Evaluation and Bonding Strength

Surface roughness and bond strength are important for evaluating geopolymer-based pavement repair materials. A strong bond between the repair layer and existing concrete or asphalt substrate is needed to prevent debonding, delamination, and premature patch failure. Rougher surfaces can improve mechanical interlocking and contact area at the interface. However, limited studies have examined the relationship between substrate roughness and bond strength in one-part rubberised geopolymer

repair materials. Therefore, this relationship is important for assessing durable semi-rigid pavement repair performance.

Tayeh et al. (2012) evaluated substrate surface roughness influences the bonding strength between an ultra-high-performance fibre concrete overlay and normal concrete substrate. Five surface conditions as-cast, grooved, drilled holes, sandblasted, and wire-brushed were compared using slant shear. Sandblasting produced the highest bond strength 17.8 MPa in slant shear at 28 days, indicating that increased roughness enhances mechanical interlocking and promotes stronger interface performance.

Abed Al-Jabar et al. (2021) reviewed the influence of substrate surface roughness on the bonding strength of geopolymer repair materials to OPC concrete substrates. Different surface roughened surfaces such as wire-brushing or drilled holes were discussed in relation to slant shear and splitting tensile bond performance. The review highlighted that, in geopolymer, high bond strength can still be achieved even with low surface roughness, whereas commercial repair products were more dependent on roughness; overall, surface roughness affects bonding mainly by enhancing interfacial contact and mechanical interlocking, although the extent of its influence varies with binder chemistry and interface reactions.

Daneshvar et al. (2021) investigated casting and curing temperature affects the bonding strength of epoxy bonded concrete composites. The concrete substrate surface was prepared by shot blasting to create a roughened interface prior to epoxy application. Bond performance was evaluated using pull-off, and bi-surface shear tests, and the results showed that increasing temperature from 5 to 55°C significantly reduced interfacial bond strength up to 64 to 65% reduction in tension parameters. The reduction was mainly attributed to temperature driven changes in epoxy, including faster epoxy setting relative to cement hydration and increased epoxy loss into pores, which weakened the interface.

Wang et al. (2021) investigated the interfacial bonding behaviour between geopolymer repair materials and concrete substrates with different surface conditions. The substrate surfaces were prepared using 5mm roughness treatments prior to repair application. Bond performance was evaluated using pull-off, and slant shear, and the results showed that increased surface roughness significantly enhanced bond strength due to improved mechanical interlocking and stress transfer at ITZ.

Felekoğlu (2024) investigated the interfacial bonding performance of geopolymer repair mortars applied to concrete substrates with different surface

preparation conditions. Substrate surfaces were prepared using smooth surface and wire brush roughness prior to repair application. Bond strength was evaluated using the slant shear test, and the results showed that roughened substrates achieved significantly higher bond strength compared to smooth surface, with reported shear bond values exceeding 10 MPa at 28 days. The improvement was attributed to enhanced mechanical interlocking and stronger stress transfer across the geopolymer concrete interface, confirming the critical role of surface roughness in bond development.

Overall, substrate surface roughness improves bond strength by enhancing mechanical interlocking, contact area, and stress transfer at the interface. Roughened surfaces such as sandblasted, wire-brushed, drilled-hole, and shot-blasted surfaces generally provide better bonding than smooth surfaces. However, bond performance also depends on repair material type, binder chemistry, curing condition, and interface reaction. Therefore, proper surface preparation is important to reduce debonding and premature repair failure. Table 2.10 summarises previous studies on surface preparation and interfacial bond strength of geopolymer and OPC repair materials.

Table 2.10
Summary of Surface Preparation and Bond Strength Evaluation Studies

Reference	Surface Preparation	Bond Test Method	Finding
(Tayeh et al., 2012)	- As cast - Grooved - Drill holes - Sandblast - Wire brush	Slant shear test	Bond strength increased with surface roughness; sandblasting gave the highest bond
(Abed Al-Jabar et al., 2021)	- As cast - Drill hole - Wire brush	-Slant shear test - Splitting tensile test	Bond strength increased with surface roughness
(Daneshvar et al., 2021)	Shot Blasting	- Pull-off test - Bi-surface shear test	Bond strength dropped with temperature (up to 65% from 5–55°C); best bond at ≤25°C
(Wang et al., 2021)	5mm roughness	- Pull-off test - Slant shear test	GGBS-based geopolymers bonded better; FA-based showed weaker bond due to lower compatibility and a weaker ITZ
(Felekoğlu, 2024)	- Smooth surface by trowelling - Wire brush	Slant Shear Test	Lower-stiffness cementitious micro-concrete repair mortar produced more stable bonding with the high-strength concrete substrate, especially on roughened surfaces

2.7.7 Rutting Resistance

Rutting resistance is an important property of pavement repair materials because it indicates their ability to resist permanent deformation under repeated traffic loading. Good rutting resistance is required to maintain surface stability, riding quality, and pavement safety. Although rutting behaviour has been widely studied in asphalt mixtures, limited studies have evaluated rutting resistance in one-part rubberised geopolymer repair materials. Therefore, understanding rutting resistance is important for assessing the suitability of rubberised geopolymer-based semi-rigid materials for surface road repair applications.

Haritonovs et al. (2012) evaluated the rutting resistance of asphalt mixtures incorporating dolomite sand waste and basic oxygen furnace (BOF) steel slag as alternative aggregates. Rutting performance was assessed using the wheel-tracking test at 60 °C, where rutting depth, wheel-tracking slope, and proportional rutting depth were measured under repeated loading. These parameters were used to indicate the degree of permanent deformation and visco-plastic flow of the asphalt mixture during loading. The results showed that mixtures containing 100% joint products, consisting of quartz sand and bitumen, exhibited improved rutting resistance, with rutting depth as low as 1.54 mm compared with conventional mixtures. The enhanced performance was attributed to the high angularity and stiffness of steel slag aggregates, which improved resistance to permanent deformation and limited visco-plastic flow under traffic loading.

Lv et al. (2020) investigated asphalt rutting resistance by evaluating twenty-six (26) mixtures with different aggregate gradations using the Hamburg Wheel Tracking (HWT) test at 50 °C. The results showed that rutting performance was strongly controlled by the aggregate skeleton, where excessive fine content increased rut depth and creep slope. Increasing the 4.75 mm sieve passing beyond 41% caused a sharp reduction in rutting resistance and initiated stripping behaviour. In contrast, mixtures with a coarser skeleton and controlled fine fraction exhibited superior rutting resistance due to improved stone on stone contact and reduced aggregate displacement under repeated loading.

Xiang et al. (2024) investigated the rutting resistance of rubberised reclaimed asphalt mixtures incorporating reclaimed asphalt pavement (RAP) and crumb rubber

(CR) using the Hamburg Wheel-Tracking (HWT) test. The study showed that increasing RAP content, CR dosage, and accelerated ageing time improved resistance to rutting deformation. Rutting depth decreased, while dynamic stability increased with ageing, indicating better resistance to permanent deformation at high temperature. The results also showed that CR and RAP improved mixture elasticity, delayed stripping, and reduced permanent deformation.

Overall, rutting resistance is influenced by aggregate type, gradation, binder composition, CR content, and repeated loading conditions. Angular aggregates, coarser skeleton structure, controlled fine content, and CR or RAP addition can improve resistance to permanent deformation. However, most studies focused on asphalt mixtures, while rutting resistance of one-part rubberised geopolymer repair materials remains limited. Therefore, further study is needed to evaluate the rutting performance of rubberised geopolymer-based semi-rigid repair materials. Table 2.11 summarises rutting resistance outcomes reported in previous studies.

Since the performance of one-part geopolymer repair materials depends on binder formation and matrix development, their chemical composition, phase formation, and microstructure must be understood. Therefore, the following section discusses the chemical, phase, and microstructural characteristics of one-part geopolymer.

Table 2.11
Summary of Rutting Resistance Studies

Reference	Varius parameter	Result	Finding
(Haritonovs et al., 2012)	Aggregate type: dolomite sand waste and basic oxygen furnace (BOF) steel slag	Rut depth reduced to 1.54 mm	BOF steel slag improved rutting resistance by increasing aggregate angularity and stiffness, which reduced permanent deformation and visco-plastic flow under repeated loading
(Lv et al., 2020)	Bitumen content in the range 5.4 to 7.0 %	Rutting depth increased sharply when loading exceeded 4.75 million passes	Coarser gradation with strong stone-on-stone contact improves rutting resistance
(Xiang et al., 2024)	-Asphalt content (4.0 to 7.0%) -4.75 mm key sieve passing (20–68%) -Coarse particle gradation variation (7:1 to 1:11) - Fine particle gradation variation (0.450 to 0.512)	Reduced rut depth and increased dynamic stability with higher RAP or CR and aging	Rutting performance was measured through accumulated rutting depth under repeated wheel loading. Coarser gradation with stronger stone-on-stone contact improved resistance to permanent deformation

2.8 Chemical, Phase Composition and Microstructure Analysis for One-Part Geopolymer

The performance of one-part geopolymer materials depends on their chemical composition, phase formation, and microstructural development. These characteristics influence precursor reactivity, gel formation, strength development, durability, and matrix compactness. In one-part geopolymer systems, the reaction begins when water is added to dry precursor materials and solid alkaline activators, leading to dissolution, gel formation, and hardening. The following subsections discuss the chemical composition, phase properties, and microstructural characteristics of one-part geopolymer materials. The chemical composition analysis focuses on the major oxide constituents of the precursor materials and their influence on geopolymerisation. Phase properties are evaluated using X-ray diffraction (XRD) to identify crystalline and amorphous phases formed during the reaction process. Microstructural characteristics are examined using scanning electron microscopy (SEM), backscattered electron (BSE) imaging, and energy-dispersive X-ray spectroscopy (EDS) to assess gel formation, pore structure, and matrix densification. Overall, these analyses are important to justify the suitability of GGBS and ceramic waste as precursor materials and to support the development of one-part geopolymer-based semi-rigid repair materials for pavement applications.

2.8.1 Chemical Composition Properties

Chemical composition is important in evaluating the suitability of precursor materials for geopolymer synthesis. Major oxides such as silicon dioxide (SiO_2), aluminium oxide (Al_2O_3), and calcium oxide (CaO) influence precursor reactivity, gel formation, strength development, and microstructure. Although chemical composition has been widely studied in two-part geopolymer systems, studies on one-part geopolymer repair materials remain limited. Therefore, this section reviews the chemical composition of GGBS and ceramic waste (CW) to explain their role in geopolymerisation.

Ground granulated blast furnace slag (GGBS) is a widely used supplementary cementitious material derived from the by-product of iron production in the

metallurgical industry. Phummiphan et al. (2018) reported that calcium oxide (CaO) was the dominant oxide in GGBS, comprising approximately 30.38 wt%, followed by silicon dioxide (SiO_2) at 26.78 wt%. Similarly, Migunthanna et al. (2021) used XRF analysis to characterise slag particles and found that CaO and SiO_2 were the two major oxides, accounting for 61.13 wt% and 27.54 wt%, respectively.

In a study by Azevedo et al. (2020), XRF analysis showed that ceramic waste (CW) was mainly composed of silica, accounting for approximately 57.20 wt%, while alumina oxide contributed about 32.20 wt%. Similar trends were reported by Faldessai et al. (2023), who observed comparable chemical characteristics, with silica content of 57.90 wt% and alumina as one of the main oxides (19 wt%). These findings indicate that CW generally exhibits an aluminosilicate-rich composition, which supports its potential use as a sustainable precursor or supplementary material in cementitious and geopolymer binders.

Overall, previous studies show that GGBS is mainly in CaO and SiO_2, while CW contains high amounts of SiO_2 and Al_2O_3. This indicates that GGBS can contribute to calcium- gel formation and early strength development, whereas CW can provide aluminosilicate components for geopolymerisation. Therefore, the combination of GGBS and CW is suitable for developing one-part geopolymer binders, as both materials provide the main oxides required for gel formation and matrix development. Table 2.12 summarises the chemical composition of GGBS and CW, providing a useful basis for discussing precursor suitability and expected geopolymerisation behaviour.

Table 2.12
Chemical Composition of GGBS and CW Aluminosilicate Precursors

Reference	Aluminosilicate precursors	Chemical composition of aluminosilicate precursors (%)							
		SiO_2	Al_2O_3	Fe_2O_3	TiO_2	CaO	MgO	Na_2O	Loss on ignition
(Phummiphan et al., 2018)	GGBS	26.78	6.96	18.65	0.85	30.38	9.70	-	-
(Azevedo et al., 2020)	CW	57.20	32.20	3.50	1.00	-	-	0.78	-
(Migunthanna et al., 2021)	GGBS	27.54	2.84	0.78	1.05	61.13	-	-	-
(Faldessai et al., 2023)	CW	57.90	19.00	2.80	-	9.60	3.40	-	-

Note: SiO_2 -Silica Dioxide, Al_2O_3 - Alumina oxide, Fe_2O_3 - Iron oxide, TiO_2 – Titanium dioxide, CaO - Calcium oxide, MgO - Magnesium oxide, Na_2O - Sodium oxide.

2.8.2 Phase Properties

Phase properties are important for understanding reaction products and mineralogical changes during geopolymerisation. X-ray diffraction (XRD) is commonly used to identify crystalline phases, amorphous phases, unreacted particles, and binding gels such as calcium silicate hydrate (C–S–H), calcium aluminosilicate hydrate (C–A–S–H), sodium aluminosilicate hydrate (N–A–S–H), and hybrid calcium–sodium aluminosilicate hydrate (C–N–A–S–H), which are the primary reaction products responsible for strength development and microstructural densification in geopolymer systems. Although phase development has been widely studied in two-part geopolymer systems, studies on one-part geopolymer repair binders remain limited. Therefore, this section reviews the phase properties of GGBS, fly ash, and ceramic waste geopolymer materials to explain their reaction behaviour and suitability for one-part geopolymer repair applications.

Bernal et al. (2013) reported that XRD results for alkali-activated GGBS pastes at 8 and 14 days, and the interior region after long-term exposure show that a small amount of akermanite and gehlenite remains, indicating incompletely reacted slag particles, as shown in Figure 2.5. The main reaction product is a poorly crystalline calcium silicate hydrate (C–S–H). Hydrotalcite is also detected as a secondary reaction product, consistent with common observations in alkali-activated slag. With curing, zeolitic phases can develop, where a gismondine type product is identified after 14 days and thomsonite is observed in aged pastes. In long-term cured samples, a small amount of katoite (siliceous hydrogarnet) is reported, suggesting that high silicate availability can favour katoite formation. Some calcium aluminate phases may be present, but they are not always distinguishable by XRD because they can be intimately intermixed with the C–S–H structure.

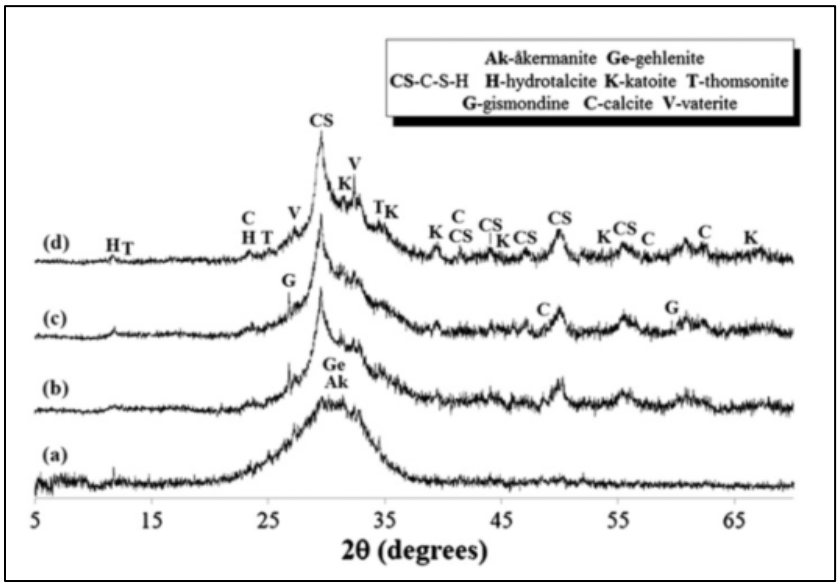


Figure 2.5 XRD Patterns of Alkali-Activated GGBS Pastes at Different Curing Ages, Showing the Evolution of Crystalline Phases and Reaction Products (Bernal et al., 2013)

According to Zhang M. et al. (2024), the XRD patterns of GGBS/FA geopolymers show broadly similar overall trends across different FA-to-GGBS ratios, with the main differences occurring in peak intensities rather than completely new phase as shown in Figure 2.6. Peaks at approximately 14° and 28° (2θ) were assigned to $MgSO_3 \cdot H_2O$, indicating Mg and S from slag that crystallise stably and remain largely unreactive, while characteristic reflections of calcite, nesquehonite and albite were also detected. Although Ca from GGBS contributes to gel formation, a fraction persists as calcite, with its peak activity increasing at higher GGBS content. In ternary mixes containing metakaolin, a clearer broad hump at 20 to 30° (2θ) and a slight peak near 56° indicate enhanced formation of amorphous gel phases, such as calcium-(alumino)-silicate-hydrate, C-(A)-S-H and sodium-alumino-silicate-hydrate, N-A-S-H gels.

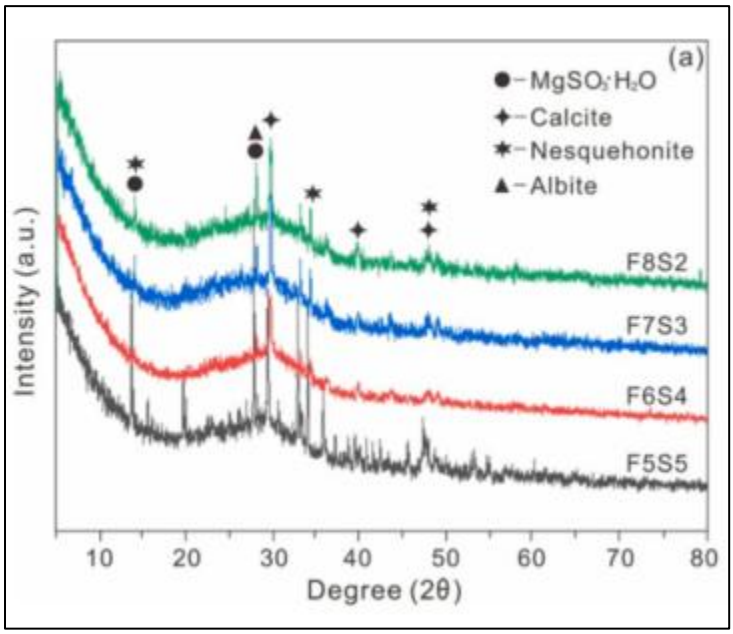


Figure 2.6 XRD Patterns of FA/GGBS Geopolymers with Different FA-to-GGBS Ratios (Zhang M. et al., 2024)

Li J. et al. (2024) reported that, based on the XRD spectra in Figure 2.7, the geopolymerisation progress is mainly indicated by the broad amorphous hump. For low-calcium circulating fluidised bed fly ash (LCFA), the hump shifts from 15°–30° (2θ) to 20°–40° (2θ) by 1 day, reflecting dissolution of Al and Si species and gel formation N-C-A-S-H gel (sodium–calcium–aluminosilicate hydrate), with calcium sulfate ($CaSO_4$) forming sodium sulfate (Na_2SO_4) and hydroxysodalite. For high-calcium circulating fluidised bed fly ash (HCFA), the hump shifts to 20°–37° (2θ), but with a smaller area, indicating lower geopolymerisation and less gel formation. Characteristic peaks of C–S–H and $CaSO_4 \cdot 2H_2O$ are observed, with the latter disappearing by 90 days, suggesting transformation into C–S–H or C-A-S-H. Calcite remains stable, and later increases in crystalline phases suggest a shift towards crystallisation, reducing gel cross-linking and matrix densification.

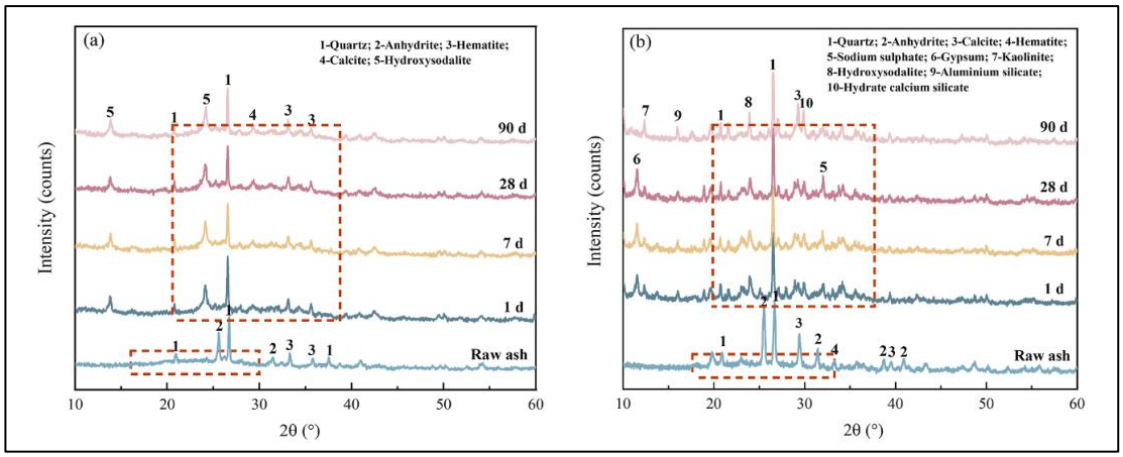


Figure 2.7 XRD Spectra of (a) LCFA-Based Geopolymer, (b) HCFA-Based Geopolymer Prepared at NaOH Concentration of 8 mol/L at Different Curing Ages (Li J. et al., 2024)

Overall, previous studies show that the phase development of geopolymer binders depends strongly on precursor composition, calcium content, activator condition, and curing age. GGBS binder commonly forms calcium reaction products such as C–S–H or C–A–S–H, while FA binder promotes aluminosilicate gel formation such as N–A–S–H or C–N–A–S–H. The presence of broad amorphous humps in XRD patterns indicates gel formation, whereas remaining crystalline peaks show unreacted or partially reacted precursor phases. These findings suggest that the combination of calcium and aluminosilicate materials can support gel formation and matrix development, which are important for strength and durability in one-part geopolymer repair materials.

2.8.3 Microstructure Properties

Microstructural properties are important for understanding the internal structure and reaction development of geopolymer binders. Scanning electron microscopy (SEM), backscattered electron (BSE) imaging, and energy-dispersive X-ray spectroscopy (EDS) are commonly used to observe pore structure, gel formation, unreacted particles, microcracks, and elemental distribution. These analyses help explain the relationship between precursor composition, reaction products, matrix densification, and strength development. Therefore, this section reviews the microstructural characteristics of FA, GGBS, and CW geopolymer materials to support the development of one-part geopolymer repair binders.

Lee et al. (2014) examined alkali-activated fly ash slag binders using scanning electron microscopy (SEM), backscattered electron (BSE) imaging, and energy-dispersive X-ray spectroscopy (EDS) to relate reaction products to the hardened microstructure. Increasing slag replacement produced a denser matrix with fewer visible pores, which corresponded with improved strength. However, microcracks were also observed at higher slag content and were associated with shrinkage of the reaction products. The hardened binder was mainly characterised by hybrid calcium–sodium–aluminosilicate hydrate (C–N–A–S–H) gel, with unreacted or partially reacted fly ash and slag particles embedded within the gel matrix. The energy-dispersive X-ray spectroscopy (EDS) results further showed that the calcium-to-silicon (Ca/Si) ratio increased with slag addition, from 0.26 for S10 to 0.46 for S20. In this context, S10 and S20 refer to mixtures containing 10% and 20% slag replacement, respectively. This increase confirms greater calcium participation in gel formation and matrix densification.

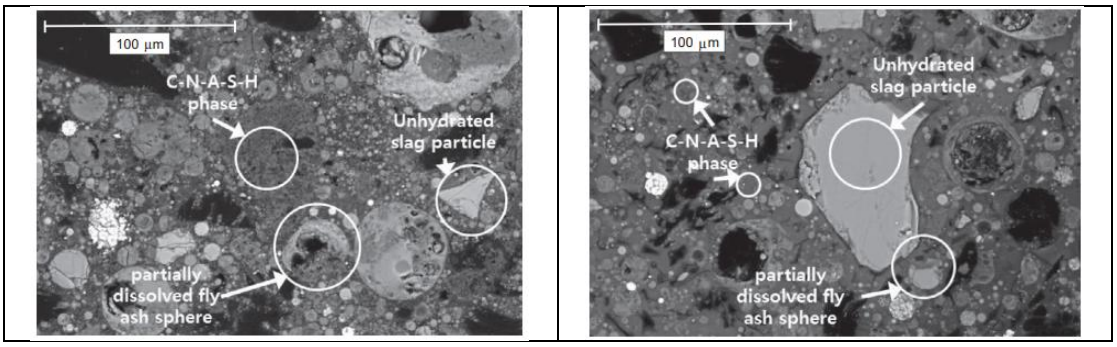


Figure 2.8 Backscattered Electron (BSE) Images of S10 and S20 Samples at 28 Days (Lee et al., 2014)

Li J. et al. (2024), SEM images in Figure 2.9 provide insight into the microstructural evolution of LCFA-based geopolymers at different curing times. In the LCFA-based geopolymer gel formation is first visible at 1 day, with the presence of pores and some early-stage gel development. At 7 days and 28 days, the gel becomes more prominent, and by 90 days, a dense C–S–H gel network is observed, confirming significant geopolymerisation and gel formation, as indicated by the N-A-S-H type structure (arrow in the 90-day image). The EDS spectra support this observation, with dominant peaks of Si, Na, and Al, confirming the formation of a sodium-alumino-silicate network.

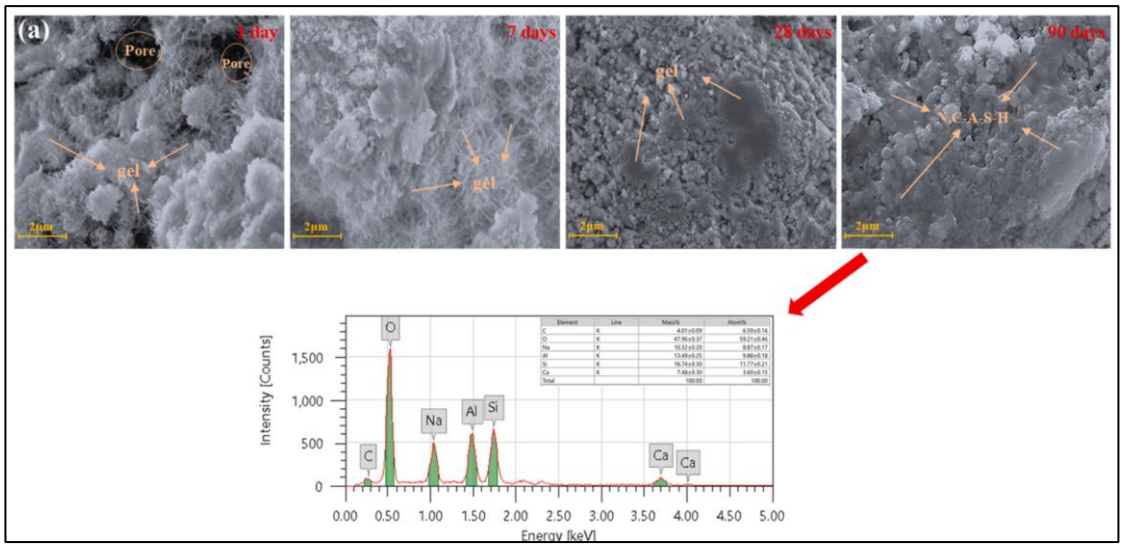


Figure 2.9 SEM Images of LCFA-Based Geopolymer Gel Curing at 90 days (Li J. et al., 2024)

Overall, previous studies show that geopolymer microstructure is strongly influenced by precursor type, slag content, curing age, and gel formation. Higher slag content generally promotes matrix densification through calcium-rich gel formation, while fly ash contributes to aluminosilicate gel development. SEM and BSE observations commonly show that a denser matrix with fewer pores is associated with improved strength, whereas microcracks, unreacted particles, and weak gel continuity may reduce performance. These findings indicate that microstructural development is important in controlling the mechanical and durability properties of one-part geopolymer repair materials. Therefore, the following section summarises the key findings from the literature and identifies the research gaps related to one-part rubberised geopolymer-based semi-rigid repair materials for pavement applications.

2.9 Summary and Gap of Research

This chapter reviewed studies on one-part geopolymer systems, precursors, crumb rubber (CR) treatment, rubberised semi-rigid pavement materials, reaction mechanisms, mechanical properties, bonding behaviour, rutting resistance, and microstructural development. The literature shows that geopolymer materials are sustainable alternatives to conventional cementitious materials, while one-part geopolymer systems are more practical for field application because they require only the addition of water during mixing.

Previous studies showed that precursor composition, activator content, curing condition, and gel formation influence the fresh, mechanical, durability, and microstructural properties of geopolymer materials. GGBS contributes to early strength development, while fly ash (FA) and ceramic waste (CW) provide aluminosilicate phases for geopolymerisation. However, most studies focused on two-part geopolymer systems, and studies on one-part geopolymer repair materials remain limited. CR can improve flexibility, energy absorption, abrasion resistance, and deformation resistance. However, high CR content may reduce strength and increase porosity, permeability, and water absorption due to weak rubber bonding. Previous studies showed that NaOH treatment is a practical and effective method for improving CR surface properties because it can increase surface roughness, remove impurities, and enhance rubber bonding. Other treatments such as $KMnO_4$, H_2SO_4, cement slurry coating, and micro-silica coating have also been investigated, but NaOH remains commonly used due to its availability, and cost-effectiveness.

The review also shows that surface roughness and bond strength are important for pavement repair performance, while rutting resistance is needed to resist permanent deformation under traffic loading. However, limited studies have investigated surface roughness, bond strength, and rutting resistance in one-part rubberised geopolymer repair materials. Therefore, the main research gap is the studies on one-part rubberised geopolymer-based semi-rigid repair materials incorporating treated CR for pavement repair applications. This study addresses the gap by evaluating fresh properties, mechanical strength, water absorption, abrasion resistance, surface roughness, bond strength, rutting resistance, and microstructural characteristics. Table 2.13 summarises previous studies on one-part and two-part geopolymer the research gap.

Table 2.13
Summary of Previous Studies and Research Gap

No	Author	Geopolymer Concrete	Rubberised Geopolymer Concrete	Geopolymer Method		Testing			Pavement / Repair Application
				One-Part	Two-Parts	Surface Roughness	Bonding Strength	Rutting Resistance (HMA)	
1	(Haritonovs et al., 2012)	-	-	-	-	-	-	✓	✓ (asphalt pavement)
2	(Tayeh et al., 2012)	-	-	-	✓	✓	✓	-	✓ (overlay repair on concrete)
3	(Bernal et al., 2013)	✓	-	-	✓	-	-	-	-
4	(Lee et al., 2014)	✓	-	-	✓	-	-	-	-
5	(Azmi et al., 2016)	-	✓	-	✓	-	-	-	-
6	(Thomas et al., 2016)	-	✓	-	✓	-	-	-	-
7	(Bisht & Ramana, 2017)	-	✓	-	✓	-	-	-	-
8	(Laskar & Talukdar, 2017)	✓	-	-	✓	-	-	-	-
9	(Phummiphan et al., 2018)	✓	-	-	✓	-	-	-	Pavement base material
10	(Wongsa et al., 2018)	✓	-	-	✓	-	-	-	-
11	(Tahir et al., 2019)	✓	-	-	✓	-	-	-	-
12	(Lv et al., 2020)	-	-	-	-	-	-	✓	✓ (asphalt rutting)
13	(Thao et al., 2020)	✓	-	-	✓	-	-	-	✓ (semi-rigid pavement)
14	(Azevedo et al., 2020)	✓	-	-	✓	-	-	-	-
15	(Abed Al-Jabar et al., 2021)	✓	-	-	✓	✓	✓	-	✓ (repair interface)
16	(Asayesh et al., 2021)	✓	-	-	✓	-	-	-	✓ (repair pavement)

Table 2.13
Summary of Previous Studies and Research Gap (Cont'd)

No	Author	Geopolymer Concrete	Rubberised Geopolymer Concrete	Geopolymer Method		Testing			Pavement / Repair Application
				One-Part	Two-Parts	Surface Roughness	Bonding Strength	Rutting Resistance (HMA)	
17	(Wang et al., 2021)	✓	-	-	✓	✓	✓	-	✓ (repair bonding)
18	(Daneshvar et al., 2021)	✓	-	-	✓	✓	✓	-	✓ (repair bonding)
19	(Feng L.-Y. et al., 2021)	✓	-	-	✓	-	-	-	-
20	(Girish et al., 2022)	✓	-	-	✓	-	-	-	✓ (rigid pavement)
21	(Hamid Abed et al., 2022)	✓	-	-	✓	-	-	-	-
22	(Migunthanna et al., 2021)	✓	-	✓	-	-	-	-	✓ (rigid pavement)
23	(Liu et al., 2022)	✓	-	-	✓	-	-	-	-
24	(Patel et al., 2022)	✓	-	-	✓	-	-	-	✓ (rigid pavement)
25	(Faldessai et al., 2023)	-	✓	-	✓	-	-	-	-
26	(Orhan et al., 2023)	-	✓	-	✓	-	-	-	-
27	(Osman & Irshidat, 2023)	✓	-	-	✓	-	-	-	-
28	(Prasad et al., 2023)	✓	-	-	✓	-	-	-	-
29	(Zakeremamreza et al., 2023)	-	✓	-	✓	-	-	-	-
32	(Zhao J. et al., 2023)	-	✓	✓	✓	-	-	-	-
33	(Felekoğlu, 2024)	-	-	-	-	✓	✓	-	✓ (repair bonding)
34	(Raut et al., 2024)	-	✓	-	✓	-	-	-	-

Table 2.13
Summary of Previous Studies and Research Gap (Cont'd)

No	Author	Geopolymer Concrete	Rubberised Geopolymer Concrete	Geopolymer Method		Testing			Pavement / Repair Application
				One-Part	Two-Parts	Surface Roughness	Bonding Strength	Rutting Resistance (HMA)	
35	(Li J. et al., 2024)	✓	-	-	✓	-	-	-	-
36	(Xiang et al., 2024)	-	-	-	-	-	-	✓	✓ (rubberised asphalt)
37	(Zhang M. et al., 2024).	✓	-	-	✓	-	-	-	-
38	This study	-	✓	✓	-	✓	✓	✓	✓ (one-part semi-rigid repair)

CHAPTER 3
RESEARCH METHODOLOGY

3.1 Introduction

This chapter describes the research methodology used to develop and evaluate a one-part semi-rigid geopolymer repair material for surface road repair applications. The material was formulated using GGBS-FA and GGBS-WCT-based one-part geopolymer binders, with treated crumb rubber (CR) used as a partial fine aggregate replacement to improve flexibility and deformation resistance. The methodology was divided into five (5) experimental phases. Phase 1 involved raw material characterisation, while Phase 2 focused on the development and optimisation of the one-part geopolymer repair binders. Phase 3 examined the selected binder using X-ray fluorescence (XRF), X-ray diffraction (XRD), scanning electron microscopy (SEM), and scanning electron microscopy coupled with energy-dispersive X-ray spectroscopy (SEM–EDX) to evaluate its chemical, phase, and microstructural properties. Phase 4 involved the development and testing of the one-part semi-rigid geopolymer repair material incorporating fine aggregate and treated CR. Phase 5 evaluated the bonding and pavement repair performance of the selected material when applied to OPC concrete and Hot Mix Asphalt (HMA) substrates. Overall, this chapter presents the materials, mix proportioning, specimen preparation, substrate preparation, testing procedures, and data analysis methods adopted in this study.

3.2 Research Framework

This study was structured into five (5) phases to provide workflow for developing and evaluating the one-part semi-rigid geopolymer repair material. The research framework begins with raw material characterisation, followed by the development and optimisation of one-part geopolymer repair binders. The GGBS-WCT was then further characterised to examine its chemical, phase, and microstructural properties. Next, the GGBS-WCT binder was used to develop the one-part semi-rigid geopolymer repair material by incorporating treated crumb rubber (CR) as a partial fine

aggregate replacement. The final phase evaluated the compatibility, bonding performance, and pavement repair performance of the developed repair material when applied to road surface substrates. The overall research framework for all five (5) phases is shown in Figure 3.1.

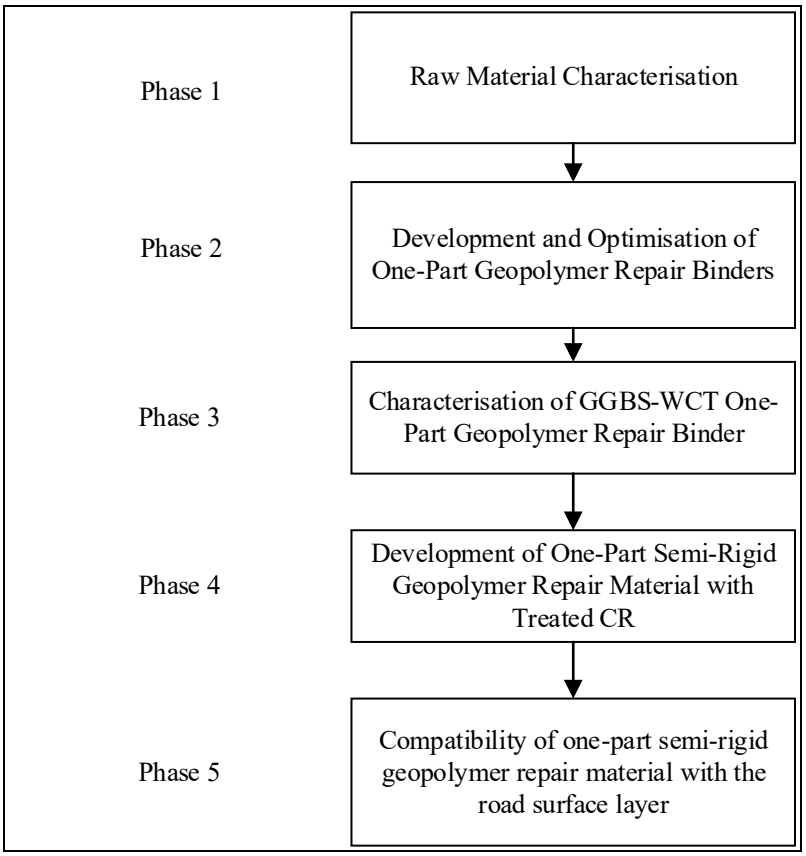


Figure 3.1 Overall Research Framework of the Experimental Programme

In Phase 1 of the study, the raw materials used to produce one-part geopolymer repair binders were characterised to establish their suitability for semi-rigid repair applications. Figure 3.2 presents the experimental workflow for the material preparation and characterisation stage. The precursors considered in this investigation were ground granulated blast-furnace slag (GGBS), Class F fly ash (FA), and waste clay tiles (WCT), which were obtained from industrial by-product sources and prepared prior to testing. X-ray fluorescence (XRF) analysis was conducted to determine the chemical composition of the precursors, while X-ray diffraction (XRD) was used to identify the crystalline phases present. In addition, scanning electron microscopy (SEM) was performed to examine the morphology and microstructural characteristics of the precursor particles. Overall, this characterisation phase was undertaken to confirm the

suitability of each precursor material for use in the development of semi-rigid geopolymer repair materials.

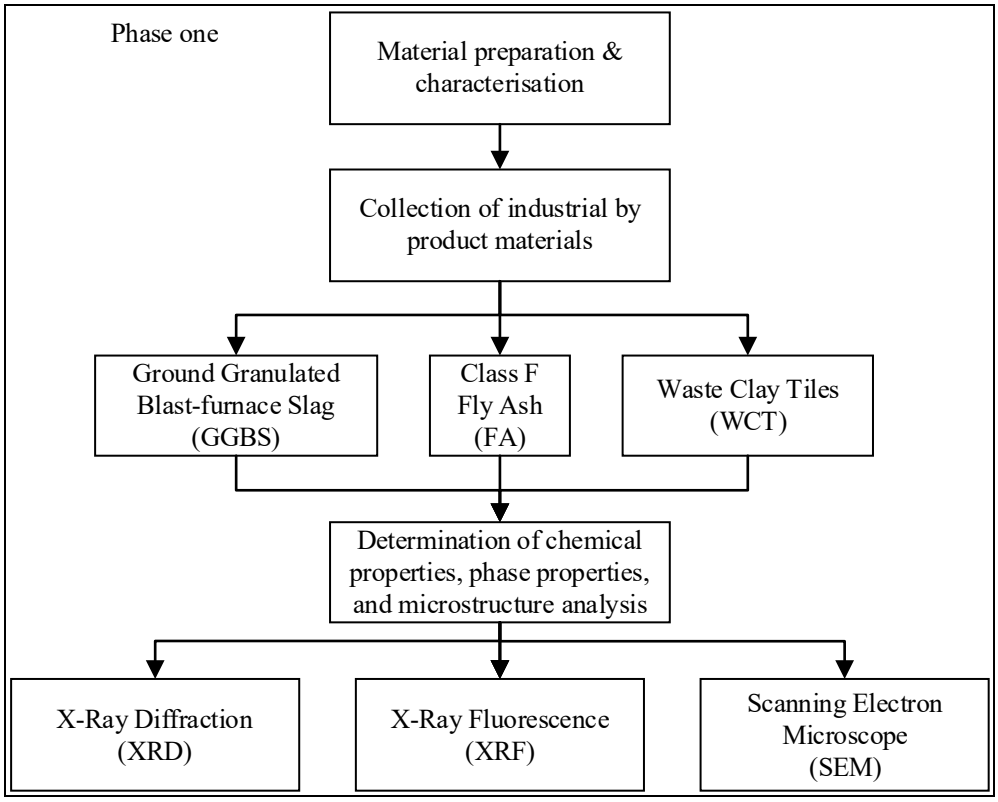


Figure 3.2 Characterisation Raw Material of One-Part Geopolymer Repair Binders (Precursor) (Phase 1)

Figure 3.3 summarises the experimental workflow for Phase 2, which focused on identifying the optimum formulation of the one-part geopolymer repair binder. In this phase, GGBS was used as the primary precursor and was blended with FA and WCT at replacement levels of 10%, 20%, 30%, 40%, and 50% to develop hybrid precursor. The solid activator used was anhydrous sodium metasilicate, and the binder was prepared using the one-part geopolymer method, where all precursor and activator components are dry-mixed and activated by the addition of water only. The one-part geopolymer repair binders were prepared at two solid precursor-to-solid activator ratios of 90:10 and 80:20. The fresh properties of the one-part geopolymer repair binders were then evaluated in terms of workability and setting time. Following casting, specimens were cured under ambient conditions (25 °C ± 2 °C) and tested at curing ages of 3, 14, and 28 days. Mechanical performance was assessed using compressive strength to determine the optimum replacement level and mix proportion.

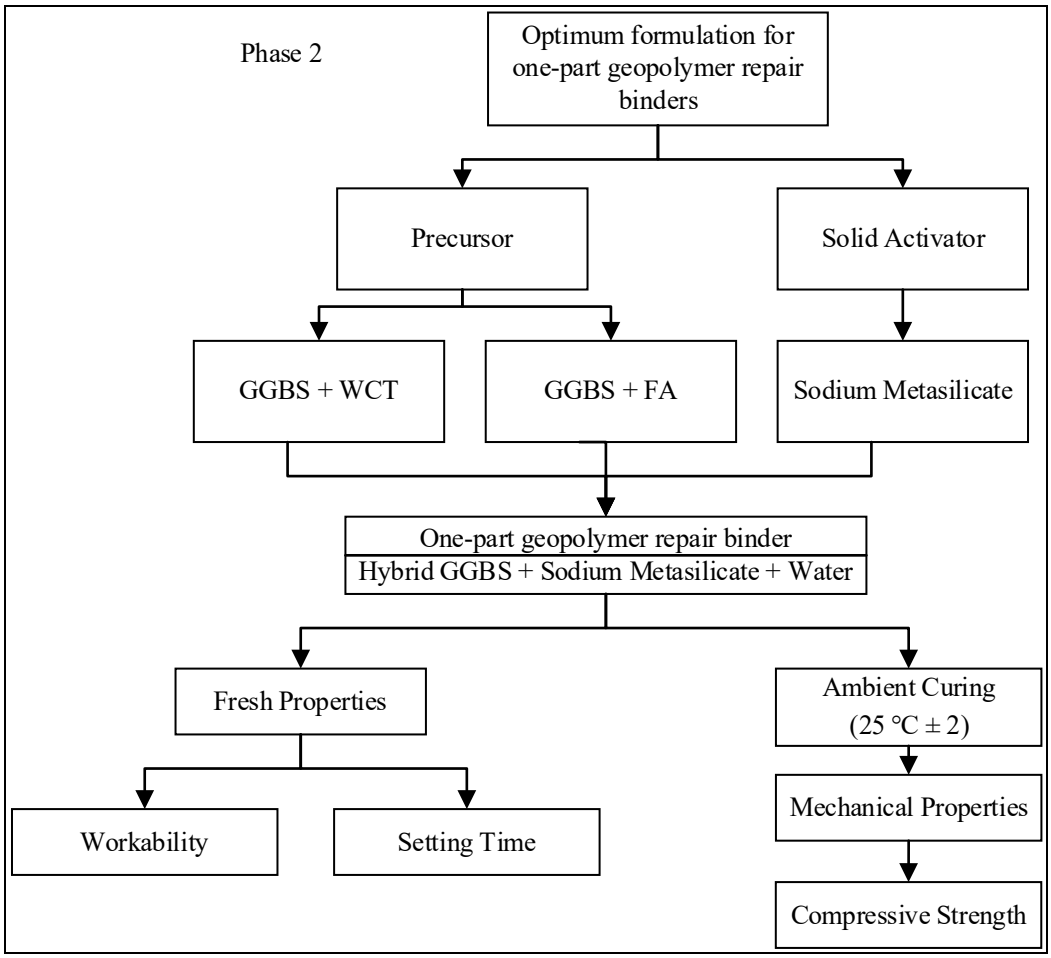


Figure 3.3 One-Part Geopolymer Repair Binder on Workability, Setting Time and Compressive Strength (Phase 2)

Figure 3.4 outlines Phase 3, which focused on characterising the geopolymerisation reaction of the GGBS–WCT based hybrid one-part geopolymer repair binder. Specimens produced using the optimum mixture from Phase 2 were subjected to chemical composition, phase, and microstructural analyses. XRF was conducted to determine the chemical composition. XRD was used to identify crystalline phases and assess the reaction products formed within the one-part geopolymer repair binders and evaluate the chemical characteristics of the binder. In addition, energy-dispersive X-ray spectroscopy (EDX) coupled with SEM was used to determine the elemental composition and elemental distribution of selected regions, supporting interpretation of geopolymer gel formation and unreacted particles. Collectively, these analyses fulfilled the Phase 3 objectives by establishing the chemical composition, phase analysis, and microstructural characteristics of the optimised binder.

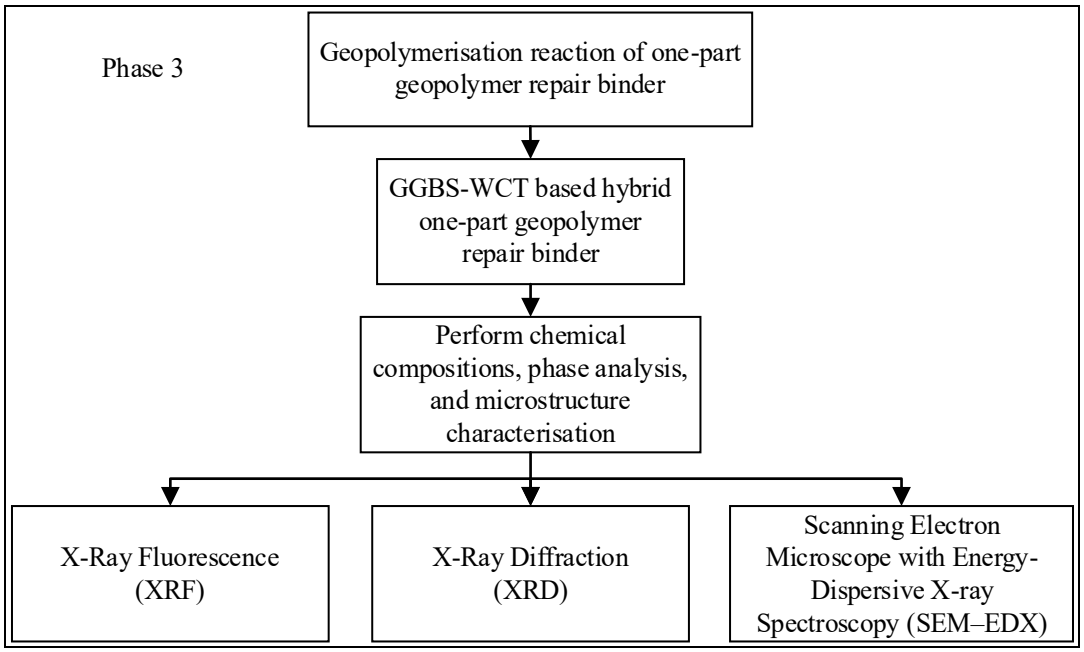


Figure 3.4 Geopolymerisation Reaction of One-Part Geopolymer Repair Binder (Phase 3)

Figure 3.5 summarises the experimental workflow for Phase 4, which aimed to determine the optimum crumb rubber (CR) content as partial sand replacement in the one-part semi-rigid geopolymer repair material. The binder used in this phase was based on the optimum formulation obtained from Phase 2, consisting of a hybrid GGBS–WCT precursor with 30% WCT and a fixed solid precursor-to-solid activator ratio of 90:10. Anhydrous sodium metasilicate was used as the solid activator, and the one-part method was prepared by dry blending the solid components prior to activation with water. For the one-part semi-rigid geopolymer repair material, aggregates (chipping and sand) were incorporated, and CR treated by immersion in 5% sodium hydroxide (NaOH) was introduced as a flexible component by partially replacing the sand at 5%, 10%, 15%, and 20% (by volume). The specimens were cured under ambient conditions (25 °C ± 2 °C) and tested at curing ages of 3 and 28 days. Durability performance was evaluated through water absorption and abrasion resistance, while mechanical performance was assessed using compressive strength. These tests were conducted to identify the optimum CR replacement level that provides good durability and mechanical properties for the one-part semi-rigid geopolymer repair material.

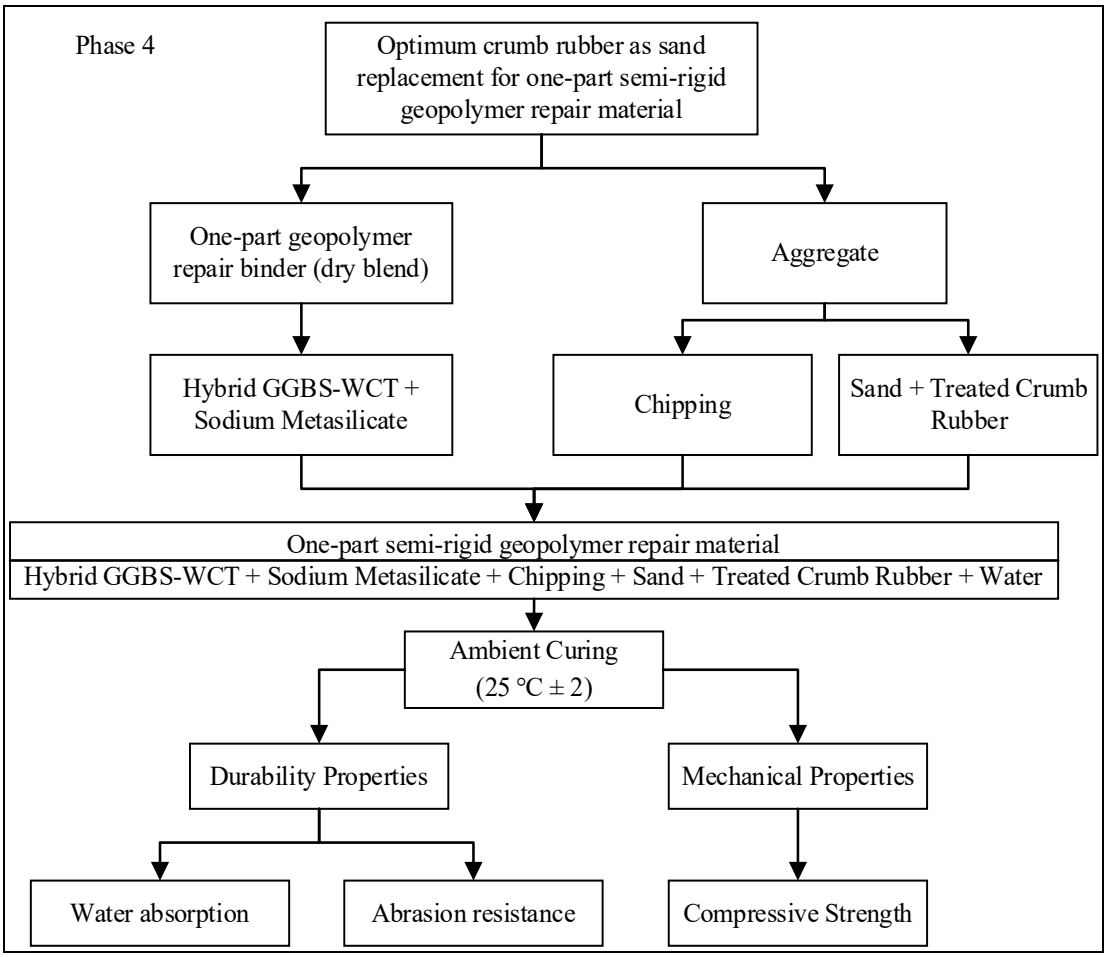


Figure 3.5 One-Part Semi-Rigid Geopolymer Repair Materials Based on Durability and Mechanical Properties (Phase 4)

The development and performance evaluation of the one-part semi-rigid geopolymer repair material is summarised in Figure 3.6 (Phase 5). Based on the results obtained in Phase 4, the hybrid GGBS–WCT formulation incorporating the optimum CR content (15%) was selected due to its optimum durability and mechanical performance. In this final phase, the one-part semi-rigid geopolymer repair material was applied as an overlay repair material on concrete and hot mix asphalt (HMA) substrates prepared under three surface conditions: as-cast (AC), drilled holes (DH), and wire brushing (WB). Interfacial bonding behaviour between the overlay and substrates was evaluated using the bi-surface shear test, performed on composite specimens representing each surface condition. In addition, the rutting performance of the surface layer was assessed using wheel-tracking tests conducted before and after overlay application to determine the suitability and durability of the repair system for surface road repair applications.

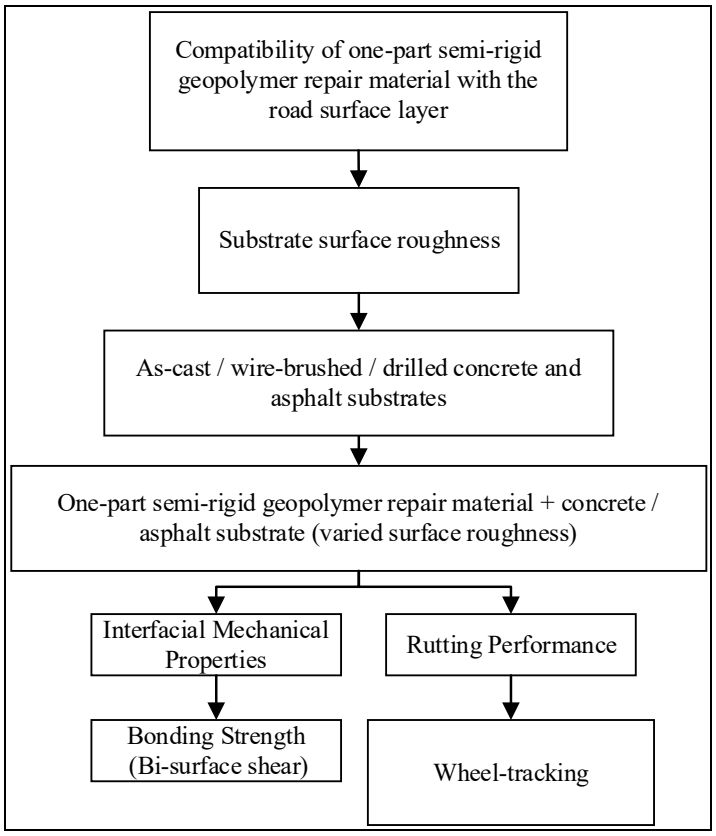


Figure 3.6 Development and Performance Evaluation of the One-Part Semi-Rigid Geopolymer Repair Material Based on Interfacial Bonding Strength and Rutting Performance (Phase 5)

The overall type of testing, standard method and number of specimens involved in this study are summarised in Table 3.1. The following sections describe the experimental activities conducted in each phase of the study, beginning with the collection, preparation, and characterisation of raw materials.

Table 3.1
Summary of Testing Approach, Standardised Methodology, and Number of Specimens

Phase 1: Characterisation raw material		
Type of testing	Standard Method	No. of specimen(s)
XRF	*PR	3
XRD	*PR	3
SEM	*PR	3
Phase 2: Optimum formulation for one-part geopolymer repair binders		
Type of testing	Standard Method	No. of specimen(s)
Workability	ASTM C1437	66
Setting Time	ASTM C191	66
Compressive Strength	ASTM C109	66

Table 3.1
Summary of Testing Approach, Standardised Methodology, and Number of Specimens (Cont'd)

Phase 3: Geopolymerisation reaction of one-part geopolymer repair binder		
Type of testing	Standard Method	No. of specimen(s)
XRF	*PR	6
XRD	*PR	6
SEM	*PR	6
Phase 4: Optimum CR as sand replacement for one-part semi-rigid geopolymer repair material		
Type of testing	Standard Method	No. of specimen(s)
Water Absorption	ASTM C642	30
Abrasion resistance	BS 812-113:1990	30
Compressive Strength	ASTM D6023	30
Phase 5: Compatibility of one-part semi-rigid geopolymer repair material with the road surface layer		
Type of testing	Standard Method	No. of specimen(s)
Surface Roughness	ISO 25178	6
Bonding Strength	ASTM C882	18
Wheel-Tracking	BS 598-110	4

Note: *PR is referred to previous research of standard method

3.3 Material Preparation & Characterisation

In this study, the primary raw materials used as aluminosilicate for the one-part geopolymer repair binders were GGBS, as well as FA and WCT. These industrial by-products were collected and prepared for further characterisation. The binder was formed using a dry binder formulation consisting of GGBS, FA, WCT, and anhydrous sodium metasilicate (Na_2SiO_3) as the solid alkaline activator. This dry mix formulation represents the one-part geopolymer method, where the geopolymerisation reaction is initiated started by the addition of water during mixing. Sand and coarse aggregate were used as aggregate materials, while crumb rubber (CR) was used as a partial sand replacement to improve the flexibility of the repair material. Asphalt binder was used to prepare asphalt specimens for compatibility and bonding evaluation. Table 3.2 provides a complete inventory of this study main compounds and materials, including information on their respective suppliers and origins. The following sub-sections elaborate each constituent used for making geopolymer specimens.

Table 3.2
Summary of Overall Materials Used

Materials	Role	Supplier
Ground Granulated Blast Furnace Slag	Aluminosilicate Source	Desjaya Concrete Products Sdn Bhd
Fly Ash	Aluminosilicate Source	Universiti Tenaga Nasional (UNITEN)
Waste Clay Tiles	Aluminosilicate Source	Linbaq Construction Company
Sodium Metasilicate	Solid Activator	Thermo Scientific
Aggregate	Coarse Aggregate / Wearing Course	Kajang Rock Quarry
Sand	Fine Aggregate	Universiti Teknologi MARA (UiTM) Shah Alam
Crumb Rubber	Flexible Agent / Fine Aggregate Replacement	Jingyun Rubber
Asphalt Binder	Bituminous Binder	Universiti Malaya

3.3.1 Ground Granulated Blast Furnace Slag (GGBS)

Ground granulated blast furnace slag (GGBS) was used as one of the aluminosilicate precursor materials in this study. The GGBS was supplied by Desjaya Concrete Products Sdn. Bhd., Kuantan, Pahang, Malaysia. GGBS is a supplementary material obtained from the residual waste generated during the production process of blast furnaces in the metallurgical sector. The residual substance produced when converting iron ore into iron is commonly referred to as slag. This material possesses a unique property of buoyancy, allowing it to float on top of the iron layer. GGBS was employed as an aluminosilicate source. The utilisation of GGBS in cement manufacturing has resulted in a surface with enhanced smoothness and reduced defects, mainly attributed to the fine particle size of GGBS. In this study, GGBS was employed as one of the aluminosilicate precursors in the formulation of the one-part geopolymer binder. Figure 3.7 shows the GGBS used in this present study.



Figure 3.7 Raw GGBS Used as an Aluminosilicate Precursor

3.3.2 Fly Ash (FA)

Fly ash (FA) was used as one of the aluminosilicate precursor materials in this study. The FA used was Class F fly ash, obtained from Universiti Tenaga Nasional (UNITEN), Kajang, Selangor, Malaysia. The material was selected due to its low-calcium aluminosilicate composition, which is suitable for geopolymer binder production. Prior to mixing, the FA was kept in a dry condition to prevent moisture absorption and material agglomeration. The FA was used in powder form as received and incorporated as part of the binder system in the geopolymer mortar mixture. Figure 3.8 displays the FA utilised in this present study.



Figure 3.8 Raw FA Used as an Aluminosilicate Precursor

3.3.3 Waste Clay Tiles (WCT)

Waste clay tiles (WCT) were used as one of the aluminosilicate precursor materials in this study. The WCT was collected from broken clay tiles at a nearby construction site owned by Linbaq Construction Company, Johor Bahru. The process of crushing broken waste clay tiles was conducted in the Civil Engineering laboratory at UiTM Shah Alam. These crushed tiles were then be utilised as a source of aluminosilicate because of its rich of its SiO_2 and Al_2O_3 which are necessary elements for the geopolymerisation reaction. Owing to its high crystalline material content, ceramic has been utilised as a way of improving geopolymer mechanical as filler and enduring characteristics. Figure 3.9 shows the WCT used in this study.



Figure 3.9 Raw WCT Used as an Aluminosilicate Precursor

Meanwhile, the local ceramic maker was the source of the WCT. To obtain the necessary material for this study, at the point of collection, uniform WCT only were gathered, i.e. of similar quality, thickness and without a glossy veneer were collected from the building site area. Subsequently, the collected material was undergoing a grinding process to reduce it to a smaller size. These were immediately machine-crushed and then sieved through a 600 μm filter to extract the larger particulate. An Los Angeles abrasion machine was then employed to attain the required particle dimensions in keeping with ASTM C618 (ASTM-C618, 2023), i.e. 66 % passing 45 μm; the sieved particles therefore underwent 6 hours of grinding. The acquired powder was then utilised in the mixing protocol. Figure 3.10 shows the preparation process of WCT powder for making geopolymer specimens.

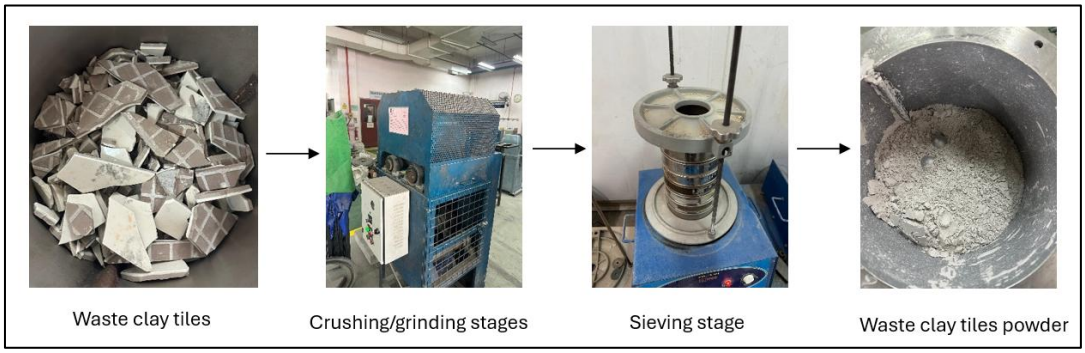


Figure 3.10 Preparation Process of WCT Powder

3.3.4 Sodium Metasilicate

The investigation utilised anhydrous sodium metasilicate as a solid activator in making geopolymer. The anhydrous form of sodium metasilicate was procured from Fisher Scientific in Malaysia. The substance referred to as sodium metasilicate,

anhydrous, is available in the form of granular powder. The study used anhydrous sodium metasilicate, as shown in Figure 3.11. The exact characteristics and properties of this substance are outlined in Table 3.3.



Figure 3.11 Sodium Metasilicate, Anhydrous Used as Solid Activator

Table 3.3
Specification of Sodium Metasilicate, Anhydrous

Properties	**Specification**
Melting Point	72.0℃
Colour	White
Physical Form	Granules (18-mesh)
Percent Purity	44 to 47.5% total solids
Molecular Weight	122.06 g/mol
Density	2.61 g/mol
Merck Index	15.8804
Sodium oxide (Na_2O)	49.1-51.7% (50.37%)
Silicon dioxide (SiO_2)	44.7-47.6% (46.67%)

3.3.5 Aggregate

This study used coarse aggregates obtained from Kajang Rock Quarry, with a nominal size of less than 10 mm, in accordance with BS EN 12620:2002 (BS-EN-12620, 2002). This aggregate size was selected to accommodate the repair layer and to ensure better material compactness, workability, and surface finishing of the geopolymer concrete. Smaller coarse aggregate also helps improve the uniformity of the repair material and reduces the risk of segregation during casting. Prior to mixing, the aggregates were soaked in water for 24 hours and then drained. The surface moisture was removed using a clean dry cloth until the aggregates reached a saturated surface-dry (SSD) condition. This procedure was carried out to ensure that the aggregates did

not absorb additional mixing water and affect the water-to-binder ratio. The aggregates used were crushed granite, known for their high strength and durability. Incorporating coarse aggregates into the mix enhanced the surface texture and frictional properties of the geopolymer binder, making it more suitable for supporting heavy traffic loads and resisting stress in pavement repair applications. Figure 3.12 presents the coarse aggregates used in this study, which had a particle size of less than 10 mm.



Figure 3.12 Coarse Aggregates with Particle Size Less than 10 mm

3.3.6 Sand

This Natural River sand was used as the fine aggregate in the geopolymer mixture. The sand was selected with particle sizes ranging from 0.30 mm to 4.75 mm, based on the sieve preparation carried out in the laboratory. Sand particles passing the 4.75 mm sieve and retained on the 0.30 mm sieve were used to obtain a more uniform grading for the mixture. Before mixing, the sand was dried to reduce excess moisture and to maintain better control of the water content in the geopolymer mixture. This preparation was carried out to minimise variation in the liquid-to-binder ratio during mixing. The prepared sand was then stored in a dry condition before being used in the geopolymer mixture. Figure 3.13 shows the natural river sand used as fine aggregate in this study.



Figure 3.13 Natural River Sand with Particle Sizes Ranging from 0.30 mm to 4.75 mm

3.3.7 Crumb Rubber (CR)

Crumb rubber (CR) was used as a partial fine aggregate replacement in this study in Phase 4 and 5. The CR was obtained from waste truck tyres and procured from a commercial tyre processing unit in Kuala Lumpur, Malaysia. From an economic perspective, the ambient grinding method was adopted to process the rubber into fine CR particles. Gill et al. (2023) reported that truck tyres are made of 42% natural rubber; therefore, processed rubber fines had a high natural rubber content and were free from metallic and other contaminants. Figure 3.14 shows that CR was used as flexible agent in this present study with particle sizes of 30 mesh. CR particles were used to partially replace fine natural aggregates. The tyre-derived rubber exhibited low water absorption and hydrophobicity, with a reported water contact angle of 95° to 122° (Assaggaf et al., 2021), making it suitable for use in moist curing environments. The purpose of using CR was to improve the flexibility and deformation resistance of the geopolymer repair material. It was also used to reduce shrinkage and improve crack resistance in pavement repair applications.



Figure 3.14 CR Used as Flexible Agent / Fine Aggregate Replacement

The treatment procedure of CR involved immersion in 5% NaOH solution, followed by washing and oven drying, as illustrated in Figure 3.15. The CR particles were treated prior to mixing. The CR particles were immersed in NaOH solution. NaOH solution (5%) was prepared in a glass beaker using distilled water and laboratory-grade NaOH flakes. The solution was then stirred using a magnetic stirrer at 600 rpm and at 60 ◦C for 24 hours. Subsequently, 400 g of CR was added gradually to the solution while covering the beaker with a glass dish. After the stirring process was completed, the CR was washed with tap water three times over a # 100 sieve and dried in an oven at 50 ◦C for 24 hours (h). The treated CR particles were used as a partial replacement for fine aggregate in the geopolymer mixture.

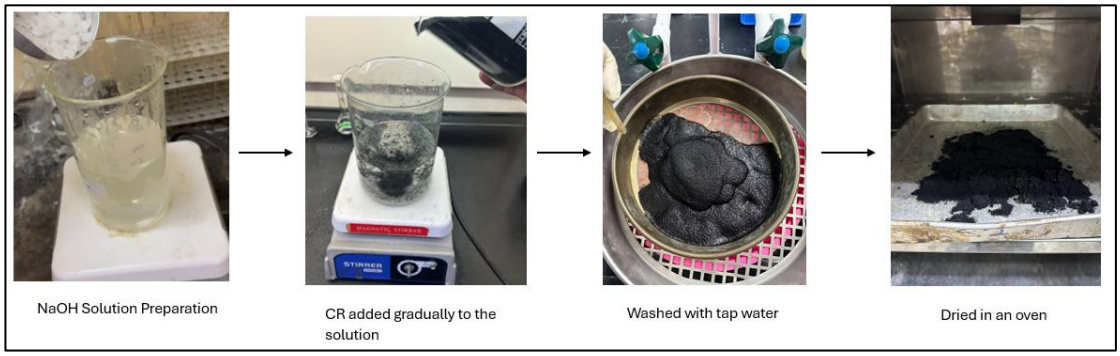


Figure 3.15 Treatment Process of CR with NaOH Solution

3.3.8 Asphalt Binder for Hot Mix Asphalt (HMA) Pavement Substrate

Asphalt binder was used in this study to prepare the Asphaltic Concrete Wearing Course 14 (ACW14) Hot Mix Asphalt (HMA) pavement substrate for the repair performance evaluation. The HMA substrate was prepared to represent the existing flexible pavement surface before the one-part semi-rigid geopolymer repair material was applied. The binder used was bitumen PEN 60/70, obtained from the Highway Engineering Laboratory, Universiti Malaya. The binder complied with the American Association of State Highway and Transportation Officials (AASHTO) Standard M320-02 (AASHTO-M-320, 2002). This bitumen grade was also selected based on the JKR Standard Specification for Road Works Section 4: Flexible Pavement (2007) (Jabatan Kerja Raya, 2007), where PEN 60/70 is commonly used wearing course mixtures. In this study, the asphalt binder was mixed with the prepared aggregate gradation to produce the ACW14 HMA specimen. The prepared ACW14 HMA

substrate was used in Phase 5 of this study for pavement repair performance evaluation, including wheel tracking and skid resistance tests.

3.3.9 Aggregate for Hot Mix Asphalt (HMA) Pavement Substrate

Aggregates are critical components in pavement construction, contributing significantly to the asphalt pavement strength, stability, and durability. Granular substances like crushed stone, gravel, sand, or recycled materials are referred to as aggregates in the context of asphalt mixtures because they combine with bitumen to form the pavement foundation. According to JKR Standard Specification for Road Works Section 4: Flexible Pavement (2007) (Jabatan Kerja Raya, 2007), coarse and fine aggregates combined with mineral filler are the required components for asphalt pavement. The particle size distribution of the aggregate used for the ACW14 specimen is shown in Figure 3.16. The experimental work and test are concentrated on the wearing course layer of asphalt pavement, with a mix design of Asphaltic Concrete Wearing Course with 14 mm nominal maximum aggregate size (ACW14) (Jabatan Kerja Raya, 1998), where the maximum aggregate size is 14mm. OPC was used 2% by mass as filler in the aggregate gradation. The aggregate gradation limit for wearing course ACW is tabulated in the Table 3.4.

Table 3.4
Aggregate Proportion for ACW14 Specimen

B.S Sieve	Passing			Design	Retain (%)	Weight (g)
	Min	Max	Mid-point			
20	100	100	100	100	0	0
14	80	95	87.5	87.5	12.5	140.6
10	68	90	79	79	8.5	95.6
5	52	72	62	62	17	191.3
3.35	45	65	53.5	53.5	8.5	95.6
1.18	30	45	37.5	37.5	16	180
0.425	17	30	23.5	23.5	14	157.5
0.15	7	16	11.5	11.5	12	135
0.075	4	10	7	7	4.5	50.6
Pan	0	0	0	0	7%=Pan (5%)	56.3
					+ Filler (2%)	22.5
					100	1125

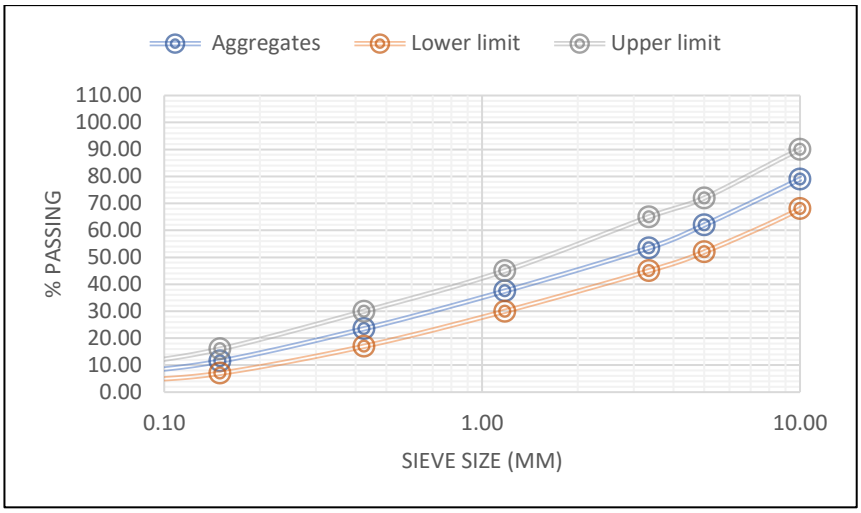


Figure 3.16 Particle Size Distribution of Aggregate for ACW14 Specimen

3.4 Parameters of Study (Phases 2 to 5)

The experiment was conducted in accordance with the framework outlined in Section 3.2, spanning Phases 2 to 5. It is aimed to determine the optimum GGBS replacement levels (10 to 50%), solid precursor-to-activator ratios (90:10, 80:20), CR replacement percentages (5 to 20%) as fine aggregate, and to evaluate the effect of substrate surface roughness on the interfacial bonding performance of geopolymer overlays on concrete and asphalt substrates. The investigated parameters and their corresponding experimental designs are summarised in Table 3.5

Parameters of Study

Phase	Material	Parameters	Design (with units)
Phase 2 and 3	One-part geopolymer repair binders	GGBS replacement FA and WCT	10, 20, 30, 40, and 50% (% of total precursor mass)
Phase 2 and 3	One-part geopolymer repair binders	Solid precursor to solid activator	90:10 and 80:20 (by mass)
Phase 4	One-part semi-rigid geopolymer repair material	Crumb rubber as sand replacement	5%, 10%, 15%, 20% (by volume of sand)
Phase 5	One-part semi-rigid geopolymer repair material with concrete and asphalt substrates	Substrate surface roughness	As cast surface (AC), wire brushed (WB) and drilled holes (DH)

. The following subsections describe the activities conducted in Phase 2 to Phase 5, including geopolymer binder development, crumb rubber as sand replacement, bonding performance evaluation, and pavement repair performance testing.

Table 3.5
Parameters of Study

Phase	Material	Parameters	Design (with units)
Phase 2 and 3	One-part geopolymer repair binders	GGBS replacement FA and WCT	10, 20, 30, 40, and 50% (% of total precursor mass)
Phase 2 and 3	One-part geopolymer repair binders	Solid precursor to solid activator	90:10 and 80:20 (by mass)
Phase 4	One-part semi-rigid geopolymer repair material	Crumb rubber as sand replacement	5%, 10%, 15%, 20% (by volume of sand)
Phase 5	One-part semi-rigid geopolymer repair material with concrete and asphalt substrates	Substrate surface roughness	As cast surface (AC), wire brushed (WB) and drilled holes (DH)

3.4.1 Mix Proportion for One-Part GGBS-FA and GGBS-WCT Geopolymer Binders (Phase 2 and 3)

Phase 2 and 3 utilises GGBS, FA and WCT as aluminosilicate sources. The solid activator employed in this study is sodium metasilicate, anhydrous. Combining these aluminosilicate precursors and solid activators was considered the total binder. The primary focus of this Phase study is to assess the optimal GGBS replacement by utilising five different concentrations 10%, 20%, 30%, 40%, and 50% of the total binder either FA or WCT. The ratios of solid precursor to solid activator selection are various mainly, two activator contents of 10%, and 20% from the total binder were used to evaluate the effect of activator content. Next, water was added to the mixture at a binder-to-water ratio 0.35. The mixing process was performed at the Laboratory of Civil Engineering at UiTM Shah Alam. The mixing procedure was conducted using a mechanical mixer of the ML 712-4 type made by TPG Motors & Drives Corporation. This mixer equipped with a single-phase induction motor and was utilised until a uniform paste consistency was achieved. Table 3.6 show details of mix proportions for all series of specimen prepared in phase 2 and 3.

Table 3.6
Mix Proportions of Different GGBS Based One-Part Geopolymer Repair Binders

Constituents in aluminosilicate precursor	GGBS (%)	FA or WCT (%)	Precursor = 90% of total binder Activator = 10% of total binder (ss-10)	Precursor = 80% of total binder Activator = 20% of total binder (ss-20)
			Specimens ID	Specimens ID
GGBS-only	100	0	GGBS100-ss10	GGBS100-ss20
GGBS + FA	90	10	GGBS90-FA-ss10	GGBS90-FA-ss20
GGBS + FA	80	20	GGBS80-FA-ss10	GGBS80-FA-ss20
GGBS + FA	70	30	GGBS70-FA-ss10	GGBS70-FA-ss20
GGBS + FA	60	40	GGBS60-FA-ss10	GGBS60-FA-ss20
GGBS + FA	50	50	GGBS50-FA-ss10	GGBS50-FA-ss20
GGBS + WCT	90	10	GGBS90-WCT-ss10	GGBS90-WCT-ss20
GGBS + WCT	80	20	GGBS80-WCT-ss10	GGBS80-WCT-ss20
GGBS + WCT	70	30	GGBS70-WCT-ss10	GGBS70-WCT-ss20
GGBS + WCT	60	40	GGBS60-WCT-ss10	GGBS60-WCT-ss20
GGBS + WCT	50	50	GGBS50-WCT-ss10	GGBS50-WCT-ss20

3.4.2 Crumb Rubber as Sand Replacement for One-Part Semi-Rigid Geopolymer Repair Material (Phase 4)

In Phase 3, fine aggregate was incorporated into the selected one-part geopolymer binder to produce the semi-rigid geopolymer repair material. The prepared sand was used as the main fine aggregate, while treated crumb rubber (CR) was introduced as a partial sand replacement. The dry binder materials, sand, and CR were first mixed to achieve uniform distribution. Water was then gradually added, and mixing was continued until a consistent repair mixture was obtained. The fresh mixture was cast into the required moulds and prepared for subsequent mechanical and performance evaluation.

CR was incorporated as a flexible component by partially replacing fine aggregate at replacement levels of 5%, 10%, 15%, and 20% by volume. The binder composition for this phase was fixed at the optimum GGBS–WCT blend (30% WCT), with the solid precursor-to-solid activator ratio maintained at 90:10. These parameters were kept constant and evaluate the influence of CR content on the performance of the one-part semi-rigid geopolymer repair material. By varying only, the CR content while maintaining all other binder parameters, the effects of CR on mechanical performance and durability could be assessed more reliably. The mix proportions for the one-part semi-rigid geopolymer repair materials containing CR as partial sand replacement are presented in Table 3.7.

Table 3.7
Mix Proportion of One-Part Semi Rigid Geopolymer Repair Material with Various CR Replacement

Constituents in aluminosilicate precursor (30% WCT)	**Sand (%)**	**CR (%)**	**Activator = 10% of total binder Precursor = 90% of total binder Specimens ID**
GGBS + WCT	100	0	GGBS-WCT-0% CR
GGBS + WCT	95	5	GGBS-WCT-5% CR
GGBS + WCT	90	10	GGBS-WCT-10% CR
GGBS + WCT	85	15	GGBS-WCT-15% CR
GGBS + WCT	80	20	GGBS-WCT-20% CR

3.4.3 Surface Preparation of OPC Concrete and HMA Substrate (Phase 5)

In this study, two types of substrates were used: Ordinary Portland Cement (OPC) concrete and Hot Mix Asphalt (HMA). The surface preparation of these substrates was crucial to ensure effective bonding between the substrate and the one-part semi-rigid geopolymer repair material. The asphalt binder and aggregate used to prepare the HMA substrate have been described previously in Sections 3.3.8 and 3.3.9. For the OPC concrete substrate, the mix was designed using Grade 30 concrete. After casting, the specimens were water-cured for three months to achieve a stable hardened substrate condition and to simulate the condition of an existing concrete pavement before repair. Three surface conditions were then prepared: as-cast (AC), which served as the control with no surface treatment, wire brushing (WB), and drilled holes (DH). The WB treatment was carried out using a mechanical wire brush, whereas the DH treatment was produced using a rotary hammer drill. These surface preparations were adopted to enhance mechanical interlocking and improve interfacial bonding.

The second substrate, HMA, was prepared using a typical dense-graded asphalt mixture consisting of asphalt binder, coarse and fine aggregates, and mineral filler. The asphalt mixtures were heated and mixed to achieve uniform binder coating, compacted to form specimens, and allowed to stabilise under ambient conditions. Following stabilisation, the HMA surfaces were prepared using the same three surface conditions (AC, WB, and DH) to simulate practical road maintenance scenarios and to enable consistent comparison with the OPC concrete substrate. The use of both OPC concrete and HMA substrates enabled direct comparison of bonding behaviour and overall compatibility of the one-part semi-rigid geopolymer repair material with different pavement surface layers.

3.5 Moulding and Curing

After mixing, two types of specimens were prepared in Phase 2 and 3, one-part geopolymer repair binder specimens and one-part semi-rigid geopolymer repair material specimens. The one-part geopolymer repair binder consisted only of the geopolymer binder. In Phase 4 and 5, the one-part semi-rigid geopolymer repair material consisted of the geopolymer binder combined with aggregates and crumb rubber (CR). The specimens were cast into pre-oiled moulds according to the testing procedure. For compressive strength testing, cube specimens of 50 mm × 50 mm × 50 mm were prepared. For bonding strength evaluation, 150 mm × 150 mm × 150 mm composite cube specimens were produced using steel moulds containing substrate and the one-part semi-rigid geopolymer repair material. In addition, cuboid specimens (55 mm × 90 mm × 10 mm) were cast for the abrasion resistance test.

The mixture was then compacted into three distinct layers and subjected to vibration for two minutes. Subsequently, the specimen was subjected to ambient temperature conditions (25 ± 2 °C) prior to testing, followed by demoulding after achieving full hardening (28 days). After casting, the specimens were cured at ambient temperature and subsequently demoulded after 24 hours. Tests were performed at 3, 14, and 28 days (Phase 2), at 3 and 28 days (Phase 4), and at 3 days (Phase 5). Following the casting process, all specimens were sealed using vinyl plastic sheets to mitigate any potential moisture loss. This measure ensured a stable curing environment, promoting consistent geopolymerisation and the development of desired mechanical and durability properties.

3.6 Preparation and Mix Design of Ordinary Portland Cement (OPC) Concrete Substrate

The OPC Cement Type 1: 42.5N was used as a substrate binder to produce the concrete substrate for the bonding test. It was prepared by mixing the OPC cement, coarse aggregates, fine aggregates and water. By referring to the Faury concrete mix design method, a C30/37 strength class of OPC concrete was designed (Pacheco-Torgal et al., 2008). The hardened OPC concrete substrate was used in contact with the one-part semi-rigid geopolymer repair material to simulate its function as a repair material

for the existing concrete. The OPC concrete substrate was immersed in water for curing purposes and left for three months for the actual damaged concrete substrate condition. This curing period was believed to give the concrete a complete hydration as the existing concrete substrate infield practice.

The mix proportion and strength of OPC concrete are shown in Table 3.8. The OPC concrete was used as a substrate for bonding strength by bi shear test to prepare the actual concrete structure surface. OPC concrete grade 30 was designed as a substrate. The local river sand and crushed limestone were used as fine aggregate and coarse aggregate, respectively.

Table 3.8
Mix Proportion and Strength of OPC

Components	OPC (kg/m^3)	Aggregates (kg/m^3)		Water (kg/m^3)	Compressive strength (MPa)
		Fine	Coarse		
Proportion	380	878	952	205	32.5

Note: Compressive strength = Strength at the age of 28 days (100mm × 100mm × 100mm) specimen.

3.7 Preparation of Hot Mix Asphalt (HMA) Substrate

The preparation of the Hot Mix Asphalt (HMA) substrate was carried out for Phase 5 of this study, as shown in the experimental flowchart. As shown in the overall research framework, Phase 5 hot mix asphalt (HMA) substrates were prepared in this study to evaluate the compatibility and bonding performance of the one-part semi-rigid geopolymer repair material with asphalt pavement layers. The asphalt used in the specimens was HMA meeting the requirements of Malaysia Standard Specification for Road Works (Jabatan Kerja Raya, 2007), with bitumen contents of 6.2 % and ordinary Portland cement (OPC) as mineral filler 2%. The asphalt binder and aggregate gradation used for preparing the ACW14 HMA substrate have been described previously in Sections 3.3.8 and 3.3.9. The mixed and compacted specimens with slab compactor utilised for the wheel tracking test. The total of three (3) specimens of asphalt mix slab as substrate were made. Wheel tracking test was conducted to assess the rutting resistance of HMA and bi shear test to access the bonding between HMA with one-part hybrid geopolymer repair material.

This section provides an overview of the HMA substrate preparation process. The following subsections describe the main procedures involved, including aggregate sieving and gradation, aggregate mixing with bitumen, slab compaction, and specimen preparation for testing. The sieving and gradation process was conducted to obtain the required aggregate particle size distribution for the HMA mixture. The aggregate mixing process was carried out to ensure proper coating of aggregates with bitumen. The compaction process was performed to produce asphalt slab specimens with the required dimensions and density. Finally, the prepared HMA specimens were used for wheel-tracking and bonding performance evaluations.

3.7.1 Sieving and Gradation

Sieving and gradation were conducted as part of the preparation of the hot mix asphalt (HMA) specimens. The sieve analysis test was used to calculate the gradation (particle size) of coarse and fine aggregates. The aggregate's grain size characteristics were analysed with a sieve test. The experiment was carried out using a mechanical sieve shake. The machine sacked the aggregate before putting it on top. The Sieve Shaker, shown in Figure 3.17, was used to remove debris from the aggregate during the screening process. After that, the aggregates be sieved through a series of progressively smaller sieves to separate the particles depending on size. Typically, a machine with a sieve has the largest sieve towards the top and the smallest near the bottom. Aggregates were dried and of a known, consistent weight. After the separation completed, the aggregate weight was compared to the weight of each individual particle on each sieve. The proportion of particles retained by weight for each sieve size was determined by first measuring all the particles retained from each sieve.



Figure 3.17 Sieve Shaker Used for Sieving

3.7.2 Aggregate Mixing

Penetration grade bitumen 60/70 was selected as the asphalt binder because it is suitable for Malaysian environmental conditions, while the aggregates were selected based on the required aggregate properties and gradation tests. After selecting the material, the aggregate gradation was decided, and an ACW14 (Jabatan Kerja Raya, 1998) wearing course type mix was selected. The formulation for the mix design was adopted specifically for the preparation of asphalt pavement specimens. The percentage of the asphalt content was then determined by trial and error to meet the grading criteria. Sieved specimens were mixed with bitumen 60/70 at a temperature of 160 °C until the binder completely coated the aggregate. The mixture was then poured into a heated slab mould with a 400 mm x 300 mm x 120 mm. The mould was then placed in the compaction machine and the height of the specimens after the compaction was set to 50mm for a total of 20 cycles. Figure 3.18 depicts the asphalt slab compactor machine used to compress the specimen. By separating the specimen from the extruder's mould, the specimens are extracted. The specimen was left at room temperature for 24 hours to cool and harden.



Figure 3.18 Asphalt Slab Compactor

3.8 Substrate Surface Treatment

In Phase 5, Prior to the application of the repair material, all substrates were subjected to controlled surface treatments to produce varying levels of surface roughness and interfacial characteristics. Three surface preparation methods were adopted in this study: as-cast (AC), wire-brushed (WB), and drilled holes (DH). The AC condition was left untreated and served as the control surface, representing the original substrate condition without any mechanical modification. This surface was characterised by relatively smooth texture and the possible presence of surface laitance. For the wire-brushed WB condition, the substrate surface was mechanically treated using a steel wire brush as shown in Figure 3.19(a). This process removed loose surface particles and laitance, while exposing the underlying surface texture. The resulting micro-textured surface was intended to enhance surface roughness and improve frictional interaction at the interface.

The DH condition involved the creation of uniformly spaced holes drilled into the substrate surface to promote mechanical interlock as illustrated in Figure 3.19(b). The holes were designed with a nominal depth of 30 mm, with an allowable tolerance of ±2 mm, and arranged in a consistent pattern across the substrate surface. For cored substrates with limited surface area, the drilled holes were positioned symmetrically to ensure uniform stress distribution and to accommodate the reduced specimen dimensions. This surface preparation approach enabled the evaluation of the influence of surface roughness and mechanical interlocking on the interfacial bonding and overall performance of the repair.

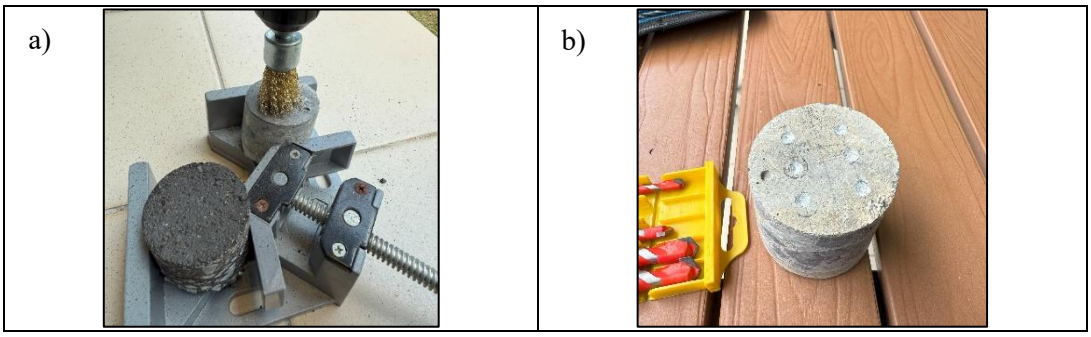


Figure 3.19 Surface Preparation Methods Applied to Concrete Substrates: (a) Wire-Brushed and (b) Drilled Holes

3.9 Testing of One-Part Geopolymer Repair Binders and One-Part Semi-Rigid Geopolymer Repair Material for Surface Road Repair Pavement (Phase 2 to Phase 5)

The testing was conducted from Phase 2 to Phase 5. In Phase 2 involved testing workability, setting time, and compressive strength tests were carried out to evaluate the performance of the one-part geopolymer repair binders. In Phase 4, water absorption, abrasion resistance, and compressive strength tests were conducted to assess the properties of the one-part semi-rigid geopolymer repair materials. In Phase 5, surface roughness, rutting resistance, compressive strength, and bonding strength tests were performed to evaluate the repair performance of the geopolymer material when applied to concrete and HMA substrates. Furthermore, characterisation tests were conducted in Phase 1 and Phase 3. Chemical composition analysis using XRF was performed to determine the elemental composition essential for geopolymerisation. Phase characterisation using XRD was conducted to identify the crystalline and amorphous phases influencing the setting and strength development. Microstructure characterisation using SEM was carried out to examine the morphology, pore distribution and SEM–EDX was employed to determine the elemental composition and distribution within selected microstructural. The following sub-section explains the testing conducted on the geopolymer, including its mechanical and microstructural, as well as the bonding strength between geopolymer and concrete/HMA substrates, and rutting performance.

3.9.1 Workability Test

The workability test was carried out to determine the fresh consistency of the one-part geopolymer repair binder in Phase 2. In this study, the flow table test was adopted in accordance with ASTM C1437 (ASTM-C1437, 2020). The fresh mixture was placed into the flow mould at the centre of the flow table. After the mould was lifted vertically, the flow table was operated according to the standard procedure to allow the mixture to spread. The spread diameter was measured in two perpendicular directions, namely D_1 and D_2. The average spread diameter was then calculated as the workability value using Equation 3.2. The apparatus used for the workability test is shown in Figure 3.20.

$$\text{Wb} = \frac{D_1 + D_2}{2} \tag{3.2}$$

where:

Wb = Workability, expressed as mean spread diameter (mm);

D_1 = Diameter of flow in one direction (mm); and

D_2 = Diameter of flow in the perpendicular direction (mm)



Figure 3.20 Flow Table Set for Measuring the Diameter of One-Part Geopolymer Repair Binders Spread

3.9.2 Setting Time Test

As specified by the ASTM C191 (ASTM-C191, 2007) standard, the Vicat equipment was utilised to measure the commencement and conclusion times of the one-part geopolymer repair binders setting process in Phase 2. The initial setting (t_1), refers

to the duration for the concrete to attain a penetration resistance of 25 ± 1 mm. In contrast, the final setting time (t_2) is characterised by the point at which the needle no longer visibly sinks into the fresh geopolymer mixture.

The reading was taken every 10 minutes until the t_1 and t_2 were recorded. Figure 3.21 measures the one-part geopolymer repair binders initial and final setting time. These values were then used to calculate the total setting time, as shown in Equation 3.3. According to the established protocol, the determination of setting time using the Vicat apparatus necessitates the measurement to be conducted on a paste that adheres to the typical consistency requirement.

$$\text{Setting Time } (S_t) = t_2 - t_1 \tag{3.3}$$

where:

S_t = Setting time (minutes, min);

t_1 = Time at which the needle penetrates to a depth of 25 ± 1 mm; and

t_2 = Time at which the needle fails to visibly penetrate the paste



Figure 3.21 Setting Time Apparatus for Measuring Setting Time of Geopolymer Paste

3.9.3 Compressive Test

The process of obtaining specimens of the one-part geopolymer repair binders in Phase 2 and one-part semi-rigid geopolymer repair material in Phase 4 was conducted following the guidelines outlined in ASTM C109 (ASTM-C109, 2020). The one-part geopolymer repair binders and one-part semi-rigid geopolymer repair material cubes used as test specimens were produced, subjected to the ambient curing. The maximum compressive loads were determined through compression testing at the Concrete

Laboratory located at UiTM Shah Alam, Selangor. The cast specimens underwent ambient curing at standard room temperature for geopolymer paste 3, 14, and 28 days (phase 2) while for geopolymer concrete at 3 and 28 days (phase 4). The test was conducted using three specimens for each trial. Utilising three specimens for each period to obtain the mean compressive strength values. It is crucial to ensure that all bearing surfaces of the testing equipment are thoroughly wiped clean before conducting compression tests. The compression machine utilised in this experiment is depicted in Figure 3.22. Compressive strength was calculated using the formula presented in Equation 3.4.

$$\text{Compressive strength (Cs)} = \frac{\text{P(Load)}}{\text{A(Area)}} \tag{3.4}$$

where:

Cs = Compressive strength (Megapascal, MPa);

P = Maximum load (Newton, N); and

A = Surface area (millimetre square, mm^2)



Figure 3.22 Universal Testing Machine (UTM) 1000kN Machine Used to Compress the Geopolymer Specimens

3.9.4 Chemical Composition Characterisation

The chemical compositions of the raw materials in Phase 1, including GGBS, FA, and WCT, and the selected one-part geopolymer repair binders in Phase 3 were determined using a benchtop X-ray fluorescence (XRF) spectrometer manufactured by PAN analysis, specifically the PW4030 model, as shown in Figure 3.23. This

spectrometer is an energy-dispersive microprocessor controlled analytical instrument integrated with the MiniPal software. The specimen was introduced into the spectrometer chamber and subjected to a maximum voltage of 30 kV. Additionally, a maximum current of 1 mA was employed to generate X-rays that stimulate the specimen for a predetermined duration of 10 minutes. The precision of the XRF analysis is 1%. The elemental composition of the specimens was determined and measured using XRF technique, which involved subjecting the materials to XRF radiation. The radiation emitted exhibits distinct characteristics unique to each element, with the strength of the radiation being directly proportional to the concentration of the respective element. This allows for quantitative determination of the element's concentration.



Figure 3.23 XRF Spectrometer Used to Determine Chemical Composition

3.9.5 Phase Characterisation

The phase composition of raw GGBS, FA, and WCT in Phase 1, and the selected GGBS-WCT-based hybrid one-part geopolymer repair binder in Phase 3, was determined using X-ray diffraction (XRD) characterisation. XRD patterns were acquired utilising the XRD-6000, a Shimadzu x-ray diffractometer equipped with Cu-Kα radiation. The specimens utilised for the experimentation are in a powdered state. The XRD scan was encompassing a range of 10^{o} to 80^{o} 2θ values, with a scanning increment of 0.020^{o} per second. The XRD was be furnished with auto-match software as a conventional instrument to identify crystalline phases. The XRD pattern was be analysed using the X'pert Highscore Plus software, which utilises the International Centre for Diffraction Data (ICDD) PDF-2 database. The XRD utilised in this study is the Rigaku Model Ultima IV, shown in Figure 3.24 .



Figure 3.24 XRD Diffractometer Used to Determine Phase Characterisation

3.9.6 Microstructure Characterisation

The JSM-6460LA model Scanning Electron Microscope (SEM) was used in Phase 1 to analyse the morphology of raw GGBS, FA, and WCT, and in Phase 3 to examine the microstructure of the selected GGBS-WCT-based hybrid one-part geopolymer repair binder, as shown in Figure 3.25. The analysis was conducted using secondary electron detectors. The microstructure investigation of raw material and hardened geopolymer specimen was conducted by dispersing the powders over carbon tape. The cross-sectional analysis of raw material and one-part geopolymer repair binders specimens involves obtaining a specimen using a cutting technique. Subsequently, prior to the start of the testing process, all undergo specimens were a palladium coating procedure utilising the Auto Fine Coater JEOL JFC 1600 model. Simultaneously, the surface elemental composition was determined through the utilisation of Energy Dispersive X-ray (EDX) spectroscopy, employing the same methodology.


Figure 3.25 SEM Instrument Used to Determine Microstructural Characteristics

3.9.7 Water Absorption

The water absorption test was conducted on the one-part semi-rigid geopolymer repair material specimens prepared in Phase 4. To perform the water absorption test in accordance with ASTM C642 (ASTM-C642, 2022), specimen GGBS-WCT-based one-part semi-rigid geopolymer repair material varying amounts of CR were dried in an oven at 110°C until a stable mass was achieved. They were then cooled in a desiccator, and the dry mass (M_d) was recorded as shown in Figure 3.26. The specimens were subsequently submerged in water for 3 and 28 days, allowed to air dry, and the saturated surface-dry mass (M_{ssd}) was recorded. Water absorption percentages were calculated using the formulas in Equation 3.5, and the effect of CR content on water absorption was evaluated

$$\text{Water Absorption (\%)} = \frac{M_{ssd} - M_d}{M_d}\ x\ 100 \tag{3.5}$$

where,

M_d = Mass of dried specimens (g); and

M_{ssd} = Mass of saturated surface-dried specimens (g)



Figure 3.26 Determination of Specimen Mass for CR Sample

3.9.8 Abrasion Resistance (AR)

The methods outlined in BS 812-113:1990 (BS-812-113, 1990) were strictly followed to determine the abrasion resistance (AR) of the aggregate specimens in Phase 4. The relevant sections of the standard were followed to during the preparation, conditioning, and testing of the aggregates used in this investigation. The abrasion

resistance test was conducted at the Highway Laboratory, University of Malaya, to evaluate the loss of particle mass under standardised conditions as shown in Figure 3.27.

Each specimen of GGBS-WCT based hybrid one-part semi-rigid geopolymer repair material was weighed and placed in the abrasion testing machine, as prescribed by the standard, along with the required number and size of steel spheres. The drum was rotated at a speed of 30–33 revolutions per minute for a total of 500 revolutions, in accordance with the standard requirement. Upon completion of the test cycle, the specimens were removed, cleaned, and reweighed. Abrasion resistance (AR) was calculated using the equation proposed by Feng and Liu (2021) and reported in $mm^2 \cdot hr/g$, providing an index of the material resistance to surface material loss under mechanical wear. The loss in mass was calculated to determine the abrasion value using Equation 3.6.

$$\text{AR} = \frac{TA}{M_t} \tag{3.6}$$

where,

AR = Abrasion resistance, $(mm^2 \cdot hr/g)$;

A = Area of specimens (mm^2);

T = Test duration *(hr)*; and

M_t = Mass loss after abrasion *(g)*

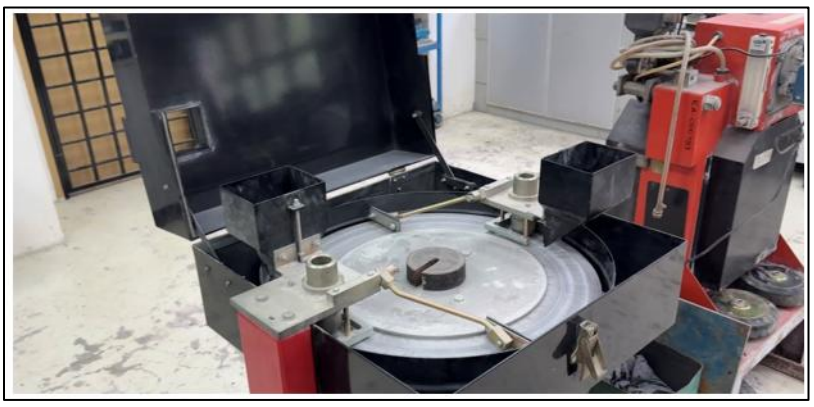


Figure 3.27 Surface Abrasion Testing Machine

3.9.9 Surface Roughness Evaluation

In Phase 5, two types of surface preparations were implemented on the surface of the concrete substrate which are DH, and WB. Surface roughness of the prepared substrates was measured using Alicona 3D Surface Metrology System, a high-resolution 3D optical metrology system. Measurements were conducted in accordance with ISO 25178 (ISO-25178, 2021) for areal surface texture to obtain roughness average (Ra) for comparison. For each sample, the surface roughness was measured thrice, and the average value was obtained as the final Ra value.



Figure 3.28 Alicona 3D Surface Metrology Instrument

3.9.10 Bi-Surface Shear

The bond between the one-part semi-rigid geopolymer repair material and hardened OPC concrete/HMA substrates was evaluated using a bi-surface shear test on specially cast composite cube specimens. For this test, OPC concrete/HMA substrate cube size 150mm x 150mm x 100mm was cast and cured for over three months of curing. One-part semi-rigid geopolymer repair material was poured over the remaining half to form a complete 150mmx150mmx50mm cube. Half part of the composite was made up of one-part semi-rigid geopolymer repair material and the remaining half cast with OPC concrete or HMA substrate. This composite specimen was tested under ASTM C882 (ASTM-C882, 2020). Figure 3.29 shows the composite specimen to determine the bond between repair materials and concrete substrate.

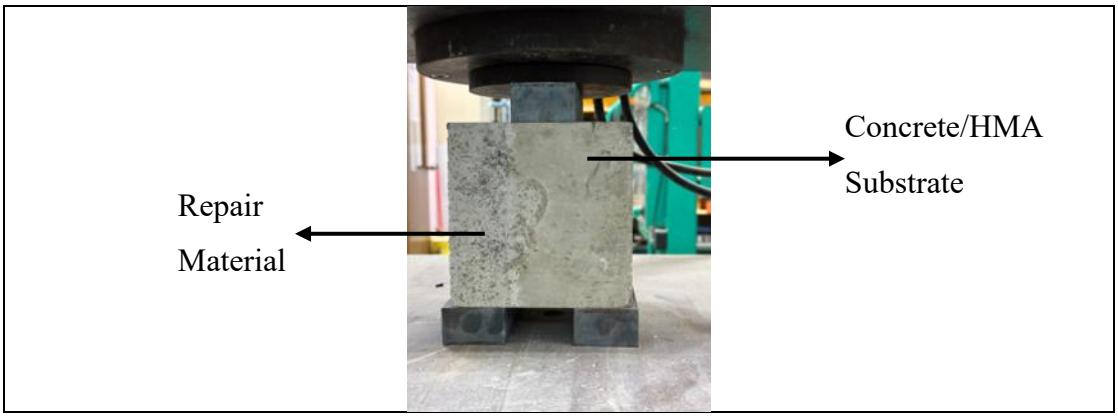


Figure 3.29 Composite Specimen for Bi-Surface Shear Test

The composite specimens were tested in a constant loading rate of 0.50 MPa/s. The average of three specimens was reported as results of bonding strength between one-part semi-rigid geopolymer repair material and concrete substrate. The bonding strength for the bi shear strength was calculated by dividing the maximum load by the bond area as shown in Equation 3.7

$$S = \frac{P}{A} \tag{3.7}$$

where,

S: Bond strength (Megapascal, MPa);

P = Maximum load (Newton, N); and

A = Bond area (millimetre square, mm^2)

3.9.11 Wheel Tracking Test

A wheel tracking test was conducted to assess the rutting resistance of HMA and to determine the rutting behaviour of each specimen. One of the major problems with asphalt pavement is rutting, which can occur particularly during hot climates. The slab specimens were prepared using a slab compactor in a mould of size 400mm × 300mm × 120mm, as in Figure 3.30. The final height of the specimens after the compaction was set to 50mm for a total of 20 cycles. The 20kN load was applied for

the ten cycles, followed by 5kN for the last ten cycles. The weight of the asphalt mix slab specimen is presented in the Table 3.9.



Figure 3.30 Asphalt Rolling Compactor Machine

Table 3.9
Slab weight for Control Mixture

Slab specimens		
Volume cm^3	Total weight, g	Specific Gravity
6000	13818.19	2.3

The dimension of the slab mould in the wheel tracking machine is 300 mm × 300 mm × 50 mm. After the mixture was compacted in an asphalt rolling compactor, the slab specimens were cut according to the size of the wheel tracking machine mould using a cutter machine. In a wheel tracking test, a loaded wheel was travel horizontally on a slab specimen, like those experienced on real road pavement. The BS 598-110 (BS-598-110, 1998) standard procedure was used to perform this test. The wheel tracking machine was made up of a 200 mm diameter by 50 mm wide steel wheel that moved for 45 minutes at a constant speed at 42 passes or 21 cycles per minute. The 520 ± 5 N load was applied to the centre line at the top surface of the slab specimen. The slab specimen was placed in an insulated heated cabinet, and the temperature was set to the desired temperature. For this study, the temperatures were set to 45ºC for each slab specimen. Every five minutes, the reading of the rutting depth was taken through the dial gauge that connected to the wheel tracking test machine. The test was carried out for 45 minutes or until the rutting depth of the specimens reached 15mm or whichever occurred first. The thermometer was placed in the heated cabinet to measure and ensure constant temperature during the test was maintained.

3.10 Data Collection and Analysis

Data collection and analysis were conducted according to the five (5) experimental phases of this study. The purpose of this section is to explain the type of data collected in each phase and the method used to analyse the data before the results were presented and discussed in Chapters 4 and 5. In Phase 1, data were collected from the characterisation of raw materials, including GGBS, FA, and WCT. The chemical composition data were obtained from X-ray fluorescence (XRF), while the phase composition was obtained from X-ray diffraction (XRD). The morphology and particle characteristics were observed using scanning electron microscopy (SEM). These data were analysed to determine the suitability of the raw materials as aluminosilicate sources for one-part geopolymer repair binder.

In Phase 2, the collected data included workability, setting time, and compressive strength of the one-part geopolymer repair binders. These data were used to evaluate the effect of GGBS replacement levels and solid precursor-to-solid activator ratios on the performance of the GGBS-FA and GGBS-WCT binder The results were analysed based on average values, percentage differences, and comparison between mix designs to identify the most optimum binder formulation. In Phase 3, characterisation data were collected from the selected one-part geopolymer repair binder after geopolymerisation. XRF, XRD, SEM, and SEM–EDX analyses were used to examine the chemical composition, phase formation, morphology, and elemental distribution of the selected binder. These data were analysed the reaction products and microstructural development for the mechanical performance of the geopolymer binder.

In Phase 4, data were collected from the one-part semi-rigid geopolymer repair material using crumb rubber (CR) as a partial fine aggregate replacement. The tests included workability, setting time, compressive strength, water absorption, and abrasion resistance. The results were analysed the influence of CR replacement on the fresh, hardened, and durability-related properties of the repair material. In Phase 5, data were collected from the bonding and pavement repair performance tests. These included surface roughness, bonding strength, rutting resistance, skid resistance, and compressive strength of the repair on OPC concrete and HMA substrates. The results were analysed to evaluate the effect of substrate surface preparation on interfacial bonding and pavement repair performance. Statistical analysis was conducted using the

Statistical Package for the Social Sciences (SPSS) to support the interpretation of the experimental data. An independent-samples t-test was used to compare selected quantitative results, including compressive and bonding strength. The significance level was set at 0.05, where a p-value less than 0.05 indicated a statistically significant difference between the compared groups. The statistical findings were used to support the selection of the optimum repair mixture.

3.11 Summary

The research methodology adopted in this study was divided into five (5) main phases. The phase 1 focused on the characterisation of the raw materials, including GGBS, FA, and WCT. These materials were analysed for their chemical composition, phase, and microstructural properties using XRF, XRD, and SEM. The phases 2 involved the optimisation of the one-part geopolymer repair binders through the different GGBS replacement and precursor to activator ratios. This phase included testing for workability, setting time, and compressive strength to determine the most optimum mix design. In the phases 3, the reaction of geopolymerisation was investigated the chemical, phase, and microstructural in the GGBS-WCT-based hybrid one-part geopolymer repair binders. This step ensured a deeper understanding of the reaction mechanisms for the performance of the one-part geopolymer repair binders. The phases 4 focused on the development of one-part semi-rigid geopolymer repair material incorporating CR as a flexible agent. Various replacement of CR was tested as sand replacement, and the mechanical properties such as compressive strength, abrasion resistance, and water absorption were evaluated.

Phase 5 evaluated the bonding performance between the geopolymer repair material and OPC concrete and HMA substrates using AS, WB, and DH surface treatments under ambient curing. The optimised surface condition was further assessed by wheel-tracking to determine its durability for pavement repair applications. Overall, the experimental programme covered material characterisation, binder optimisation, reaction mechanisms, material development, and bonding performance to comprehensively evaluate the one-part semi-rigid geopolymer repair material.

CHAPTER 4
CHARACTERISTICS OF RAW MATERIALS (PHASE 1), OPTIMISATION OF GGBS–FA AND GGBS–WCT ONE-PART GEOPOLYMER BINDERS (PHASE 2) AND GEOPOLYMERISATION REACTION (PHASE 3)

4.1 Introduction

This chapter presents the characteristics of the raw materials, namely ground granulated blast-furnace slag (GGBS), fly ash (FA), and waste clay tile (WCT). The raw materials were characterised using X-ray diffraction (XRD) and X-ray fluorescence (XRF), together with microstructural examination using scanning electron microscopy (SEM). The findings reported in this chapter cover Phases 1 to 3. Specifically, the chemical composition, phase, and microstructure analysis of the raw materials are discussed, followed by the optimisation results of the one-part geopolymer binder in terms of workability, setting time, and compressive strength.

4.2 Phase 1: Chemical Composition, Phase and Microstructure Analysis

This section presents the chemical composition, phase, and microstructural characteristics of the raw materials used in this study. The analyses were conducted to identify the major chemical oxides, crystalline and amorphous phases, and particle morphology of the materials. Chemical composition analysis was used to determine the oxide contents of the raw materials, particularly silica, alumina, calcium oxide, and iron oxide, which are important for geopolymerisation. Phase analysis was carried out to identify the mineral phases present in the materials. Microstructure analysis was performed to observe the particle shape, surface texture, and morphology. The results from these analyses provide a basis for understanding the reactivity and suitability of the materials for producing one-part geopolymer binders.

4.2.1 Chemical Composition Analysis

The SiO_2/Al_2O_3 molar ratio obtained was approximately 3, suggesting the probable formation of a sialate-disiloxo (–Si–O–Al–O–Si–O–Si–) geopolymer structure, as discussed in Section 2.5.1. Similar finding of GGBS has been reported by Davidovits (2008) who observed that effective geopolymer precursors typically exhibit a combined SiO_2 and Al_2O_3 content ranging from 40% to 47%. This compositional range is considered because it ensures optimal availability of reactive silica and alumina species required for the geopolymerisation process, contributing to improved mechanical properties and setting performance. In addition, CaO was identified as the dominant oxide due to the use of limestone during iron ore reduction in blast-furnace operations, which results in a CaO-rich slag material. The presence of MgO (3.20 wt.%) can be attributed to the use of dolomite as a flux during steelmaking. Dolomite acts as a heat-resistant material and contributes MgO to the slag, while iron ore typically contains gangue materials such as silica (SiO_2) and alumina (Al_2O_3), along with trace amounts of sulphur (S) and phosphorus (P).

Table 4.1 tabulates the chemical composition of GGBS obtained by XRF analysis. The major oxide composition of GGBS calcium oxide (CaO), silicon dioxide (SiO_2), and aluminium oxide (Al_2O_3), with contents of 50.37 wt.%, 30.40 wt.%, and 10.50 wt.%, respectively. The high CaO content indicates the GGBS, which contributes to enhanced early-age reactivity and strength development in geopolymer. The combined content of SiO_2 and Al_2O_3 was approximately 40.9 wt.%, indicating sufficient availability of reactive silica and alumina required for geopolymerisation. Minor oxides such as magnesium oxide (MgO), iron oxide (Fe_2O_3), titanium dioxide (TiO_2), and potassium oxide (K_2O) were also detected in small quantities. The relative proportions of these oxides determine the glass structure, reactivity, and the nature of hydration products formed (Humad et al., 2019).These oxides may influence the reaction rate and microstructural development but do not affect the geopolymerisation process. Overall, the chemical composition confirms that GGBS is a suitable precursor material for one-part geopolymer binders, as the reactive silica and alumina phases can be activated in an alkaline environment.

The SiO_2/Al_2O_3 molar ratio obtained was approximately 3, suggesting the probable formation of a sialate-disiloxo (–Si–O–Al–O–Si–O–Si–) geopolymer

structure, as discussed in Section 2.5.1. Similar finding of GGBS has been reported by Davidovits (2008) who observed that effective geopolymer precursors typically exhibit a combined SiO_2 and Al_2O_3 content ranging from 40% to 47%. This compositional range is considered because it ensures optimal availability of reactive silica and alumina species required for the geopolymerisation process, contributing to improved mechanical properties and setting performance. In addition, CaO was identified as the dominant oxide due to the use of limestone during iron ore reduction in blast-furnace operations, which results in a CaO-rich slag material. The presence of MgO (3.20 wt.%) can be attributed to the use of dolomite as a flux during steelmaking. Dolomite acts as a heat-resistant material and contributes MgO to the slag, while iron ore typically contains gangue materials such as silica (SiO_2) and alumina (Al_2O_3), along with trace amounts of sulphur (S) and phosphorus (P).

Table 4.1
Chemical Composition GGBS

Chemical oxide	**Composition (wt.%)**
Aluminium oxide (Al_2O_3)	10.5
Calcium oxide (CaO)	50.37
Silicon dioxide (SiO_2)	30.4
Magnesium oxide (MgO)	3.2
Iron oxide (Fe_2O_3)	3.30
Potassium oxide (K_2O)	0.48
Titanium dioxide (TiO_2)	0.98

In accordance with ASTM C618 (ASTM-C618, 2023), the FA utilised in this research contains silicon dioxide (SiO_2), aluminium oxide (Al_2O_3), and iron oxide (Fe_2O_3) with a cumulative content exceeding 70%, satisfying the requirement for FA Class F. FA Class F is recognised as a pozzolanic material and is suitable as an aluminosilicate precursor for geopolymer binder production. Based on the XRF results, SiO_2 exhibited the highest proportion in the FA, accounting for 59.49% of the overall composition. The high silica content is beneficial for geopolymerisation, as it promotes the formation of soluble silicate and supports polycondensation during binder gel development.

The SiO_2/Al_2O_3 ratio of FA obtained in this study was approximately 2.9, indicating a silica aluminosilicate composition that is good for forming a stable geopolymeric network under alkaline activation. With the introduction of an alkali activator, the high SiO_2 and Al_2O_3 contents are expected to contribute to the

development of a dense binder gel, and a sialate–siloxo type framework may be formed. Overall, the chemical composition confirms that the FA has strong potential for use as a raw material in one-part geopolymer binders.

Table 4.2 presents the chemical composition of FA determined by XRF analysis. The major oxide constituents of FA are silicon dioxide (SiO_2), aluminium oxide (Al_2O_3), and calcium oxide (CaO), with contents of 59.49 wt.%, 20.01 wt.%, and 8.74 wt.%, respectively. In accordance with ASTM C618 (ASTM-C618, 2023), the FA utilised in this research contains silicon dioxide (SiO_2), aluminium oxide (Al_2O_3), and iron oxide (Fe_2O_3) with a cumulative content exceeding 70%, satisfying the requirement for FA Class F. FA Class F is recognised as a pozzolanic material and is suitable as an aluminosilicate precursor for geopolymer binder production. Based on the XRF results, SiO_2 exhibited the highest proportion in the FA, accounting for 59.49% of the overall composition. The high silica content is beneficial for geopolymerisation, as it promotes the formation of soluble silicate and supports polycondensation during binder gel development.

The SiO_2/Al_2O_3 ratio of FA obtained in this study was approximately 2.9, indicating a silica aluminosilicate composition that is good for forming a stable geopolymeric network under alkaline activation. With the introduction of an alkali activator, the high SiO_2 and Al_2O_3 contents are expected to contribute to the development of a dense binder gel, and a sialate–siloxo type framework may be formed. Overall, the chemical composition confirms that the FA has strong potential for use as a raw material in one-part geopolymer binders.

Table 4.2
Chemical Composition FA

Chemical oxide	**Composition (wt.%)**
Aluminium oxide (Al_2O_3)	20.01
Calcium oxide (CaO)	8.74
Silicon dioxide (SiO_2)	59.49
Magnesium oxide (MgO)	2.94
Iron oxide (Fe_2O_3)	4.10
Potassium oxide (K_2O)	1.04
Titanium dioxide (TiO_2)	1.85

The high SiO_2 content indicates that WCT is a silica aluminosilicate material, making it a suitable precursor for geopolymerisation. The combined presence of SiO_2 and Al_2O_3 satisfies the minimum requirements for effective alkali activation and

geopolymer binder formation. According to de Azevedo et al. (2020), a SiO_2/Al_2O_3 ratio of 1.0 or higher is sufficient to promote the formation of sialate-based geopolymeric structures, making them suitable for ceramic-related applications. Based on the XRF results, the WCT exhibited a SiO_2/Al_2O_3 ratio of approximately 3.0, exceeding the minimum requirement. This composition suggests that a silica geopolymeric network, such as a sialate–disiloxo type structure, may form during the geopolymerisation process.

Table 4.3 presents the chemical composition of waste clay tile (WCT) determined by XRF analysis. The XRF measurements were conducted using an S1 TITAN handheld XRF spectrometer to quantify the oxide composition of the WCT. The major oxide constituents were silicon dioxide (SiO_2), aluminium oxide (Al_2O_3), and calcium oxide (CaO), with contents of 68.0 wt.%, 17.5 wt.%, and 2.72 wt.%, respectively, giving a combined percentage of 88.22 wt.%. The high SiO_2 content indicates that WCT is a silica aluminosilicate material, making it a suitable precursor for geopolymerisation. The combined presence of SiO_2 and Al_2O_3 satisfies the minimum requirements for effective alkali activation and geopolymer binder formation. According to de Azevedo et al. (2020), a SiO_2/Al_2O_3 ratio of 1.0 or higher is sufficient to promote the formation of sialate-based geopolymeric structures, making them suitable for ceramic-related applications. Based on the XRF results, the WCT exhibited a SiO_2/Al_2O_3 ratio of approximately 3.0, exceeding the minimum requirement. This composition suggests that a silica geopolymeric network, such as a sialate–disiloxo type structure, may form during the geopolymerisation process.

Table 4.3
Chemical Composition WCT

Chemical oxide	**Composition (wt.%)**
Aluminium oxide (Al_2O_3)	17.5
Calcium oxide (CaO)	2.72
Silicon dioxide (SiO_2)	68.0
Magnesium oxide (MgO)	1.62
Iron oxide (Fe_2O_3)	1.48
Potassium oxide (K_2O)	2.72
Titanium dioxide (TiO_2)	0.25

4.2.2 Phase Analysis

Figure 4.1 presents the XRD pattern of the GGBS. The diffractogram was processed and plotted using PANalytical HighScore software. A broad diffuse scattering band is observed across the scanned range, with a pronounced hump between approximately 20° and 40° (2θ). This feature is characteristic of a predominantly amorphous (glassy) phase, indicating a high proportion of disordered material. In contrast, the sharper reflections observed at higher angles represent crystalline phases present in smaller proportions. The most intense diffraction peaks were recorded at 2θ = 29.48° and 31.87°, which were assigned to calcium silicate-related phases (PDF No. 00-031-0301). Additional minor peaks were detected at 2θ = 43.97° and 49.69°, corresponding to epidote (PDF No. 00-017-0514). Overall, the dominance of the amorphous hump relative to the individual crystalline peaks suggests that GGBS comprises a substantial glassy fraction with limited crystalline inclusions. This phase assemblage is good for one-part geopolymer repair binders synthesis because the amorphous fraction generally dissolves more easily in alkaline environments, supplying reactive calcium and silicate species that contribute to gel formation and strength development.

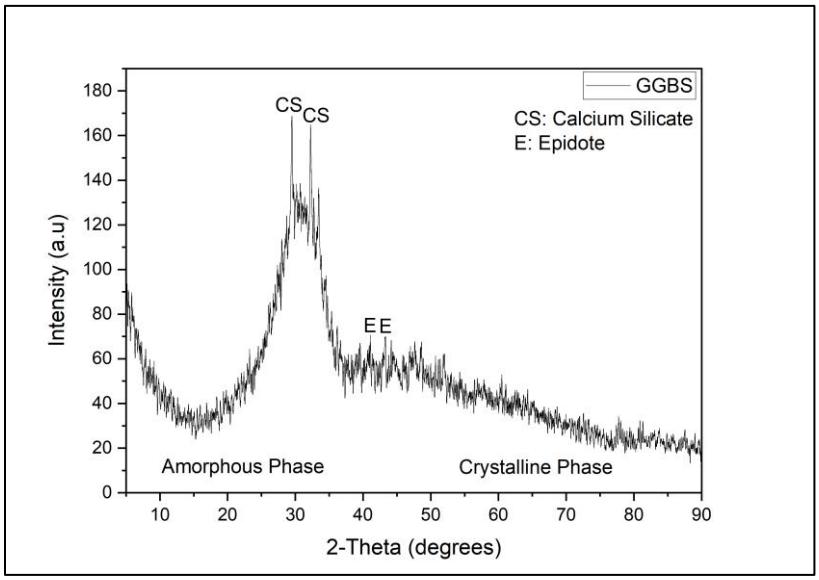


Figure 4.1 X-Ray Diffraction Patterns of GGBS (CS = Calcium Silicate (Ca_3SiO_5: PDF no. 00-031-0301); E = Epidote ($Ca_2Al_2Fe(SiO_4)$ ($Si2O_7$)) : PDF no. 00-017-0514)

The occurrence of calcium-bearing phases is consistent with the origin of GGBS as a by-product of the blast-furnace ironmaking process. During iron production, iron ore is smelted with limestone and coke at high temperatures (typically around 1500 °C), producing molten slag that is subsequently processed into GGBS (Ahmad et al., 2022). The slag melt contains mineral constituents including silicates, aluminates, and calcium-rich species. This interpretation is supported by the XRF results, which indicated a high CaO content (50.37 wt.%), confirming that calcium is a dominant component of the GGBS. Accordingly, the pronounced calcium silicate-related peaks in the XRD pattern reflect the high proportion of Ca-based phases in the material. Finally, the broad hump observed between 20° and 40° (2θ) signifies the presence of reactive amorphous phases, which are widely recognised as the primary contributors to reactivity in alkali-activated systems. The availability of reactive calcium and silica from this glassy fraction is therefore expected to enhance geopolymerisation reaction and support the development of a dense binder matrix.

Figure 4.2 shows the XRD pattern of the FA. A broad diffuse hump is observed within the 2θ range of approximately 20° to 35°, which is characteristic of a glassy amorphous phase. This amorphous component is widely recognised as the primary source of reactivity in FA. Overlay on this amorphous background, several distinct crystalline peaks are present, indicating that FA consists of a combination of amorphous and crystalline phases. The dominant crystalline phase identified in the FA was quartz (SiO_2), with major diffraction peaks observed at 2θ values of 20.93° and 26.78° (PDF No. 01-078-1254). In addition, peaks corresponding to sillimanite (Al_2SiO_5) were detected at 2θ values of 16.60°, 26.39°, 33.36°, 35.42°, 42.77°, and 60.80° (PDF No. 01-083-1562). Quartz is known to be highly crystalline and chemically stable and therefore contributes minimally to geopolymer reactivity. Its presence primarily acts as an inert filler rather than a reactive precursor.

The existence of a broad amorphous hump with pronounced quartz and sillimanite peaks suggests that the reactivity of FA is controlled predominantly by its glassy fraction rather than its crystalline constituents. This observation is consistent with Huseien et al. (2020), who reported that the amorphous phase in FA plays a critical role in dissolution and gel formation during alkali activation. Although sillimanite is an aluminosilicate mineral, its crystalline nature limits its dissolution rate under alkaline conditions, and thus its contribution to geopolymerisation is expected to be secondary compared to the amorphous phase. The dominance of quartz in the XRD pattern can be

attributed to the silica origin of the FA. This interpretation is consistent with the XRF results, which indicated a high SiO_2 content. However, despite the amount of silica, the relatively high crystallinity of FA compared to GGBS suggests a lower reactivity, which may necessitate higher activator dosage or longer curing durations to achieve comparable geopolymerisation efficiency. Similar observations were reported by Altheeb (2023), who highlighted that FA-based geopolymers with heavily on the dissolution of amorphous aluminosilicate phases for effective binder formation.

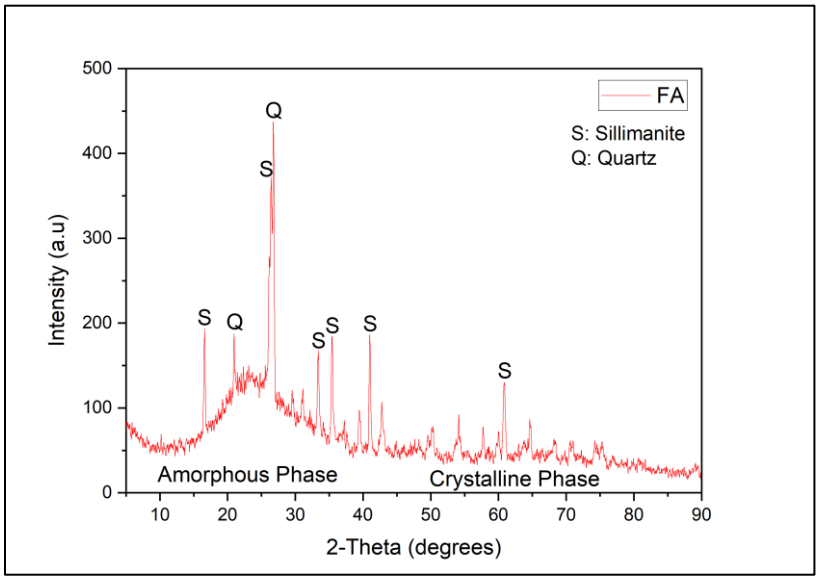


Figure 4.2 X-Ray Diffraction Patterns of FA (Q = Quartz (SiO_2: PDF no. 01-078-1254); S = Sillimanite ($Al_2(SiO_4)$ O): PDF no. 01-083-1562)

Figure 4.3 presents the XRD pattern of the WCT. The XRD results reveal a predominantly crystalline phase assemblage, as evidenced by the presence of sharp and well-defined diffraction peaks across the scanned 2θ range, indicating limited amorphous content within the WCT specimens. The dominant crystalline phase identified was quartz (SiO_2), with major diffraction peaks observed at 2θ values of 20.92°, 26.69° and 50.17° (PDF No. 01-078-1254). In addition, mullite ($3Al_2O_3 \cdot 2SiO_2$) was detected at 2θ values of 36.61°, 39.52°, and 42.54° (PDF No. 01-079-1456). These findings are consistent with previous studies on ceramic waste materials, which report quartz and mullite as the principal mineralogical phases formed during high-temperature ceramic firing processes (Li et al., 2022).

Mullite is a thermodynamically stable aluminosilicate phase that typically forms at temperatures between 950 °C and 1100 °C during ceramic impurity and is associated with enhanced mechanical strength and thermal stability in fired clay products

(Lampropoulou & Papoulis, 2021). However, aluminosilicate composition, the crystalline nature of mullite significantly limits its dissolution rate under alkaline activation. Similarly, quartz is a highly crystalline and chemically stable phase and therefore contributes minimally to geopolymerisation reactions, primarily acting as an inert filler within alkali activated.

The presence of crystalline quartz and mullite, together with the absence of a clear amorphous hump in the XRD pattern, suggests that the reactivity of WCT is considerably lower than that of more glassy precursors such as GGBS and FA. This interpretation is consistent with the XRF results, which indicated a high SiO_2 content (68.0 wt.%), largely associated with crystalline quartz rather than reactive amorphous silica. Consequently, an increase in quartz peak intensity corresponds to a higher proportion of unreactive silica, which may result in a higher proportion of unreacted particles within the geopolymer reaction. Nevertheless, WCT can still function as a secondary aluminosilicate source or filler material in geopolymer matrices. Under alkaline activation, limited dissolution of aluminosilicate species from glassy regions or surface defects may contribute to the formation of geopolymeric gels, such as N–A–S–H or hybrid C–(A)–S–H gels when combined with calcium-rich precursors. Therefore, the role of WCT in one-part geopolymer repair binders is expected to be supplementary rather than primary, influencing microstructural packing, dimensional stability, and long-term durability rather than driving reaction.

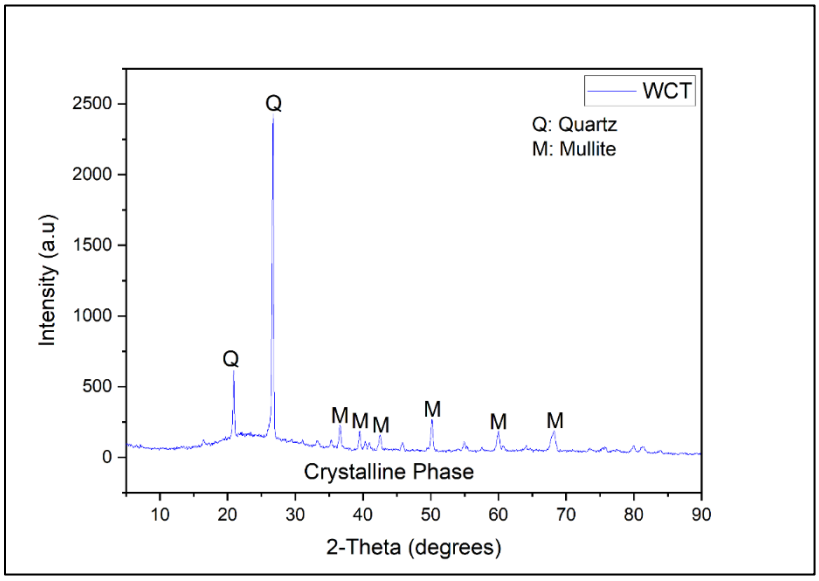


Figure 4.3 X-Ray Diffraction Patterns of WCT (Q = Quartz (SiO2: PDF no. 01-078-1254); M = Mullite ($3Al_2O_3 \cdot 2SiO_2$): PDF no. 01-079-1456)

4.2.3 Microstructure Analysis

A microstructural examination of GGBS was conducted using scanning electron microscopy (SEM) in backscattered electron (BSE) mode, as shown in Figure 4.4. The micrographs were captured at a magnification of 500× to assess particle morphology and surface characteristics. The raw GGBS particles exhibited irregular and angular morphologies, characterised by sharp edges and non-uniform outlines. Most particles appeared as compact, fractured grains with rough surface textures. Particle sizes measured within the field of view ranged from approximately 16 μm to 45 μm. The angular geometry and rough surface texture suggest a relatively high specific surface area, which is expected to enhance dissolution under alkaline activation but may simultaneously increase water demand in fresh geopolymer mixtures. In contrast, the presence of smooth, glassy surface patches is consistent with the amorphous phase identified in the XRD analysis, confirming the presence of both reactive glassy domains and less reactive crystalline regions within the GGBS particles.

The observed morphology is characteristic of rapidly cooled blast-furnace slag and reflects the combined influence of the ironmaking process and subsequent grinding operations. Similar angular and rough surface features have been reported by Jamil et al. (2021), who attributed such morphologies to mechanical size reduction processes, including ball milling and vibratory milling. These processing methods introduce surface defects and microcracks, which can further promote ion release and accelerate geopolymerisation reactions. This microstructural is advantageous for geopolymer binder production, as it promotes the release of reactive calcium and silicate species, thereby contributing to rapid gel formation and improved mechanical performance.

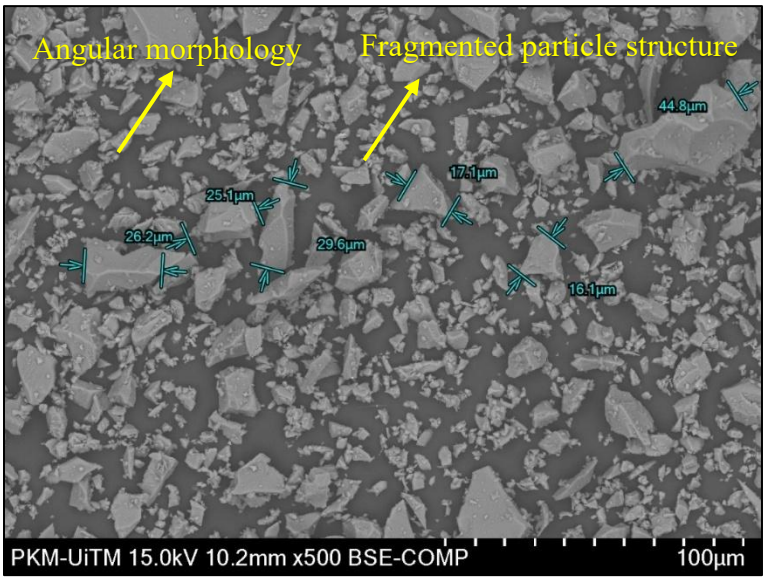


Figure 4.4 SEM Micrograph of GGBS Particles at 500× Magnification (BSE mode)

The microstructural characteristics of the raw FA were examined using SEM in BSE mode, as shown in Figure 4.5. The FA particles mainly exhibit a spherical morphology with smooth external surfaces, together with a smaller proportion of irregularly shaped particles and agglomerated particles. A significant number of hollow spherical particles, commonly referred to as cenospheres, were observed throughout the microstructure. The particle sizes within the analysed field ranged from approximately 10 µm to 35 µm. The formation of these spherical and hollow structures is characteristic of FA produced during coal combustion, where molten mineral matter undergoes rapid cooling. The smooth and spherical morphology of FA particles is known to impart a ball-bearing effect, which enhances particle packing efficiency and improves the workability of fresh geopolymer mixtures.

From a reactivity perspective, the spherical morphology improved dispersion of particles and more uniform contact with the alkaline activator, which can promote early-stage dissolution of the amorphous aluminosilicate phase. This behaviour has been reported to contribute to enhanced geopolymerisation rate during the initial reaction stages (Yan et al., 2024). However, these acceptable rheological characteristics, the smooth surface texture and relatively low specific surface area of FA particles can also limit the rate of dissolution compared to more angular and rough precursors such as GGBS. This microstructural feature is consistent with the slow reaction rate and delayed strength development commonly observed in FA-based geopolymer. In contrast, irregular particles and ferrosphere-rich area containing higher iron oxide content were

only rarely observed. Their limited presence suggests that the geopolymerisation behaviour of the FA in this study was primarily influenced by the spherical glassy particles rather than iron-rich crystalline inclusions. Agglomerated structures were also observed locally, which may reduce effective surface area and contribute to incomplete reaction of some FA particles, resulting in unreacted particle cores within the geopolymer matrix.

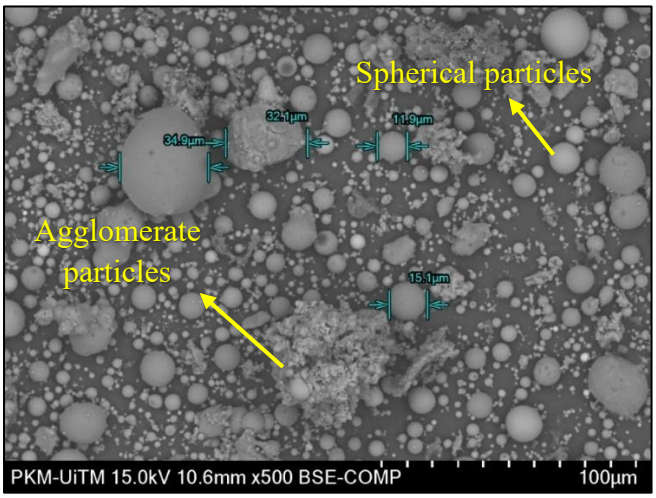


Figure 4.5 SEM Micrograph of FA Particles at 500× Magnification (BSE mode)

Figure 4.6 shows the SEM image of the WCT. The microstructure is characterised by angular and irregular particles with sharp edges and fractured, shard-like morphologies, reflecting the crushing and milling processes applied during material preparation. The particle surfaces are largely rough and uneven, with fine particles distributed between larger fragments, partially filling inter-particle voids. The measured particle sizes within the imaged area range from approximately 8.72 µm to 17.7 µm, which are notably smaller than those observed for FA and comparable to the finer fraction of GGBS. The angular geometry and textured surfaces indicate a relatively high specific surface area, which can increase inter-particle friction and consequently, increase water demand in fresh geopolymer mixtures. Unlike the spherical morphology of FA, the absence of a ball-bearing effect in WCT particles may adversely affect workability unless compensated through mix optimisation or the inclusion of more reactive or finer precursors.

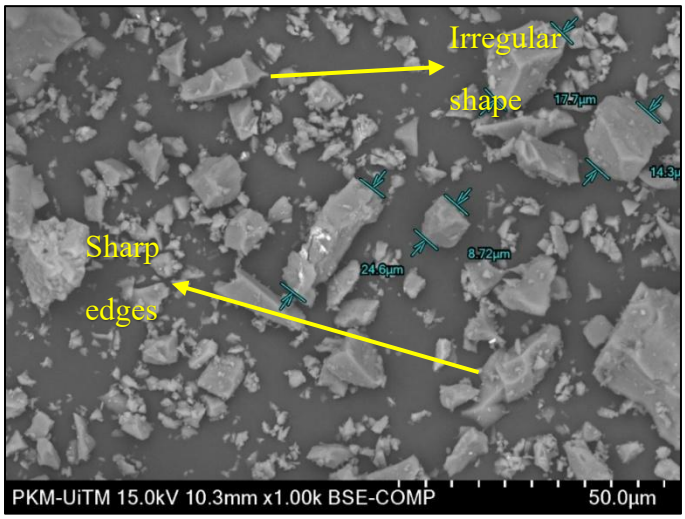


Figure 4.6 SEM Micrograph of WCT Particles at 500× Magnification (BSE mode)

From a reactivity standpoint, the angular morphology and rough surfaces may enhance mechanical interlocking and particle matrix bonding within the hardened geopolymer. However, the mainly crystalline nature of WCT, as evidenced by XRD analysis identifying quartz and mullite as the principal phases, limits its chemical reactivity under alkaline activation. As a result, the increased surface roughness, dissolution of aluminosilicate species from WCT is expected to be restricted, and a significant fraction of the particles may remain partially unreacted within the geopolymer matrix. These observations are consistent with the findings of Fu et al. (2023), who reported that ceramic tile waste typically exhibits angular, shard-like particles dominated by crystalline quartz and mullite phases. Consequently, WCT is more appropriately regarded as a secondary aluminosilicate source or filler material in geopolymer matrices, contributing primarily to microstructural densification, interfacial bonding, and dimensional stability rather than serving as a highly reactive precursor.

4.3 Phase 2: Optimisation of GGBS Replacement and Solid Precursor to Solid Activator

This section presents the Phase 2 optimisation of the one-part geopolymer binder by evaluating the effects of GGBS replacement and the solid precursor solid activator ratio. The GGBS content was varied at 10%, 20%, 30%, 40%, and 50% by replacement of the precursors (FA and WCT). In addition, solid precursor to solid activator ratios were investigated, namely 90:10 and 80:20, based on the total binder.

The performance of each mix was assessed in terms of fresh properties (workability and setting time) and hardened performance, with compressive strength used as reference. The optimum combination was determined by balancing constructability requirements with strength development suitable for repair binder applications.

4.3.1 Workability Analysis

Figure 4.7 shows the workability of fresh one-part geopolymer repair binders with an activator content of 10% of the total binder and a common water-to-binder ratio of 0.35. The measured flow diameters for the GGBS-FA and GGBS-WCT was in the range of 160 mm to 260 mm. The GGBS mixture showed the lowest workability, which can be attributed to the high calcium content and angular particle morphology of GGBS that promote rapid early reaction and increased inter-particle friction. As the proportion of FA or WCT increased through partial replacement of GGBS, a general improvement in workability was observed. This effect was most pronounced for binders containing 50% FA and 50% WCT (i.e., GGBS50–FA–ss10 and GGBS50–WCT–ss10).

The increase in workability with FA incorporation is primarily attributed to the spherical morphology and smooth surface texture of FA particles, as confirmed by SEM analysis, which impact a ball-bearing effect that reduces friction and improves particle filling. In contrast, WCT containing binders exhibited comparatively lower workability than FA blends at similar replacement levels. This behaviour is consistent with the angular, shard-like morphology of WCT particles observed in SEM micrographs, which increases inter-particle friction and limits flow despite partial void-filling by fine particles. These observations demonstrate that workability is strongly governed by precursor morphology. Specifically, spherical FA particles promote lubricating action and reduced interlocking, whereas angular WCT particles increase resistance to flow. Similar trends have been reported by Akmalaiuly et al. (2023), who observed enhanced fresh-state rheology in FA-rich geopolymer due to improved lubrication and packing efficiency.

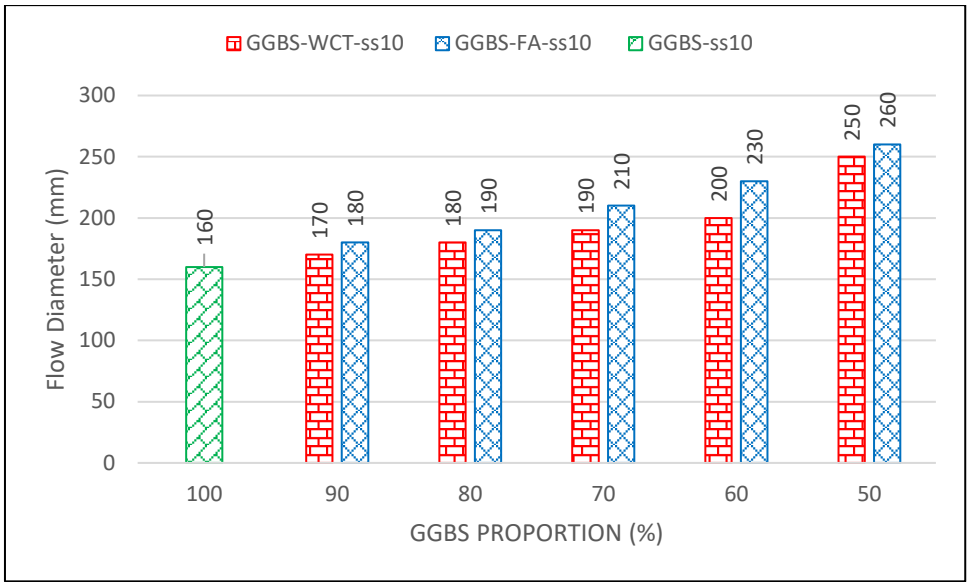


Figure 4.7 Workability of GGBS–FA and GGBS–WCT One-Part Geopolymer Repair Binders with 10% Activator Content

To further evaluate the influence of activator content, the solid activator dosage was increased from 10% to 20% of the total binder, as illustrated in Figure 4.8. A consistent reduction in workability was observed across all mixtures. The GGBS binder exhibited a reduction of approximately 25% in flow diameter, while GGBS–FA and GGBS–WCT based hybrid one-part geopolymer repair binders showed reductions exceeding 20% compared to their corresponding 10% activator. This decrease in workability is attributed to the increased concentration of sodium metasilicate, which accelerates early-stage dissolution and promotes rapid formation of initial gel products. The negative correlation between activator content and workability indicates that higher alkali availability increases early geopolymerisation reactions, reducing the time for effective flow. Although powder-activated geopolymer generally exhibit a more gradual alkali release compared to liquid-activated (Mohammed et al., 2019), increasing the solid activator content still significantly influences fresh-state. Consequently, excessive activator dosage can compromise workability potential gains in reaction and strength development.

Overall, the workability behaviour of the one-part geopolymer repair binders is controlled by a combined effect of precursor morphology and activator dosage. FA incorporation enhances flowability through particle shape effects, whereas higher GGBS and activator contents reduce workability due to accelerated reaction and increased inter-particle friction. These findings highlight the need to balance fresh-state

constructability with chemical reactivity when determining the optimum binder composition for repair applications.

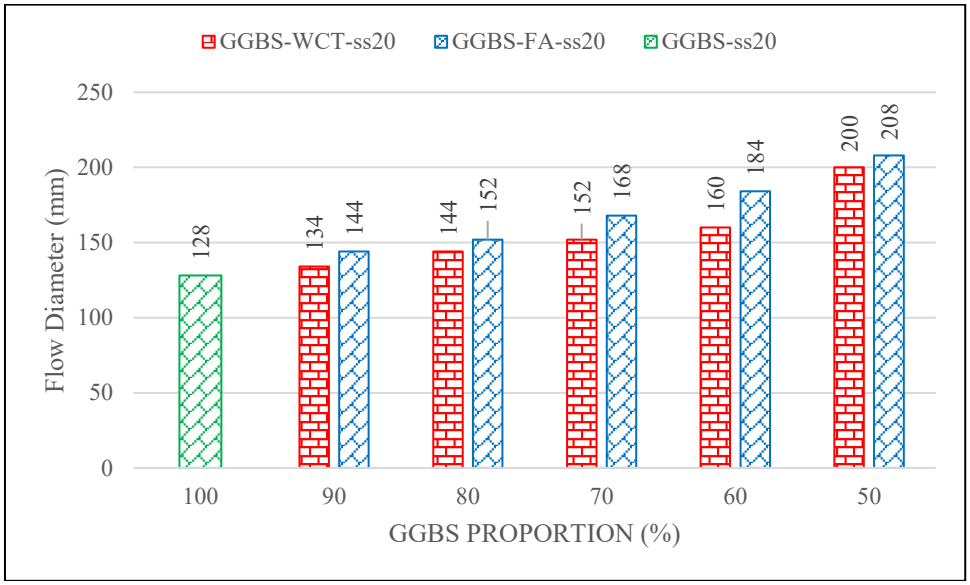


Figure 4.8 Workability of GGBS–FA and GGBS–WCT One-Part Geopolymer Repair Binders with 20% Activator Content

4.3.2 Setting Time Analysis

Figure 4.9 presents the setting time behaviour of the one-part geopolymer repair binders prepared with an activator content of 10% the total binder. The results show that the difference between the initial and final setting times gradually decreased with changes in binder composition, indicating an acceleration of hardening as reaction increased. For both GGBS–FA and GGBS–WCT based hybrid one-part geopolymer repair binders, the final setting times were within the range of approximately 62 to 84 minutes, which is considered suitable for practical repair applications. Among the mixtures, the binders with low GGBS replacement levels, namely GGBS10–FA–ss10 and GGBS10–WCT–ss10, exhibited relatively short initial setting times of 32 minutes and 22 minutes, respectively.

This behaviour can be attributed to the higher availability of calcium ions released from GGBS, which accelerates early geopolymerisation reactions and promotes rapid gel formation. The role of calcium in reducing setting time, as Ca^{2+} ions enhance charge balancing and faster condensation of aluminosilicate species compared to sodium (Ghafoor et al., 2025; Wei et al., 2024). In general, increasing GGBS content

resulted in shorter initial and final setting times, reflecting the enhanced reaction associated with calcium-rich precursors. This trend was particularly evident in the GGBS–WCT based hybrid one-part geopolymer repair binders, where setting time decreased progressively as the GGBS proportion increased. The presence of crystalline quartz and mullite in WCT may have contributed to a slower reaction rate, as these phases are relatively stable and less reactive during geopolymerisation.

In contrast, the GGBS–FA based hybrid one-part geopolymer repair binders exhibited an increase in setting time as the GGBS content decreased and FA replacement increased. This behaviour is attributed to the lower calcium content and slower dissolution rate of FA, which delays the formation of calcium containing reaction. Moreover, FA particles absorb less water and possess smoother spherical surfaces, resulting in higher free water availability in the fresh paste, which delays the hardening process. The lack of early-age C–A–S–H formation in FA-rich has been reported to contribute to delayed setting compared to GGBS binders (Cheah et al., 2017). Although no significant difference was observed in the initial setting times between GGBS–FA and GGBS–WCT at comparable GGBS contents, the final setting time was consistently shorter for GGBS–FA mixtures. This indicates that, while early hardening may be similar, the subsequent hardening process is influenced by differences in dissolution behaviour and gel development between FA and WCT binders.

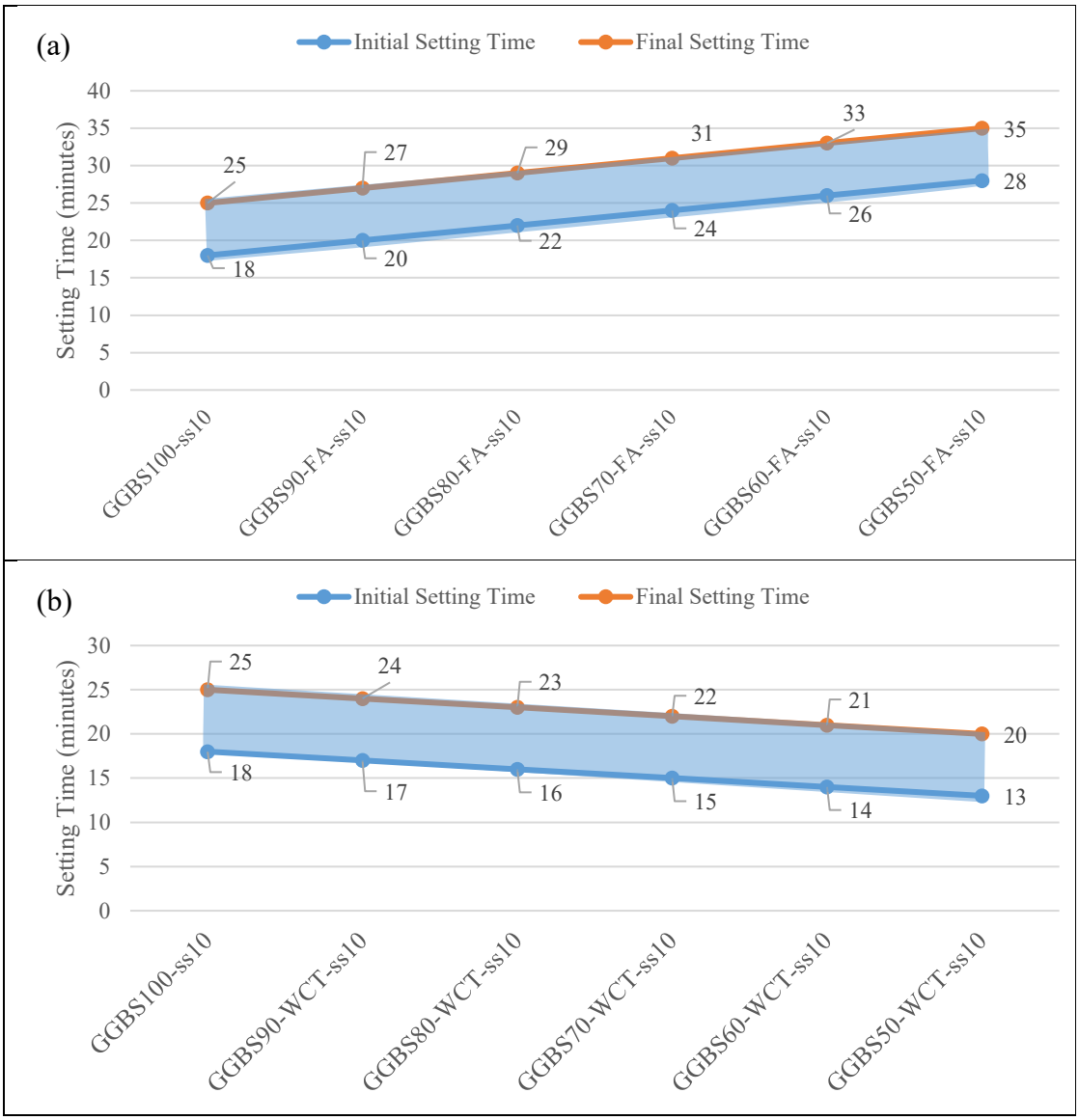


Figure 4.9 Setting Time Development of One-Part Geopolymer Repair Binders with 10% Activator Content: (a) GGBS–FA and (b) GGBS–WCT

Figure 4.10 illustrates the effect of increasing the solid activator content from 10% to 20% of the total binder on the setting time behaviour of the one-part geopolymer repair binders. High reduction in both initial and final setting times was observed across all binder compositions, indicating a high sensitivity of setting behaviour to activator dosage. For the GGBS binder, increasing the activator content resulted in a significant shortening of the final setting time, reflecting accelerated reaction induced by the higher concentration of sodium metasilicate. Similar trends were observed for the GGBS–WCT and GGBS–FA, although the amount of reduction varied depending on precursor composition.

In general, GGBS–WCT binder exhibited a more significantly decrease in setting time compared to GGBS–FA binder, The observed reduction in setting time with increased activator dosage can be attributed to the enhanced alkalinity and ionic concentration, which promotes rapid dissolution of reactive aluminosilicate species and accelerates gel nucleation. In powder-activated the dissolution of anhydrous sodium metasilicate is accompanied by localised heat release, further intensifying early reaction (Chen et al., 2021). This effect shortens the time required for the formation of reaction products, including sodium aluminosilicate hydrate (N–A–S–H) and calcium-containing gels such as C–(A)–S–H in calcium-rich mixtures.

In GGBS–FA binder, although increased activator content accelerated setting, the effect was moderated by the lower calcium availability and slower dissolution rate of FA. Conversely, in GGBS–WCT, the setting behaviour remained strongly by GGBS content, as the largely crystalline nature of WCT contributes minimally to early chemical reactions. As a result, the reduction in setting time with higher activator dosage is primarily controlled by the interaction between sodium metasilicate and calcium-bearing phases originating from GGBS. From a practical perspective, while increasing the solid activator content enhances early hardening and may be advantageous for rapid repair applications, excessive acceleration can compromise workability and placement time, as discussed in Section 4.5.1. Therefore, the selection of activator dosage must balance early setting requirements with sufficient open time to ensure constructability and uniform application in repair.

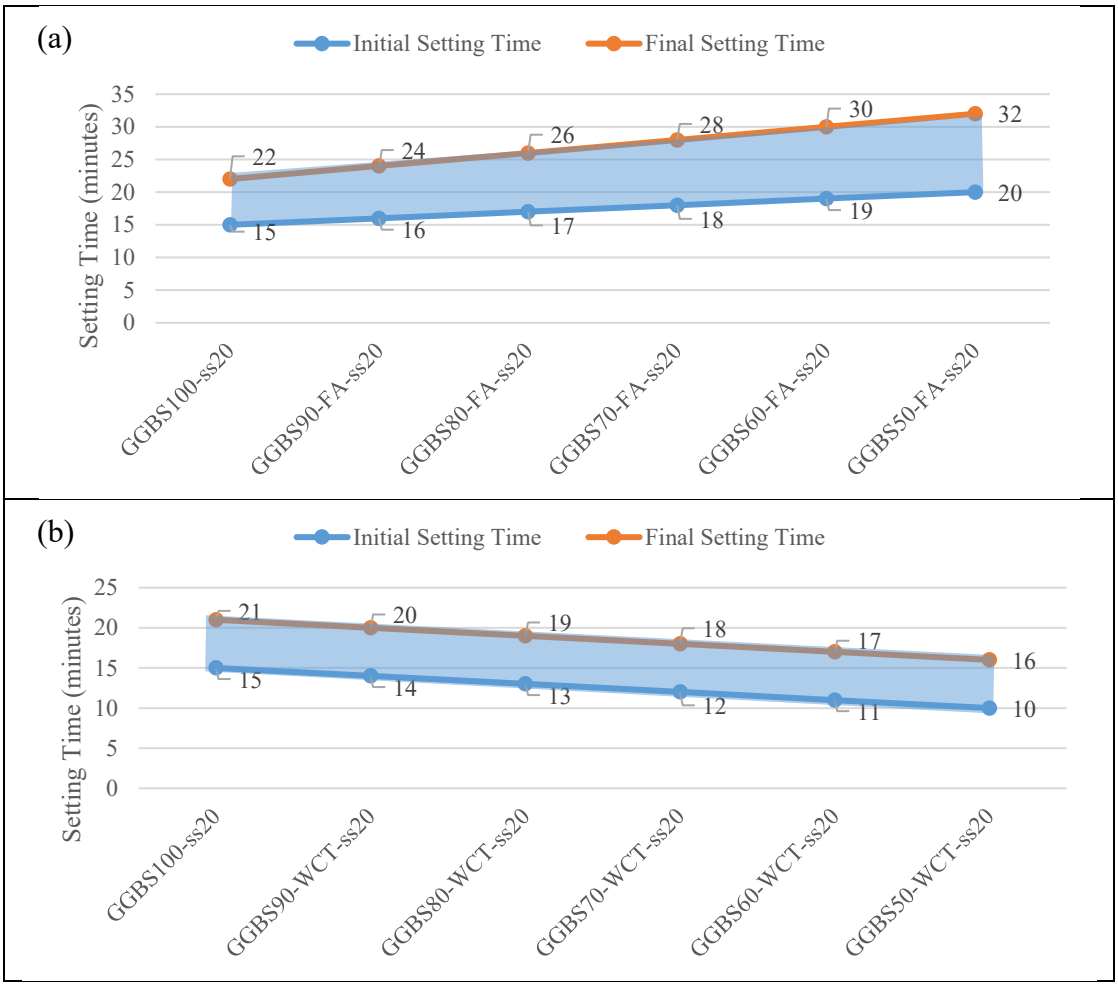


Figure 4.10 Setting Time Development of One-Part Geopolymer Repair Binders with 20% Activator Content: (a) GGBS–FA and (b) GGBS–WCT

4.3.3 Compressive Strength Analysis

Figure 4.11 presents the compressive strength development of GGBS-based one-part geopolymer repair binders at curing ages of 3, 14, and 28 days under ambient conditions. The GGBS specimen with 10% activator content (GGBS100–ss10) exhibited a high early compressive strength of 54.17 MPa at 3 days, increasing to 63.15 MPa at 14 days and 72.22 MPa at 28 days. This behaviour confirms the strong contribution of calcium-rich GGBS to rapid strength development through early formation of calcium containing binding phases under sodium metasilicate activation. However, although the GGBS demonstrated rapid early strength gain, its long-term strength development decreased relative to some mixtures, indicating that high calcium availability alone does not necessarily optimise later-age performance.

For the GGBS–FA based hybrid one-part geopolymer repair binders, the compressive strength results indicate a clear dependence on GGBS content. Among these mixtures, GGBS70–FA–ss10 achieved the highest 28-day compressive strength of 69.16 MPa. Increasing the FA content from 40% to 50% did not result in further strength enhancement, suggesting that excessive replacement of GGBS by FA reduce the calcium required for the formation of C–A–S–H gels. In FA-rich mixtures strength development is primarily led by the formation of N–A–S–H gel networks (Buruberri et al., 2019; Doan et al., 2024), which are known to show slower reaction rates and lower early-age strength compared to calcium-rich mixtures. This observation highlights a key limitation of FA as a primary precursor in one-part geopolymer binders under ambient curing, particularly for applications requiring rapid strength gain.

In contrast, the based hybrid one-part geopolymer repair binders consistently show higher compressive strength compared to both GGBS and GGBS–FA binders. Notably, the lowest 28-day strength recorded for GGBS90–WCT–ss10 mixtures (70.75 MPa) exceeded the maximum strength achieved by the GGBS–FA mixtures by approximately 3%. While WCT is largely crystalline and show limited initial reactivity, its high SiO_2 content (68.0%), as identified by XRF analysis (Table 4.3), provides a chemically good environment for geopolymerisation when combined with calcium supplied by GGBS. This finding supports previous studies indicating that precursor chemistry, rather than crystallinity alone, plays a decisive role in governing gel formation and mechanical performance in solid-activated binders (Çelikten et al., 2024).

The improved performance of WCT based hybrid one-part geopolymer repair binders cannot be attributed to filler effects alone. Although the angular morphology of WCT particles may enhance mechanical interlocking, the observed strength enhancement suggests hybrid gel network formation within the matrix. The calcium alumino-silicate hydrate (C–A–S–H) gels and aluminosilicate networks contributes to a denser and more continuous binding structure (He et al., 2020; Zhang et al., 2023). This hybrid gel mixtures contrasts with FA-dominated binders, where strength is largely governed by N–A–S–H bonding, which is less effective in promoting early reduction (Buruberri et al., 2019).

Furthermore, the relative performance differences between FA and WCT based hybrid one-part geopolymer repair binders highlight an important balance in precursor selection. Although FA shows a higher amorphous content than WCT, its lower silica

availability and limited calcium contribution limits the extent of hybrid gel formation under the investigated activation conditions. Conversely, WCT, shows its crystalline nature, contributes a high silica supply that complements the calcium-rich GGBS, resulting in more effective chemical bonding and strength development (Yildirim et al., 2022).

For further verification, an independent t-test was carried out to determine whether there was a significant difference between the mean compressive strength values of different geopolymer binder compositions. Null Hypothesis, H_0: The geopolymer binder composition has no significant effect on the compressive strength performance. Proposed Hypothesis, H_1: The geopolymer binder composition has a significant effect on the compressive strength performance. From analysis, it is found that there is no significant difference in compressive strength values between GGBS70-WCT-ss10 and GGBS100-ss10 at 0.05 level. For GGBS70-WCT-ss10, the analysis yielded a t_{stat} of 1.451 ($t_{stat} = 1.451 < t_{critical} = 4.27$, Do not reject H_0), which was not significant at the specified level ($p = 0.283$). It can be concluded that the difference between GGBS70-WCT-ss10 and GGBS100-ss10 does not significantly influence the compressive strength performance of geopolymer binder mixtures.

The highest compressive strengths at 3, 14, and 28 days were obtained for the GGBS70–WCT–ss10 mixture, which achieved 43.65 MPa, 58.40 MPa, and 73.15 MPa, respectively. This mixture, comprising 60% GGBS and 30% WCT with a 10% solid activator content, demonstrates that optimum mechanical performance is achieved through balanced precursor chemistry rather than maximising GGBS content alone. The independent t-test further showed no significant difference between GGBS70–WCT–ss10 and GGBS100–ss10 ($t_{stat} = 1.451$, $p = 0.283 > 0.05$), indicating comparable strength performance while utilising WCT as a replacement GGBS. The results confirm that the quantity, continuity, and formation rate of geopolymeric gel phases are the dominant factors governing mechanical performance in hybrid binders (Zhang et al., 2023).

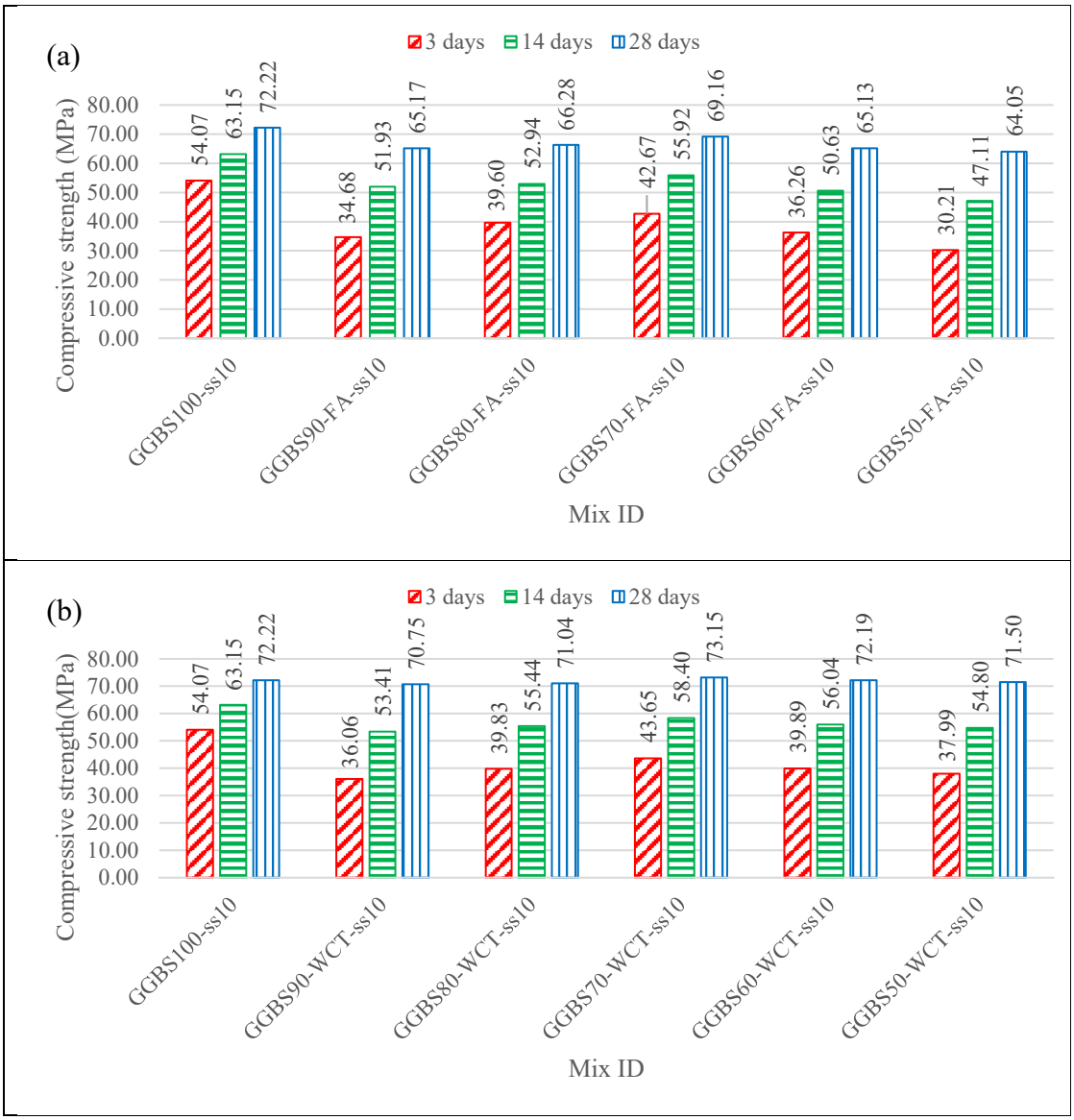


Figure 4.11 Compressive Strength Development of One-Part Geopolymer Repair Binders with 10% Activator Content: (a) GGBS–FA and (b) GGBS–WCT

The activator content of the studied mixtures was increased from 10% to 20% of the total binder to investigate its influence on compressive strength development. As shown in Figure 4.12, increasing the activator dosage resulted in a reduction in compressive strength at all curing ages for all binder compositions. For the GGBS based hybrid one-part geopolymer repair binders, increasing the activator content led to strength reductions of approximately 9%, 8%, and 7% at 3, 14, and 28 days, respectively. Similar trends were observed for the GGBS–WCT based hybrid one-part geopolymer repair binders, which exhibited reductions exceeding 10% at early ages and approximately 7% at 28 days. In the case of GGBS–FA based hybrid one-part geopolymer repair binders, the highest 28-day compressive strength obtained at 20%

activator was 64.97 MPa, representing a reduction of approximately 7% compared to the corresponding 10% activator mixtures. For the GGBS–WCT based hybrid one-part geopolymer repair binders, the highest 28-day strength recorded at 20% activator was 68.96 MPa, corresponding to a reduction of approximately 5.7% relative to the 10% activator mixture.

The reduction in compressive strength with increasing activator dosage can be attributed to several interacting mechanisms. First, in one-part geopolymer repair binders, the solid activator contributes to the total binder and partially replaces reactive precursor material. Increasing the activator proportion therefore reduces the relative amount of aluminosilicate source available for gel formation, which can limit strength development. Similar observations have been reported in solid-activated binders, where excessive activator content dilutes the reactive precursor fraction and negatively affects mechanical performance (Migunthanna et al., 2021). Secondly, higher activator contents introduce excess alkali species into the geopolymer matrix. While sufficient alkalinity is required to initiate dissolution, excessive alkali concentrations can lead to the presence of unreacted or weakly bound alkali salts within the hardened matrix, increasing porosity and reducing structural integrity (Cong & Cheng, 2021). This effect is particularly detrimental under ambient curing conditions, where rapid alkali release may not be fully balanced by gel formation.

Thirdly, excessive alkalinity enhances silica dissolution beyond the optimal level required for geopolymer gel formation. The presence of excess dissolved silica can disrupt the Si/Al balance, leading to poorly polymerised networks and the formation of weak or unstable phases, ultimately reducing compressive strength. Similar strength reductions associated with over-activation have been reported in alkali-activated slag and hybrid geopolymer (Escalante-García et al., 2003). Overall, although increasing activator content accelerates early reaction, the results clearly demonstrate that excessive activator dosage is negatively affects to compressive strength development. Based on the experimental findings, an activator content of 10% by mass of the total binder provides a better balance between optimal alkalinity, effective gel formation, and mechanical performance. Therefore, 10% solid activator was identified as the optimum dosage for GGBS-based one-part geopolymer repair binders activated with anhydrous sodium metasilicate.

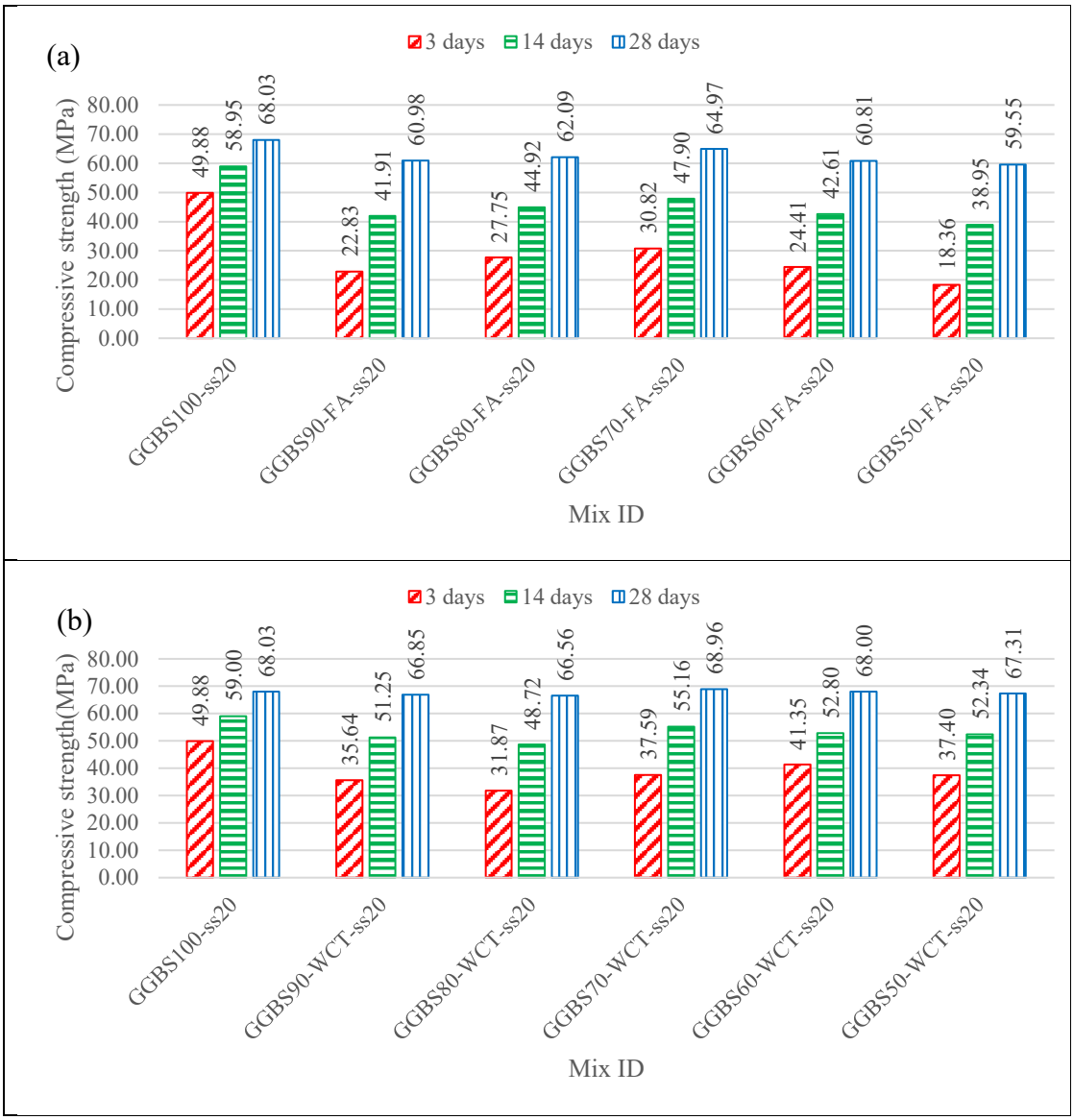


Figure 4.12 Compressive Strength Development of One-Part Geopolymer Repair Binders with 20% Activator Content: (a) GGBS–FA and (b) GGBS–WCT

4.4 Phase 3: Geopolymerisation Reaction of GGBS-WCT Based Hybrid One-Part Geopolymer Repair Binders

Geopolymerisation involves the alkaline dissolution of aluminosilicate precursors, followed by gel formation reactions that develop a rigid, three-dimensional aluminosilicate gel network. In GGBS–WCT base hybrid one-part geopolymer repair binders, reaction behaviour is primarily controlled by interactions between the solid alkali activator and the reactive aluminosilicate contributed by GGBS and WCT. These interactions influence the nature of the reaction products and, consequently, the resulting matrix structure. In this phase, a series of binder formulations incorporating

10%, 20%, 30%, 40%, and 50% WCT (as precursor replacement levels) were evaluated while maintaining the solid precursor-to-solid activator ratio at 90:10 (optimum from Phase 2) to investigate reaction evolution. The geopolymerisation reaction was characterised using XRF to determine chemical composition, XRD for phase identification, and SEM (with EDX, where applicable) to examine microstructural and elemental features.

4.4.1 Chemical Composition of GGBS–WCT Based Hybrid One-Part Geopolymer Repair Binders

The chemical composition of GGBS–WCT based hybrid one-part geopolymer repair binders plays an important role in determining the geopolymerisation reactions, gel structures, and mechanical properties at 28 days. XRF analysis was conducted to evaluate the chemical composition trends across varying levels of WCT substitution (0% to 50%). The analysis focused on key oxides SiO_2, CaO, Al_2O_3, and Fe_2O_3 which play key roles in the formation and development of geopolymer gels.

Based on the raw material characterisation discussed in Section 4.2, WCT is characterised by high silica and low calcium contents, while GGBS is calcium-rich with moderate silica and alumina contents. As shown in Figure 4.13, SiO_2 content increased continuously from 47.26 wt% in GGBS100 to 52.14 wt% in GGBS50–WCT, reflecting the increasing contribution of silica WCT. This trend indicates a shift in the geopolymerisation reaction towards higher silica and alumina availability and reduced calcium content as WCT replacement increases. The high SiO_2 content originates from feldspar and clay minerals used in ceramic tile manufacturing (Azevedo et al., 2020; Fu & Lee, 2024). Although WCT contains crystalline silica, the overall increase in available silica enhances geopolymerisation under solid activator conditions by promoting aluminosilicate network.

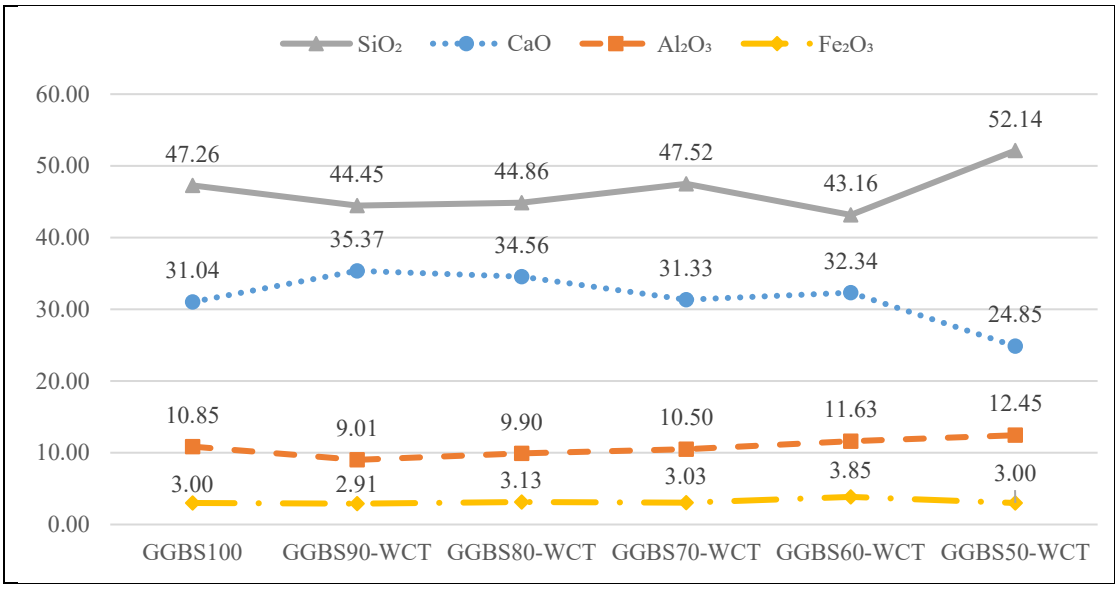


Figure 4.13 Chemical Composition of GGBS–WCT One-Part Geopolymer Repair Binders

However, CaO content decreased from 31.04 wt% to 24.85 wt% with increasing WCT replacement, corresponding to the reduced proportion of GGBS in the binder. This reduction in calcium availability limits the extent of calcium aluminosilicate hydrate (C–A–S–H) gel formation, as expressed in Equation (4.1), and progressively change the reaction mechanism towards sodium aluminosilicate gel formation. Under suitable alkalinity, sodium ions activate the formation of N–A–S–H gel, as represented in Equation (4.2). In hybrid containing both calcium and sodium species, mixed C–(N)–A–S–H gels are commonly formed Equation (4.3), combining the advantages of rapid calcium hardening and stable aluminosilicate network formation (Provis & Deventer, 2014; Zhang Z. et al., 2024).

$$Ca^{2+} + [SiO_4]^{4-} + [AlO_4]^{5-} + H_2O \rightarrow (C–A–S–H)\ gel \quad (4.1)$$

$$Na^{+} + [SiO_4]^{4-} + [AlO_4]^{5-} + H_2O \rightarrow (N–A–S–H)\ gel \quad (4.2)$$

$$Ca^{2+} + Na^{+} + [SiO_4]^{4-} + [AlO_4]^{5-} + H_2O \rightarrow (C–(N)–A–S–H)\ gel \quad (4.3)$$

The formation of this hybrid gel enhances both early strength and long-term durability due to strong bonding interactions between calcium-rich and sodium-based gel networks. Al_2O_3 content also increased slightly, from 10.85 wt% to 12.45 wt%, with increasing WCT replacement, contributing to enhanced aluminosilicate framework development even at moderate levels. Fe_2O_3 content remained relatively stable (2.91–

3.85 wt%) across all mixtures, indicating minimal impact on geopolymer gel formation or reactivity. However, iron may still participate in minor substitutions or crystalline phase (Jumaa et al., 2022).

Molar ratio analysis illustrates the evolution of geopolymer gel chemistry. As shown in Figure 4.14 the Si/Al ratio increased to a highest value of 4.93 at 10% WCT replacement before decreasing slightly to 4.19 at 50% WCT. The Ca/Al ratio decreased from 2.86 to 2.00 with increasing WCT content, reflecting reduced calcium availability for C–A–S–H formation. Meanwhile, the Al/Si ratio remained relatively stable between 0.20 and 0.24, indicating that the aluminosilicate framework remained within a good compositional range for geopolymer gel formation. An increase in Si/Al ratio generally promotes the formation of amorphous N–A–S–H gel networks; however, very high Si/Al ratios do not always translate into higher strength, as gel composition and calcium availability remain key factors.

As WCT replaces GGBS, the decreasing Ca/Al ratio indicates a progressive transition from calcium-dominated C–A–S–H gels towards hybrid C–(N)–A–S–H gels or N–A–S–H. This compositional shift influences both setting behaviour and strength development. According to Ghafoor et al. (2025), higher GGBS contents shorten setting time by accelerating early dissolution and gel nucleation, while reduced calcium availability has the opposite effect, leading to extended setting and delayed hardening. Maintaining an appropriate alumina supply through the solid activator (Al/Si = 0.2–0.25) is therefore critical to maintain gel structure and sustain strength development as silica content increases.

Among the compositions, the GGBS70–WCT binder (30% WCT replacement) exhibited the most balanced oxide composition and molar ratios (Si/Al = 4.53; Ca/Al = 2.98; Al/Si = 0.22), corresponding to the highest compressive strength observed in this study. This composition maintains sufficient calcium to develop a dense C–(A)–S–H network while providing sufficient silica and alumina to form stable N–A–S–H networks. The resulting hybrid gel structure promotes both early mechanical strength and long-term chemical stability (Azevedo et al., 2020; Zhang Z. et al., 2024).

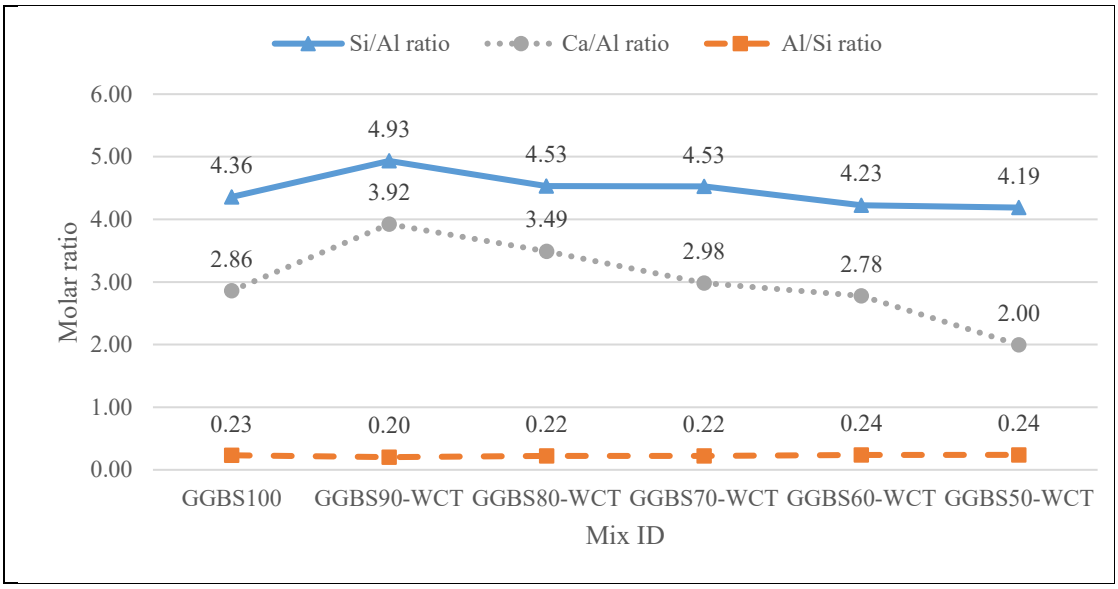


Figure 4.14 Molar Ratio of GGBS–WCT One-Part Geopolymer Repair Binders

4.4.2 Phase Analysis of GGBS-WCT Based Hybrid One-Part Geopolymer Repair Binders

XRD analysis was conducted to identify the crystalline and amorphous phases formed in GGBS–WCT based hybrid one-part geopolymer repair binders activated using 10% solid activator and cured under ambient conditions for 28 days. Figure 4.15 presents the XRD patterns of binders with WCT replacement levels ranging from 0% (GGBS100) to 50% (GGBS50–WCT). The GGBS100 specimen exhibited a largely amorphous character, characterised by a broad hump centred between 20° and 35° (2θ). This observation is commonly associated with the formation of calcium–alumino–silicate–hydrate (C–A–S–H) type gels, which act as the primary binding phase in calcium-rich geopolymer. The dominance of this amorphous indicates extensive dissolution of GGBS and rapid gel formation under alkaline activation.

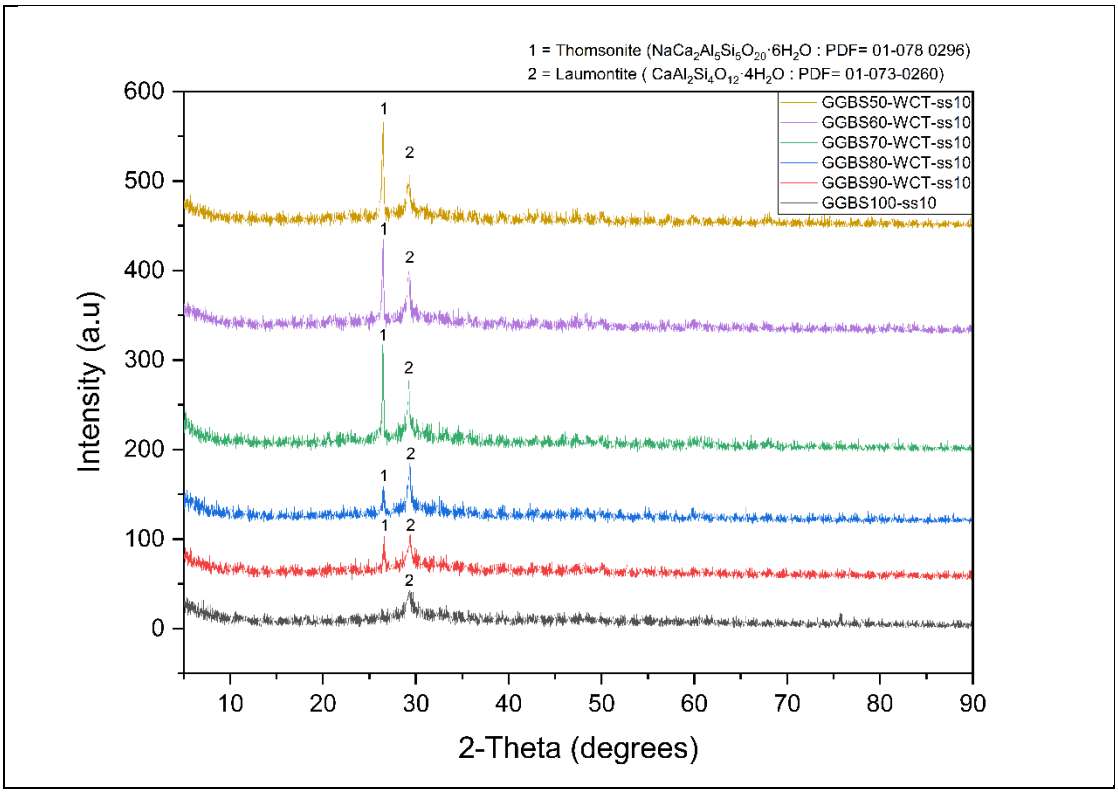


Figure 4.15 Diffractogram Patterns of Different Specimens, GGBS-WCT (1 = Thomsonite ($NaCa_2Al_5Si_5O_{20}·6H_2O$: PDF no. 01-078-0296); (2 = Laumontite ($CaAl_2Si_4O_{12}·4H_2O$: PDF no. 01-073-0260)

With increasing WCT content, the XRD patterns progressively revealed sharper crystalline peaks corresponding to quartz (SiO_2) and mullite ($3Al_2O_3·2SiO_2$), originating from unreacted ceramic phases in WCT. These phases are largely inert under alkaline conditions and therefore do not contribute directly to gel formation; however, they may act as filler particles and nucleation sites that locally enhance microstructural densification (Azevedo et al., 2020; Fu & Lee, 2024). The increasing intensity of quartz and mullite peaks with higher WCT replacement confirms the partial reactivity of WCT and the continued presence of crystalline ceramic particles within the geopolymer matrix. Notably, at WCT contents (particularly 30% WCT), additional crystalline phases corresponding to zeolitic minerals were detected, including thomsonite ($NaCa_2Al_5Si_5O_{20}·6H_2O$) and laumontite ($CaAl_2Si_4O_{12}·4H_2O$). These phases are characteristic of sodium activated aluminosilicate and form under conditions of sufficient alkalinity and soluble Al–Si species availability (Chen C. et al., 2023). Their presence suggests that part of the silica and alumina released from WCT actively participated in geopolymerisation, contributing to the development of a more ordered aluminosilicate network.

The formation mechanisms of these zeolitic phases can be represented by Equations (4.4) and (4.5), where alkaline activation promotes the reorganisation of SiO_4 and AlO_4 tetrahedra into hydrated aluminosilicate structures. These zeolite-like phases, although crystalline, are structurally related to geopolymeric gels and have been reported to enhance long-term chemical stability and durability (Papa et al., 2017).

$$Na^{+} + 2Ca^{2+} + 5Al\,(OH)_4^{-} + 5SiO_2 + H_2O \rightarrow NaCa_2Al_5Si_5O_{20}\cdot 6H_2O \quad (4.4)$$

$$Ca^{2+} + 2Al\,(OH)_4^{-} + 4SiO_2 + H_2O \rightarrow CaAl_2Si4O_{12}\cdot 4H_2O \quad (4.5)$$

At higher WCT replacement levels (50% WCT), the XRD patterns displayed a stronger crystalline character dominated by quartz and mullite, accompanied by a reduced amorphous contribution and lower number of zeolitic peaks. This suggests that excessive WCT content limits the dissolution of reactive SiO_2 and Al_2O_3, thereby reducing gel formation and slowing geopolymerisation. The reduced availability of reactive aluminosilicate species at high WCT contents explains the observed decline in compressive strength at later ages, as previously discussed. Similar dilution effects have been reported when inert or low-reactivity ceramic wastes are incorporated beyond their optimum replacement level (Azevedo et al., 2020; Zhang Z. et al., 2024). Among all formulations, the GGBS70–WCT (30% WCT) binder exhibited the most balanced phase composition, combining a high proportion of amorphous gel with well-defined zeolitic phases. This hybrid phase composition supports the C–A–S–H and N–A–S–H type gels, forming a hybrid C–(N)–A–S–H network. Such hybrid gel are widely recognised for providing both rapid early-age strength and enhanced long-term durability, making them particularly suitable for semi-rigid pavement repair applications (Fu & Lee, 2024; Zhang Z. et al., 2024).

Overall, the XRD results confirm that controlled incorporation of WCT promotes beneficial phase evolution through partial geopolymerisation and zeolite formation, whereas excessive WCT content leads to phase dilution and reduced binder efficiency. These findings highlight the importance of optimising WCT replacement to balance reactivity and microstructural stability in hybrid one-part geopolymer repair binders.

4.4.3 Microstructure Analysis of GGBS-WCT Based Hybrid One-Part Geopolymer Repair Binders

Figure 4.16 (a to f) illustrates the SEM micrographs and corresponding EDX spectra GGBS–WCT hybrid one-part geopolymer repair binders with increasing WCT replacement levels from 0% to 50%, cured under ambient conditions. The microstructural development clearly reflects the progressive transition from calcium-dominated gel to sodium-rich aluminosilicate networks as the WCT content increases.

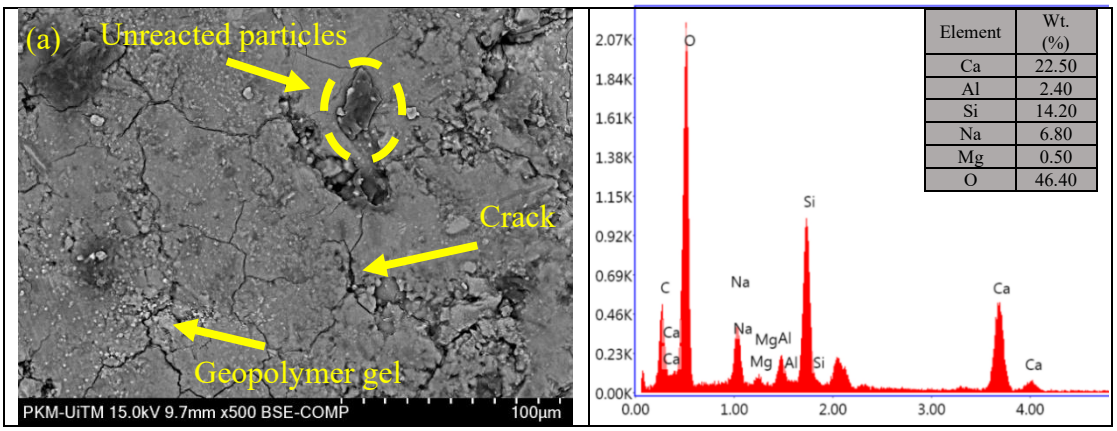
At 0% and 10% WCT, the geopolymer matrix is dense and well interconnected with limited porosity, as SEM shows a continuous gel phase surrounding partially reacted particles. EDX indicates high Ca and low Na at 0% WCT, confirming C–A–S–H as the dominant reaction product, supported by Ca/Si ratios of 1.58 (0% WCT) and 1.37 (10% WCT). At 10% WCT, increased Na and Al suggest the initial stage of hybrid C–(N)–A–S–H gel formation, while a moderate Si/Al ratio supports adequate network crosslinking. SEM samples were obtained from fractured compressive strength specimens to relate the observed microstructure to the measured strength performance at the same curing age. Since the specimens had undergone loading, some localised microcracks may have been induced during the compressive strength test.

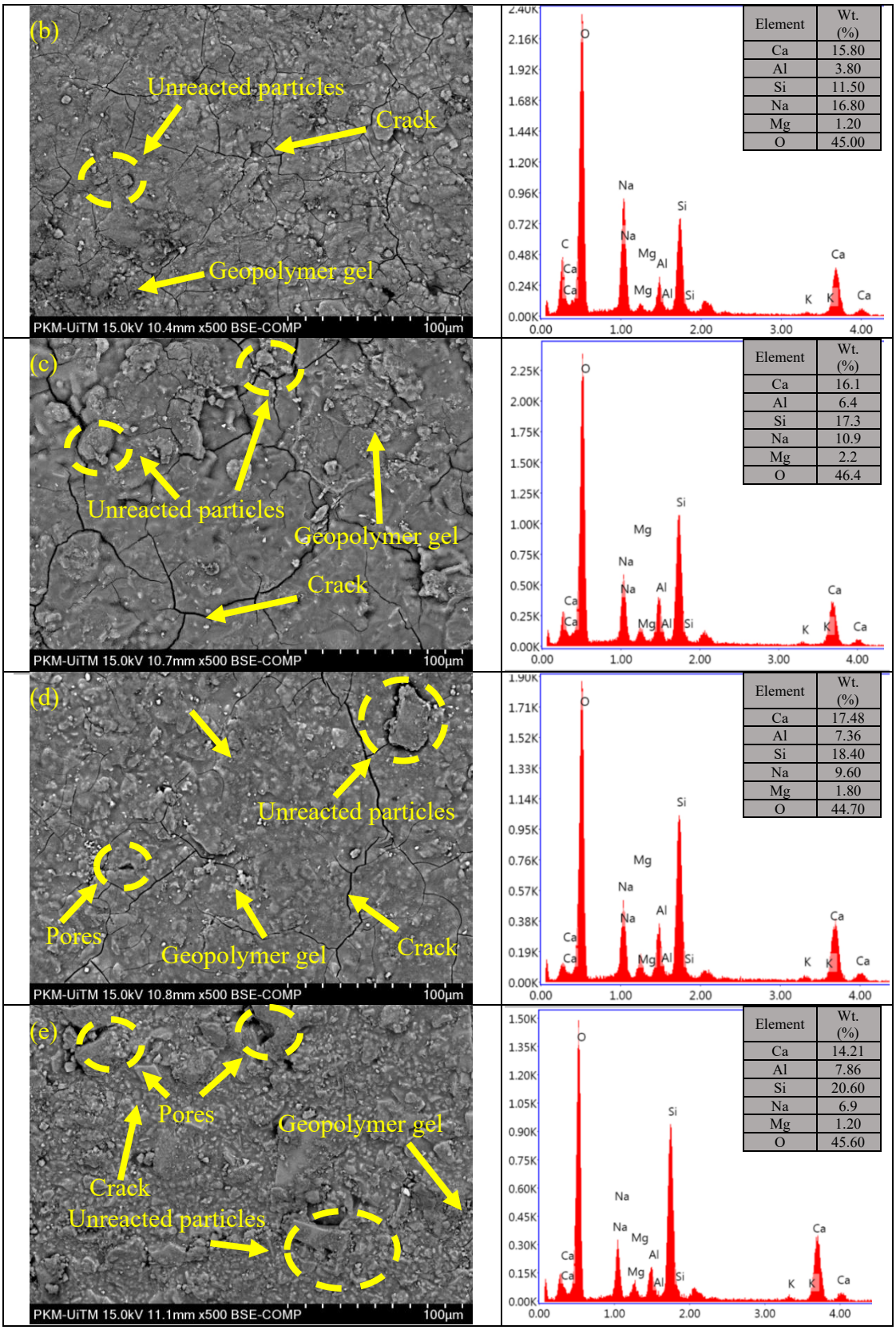
At 20% to 30% WCT, the geopolymer exhibits a highly compact and homogeneous microstructure, with a dense continuous gel matrix, minimal cracking, and reduced pore connectivity. SEM indicates effective binding between GGBS and WCT with limited unreacted area, while EDX shows reduced Ca alongside increased Si, Al, and Na, confirming a shift from Ca-dominated gels toward a hybrid gel structure. The Ca/Si ratio decreases to 0.93 to 0.95 and the Si/Al ratio stabilises at 2.7 to 2.8, which is consistent with the formation of a hybrid C–(N)–A–S–H network where calcium promotes early densification and sodium aluminosilicate enhance polymerisation and gel continuity. This balanced gel chemistry improves interfacial bonding and matrix connectivity, leading to lower porosity and more uniform stress distribution. Consequently, these mixes achieved the highest compressive strengths, indicating that 20% to 30% WCT provides an optimum chemical–microstructural balance, consistent with the hybrid gel formation reported by Luo et al. (2023).

At 40% to 50% WCT, the microstructure shows less dense microstructure, characterised by visible voids, microcracks, and unreacted ceramic particles within a

discontinuous gel matrix, indicating reduced gel continuity and weaker interparticle bonding. EDX support that reduce calcium availability, as Ca/Si decreases to 0.69 and 0.44 for 40% and 50% WCT, respectively, while Si/Al remains relatively stable (2.62–2.72), suggesting a change from calcium-rich or hybrid C–(N)–A–S–H gels toward Na-dominated N–A–S–H networks. Although N–A–S–H gels are chemically stable, calcium dilution limits matrix densification and reduces mechanical integrity, while higher Na^+ charge balancing increases potential to drying and shrinkage-induced cracking. These features are consistent with low calcium geopolymer binders reported to exhibit higher porosity and crack sensitivity (Lee & Lee, 2015).

SEM–EDX confirms that WCT plays a dual role in the GGBS–WCT hybrid binder matrix. At moderate replacement levels, WCT supplies silica and alumina that support geopolymerisation and promote a dense hybrid gel network with balanced calcium and alumina contributions. In contrast, excessive WCT dilutes calcium, suppresses C–A–S–H formation, and change the binder toward Na-dominated gels, resulting in a less compact matrix with higher porosity and cracking propensity, which reduces mechanical performance. Overall, GGBS70–WCT (30% WCT) exhibits the most good microstructure, characterised by a dense hybrid C–(N)–A–S–H network, minimal cracking, and strong interfacial bonding, explaining its superior compressive strength and suitability for semi-rigid geopolymer repair applications.




(b)
Unreacted particles
Crack
Geopolymer gel
PKM-UiTM 15.0kV 10.4mm x500 BSE-COMP
100µm
Element | Wt. (%)
Ca | 15.80
Al | 3.80
Si | 11.50
Na | 16.80
Mg | 1.20
O | 45.00
(c)
Unreacted particles
Geopolymer gel
Crack
PKM-UiTM 15.0kV 10.7mm x500 BSE-COMP
100µm
Element | Wt. (%)
Ca | 16.1
Al | 6.4
Si | 17.3
Na | 10.9
Mg | 2.2
O | 46.4
(d)
Unreacted particles
Pores
Geopolymer gel
Crack
PKM-UiTM 15.0kV 10.8mm x500 BSE-COMP
100µm
Element | Wt. (%)
Ca | 17.48
Al | 7.36
Si | 18.40
Na | 9.60
Mg | 1.80
O | 44.70
(e)
Pores
Geopolymer gel
Crack
Unreacted particles
PKM-UiTM 15.0kV 11.1mm x500 BSE-COMP
100µm
Element | Wt. (%)
Ca | 14.21
Al | 7.86
Si | 20.60
Na | 6.9
Mg | 1.20
O | 45.60

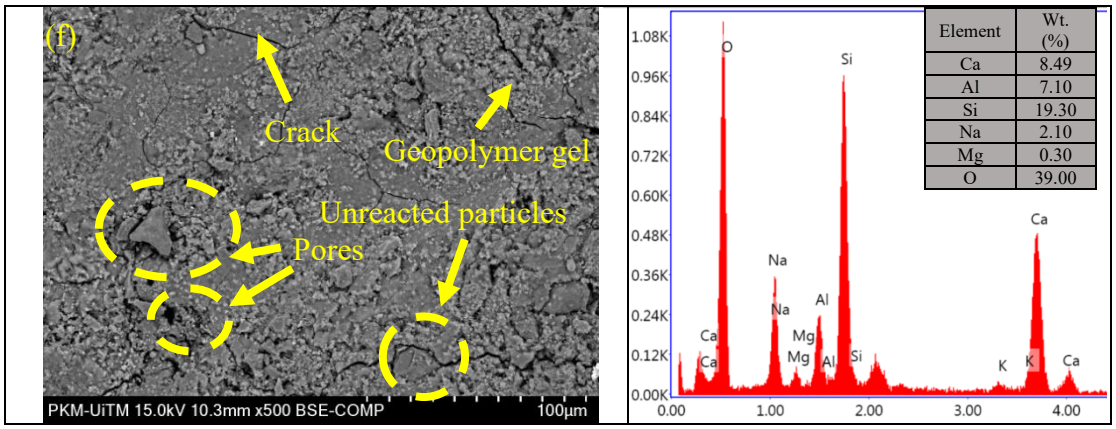


Figure 4.16 Micrographs and Corresponding EDX Spectra of GGBS–WCT Hybrid One-Part Geopolymer Repair Binders at 500× Magnification (a) 0% WCT, (b) 10% WCT, (c) 20% WCT, (d) 30% WCT, (e) 40% WCT, and (f) 50% WCT

4.4.4 Summary

This chapter presented the characterisation, optimisation, and geopolymerisation reaction of GGBS–FA and GGBS–WCT one-part geopolymer repair binders. The raw material results showed that GGBS is a calcium-rich precursor, FA improves workability due to its spherical particle shape, while WCT provides high silica content and angular particles that support mechanical interlocking and hybrid gel formation. Based on the optimisation results, both GGBS–FA and GGBS–WCT formulations were suitable for one-part geopolymer binders. However, GGBS–WCT showed better overall performance, especially in compressive strength. The highest strength for GGBS–FA was obtained by GGBS70–FA–ss10 with 69.16 MPa, while GGBS70–WCT–ss10 achieved the highest 28-day strength of 73.15 MPa. The independent *t*-test further showed no significant difference between GGBS70–WCT–ss10 and GGBS100–ss10 (t_{stat} = 1.451, p = 0.283 > 0.05), indicating comparable strength performance while utilising WCT as a partial replacement for GGBS. Therefore, GGBS–WCT was selected as the optimum binder formulation. The optimum mix was identified as GGBS70–WCT–ss10, consisting of 70% GGBS, 30% WCT, and 10% solid activator. This mix was selected because it provided the best balance between workability, setting time, and compressive strength. The 10% solid activator was more suitable than 20% because higher activator content reduced workability and strength due to excessive alkali and lower reactive precursor content. The superior performance of GGBS70–WCT–ss10 was attributed to the balanced calcium, silica, and alumina

composition, which promoted the formation of hybrid C–(N)–A–S–H gel. XRD and SEM–EDX results confirmed that this mix formed a dense and compact matrix with better gel continuity, reduced pores, and limited unreacted particles. In contrast, higher WCT replacement levels caused calcium dilution, more unreacted ceramic particles, and a less compact matrix. Overall, GGBS–WCT was more suitable than GGBS–FA, and GGBS70–WCT–ss10 was selected as the optimum binder mix. Therefore, this mix was used for the next phase of the study, which focused on the development of one-part semi-rigid geopolymer repair material incorporating crumb rubber.

CHAPTER 5
OPTIMISATION OF CRUMB RUBBER CONTENT (PHASE 4) AND COMPATIBILITY OF ONE-PART SEMI-RIGID GEOPOLYMER REPAIR MATERIAL WITH ROAD SURFACE LAYERS (PHASE 5)

5.1 Introduction

This chapter presents the results and discussion for Phase 4 and Phase 5 of the study. Phase 4 focuses on optimising treated crumb rubber (CR) as a partial replacement for fine aggregate in a one-part semi-rigid geopolymer repair material used for pavement repair applications. The repair material was developed using the optimum binder obtained from the previous phase, consisting of 70% GGBS and 30% WCT with 10% solid activator, designated as GGBS70–WCT–ss10. CR replacement levels of 0%, 5%, 10%, 15%, and 20% were investigated to identify the optimum mixture based on key durability and mechanical properties. The material performance was evaluated through water absorption, abrasion resistance, and compressive strength, which collectively reflect transport behaviour, surface degradation resistance, and load-carrying capacity relevant to road repair conditions. Following the mix optimisation, Phase 5 assesses the compatibility of the developed repair material with typical road surface layers, with emphasis on its interfacial behaviour when applied to concrete and asphalt substrates. The chapter examines the influence of CR content on bonding performance and further evaluates substrate surface roughness affects bond strength. In addition, the discussion considers the overall functional suitability of the repair material, including its rutting resistance and practicality for pavement applications.

5.2 Water Absorption Analysis

The water absorption behaviour of the one-part semi-rigid geopolymer repair material incorporating treated CR was evaluated under ambient curing at 3 and 28 days for sand replacement levels of 0%, 5%, 10%, 15%, and 20%. As presented in Figure 5.1, all mixtures showed water absorption values within a relatively small range,

indicating a generally constant resistance to water absorption across the investigated CR contents. At 3 days, absorption ranged from 5.35% to 6.19%, in contrast at 28 days it ranged from 6.18% to 6.33%. The limited difference between mixtures suggests that the addition of treated CR did not cause a significant deterioration in the material water absorption performance within the replacement range.

A small increase in water absorption was observed at 28 days for all mixtures compared with 3 days. Although one-part semi-rigid geopolymer repair material can show improved transport resistance with continued reaction, curing under ambient conditions may introduce moisture loss and moisture gradients, which can increase the accessibility of flow paths for water during the absorption test. This behaviour has been reported in geopolymer concrete where curing environment influences the evolution of transport-related properties over time (Aly et al., 2019). In the present study, the change in water absorption remained minimal, indicating that the long-term absorption response was likely controlled by a combination of ongoing matrix development and the curing exposure history, rather than a major change in binder performance.

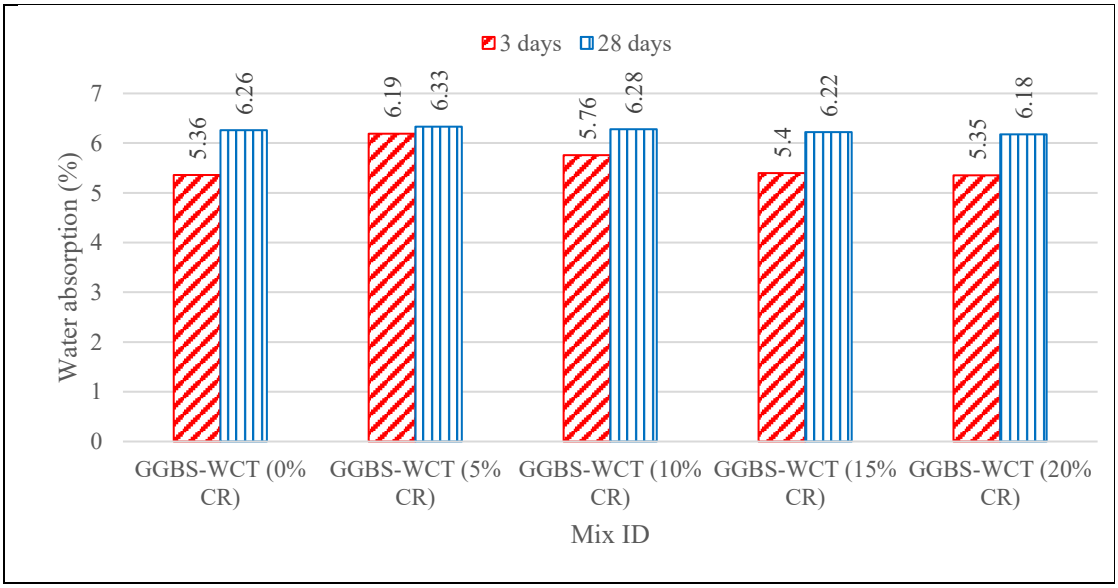


Figure 5.1 Variation of Water Absorption with CR Replacement Level for GGBS–WCT Based Hybrid One-Part Semi-Rigid Geopolymer Repair Material

The 5% CR mixture recorded the highest absorption at both ages, 6.19% at 3 days and 6.33% at 28 days, which may reflect selective effects such as entrapped air, incomplete compaction at that replacement level. In contrast, higher CR contents 15–20% did not increase absorption and produced comparatively lower, with the 20% CR mix recording 5.35% at 3 days and 6.18% at 28 days. This outcome is consistent with

the view that alkali treatment can enhance rubber binder interaction, which may reduce interfacial gaps that otherwise serve as preferential water ingress routes (Guo et al., 2017). However, it is also recognised that rubber addition can introduce voids or weak zones if bonding and densification are not adequately achieved, which may increase water absorption (Ahmad Zailani et al., 2025). Therefore, the absorption results should be interpreted as reflecting the balance between improved interface quality due to treated CR and any casting-related or interfacial defects introduced by rubber inclusion.

Overall, the results indicate that incorporating treated CR help comparable water absorption performance across all replacement levels studied. Importantly, because the differences between mixtures were small particularly at 28 days water absorption alone is not sufficient to define the optimum CR content. The final optimum selection should therefore be supported by combined evaluation with abrasion resistance, and compressive strength outcomes discussed in subsequent sections.

5.3 Abrasion Resistance Analysis

The abrasion resistance of the GGBS–WCT hybrid one-part semi-rigid geopolymer repair material incorporating treated CR was evaluated at 3 and 28 days, as presented in Figure 5.2. Abrasion resistance (AR) was calculated using the equation proposed by Feng and Liu (2021) and reported in $mm^2 \cdot hr/g$, providing an index of the material resistance to surface material loss under mechanical wear. This property is particularly relevant for pavement repair material, where the exposed surface is subjected to repeated tyre surface contact and frictional action.

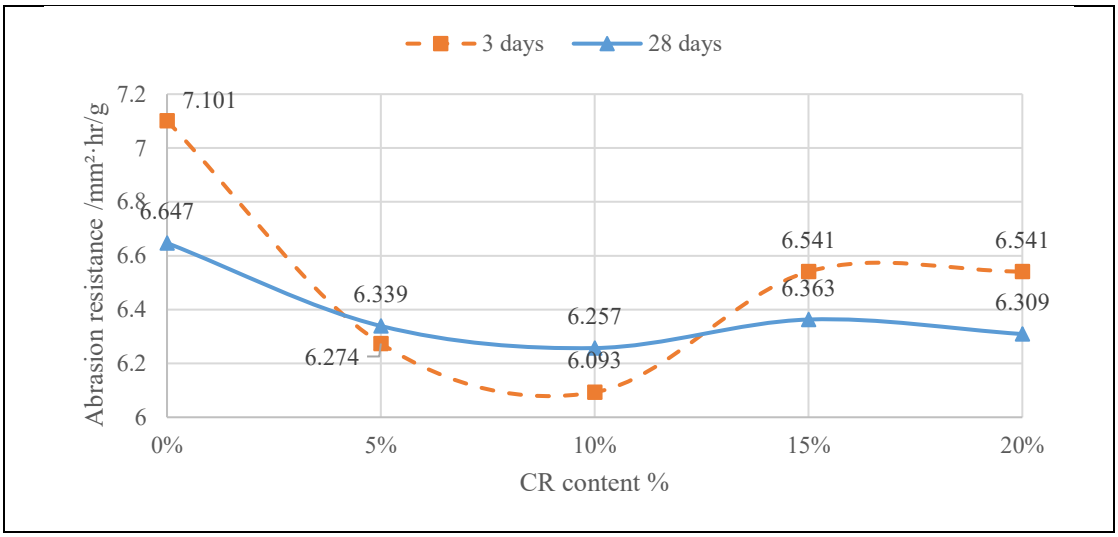


Figure 5.2 Abrasion Resistance of GGBS–WCT Based Hybrid One-Part Semi-Rigid Geopolymer Repair Material with Varying CR

Overall, the results indicate that the 0% CR achieved the highest abrasion resistance at both ages, recording 7.101 mm²·hr/g at 3 days and 6.647 mm²·hr/g at 28 days. This confirms that the one-part semi-rigid geopolymer repair material provided the most wear-resistant surface, likely due to a more continuous and rigid binder aggregate skeleton. Adding CR generally reduced abrasion resistance, although the response was not uniform across replacement levels. The lowest AR show at 10% CR, with values of 6.093 mm²·hr/g at 3 days and 6.257 mm²·hr/g at 28 days. This reduction suggests that, at this replacement level, the rubber phase likely acted as a mechanically softer inclusion that reduced surface hardness or promoted localised wear under abrasion action. In rubberised mixtures, this behaviour is often linked to weaker interfacial behaviour and the tendency for rubber particles to deboned or pull out under repeated surface stress, creating local defects that accelerate material removal an observation consistent with the mechanism discussed by Bisht and Ramana (2017).

At higher CR contents, abrasion resistance recovered and showed its best performance among CR replacement mixtures at 15% CR, reaching 6.541 mm²·hr/g at 3 days and 6.363 mm²·hr/g at 28 days. This improvement indicates that, beyond a minimum content, the elastic and energy-dissipating behaviour of rubber can partially offset wear progression by reducing brittle surface damage, as highlighted Feng and Liu (2021). However, it is important to highligh that even at 15% CR, AR remained below the control mix, demonstrating that rubber addition did not surpass the wear resistance of the 0% CR mixture. At 20% CR, abrasion resistance decreased slightly again to 6.541 mm²·hr/g at 3 days and 6.309 mm²·hr/g at 28 days, implying that excessive replacement

begins to compromise the load-bearing solid skeleton near the surface. This is associated with reduced matrix compactness and increased susceptibility to localised wear features, aligning with the balance between durability and mechanical integrity highlighted by Thomas et al. (2016). In summary, the abrasion data show that the 0% CR mixture provided the highest wear resistance, while among the CR mixtures, 15% CR delivered the most best abrasion performance. Therefore, 15% CR can be considered the optimum replacement level within the CR series for abrasion behaviour.

5.4 Compressive Strength Analysis

The compressive strength of the GGBS–WCT based hybrid one-part semi-rigid geopolymer repair material incorporating treated CR as partial sand replacement (0%, 5%, 10%, 15%, and 20%) is presented in Figure 5.3 for 3 and 28-day curing ages. Overall, increasing CR content produced a clear reduction in compressive strength at both ages, indicating that strength development in this composite was strongly influenced by the replacement of aggregate sand with rubber. At 28 days, the control mixture (0% CR) achieved the highest compressive strength of 70.72 MPa. Adding 5% CR reduced the strength to 65.54 MPa, representing a 7.32% decrease compared with the control. Above 5% CR, the reduction more visible, with the 10%, 15%, and 20% CR mixtures recording 52.80 MPa, 43.25 MPa, and 38.86 MPa, respectively. The 20% CR mixture corresponded to a 45.05% reduction compared with the control, confirming that high rubber replacement substantially weakens the load-bearing skeleton of the hardened repair material.

A similar trend was observed at 3 days, where the control mixture recorded 49.37 MPa, followed by 47.24 MPa (5% CR), 43.00 MPa (10% CR), 35.25 MPa (15% CR), and 31.61 MPa (20% CR). These results indicate that the reduction in strength due to CR was already shows at early age, suggesting that rubber inclusion affects not only later age capacity but also early age load resistance. However, all mixtures showed strength gain between 3 and 28 days, demonstrating continued hardening of the geopolymer matrix under ambient curing.

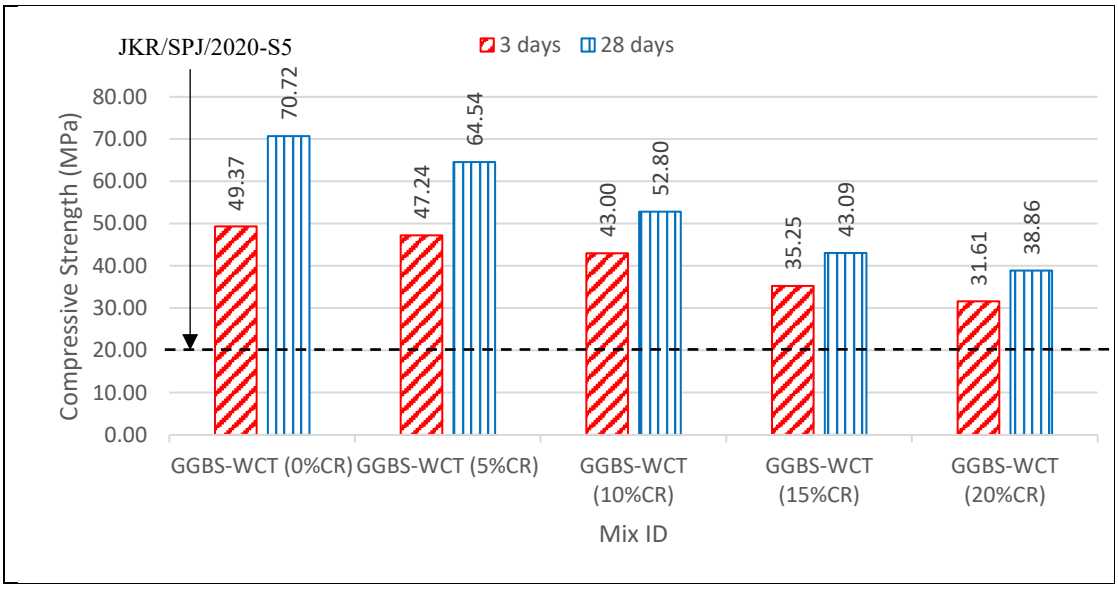


Figure 5.3 Compressive Strength of GGBS–WCT-Based Hybrid One-Part Semi-Rigid Geopolymer Repair Material with Varying CR Replacement Levels

This reduction in compressive strength with increasing CR is consistent with the lower stiffness of rubber compared with sand, which reduces the effectiveness of load transfer and promotes concentrated deformation under compression. In addition, literature on rubberised cementitious materials has attributed strength losses to weaker rubber binder interfacial behaviour the presence of interfacial gaps and voids (Siddika et al., 2019). While treated CR can improve rubber binder interaction, rubber particles remain mechanically softer than aggregates and may still act as stress concentrators under compressive loading. Further reductions at higher CR contents may also be associated with increased void propensity and weakened overall structure, as discussed by Zhao J. et al. (2023) and Raut et al. (2024). According to JKR/SPJ/2020-S5 (Jabatan Kerja Raya, 2020) specifies a minimum compressive strength of 20 MPa prior to traffic exposure. All mixtures in this study exceeded this requirement at both 3 and 28 days, indicating that the developed repair materials are suitable for early traffic exposure under standard conditions. Even so, the marked reductions at higher CR contents particularly at 20% suggest that such mixtures may be less appropriate for high-load pavement zone.

For further verification, an independent *t*-test was carried out to determine whether there is a significant difference between the two means of compressive strength values for different CR percentages. Null Hypothesis, H_0: The CR percentage does not influence the compressive strength performance. Proposed Hypothesis, H_1: The CR percentage influences the compressive strength performance. From the analysis, it is

found that there is a significant difference in compressive strength values between GGBS-WCT (15% CR) and GGBS-WCT (0% CR) at 0.05 level. The GGBS-WCT (15% CR) mixture recorded a mean compressive strength of 43.09 MPa, while GGBS-WCT (0% CR) recorded a higher mean value of 70.72 MPa. The analysis yielded a t_{stat} of -154.698. Since the t_{stat} value is greater than the critical value ($t_{stat} = 154.698 > t_{critical} = 2.776$, Reject H_0), the result was significant at the specified level ($p < 0.001$). It can be concluded that the incorporation of 15% CR significantly influenced the compressive strength performance of the geopolymer mixture, resulting in a reduction in strength compared with the mixture without CR.

In terms of optimisation, although the 5% CR mixture provided the highest strength among the CR replacement mixes, the optimum replacement level was determined based on overall performance rather than compressive strength alone. The independent *t*-test showed that 15% CR significantly reduced the compressive strength of the GGBS–WCT geopolymer mixture from 70.72 MPa to 43.09 MPa ($p < 0.001$). Therefore, the null hypothesis was rejected, confirming that CR content significantly influenced compressive strength performance. The 15% CR mixture was selected as the optimum because it delivered the most good abrasion resistance among the CR replacement mixes while maintaining acceptable water absorption behaviour and adequate compressive strength 43.09 MPa at 28 days and 35.25 MPa at 3 days. This supports the view that a moderate-to-high CR replacement can provide a practical balance between functional performance and sustainability benefits through greater utilisation of recycled rubber (Bisht & Ramana, 2017; Luhar et al., 2021). Accordingly, although compressive strength decreased with increasing CR content, the 15% CR mixture remained structurally adequate, as its compressive strength at both ages exceeded the minimum requirement of 20 MPa specified in JKR/SPJ/2020-S5 (Jabatan Kerja Raya, 2020).

5.5 Phase 5: Compatibility of One-Part Semi-Rigid Geopolymer Repair Material with the Road Surface Layer

This section presents the experimental findings on the bonding performance of the one-part semi-rigid geopolymer repair material using the optimum GGBS–WCT (15% CR) selected from Phase 4, when applied to concrete and asphalt substrates. The

influence of substrate surface preparation as-cast (AC), wire-brushed (WB), and drilled holes (DH) was examined to determine surface roughness affect the interfacial bond behaviour of the repair material in pavement applications. The experimental focused on surface roughness analysis and bi-surface shear testing. In addition, rutting resistance was assessed to evaluate the performance of the one-part semi-rigid geopolymer repair material under loading and to determine its suitability for service conditions where permanent deformation may govern pavement performance. Overall, the outcomes highlight the importance of suitable surface preparation in enhancing bonding and the functional performance of the repair layer, where good bonding is needed to transfer loads properly and maintain long-term performance.

5.5.1 Surface Roughness Analysis

To improve the bonding performance between an overlay repair layer and its substrate, the interface must provide sufficient resistance against slip and separation under service loading. Substrate surface roughness is a key contributor because it increases the potential for mechanical interlocking and interfacial friction, which can be particularly important when the interface is subjected to shear in pavement applications (Lyu et al., 2024). Based on Nurdeen Mohamed et al. (2024), increasing surface roughness generally enhances the bonding strength between an overlay material and the substrate by improving interlock at the interface.

In this study, the average roughness, Ra, was measured for three surface preparation conditions, AC, WB, and DH, for both concrete and asphalt substrates. The results in Figure 5.4 show that AC produced the lowest Ra values, while mechanical treatments increased roughness, with DH producing the strongest surface texture. For the concrete substrate, Ra increased from 1.74 μm for AC to 2.40 μm for WB, then rose substantially to 11.24 μm for DH. A similar trend was observed for asphalt, where Ra increased from 2.44 μm for AC to 4.60 μm for WB, and reached 10.34 μm for DH. The higher baseline roughness of asphalt under AC can be linked to its uneven surface composition, while wire brushing likely increased Ra by partially removing the bitumen surface film and exposing fine aggregates.

The DH surface preparation generated the highest roughness for both substrates, indicating that drilling was the most effective method for creating macro-scale

anchoring points that can promote mechanical interlocking between the repair layer and the substrate. This aligns with the general understanding that surface roughness such as WB and drilling improve bond performance mainly by strengthening the mechanical component of bonding (Lyu et al., 2024). However, it is important to recognise that aggressive roughening can also introduce negative effects, such as microcracking, depending on the substrate condition and the method used. In practice, this means the benefit of increased roughness must be balanced against the risk of creating defects that can become primary locations for crack initiation or debonding (Felekoğlu, 2024).

Overall, the roughness results confirm that the three substrate surface conditions provided clearly different interface conditions, which is necessary for interpreting the subsequent bonding test outcomes. In addition, since bond performance is controlled by the combined effects of adhesion and mechanical interlock, the DH surfaces were expected to provide the most favourable interface condition for shear-type bonding evaluation, whereas AC surfaces represent the lowest-interlock condition and therefore the most demanding case for the repair material.

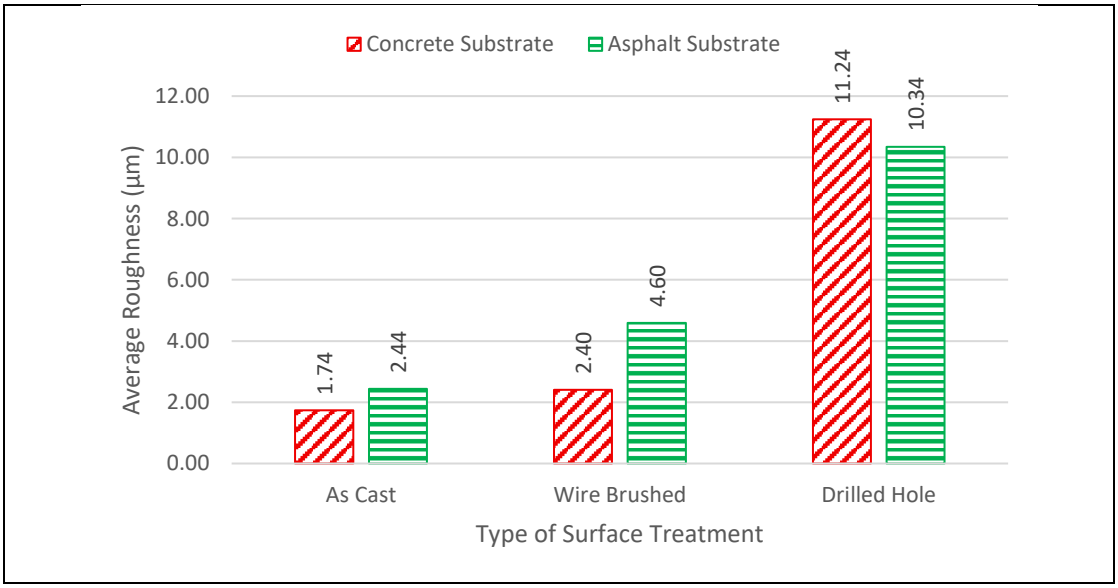


Figure 5.4 Average Roughness (Ra) of Concrete and Asphalt Substrates under AC, WB and DH Surface Preparations

5.5.2 Bonding Strength Analysis

Figure 5.5 presents the 28-day bond strength of the one-part semi-rigid geopolymer repair material applied to concrete and asphalt substrates as determined

using the bi-surface shear bond test. Three surface preparation conditions, namely AC, WB, and DH. Overall, bond strength increased with more better surface preparation for both substrates, confirming that surface preparation is a controlling factor in achieving a good repair interface. According to Lyu et al. (2024); Tayeh et al. (2012) the roughness and mechanical interlock are key contributors to shear transfer across repair interfaces, provided the roughness remains within an effective range.

For the concrete substrate, the AC condition produced the lowest bond strength, 6.82 MPa, while WB and DH increased the bond strength to 7.44 MPa and 8.69 MPa, respectively. The lower strength for AC concrete can be attributed to its relatively smooth surface and the presence of a weak surface layer, which reduces mechanical interlock and limits the effective contact condition at the interface. These increases align with the surface roughness analysis (Section 5.5.1), where DH produced the highest Ra and WB produced an intermediate Ra, indicating that a rougher surface promoted stronger mechanical interlocking and a larger effective contact area. Similar improvements with surface roughening have been linked to greater adhesion and interlocking between the overlay and roughened concrete substrate (Tayeh et al., 2012).

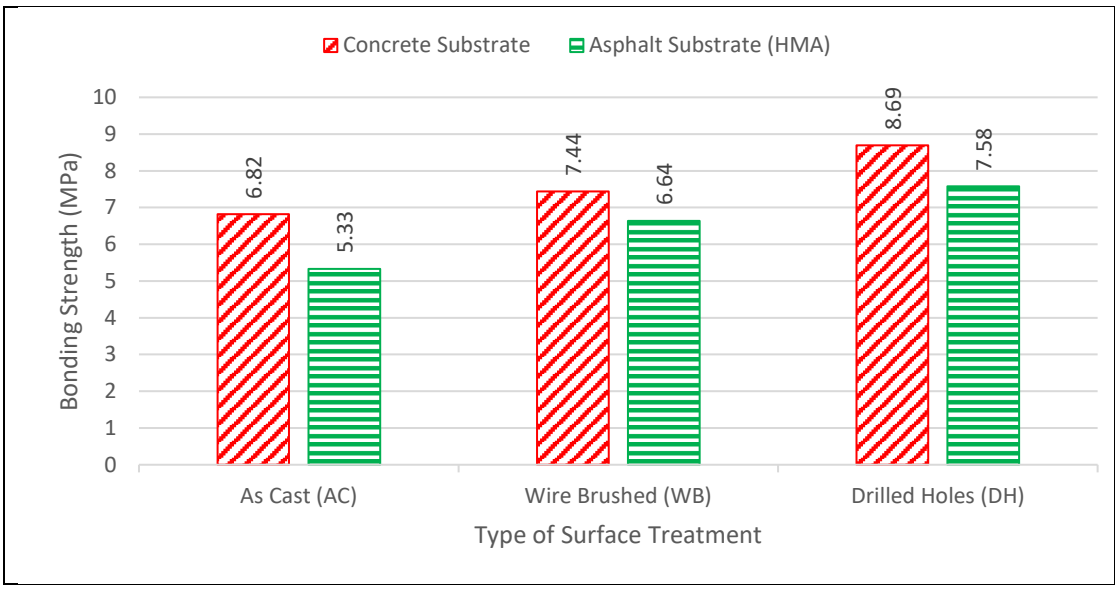


Figure 5.5 Bonding Strength of One-Part Semi-Rigid Geopolymer Repair Material under Different Surface Preparations on Concrete and Asphalt Substrates

According to Behforouz et al. (2023); Mack et al. (2023) surface roughness such as WB can improve surface roughness and promote better interfacial bonding of repair materials by increasing frictional resistance and mechanical interaction at the interfacial zone. The strongest bonding performance was achieved with the DH surface roughness,

which likely provided deeper anchorage features and improved resistance to interfacial slip under shear. This observation is consistent with Ahmad Zailani et al. (2021), who reported that drilled surfaces can significantly enhance bonding strength by providing greater surface roughness for mechanical engagement. Surfaces with the highest Ra values typically show the best interfacial strength.

For further verification, an independent t-test is carried out to determine whether there is a significant difference between the two means of bonding strength values for different concrete substrate surface treatments. Null Hypothesis, H_0: The concrete substrate surface treatment does not influence the bonding strength values. Proposed Hypothesis, H_1: The concrete substrate surface treatment influences the bonding strength values. From analysis, it is found that there is a significant difference in bonding strength values between Drilled Holes (DH) concrete substrate and As Cast (AC) concrete substrate at 0.05 level. For the Drilled Holes (DH) concrete substrate, the analysis produced a t_{stat} of 26.858 ($t_{stat} = 26.858 > t_{critical} = 2.776$, Reject H_0), which was significant at the specified level ($p < 0.001$). It can be concluded that the drilled-hole surface treatment significantly influenced the bonding strength performance of the concrete substrate by improving mechanical interlocking between the repair material and the substrate surface.

For the asphalt substrate, the same ranking was observed, where DH produced the highest bond strength, followed by WB and AC. The larger relative improvement on asphalt indicates that bonding is more sensitive to surface conditioning, since the original asphalt surface can limit mechanical interlock. The lower bond strength for AC asphalt is consistent with the hydrophobic and bitumen surface condition, which can limit interfacial bonding. In contrast, WB likely removed part of the bitumen film and exposed fine aggregates, thereby increasing effective interlock and frictional resistance, while DH provided additional anchorage that improved mechanical interlocking. This interpretation is consistent with findings reported by Ahmad Zailani et al. (2021) and Nurdeen Mohamed et al. (2024), where more aggressive surface modification improved bonding performance for flexible and bitumen substrates.

For further verification, an independent *t*-test is carried out to determine whether there is a significant difference between the two means of bonding strength values for different asphalt substrate surface treatments. Null Hypothesis, H_0: The asphalt substrate surface treatment does not influence the bonding strength values. Proposed Hypothesis, H_1: The asphalt substrate surface treatment influences the bonding strength

values. From analysis, it is found that there is a significant difference in bonding strength values between Drilled Holes (DH) asphalt substrate and As Cast (AC) asphalt substrate at 0.05 level. The Drilled Holes (DH) asphalt substrate recorded a higher mean bonding strength of 9.35 MPa, while the As Cast (AC) asphalt substrate recorded a lower mean value of 2.44 MPa. For the Drilled Holes (DH) asphalt substrate, the analysis yielded a t_{stat} of 24.823 (t_{stat} = 24.823 > $t_{critical}$ = 2.776, Reject H_0), which was significant at the specified level ($p < 0.001$). It can be concluded that the drilled-hole surface treatment significantly influenced the bonding strength performance of the asphalt substrate by improving mechanical interlocking between the repair material and the substrate surface.

Overall, the results confirm that surface preparation is essential for achieving a good repair interface, with DH providing the most effective improvement for both substrates and WB offering a practical intermediate improvement relative to AC. The combined roughness and bond data support the selection of an appropriate field surface preparation method to improve interface reliability and long-term performance (Lyu et al., 2024; Tayeh et al., 2012).

5.5.3 Rutting Resistance Analysis

Table 5.1 and Figure 5.6 present the wheel-tracking performance of HMA compared with the one-part semi-rigid geopolymer repair material applied under three substrate surface conditions, namely AC overlay, WB overlay, and DH overlay. The rutting depth patterns observed over the 45-minute loading duration show clear differences in deformation resistance, influenced by both the material properties and the quality of interaction between the substrate and the overlay. As shown in Table 5.1, the HMA specimen without geopolymer repair overlay exhibited significantly higher rutting depth compared to all one-part semi-rigid geopolymer repair material overlays. The rutting depth of the HMA without overlay specimen increased from 1.89 mm at 5 minutes to 9.45 mm at 45 minutes. The wheel-tracking test was carried out for 45 minutes or until the rut depth reached 15 mm, whichever occurred first, based on the laboratory testing procedure. In this study, the 15 mm rut depth was used as the test termination criterion, not as a performance acceptance limit. Therefore, lower rut depth values indicate better resistance to permanent deformation. This continuous

accumulation of deformation is characteristic of the viscoelastic nature of bituminous binders, where repeated loading results progressive shear flow once the critical temperature dependent stiffness limit is exceeded. Similar behaviour has been widely reported in asphalt pavement literature, where rutting is primarily attributed to viscous flow and shear deformation within the asphalt layer (Nascimento et al., 2021).

Table 5.1
Wheel-Tracking Rutting Depth of HMA and One-Part Semi-Rigid Geopolymer Repair Overlays under Different Surface Preparations

Time (minutes)	HMA without overlay (mm)	One-part semi-rigid geopolymer repair material		
		AC overlay (mm)	WB overlay (mm)	DH overlay (mm)
0	0	0	0	0
5	1.89	1.58	0.99	0.2
10	2.93	1.63	0.97	0.31
15	3.98	1.64	0.98	0.32
20	4.95	1.77	1.06	0.35
25	5.92	1.79	1.1	0.41
30	6.88	1.85	1.12	0.49
35	7.79	2.08	1.3	0.52
40	8.59	2.45	1.48	0.51
45	9.45	2.64	1.62	0.6

In addition, all one-part semi-rigid geopolymer repair material specimens showed significantly lower rutting depth, confirming higher resistance to permanent deformation. This improvement is primarily attributed the higher stiffness and lower temperature sensitivity of the geopolymer aluminosilicate matrix compared to conventional bitumen. The one-part semi-rigid geopolymer repair material provides enhanced load distribution and shear resistance, thereby limiting strain accumulation under repeated loading. This finding directly addresses the research gap identified in Table 2.13, where previous studies (Lv et al., 2020; Xiang et al., 2024) evaluated rutting behaviour basically in asphalt or rubberised asphalt mixture, without investigating the rutting performance of one-part geopolymer repair overlays applied on HMA substrates. Among the surface roughness, the AC overlay one-part semi-rigid geopolymer repair material showed moderate rutting development, increasing gradually from 1.58 mm to 2.64 mm. Although significantly lower than HMA without overly, the relatively higher rutting depth compared to WB overlay and DH overlay conditions suggests limited interfacial bonding efficiency due to the smooth as-cast surface.

Insufficient mechanical interlock at the interface reduces shear stress transfer efficiency, leading to minimal interfacial displacement under repeated loading.

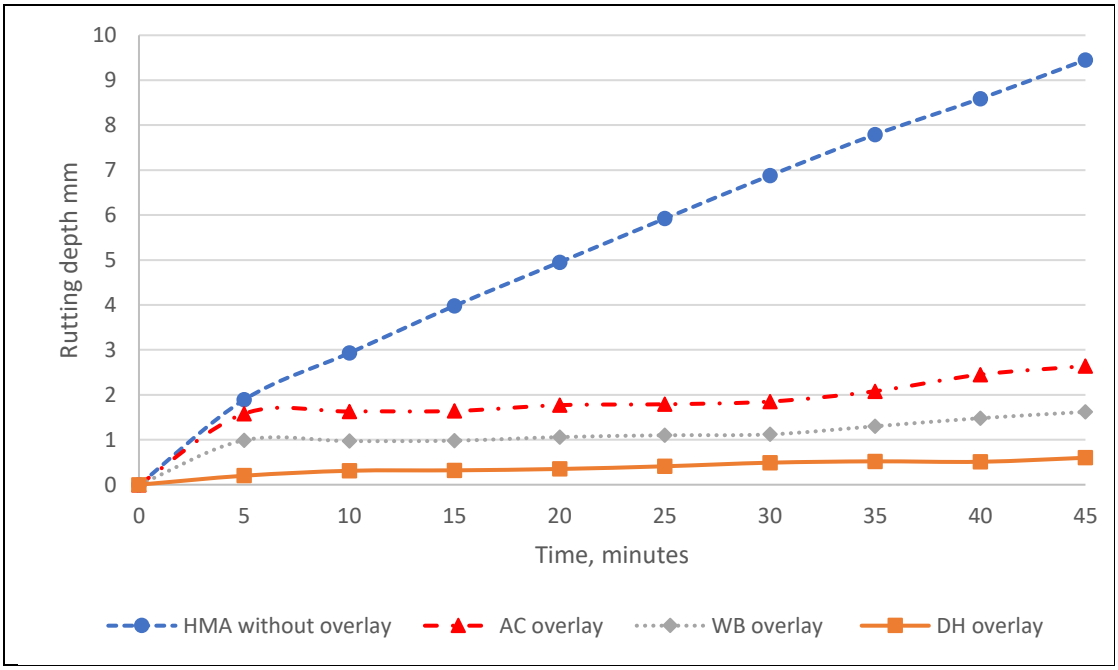


Figure 5.6 Rutting Depth versus Time for HMA and One-Part Semi-Rigid Geopolymer Repair Overlays under Different Surface Preparations

The WB overlay one-part semi-rigid geopolymer repair material demonstrated improved performance, with rutting depth ranging from 0.99 mm to 1.62 mm. The enhanced resistance can be attributed to the removal of weak superficial layer and the exposure of macro-texture, which increases interfacial resistance and mechanical interlocking between the geopolymer overlay and the substrate. Similar observations were reported by Xu et al. (2023), who demonstrated that micro-roughness enhancement significantly improves overlay stability and reduces interfacial displacement. The DH overlay one-part semi-rigid geopolymer repair material exhibited the highest rutting resistance, with rutting depth increasing only from 0.20 mm to 0.60 mm throughout the wheel-tracking test. This improved performance is attributed to the formation of strong mechanical anchorage through drilled holes, allowing the one-part semi-rigid geopolymer repair material to penetrate and harden within the substrate. The resulting multi-directional interlocking mechanism substantially improves shear transfer and minimises displacement under repeated loading. Comparable interlock strengthening mechanisms have been reported in composite repair material (El Afandi et al., 2023; Júlio et al., 2004). In terms of long-

term pavement performance, the DH treatment can improve the stability of the repair layer by reducing interfacial movement, debonding, and slippage under repeated traffic loading. Stronger anchorage also helps distribute traffic-induced stresses more effectively between the overlay and the HMA substrate, thereby reducing the potential for progressive rutting and localised repair failure. However, the drilled holes must be properly cleaned and fully filled with the repair material to avoid weak zones at the interface. Therefore, the long-term effectiveness of DH surface preparation depends on proper workmanship, adequate material penetration, and consistent field installation.

Referring to Figure 5.7, the visual rutting profiles further confirm the measured rutting depths. The HMA without overlay specimen exhibited significant deformation, while the one-part semi-rigid geopolymer repair material overlays maintained structural integrity with minimal surface rutting. The results indicate that rutting resistance was highest for the DH overlay condition, followed by WB overlay and AC overlay, while the HMA without overlay specimen exhibited the poorest rutting performance. This trend highlights the critical role of substrate preparation in controlling rutting resistance. While Tayeh et al. (2012) and Abed Al-Jabaar et al. (2021) examined bonding behaviour, and Lv et al. (2020) and Xiang et al. (2024) focused on asphalt rutting, no previous research has simultaneously evaluated surface roughness, interfacial bonding, and rutting resistance of one-part semi-rigid geopolymer repair material under representative wheel-tracking conditions. The evaluation presented in this study therefore advances the understanding of geopolymer-based repair overlays from both material and pavement performance perspectives.

The HMA control specimen had a thickness of 50 mm and was tested without overlay. For the overlay specimens, the total specimen thickness was 50 mm, consisting of a 40.55 mm HMA substrate and a 9.45 mm one-part semi-rigid geopolymer repair overlay. Therefore, the HMA column in Table 5.1 represents the control specimen without overlay, while the AC, WB, and DH columns represent HMA substrates with geopolymer repair overlays applied under different surface preparation conditions. Overall, the results confirm that the one-part semi-rigid geopolymer repair material significantly enhances rutting resistance compared to conventional HMA. The drilled-hole (DH) overlay surface roughness provides the most effective interfacial load transfer mechanism, making it particularly suitable for heavy or repeated traffic conditions where long-term deformation resistance is critical. These findings highlight

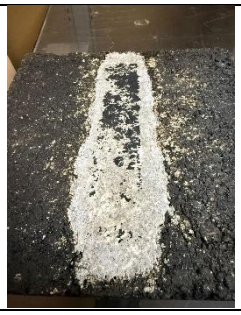
the importance of integrating material optimisation with appropriate substrate preparation to achieve durable and sustainable pavement repair.



a) HMA without overlay



b) AC overlay



c) WB overlay



d) DH overlay

Figure 5.7 Surface Rutting Profiles after Wheel-Tracking under Different Surface Preparations

5.6 Summary

This chapter presented the optimisation of treated crumb rubber (CR) content and the compatibility of the one-part semi-rigid geopolymer repair material with concrete and asphalt substrates. The repair material was produced using the optimum binder from Chapter 4, namely GGBS70–WCT–ss10, with CR used as partial sand replacement at 0%, 5%, 10%, 15%, and 20%. Based on the combined performance of water absorption, abrasion resistance, and compressive strength, 15% CR was selected as the optimum CR content. The independent *t*-test showed that 15% CR significantly reduced the compressive strength of the GGBS–WCT geopolymer mixture from 70.72 MPa to 43.09 MPa ($p < 0.001$). Therefore, the null hypothesis was rejected, confirming that CR content significantly influenced compressive strength performance. Although the control mix without CR achieved the highest strength and abrasion resistance, 15% CR showed the best balance among the rubberised mixtures. It achieved the best abrasion resistance among CR mixes and maintained acceptable compressive strength

of 35.25 MPa at 3 days and 43.09 MPa at 28 days, exceeding the 20 MPa minimum requirement in JKR/SPJ/2020-S5. For substrate compatibility, the bonding and rutting results showed that surface preparation strongly affected the performance of the repair overlay. The drilled-hole (DH) surface produced the highest roughness, strongest bonding strength, and lowest rutting depth for both concrete and asphalt substrates. For concrete, the bond strength increased from 6.82 MPa for AC to 8.69 MPa for DH, while the DH overlay recorded only 0.60 mm rutting depth after 45 minutes, compared with 9.45 mm for HMA without overlay. The independent *t*-test further confirmed that the DH treatment significantly improved bonding strength compared with AC for both concrete substrate (t_{stat} = 26.858, $p < 0.001$) and asphalt substrate (t_{stat} = 24.823, $p < 0.001$). Therefore, the null hypothesis was rejected, confirming that substrate surface treatment significantly influenced bonding strength performance. Overall, 15% CR was identified as the optimum sand replacement level, while drilled-hole surface preparation was the most effective substrate treatment. The developed one-part semi-rigid geopolymer repair material showed acceptable durability, adequate strength, good interfacial bonding, and high resistance to permanent deformation, making it suitable for pavement repair applications.

CHAPTER 6
CONCLUSION AND RECOMENDATIONS

6.1 General

This study developed a one-part semi-rigid geopolymer repair material using industrial by-products and treated crumb rubber (CR) for pavement repair applications. The findings showed that binder formulation, CR content, and substrate surface preparation significantly influenced the strength, durability properties, bonding performance, and rutting resistance of the developed repair material. Phase 1 confirmed that GGBS, FA, and WCT were suitable precursor materials for one-part geopolymer binder development. XRF results showed the presence of Ca, Si, and Al as the main elements required for binder formation. XRD and SEM results showed that GGBS had higher reactivity due to its amorphous structure, while FA and WCT contained more crystalline phases and contributed as supplementary aluminosilicate sources and filler materials.

Phase 2 showed that the GGBS–WCT binder performed better than the GGBS–FA binder in strength. The GGBS70–WCT–ss10 mixture achieved the highest 28-day compressive strength of 73.15 MPa. The 90:10 solid precursor-to-solid activator ratio provided a better balance between workability, setting behaviour, and strength development compared with the 80:20 ratio. Therefore, GGBS70–WCT–ss10 was selected as the optimum binder formulation due to its high 28-day strength. Phase 3 showed that GGBS70–WCT–ss10 produced the most compact geopolymer matrix due to its balanced Ca, Si, and Al composition, which promoted hybrid C–(N)–A–S–H gel formation. XRD and SEM–EDX results confirmed better gel continuity, fewer pores, and fewer unreacted particles compared with higher WCT mixtures. Therefore, GGBS70–WCT–ss10 was confirmed as the most suitable binder formulation for the one-part geopolymer repair material.

Phase 4 showed that 15% treated CR was the optimum replacement level for the semi-rigid geopolymer repair material. The 15% CR mixture achieved compressive strengths of 35.25 MPa at 3 days and 43.09 MPa at 28 days, exceeding the minimum requirement of 20 MPa specified in JKR/SPJ/2020-S5. Although the control mixture

without CR achieved the highest strength and abrasion resistance, the 15% CR mixture provided the best balance between strength, durability performance, deformation tolerance, and recycled rubber utilisation. Phase 5 showed that substrate surface preparation significantly affected bonding and rutting performance. The drilled-hole surface treatment gave the best performance because it improved mechanical interlocking and reduced permanent deformation under repeated wheel loading. This confirmed that proper substrate preparation was necessary to improve the compatibility between the repair material and the existing pavement substrate.

Overall, the study concluded that the optimum repair system was GGBS70–WCT–ss10 with 15% treated CR and drilled-hole substrate preparation. This repair system achieved early compressive strength of 35.25 MPa at 3 days and 43.09 MPa at 28 days, met the JKR minimum strength requirement, improved semi-rigid behaviour, enhanced bonding performance, and reduced rutting deformation. Therefore, the developed material has potential for sustainable pavement repair applications where early strength, bonding performance, and deformation resistance are required.

6.2 Recommendations

The following are the recommendations for future studies:

1. Investigation on the long-term durability behaviour of the developed one-part semi-rigid geopolymer repair material under combined service actions, including repeated traffic loading, moisture ingress, temperature variation, and chemical exposure, should be conducted to evaluate performance retention and bond stability under field-relevant conditions.

2. Further reaction verification using advanced characterisation techniques, such as Fourier Transform Infrared Spectroscopy (FTIR), Thermogravimetric Analysis/Differential Thermal Analysis (TGA/DTA), solid-state Nuclear Magnetic Resonance (NMR), and quantitative phase analysis, should be carried out to better understand the formation of C–A–S–H, N–A–S–H, and C–(N)–A–S–H gels and their relationship with strength development and matrix stability.

3. Further investigation on alternative crumb rubber pre-treatment methods and rubber–geopolymer matrix interface enhancement should be conducted to improve rubber compatibility, reduce stiffness incompatibility, and support the use of higher CR replacement levels in semi-rigid geopolymer repair materials.

6.3 Recommendation for the Industry

The findings of this study provide practical guidance for the development and application of one-part semi-rigid geopolymer repair material for pavement rehabilitation. The optimum binder formulation, GGBS70–WCT–ss10, can be used as a reference mix because it provides balanced performance in terms of workability, setting behaviour, compressive strength, and geopolymerisation reaction. The use of GGBS and WCT also supports sustainable construction by promoting the reuse of industrial and construction waste materials.

For field application, the incorporation of treated crumb rubber (CR) should be controlled at the optimum level. Based on the findings, 15% CR is recommended as the optimum sand replacement because it provides a suitable balance between strength, abrasion resistance, deformation tolerance, and recycled rubber utilisation. Excessive CR content should be avoided because it can reduce stiffness, weaken particle packing, and affect the semi-rigid behaviour required for pavement repair.

Substrate surface preparation is also an important practical requirement before applying the repair material. The results showed that rougher surfaces improved bonding and rutting resistance. Among the surface preparation methods, drilled hole (DH) treatment produced the best performance because it increased mechanical anchorage and improved load transfer between the geopolymer overlay and the existing pavement layer. Therefore, proper surface preparation should be carried out to ensure good interfacial bonding and long-term repair performance.

Overall, the developed one-part semi-rigid geopolymer repair material has practical potential as a sustainable alternative for pavement repair, particularly for localised surface rehabilitation where early strength, good bonding, and resistance to permanent deformation are required

REFERENCES

AASHTO-M-320. (2002). American Association of State Highway and Transportation Officials Standard Specification for Performance-Graded Asphalt Binder (AASHTO M 320-02).

Abbass, M., & Singh, G. (2021). Fatigue analysis of rice husk ash and basalt fibre-based sustainable geopolymer concrete in rigid pavements. *Materials Today: Proceedings*, *45*, 5014-5022. https://doi.org/https://doi.org/10.1016/j.matpr.2021.01.450

Abdila, S. R., Abdullah, M. M. A. B., Ahmad, R., Burduhos Nergis, D. D., Rahim, S. Z. A., Omar, M. F., Sandu, A. V., Vizureanu, P., & Syafwandi. (2022). Potential of Soil Stabilization Using Ground Granulated Blast Furnace Slag (GGBFS) and Fly Ash via Geopolymerization Method: A Review. *Materials*, *15*(1), 375. https://www.mdpi.com/1996-1944/15/1/375

Abed Al-Jabar, A. J., Ibrahim, S. I., & Al-Kaisy, H. A. (2021). Factors affect the bond strength of Geopolymer repair material: Review. *Journal of Physics: Conference Series*, *1973*(1), 012134. https://doi.org/10.1088/1742-6596/1973/1/012134

Ahmad, J., Kontoleon, K. J., Majdi, A., Naqash, M. T., Deifalla, A. F., Ben Kahla, N., Isleem, H. F., & Qaidi, S. M. A. (2022). A Comprehensive Review on the Ground Granulated Blast Furnace Slag (GGBS) in Concrete Production. *Sustainability*, *14*(14), 8783. https://www.mdpi.com/2071-1050/14/14/8783

Ahmad Zailani, W. W., Abdullah, M. M. A. B., Arshad, M. F., Razak, R. A., Tahir, M. F. M., Zainol, R. R. M. A., Nabialek, M., Sandu, A. V., Wysłocki, J. J., & Błoch, K. (2021). Characterisation at the Bonding Zone between Fly Ash Based Geopolymer Repair Materials (GRM) and Ordinary Portland Cement Concrete (OPCC). *Materials*, *14*(1), 56. https://www.mdpi.com/1996-1944/14/1/56

Ahmad Zailani, W. W., Abu Bakar, M. N. H., Mohd Apandi, N., Aziz Memon, N., Ismail, S., Mohd Azni, M. L. H., Sinarta, I. N., Ayu Agustini, N. K., & Koting, S. (2025). Effect of Treated Crumb Rubber on Mechanical Properties of GGBS-WCT Based Rubberised Geopolymer Concrete. *Jurnal Kejuruteraan*, *37*(6), 2749-2755. https://doi.org/10.17576/jkukm-2025-37(6)-14

Akmalaiuly, K., Berdikul, N., Pundiene, I., & Pranckeviciene, J. (2023). The Effect of Mechanical Activation of Fly Ash on Cement-Based Materials Hydration and

Hardened State Properties. *Materials (Basel)*, *16*(8). https://doi.org/10.3390/ma16082959

Almutairi, A. L., Tayeh, B. A., Adesina, A., Isleem, H. F., & Zeyad, A. M. (2021). Potential applications of geopolymer concrete in construction: A review. *Case Studies in Construction Materials*, *15*. https://doi.org/10.1016/j.cscm.2021.e00733

Altheeb, A. (2023). Engineering attributes of alkali-activated mortars containing ceramic tiles waste as aggregates replacement: Effect of high-volume fly ash inclusion. *Materials Today: Proceedings*. https://doi.org/10.1016/j.matpr.2023.04.121

Aly, A. M., El-Feky, M. S., Kohail, M., & Nasr, E.-S. A. R. (2019). Performance of geopolymer concrete containing recycled rubber. *Construction and Building Materials*, *207*, 136-144. https://doi.org/https://doi.org/10.1016/j.conbuildmat.2019.02.121

Araújo, R., Menezes, A., Cabral, K., Nóbrega, A., Martinelli, A., & Dantas, K. (2019). Evaluation of the pozzolanic activity of red ceramic waste using mechanical and physicochemical methods. *Cerâmica*, *65*, 461-469. https://doi.org/10.1590/0366-69132019653752649

Asayesh, S., Shirzadi Javid, A. A., Ziari, H., & Mehri, B. (2021). Evaluating fresh state, hardened State, thermal expansion and bond properties of geopolymers for the repairing of concrete pavements under restrained conditions. *Construction and Building Materials*, *292*, 123398. https://doi.org/https://doi.org/10.1016/j.conbuildmat.2021.123398

Assaggaf, R., Maslehuddin, M., Al-Osta, M. A., Al-Dulaijan, S. U., & Ahmad, S. (2022). Properties and sustainability of treated crumb rubber concrete. *Journal of Building Engineering*, *51*. https://doi.org/10.1016/j.jobe.2022.104250

Assaggaf, R. A., Ali, M. R., Al-Dulaijan, S. U., & Maslehuddin, M. (2021). Properties of concrete with untreated and treated crumb rubber – A review. *Journal of Materials Research and Technology*, *11*, 1753-1798. https://doi.org/https://doi.org/10.1016/j.jmrt.2021.02.019

ASTM-C109. (2020). Standard Test Method for Compressive Strength of Hydraulic Cement Mortars (Using 2-in. or [50-mm] Cube Specimens). *ASTM C109*. https://www.astm.org/c0109_c0109m-23.html

ASTM-C191. (2007). Standard Test Method for Time of Setting of Hydraulic Cement

by Vicat Needle. *ASTM C191*. https://www.astm.org/c0191_c191-23.html

ASTM-C618. (2023). ASTM C618-22:Standard Specification for Coal Fly Ash and Raw or Calcined Natural Pozzolan for Use in Concrete. *ASTM C618-23*. https://www.astm.org/c0618-23.html

ASTM-C642. (2022). Standard test method for density, absorption, and voids in hardened concrete.

ASTM-C882. (2020). Standard Test Method for Bond Strength of Epoxy-Resin Systems to Concrete by Slant Shear. *ASTM C882/C882M-20*. https://www.astm.org/c0882_c0882m-20.html

ASTM-C1437. (2020). Standard Test Method for Flow of Hydraulic Cement Mortar. *ASTM International*. https://www.astm.org/c1437-15.html

Azevedo, A. R. G., Vieira, C. M. F., Ferreira, W. M., Faria, K. C. P., Pedroti, L. G., & Mendes, B. C. (2020). Potential use of ceramic waste as precursor in the geopolymerization reaction for the production of ceramic roof tiles. *Journal of Building Engineering*, *29*, 101156. https://doi.org/https://doi.org/10.1016/j.jobe.2019.101156

Azmi, A., Abdullah, M. M. A. B., Ruzaidi, C., & Kamarudin, H. (2016). Effect Of Crumb Rubber On Compressive Strength Of Fly Ash Based Geopolymer Concrete. *MATEC Web of Conferences*, *78*, 01063. https://doi.org/10.1051/matecconf/20167801063

Bae, A., Yeom, Y., Park, S., Kwon, K., & Choi, H. (2026). Machine learning-based smoothness prediction for asphalt concrete overlay pavements considering milling effects. *Engineering Applications of Artificial Intelligence*, *165*, 113499. https://doi.org/https://doi.org/10.1016/j.engappai.2025.113499

Bahmani, H., & Mostofinejad, D. (2025). Microstructural characterization of alkali-activated concrete using waste-derived activators from industrial and agricultural sources: A review. *Case Studies in Construction Materials*, *22*, e04632. https://doi.org/https://doi.org/10.1016/j.cscm.2025.e04632

Behforouz, B., Tavakoli, D., Gharghani, M., & Ashour, A. (2023). Bond strength of the interface between concrete substrate and overlay concrete containing fly ash exposed to high temperature. *Structures*, *49*, 183-197. https://doi.org/https://doi.org/10.1016/j.istruc.2023.01.122

Bernal, S. A., Provis, J. L., Walkley, B., San Nicolas, R., Gehman, J. D., Brice, D. G., Kilcullen, A. R., Duxson, P., & van Deventer, J. S. J. (2013). Gel nanostructure

in alkali-activated binders based on slag and fly ash, and effects of accelerated carbonation. *Cement and Concrete Research*, *53*, 127-144. https://doi.org/https://doi.org/10.1016/j.cemconres.2013.06.007

Bisht, K., & Ramana, P. V. (2017). Evaluation of mechanical and durability properties of crumb rubber concrete. *Construction and Building Materials*, *155*, 811-817. https://doi.org/https://doi.org/10.1016/j.conbuildmat.2017.08.131

BS-598-110. (1998). Sampling and examination of bituminous mixtures for roads and other paved areas – Part 110: Method of test for the determination of wheel-tracking rate and depth. *BS 598-110:1998*. https://shop.bsigroup.com/ProductDetail?pid=000000000030034076

BS-812-113. (1990). Testing aggregates: Method for determination of aggregate abrasion value (AAV).

BS-EN-1338. (2003). BS EN 1338:2003 Concrete paving blocks: Requirements and test methods.

BS-EN-12620. (2002). BS EN 12620:2002 - Aggregates for concrete. In. London: British Standards Institution.

Buruberri, L. H., Tobaldi, D. M., Caetano, A., Seabra, M. P., & Labrincha, J. A. (2019). Evaluation of reactive Si and Al amounts in various geopolymer precursors by a simple method. *Journal of Building Engineering*, *22*, 48-55. https://doi.org/https://doi.org/10.1016/j.jobe.2018.11.017

Çelikten, S., Bayer Öztürk, Z., & Atabey, İ. İ. (2024). High-temperature resistance of ceramic sanitaryware waste and fly ash-based geopolymer and hybrid geopolymer mortars produced at ambient curing conditions. *Construction and Building Materials*, *446*, 137990. https://doi.org/https://doi.org/10.1016/j.conbuildmat.2024.137990

Charkhtab Moghaddam, S., Madandoust, R., Jamshidi, M., & Nikbin, I. M. (2021). Mechanical properties of fly ash-based geopolymer concrete with crumb rubber and steel fiber under ambient and sulfuric acid conditions. *Construction and Building Materials*, *281*, 122571. https://doi.org/https://doi.org/10.1016/j.conbuildmat.2021.122571

Cheah, C. B., Samsudin, M. H., Ramli, M., Part, W. K., & Tan, L. E. (2017). The use of high calcium wood ash in the preparation of Ground Granulated Blast Furnace Slag and Pulverized Fly Ash geopolymers: A complete microstructural and mechanical characterization. *Journal of Cleaner Production*, *156*, 114-123.

https://doi.org/https://doi.org/10.1016/j.jclepro.2017.04.026

Chen, Dan, H., Ding, Y., Gao, Y., Guo, M., Guo, S., Han, B., Hong, B., Hou, Y., Hu, C., Hu, J., Huyan, J., Jiang, J., Jiang, W., Li, C., Liu, P., Liu, Y., Liu, Z., Lu, G., . . . Zhu, X. (2021). New innovations in pavement materials and engineering: A review on pavement engineering research 2021. *Journal of Traffic and Transportation Engineering (English Edition)*, *8*(6), 815-999. https://doi.org/10.1016/j.jtte.2021.10.001

Chen, C., Sasaki, K., Tian, Q., & Zhang, H. (2023). Effect of Alkali Fusion Methods on the Preparation of One-Part Geopolymer From Coal Gasification Slag. *ACS Omega*, *8*(42), 39366-39375. https://doi.org/10.1021/acsomega.3c04926

Chen, J., Wu, D., Yi, M., Cai, Q., & Zhang, Z. (2021). Mechanical and durability properties of metakaolin blended with slag geopolymer mortars used for pavement repair. *Construction and Building Materials*, *281*, 122566. https://doi.org/https://doi.org/10.1016/j.conbuildmat.2021.122566

Chen, L., Liu, G., Zhang, X., & Pan, G. (2021). An innovative interface reinforcement method for steel bridge deck pavement pothole repair. *Construction and Building Materials*, *298*, 123838. https://doi.org/https://doi.org/10.1016/j.conbuildmat.2021.123838

Chen, X., & Wang, H. (2024). Asphalt pavement pothole repair with recycled material and preheating: Laboratory and field evaluation. *Journal of Cleaner Production*, *434*, 140410. https://doi.org/https://doi.org/10.1016/j.jclepro.2023.140410

Chen, Z., Qiao, J., Yang, X., Sun, Y., & Sun, D. (2023). A review of grouting materials for pouring semi-flexible pavement: Materials, design and performance. *Construction and Building Materials*, *379*. https://doi.org/10.1016/j.conbuildmat.2023.131235

Cong, P., & Cheng, Y. (2021). Advances in geopolymer materials: A comprehensive review. *Journal of Traffic and Transportation Engineering (English Edition)*, *8*(3), 283-314. https://doi.org/https://doi.org/10.1016/j.jtte.2021.03.004

Daneshvar, D., Deix, K., & Robisson, A. (2021). Effect of casting and curing temperature on the interfacial bond strength of epoxy bonded concretes. *Construction and Building Materials*, *307*, 124328. https://doi.org/10.1016/j.conbuildmat.2021.124328

Davidovits. (2008). *Geopolymer Chemistry and Applications* (Vol. 171).

Davidovits, J. (1991). Geopolymers. *Journal of thermal analysis*, *37*(8), 1633-1656.

https://doi.org/10.1007/BF01912193

Davidovits, J. (1994). Properties of geopolymer cements. First International Conference on Alkaline Cements and Concretes, Kiev, Ukraine.

Davidovits, J. (2002). *30 years of successes and failures in geopolymer applications, market trends and potential breakthroughs* Keynote Conference on Geopolymer 2002, Melbourne.

Davidovits, J. (2005). *Geopolymer, green chemistry and sustainable development solutions* World Congress Geopolymer 2005,

de Azevedo, A. R. G., Marvila, M. T., Rocha, H. A., Cruz, L. R., & Vieira, C. M. F. (2020). Use of glass polishing waste in the development of ecological ceramic roof tiles by the geopolymerization process. *International Journal of Applied Ceramic Technology*, *17*(6), 2649-2658. https://doi.org/10.1111/ijac.13585

Doan, T., Arulrajah, A., Lin, Y., Horpibulsuk, S., Chu, J., & Darmawan, S. (2024). Chemical stabilization of demolition wastes in pavement bases using one–part fly ash and slag based geopolymers. *Transportation Geotechnics*, *45*, 101192. https://doi.org/https://doi.org/10.1016/j.trgeo.2024.101192

Dong, Elchalakani, M., Karrech, A., & Yang, B. (2021). Strength and durability of geopolymer concrete with high volume rubber replacement. *Construction and Building Materials*, *274*, 121783. https://doi.org/https://doi.org/10.1016/j.conbuildmat.2020.121783

Dong, J., Liu, Y., Yuan, S., Li, K., Zhang, F., Guan, Z., Chai, H. K., & Wang, Q. (2024). Mechanical behavior and impact resistance of rubberized concrete enhanced by basalt fiber-epoxy resin composite. *Construction and Building Materials*, *435*, 136836. https://doi.org/https://doi.org/10.1016/j.conbuildmat.2024.136836

Dong, Q., Gao, J., Chen, X., & Wang, X. (2020). Development of a turpentine cutback asphalt mixture for porous pavement pothole repair. *Journal of Materials in Civil Engineering*, *32*(3), 05020001.

Dong, Q., Huang, B., & Zhao, S. (2014). Field and laboratory evaluation of winter season pavement pothole patching materials [Article]. *International Journal of Pavement Engineering*, *15*(4), 279-289. https://doi.org/10.1080/10298436.2013.814772

Duxson, P., Provis, J. L., Lukey, G. C., Mallicoat, S. W., Kriven, W. M., & van Deventer, J. S. J. (2005). Understanding the relationship between geopolymer composition, microstructure and mechanical properties. *Colloids and Surfaces*

A: Physicochemical and Engineering Aspects, *269*(1), 47-58. https://doi.org/https://doi.org/10.1016/j.colsurfa.2005.06.060

Eisa, M. S., Basiouny, M. E., & Fahmy, E. A. (2021). Effect of metakaolin-based geopolymer concrete on the length of rigid pavement slabs. *Innovative Infrastructure Solutions*, *6*(2). https://doi.org/10.1007/s41062-021-00465-5

El Afandi, M., Yehia, S., Landolsi, T., Qaddoumi, N., & Elchalakani, M. (2023). Concrete-to-concrete bond Strength: A review. *Construction and Building Materials*, *363*, 129820. https://doi.org/https://doi.org/10.1016/j.conbuildmat.2022.129820

El Alouani, M., Saufi, H., Aouan, B., Bassam, R., Alehyen, S., Rachdi, Y., El Hadki, H., El Hadki, A., Mabrouki, J., Belaaouad, S., Ez-Zaki, H., & Barka, N. (2024). A comprehensive review of synthesis, characterization, and applications of aluminosilicate materials-based geopolymers. *Environmental Advances*, *16*, 100524. https://doi.org/https://doi.org/10.1016/j.envadv.2024.100524

El Fadili, H., Ait-Khouia, Y., Ouffa, N., Taha, Y., Moukannaa, S., & Benzaazoua, M. (2025). Comprehensive review on alkaline dissolution of aluminosilicates and its role in the mechanisms and properties of geopolymers and alkali-activated materials. *Case Studies in Construction Materials*, *23*, e05330. https://doi.org/https://doi.org/10.1016/j.cscm.2025.e05330

Elgarahy, A. M., Maged, A., Eloffy, M. G., Zahran, M., Kharbish, S., Elwakeel, K. Z., & Bhatnagar, A. (2023). Geopolymers as sustainable eco-friendly materials: Classification, synthesis routes, and applications in wastewater treatment. *Separation and Purification Technology*, *324*. https://doi.org/10.1016/j.seppur.2023.124631

Elzeadani, M., Bompa, D. V., & Elghazouli, A. Y. (2021). Preparation and properties of rubberised geopolymer concrete: A review. *Construction and Building Materials*, *313*, 125504. https://doi.org/https://doi.org/10.1016/j.conbuildmat.2021.125504

Escalante-García, J. I., Gorokhovsky, A. V., Mendoza, G., & Fuentes, A. F. (2003). Effect of geothermal waste on strength and microstructure of alkali-activated slag cement mortars. *Cement and Concrete Research*, *33*(10), 1567-1574. https://doi.org/https://doi.org/10.1016/S0008-8846(03)00133-9

Faldessai, K., Lawande, S., Kelekar, A., Gurav, R., & Kakodkar, S. (2023). Utilization of ceramic waste as a partial replacement for cement in concrete manufacturing.

Materials Today: Proceedings. https://doi.org/https://doi.org/10.1016/j.matpr.2023.06.453

Faraji, M. F., Kara, H. O., Raazi, M., Ahıskalı, M., Eskici, C., Bayraktar, O. Y., Kaplan, G., Aydın, A. C., & Ozbakkaloglu, T. (2026). Development of high-performance one-part geopolymer foam concrete using ground granulated blast furnace slag, waste concrete sludge, and bamboo powder for sustainable construction. *Construction and Building Materials*, *506*, 144827. https://doi.org/https://doi.org/10.1016/j.conbuildmat.2025.144827

Felekoğlu, B. (2024). A comparative study on the bonding performance of an admixed repair mortar and high-strength flowable micro-concrete with substrate: Considerations on the physico-mechanical compatibility. *Journal of Building Engineering*, *98*. https://doi.org/10.1016/j.jobe.2024.111113

Feng, L.-Y., Chen, A.-J., & Liu, H.-D. (2021). Effect of Waste Tire Rubber Particles on Concrete Abrasion Resistance Under High-Speed Water Flow. *International Journal of Concrete Structures and Materials*, *15*(1), 37. https://doi.org/10.1186/s40069-021-00475-8

Feng, L., Ai-Jiu, & Liu, H.-D. (2021). Effect of Waste Tire Rubber Particles on Concrete Abrasion Resistance Under High-Speed Water Flow. *International Journal of Concrete Structures and Materials*, *15*(1), 37. https://doi.org/10.1186/s40069-021-00475-8

Feng, W., Liu, F., Yang, F., Jing, L., Li, L., Li, H., & Chen, L. (2021). Compressive behaviour and fragment size distribution model for failure mode prediction of rubber concrete under impact loads. *Construction and Building Materials*, *273*, 121767. https://doi.org/https://doi.org/10.1016/j.conbuildmat.2020.121767

Fu, S., & Lee, J. (2024). Recycling of ceramic tile waste into construction materials. *Developments in the Built Environment*, *18*, 100431. https://doi.org/https://doi.org/10.1016/j.dibe.2024.100431

Fu, S., Liu, R., Wei, J., lv, W., Zhang, C., & Ouyang, Z. (2023). Effect of holding time on the properties of porous ceramics with high-volume polished slag and its pore structure characteristics [Original Research]. *Frontiers in Materials*, *Volume 10 - 2023*. https://doi.org/10.3389/fmats.2023.1147120

Ghafoor, M. T., Hu, X., Li, S., & Shi, C. (2025). Role of activators in regulating the setting and hardening behavior of one-part geopolymer. *Construction and Building Materials*, *498*. https://doi.org/10.1016/j.conbuildmat.2025.144057

Ghostine, R., Bur, N., Feugeas, F., & Hoteit, I. (2022). Curing Effect on Durability of Cement Mortar with GGBS: Experimental and Numerical Study. *Materials (Basel)*, *15*(13). https://doi.org/10.3390/ma15134394

Gill, P., Jangra, P., Roychand, R., Saberian, M., & Li, J. (2023). Effects of various additives on the crumb rubber integrated geopolymer concrete. *Cleaner Materials*, *8*, 100181. https://doi.org/https://doi.org/10.1016/j.clema.2023.100181

Girish, M. G., Shetty, K. K., & Nayak, G. (2022). Synthesis of Fly-ash and Slag Based Geopolymer Concrete for Rigid Pavement. *Materials Today: Proceedings*, *60*, 46-54. https://doi.org/https://doi.org/10.1016/j.matpr.2021.11.332

Gopalakrishna, B., & Dinakar, P. (2024). The evaluation of the life cycle and corrosion properties of recycled aggregate geopolymer concrete incorporating fly ash and GGBS. *Journal of Building Engineering*, *94*, 109977. https://doi.org/https://doi.org/10.1016/j.jobe.2024.109977

Guo, S., Dai, Q., Si, R., Sun, X., & Lu, C. (2017). Evaluation of properties and performance of rubber-modified concrete for recycling of waste scrap tire. *Journal of Cleaner Production*, *148*, 681-689. https://doi.org/https://doi.org/10.1016/j.jclepro.2017.02.046

Hafezzadeh, R., Autelitano, F., & Giuliani, F. (2021). Asphalt-based cold patches for repairing road potholes – An overview. *Construction and Building Materials*, *306*, 124870. https://doi.org/https://doi.org/10.1016/j.conbuildmat.2021.124870

Hamid Abed, M., Sabbar Abbas, I., Hamed, M., & Canakci, H. (2022). Rheological, fresh, and mechanical properties of mechanochemically activated geopolymer grout: A comparative study with conventionally activated geopolymer grout. *Construction and Building Materials*, *322*, 126338. https://doi.org/https://doi.org/10.1016/j.conbuildmat.2022.126338

Haritonovs, V., Zaumanis, M., Brencis, G., & Smirnovs, J. (2012). Performance Characterization of Bituminous Mixtures With Dolomite Sand Waste and BOF Steel Slag. *Journal of Testing and Evaluation*, *40*(7), 1-6. https://doi.org/10.1520/jte20120187

He, P., Cui, J., Wang, M., Fu, S., Yang, H., Sun, C., Duan, X., Yang, Z., Jia, D., & Zhou, Y. (2020). Interplay between storage temperature, medium and leaching kinetics of hazardous wastes in Metakaolin-based geopolymer. *Journal of*

Hazardous Materials, *384*, 121377. https://doi.org/https://doi.org/10.1016/j.jhazmat.2019.121377

He, Y., Li, Y., Zhang, J., Xiong, K., Huang, G., Hu, Q., & Zhao, X. (2024a). Performance evolution mechanism and affecting factors of emulsified asphalt cold recycled mixture performance: A state-of art review. *Construction and Building Materials*, *411*, 134545. https://doi.org/https://doi.org/10.1016/j.conbuildmat.2023.134545

He, Y., Xiong, K., Zhang, J., Guo, F., Li, Y., & Hu, Q. (2024b). A state-of-the-art review and prospectives on the self-healing repair technology for asphalt materials. *Construction and Building Materials*, *421*, 135660. https://doi.org/https://doi.org/10.1016/j.conbuildmat.2024.135660

Humad, A. M., Habermehl-Cwirzen, K., & Cwirzen, A. (2019). Effects of fineness and chemical composition of blast furnace slag on properties of Alkali-Activated Binder [Article]. *Materials*, *12*(20), Article 3447. https://doi.org/10.3390/ma12203447

Huseien, G. F., Hamzah, H. K., Mohd Sam, A. R., Khalid, N. H. A., Shah, K. W., Deogrescu, D. P., & Mirza, J. (2020). Alkali-activated mortars blended with glass bottle waste nano powder: Environmental benefit and sustainability. *Journal of Cleaner Production*, *243*, 118636. https://doi.org/https://doi.org/10.1016/j.jclepro.2019.118636

IS-1237. (2012). IS 1237:2012 Cement concrete flooring tiles — Specification (Second Revision) [IS 1237:2012].

ISO-25178. (2021). Geometrical product specifications (GPS), Surface texture: Areal, Part 2: Terms, definitions and surface texture parameters.

Jabatan Kerja Raya, M. (1998). JKR ACW 14 Gradation Limits for Asphalt Wearing Course.

Jabatan Kerja Raya, M. (2007). *Standard Specification for Road Works: Section 4 – Flexible Pavement*. Kuala Lumpur, Malaysia: Public Works Department Malaysia

Jabatan Kerja Raya, M. (2020). *Standard Specification for Road Works: Section 5 – Concrete Works* (JKR/SPJ/2020-S5, Issue.

Jamil, N., Abdullah, M. M. A. B., Faizul, C. P., Mohamad, H., Arif, W., A Aziz, I., Jeż, B., & Nabiałek, M. (2021). Phase Transformation of Kaolin-Ground Granulated Blast Furnace Slag from Geopolymerization to Sintering Process.

Magnetochemistry, *7*, 32. https://doi.org/10.3390/magnetochemistry7030032

Júlio, E. N. B. S., Branco, F. A. B., & Silva, V. t. D. (2004). Concrete-to-concrete bond strength. Influence of the roughness of the substrate surface. *Construction and Building Materials*, *18*(9), 675-681. https://doi.org/https://doi.org/10.1016/j.conbuildmat.2004.04.023

Jumaa, N. H., Ali, I. M., Nasr, M. S., & Falah, M. W. (2022). Strength and microstructural properties of binary and ternary blends in fly ash-based geopolymer concrete. *Case Studies in Construction Materials*, *17*, e01317. https://doi.org/https://doi.org/10.1016/j.cscm.2022.e01317

Lampropoulou, P., & Papoulis, D. (2021). Halloysite in Different Ceramic Products: A Review. *Materials (Basel)*, *14*(19). https://doi.org/10.3390/ma14195501

Laskar, S. M., & Talukdar, S. (2017). Preparation and tests for workability, compressive and bond strength of ultra-fine slag based geopolymer as concrete repairing agent. *Construction and Building Materials*, *154*, 176-190. https://doi.org/https://doi.org/10.1016/j.conbuildmat.2017.07.187

Lee, N. K., Jang, J. G., & Lee, H. K. (2014). Shrinkage characteristics of alkali-activated fly ash/slag paste and mortar at early ages. *Cement and Concrete Composites*, *53*, 239-248. https://doi.org/10.1016/j.cemconcomp.2014.07.007

Lee, N. K., & Lee, H. K. (2015). Reactivity and reaction products of alkali-activated, fly ash/slag paste. *Construction and Building Materials*, *81*, 303-312. https://doi.org/10.1016/j.conbuildmat.2015.02.022

Li, F., Huang, S., Xu, J., & Qin, Y. (2010). Performance evaluation and technical requirements of cold patch asphalt mixture [Article]. *Tongji Daxue Xuebao/Journal of Tongji University*, *38*(10), 1463-1467. https://doi.org/10.3969/j.issn.0253-374x.2010.10.011

Li, H., Wang, R., Wei, M., Lei, N., Wei, T., & Liu, F. (2024). Characteristics of carbide-slag-activated GGBS–fly ash materials: Strength, hydration mechanism, microstructure, and sustainability. *Construction and Building Materials*, *422*, 135796. https://doi.org/https://doi.org/10.1016/j.conbuildmat.2024.135796

Li, J., Liu, J., Zhang, W., Liu, G., & Dai, L. (2019). Investigation of thermal asphalt mastic and mixture to repair potholes. *Construction and Building Materials*, *201*, 286-294. https://doi.org/https://doi.org/10.1016/j.conbuildmat.2018.12.153

Li, J., Ma, Z., Guo, Y., & Feng, Z. (2024). In-depth analysis of macro-properties and

micro-mechanism of eco-friendly geopolymer based on typical circulating fluidized bed fly ash. *Journal of Building Engineering*, *95*. https://doi.org/10.1016/j.jobe.2024.110074

Li, Y., Ding, C., Zhang, N., Wang, Q., Zhang, Y., Di, X., & Zhang, Y. (2022). High-value utilisation of ceramic waste powder in PVC-based composite and basalt fibre reinforcement effect on its performance. *Ceramics International*, *48*(13), 18083-18093. https://doi.org/https://doi.org/10.1016/j.ceramint.2022.02.282

Li, Y., Zou, Z., Zhang, J., & He, Y. (2023). Study on the evolution of airport asphalt pavement integrated distress based on association rule mining. *Construction and Building Materials*, *369*, 130565. https://doi.org/https://doi.org/10.1016/j.conbuildmat.2023.130565

Liu, J., Feng, H., Zhang, Y., & Zheng, K. (2022). Performance Investigation of Geopolymer Grouting Material with Varied Mix Proportions. *Sustainability*, *14*(20), 13046. https://www.mdpi.com/2071-1050/14/20/13046

Liu, M., Han, S., Han, X., Qi, X., & Dong, S. (2019). Microcapsule and polymer reinforcement techniques developed asphalt for use of pothole repairs in winter and rainy seasons. *Cold Regions Science and Technology*, *167*, 102865. https://doi.org/https://doi.org/10.1016/j.coldregions.2019.102865

Liu, M., Han, S., Shang, W., Qi, X., Dong, S., & Zhang, Z. (2019). New polyurethane modified coating for maintenance of asphalt pavement potholes in winter-rainy condition. *Progress in Organic Coatings*, *133*, 368-375. https://doi.org/https://doi.org/10.1016/j.porgcoat.2019.04.059

Luhar, I., Luhar, S., Abdullah, M., Nabialek, M., Sandu, A. V., Szmidla, J., Jurczynska, A., Razak, R. A., Aziz, I. H. A., Jamil, N. H., & Deraman, L. M. (2021). Assessment of the Suitability of Ceramic Waste in Geopolymer Composites: An Appraisal. *Materials (Basel)*, *14*(12). https://doi.org/10.3390/ma14123279

Luhar, S., Chaudhary, S., & Luhar, I. (2019). Development of rubberized geopolymer concrete: Strength and durability studies. *Construction and Building Materials*, *204*, 740-753. https://doi.org/https://doi.org/10.1016/j.conbuildmat.2019.01.185

Luo, S., Yang, X., Zhong, K., & Yin, J. (2020). Open-graded asphalt concrete grouted by latex modified cement mortar. *Road Materials and Pavement Design*, *21*(1), 61-77. https://doi.org/10.1080/14680629.2018.1479290

Luo, Y., Brouwers, H. J. H., & Yu, Q. (2023). Understanding the gel compatibility and

thermal behavior of alkali activated Class F fly ash/ladle slag: The underlying role of Ca availability. *Cement and Concrete Research*, *170*, 107198. https://doi.org/https://doi.org/10.1016/j.cemconres.2023.107198

Luukkonen, T., Abdollahnejad, Z., Yliniemi, J., Kinnunen, P., & Illikainen, M. (2018). One-part alkali-activated materials: A review. *Cement and Concrete Research*, *103*, 21-34. https://doi.org/10.1016/j.cemconres.2017.10.001

Lv, Q., Huang, W., Zheng, M., Sadek, H., Zhang, Y., & Yan, C. (2020). Influence of gradation on asphalt mix rutting resistance measured by Hamburg Wheel Tracking test. *Construction and Building Materials*, *238*. https://doi.org/10.1016/j.conbuildmat.2019.117674

Lyu, J., Feng, S., Zhang, Q., & Xiao, H. (2024). Review of factors affecting bond strength between ultra-high-performance concrete and normal strength substrate. *Construction and Building Materials*, *439*. https://doi.org/10.1016/j.conbuildmat.2024.137416

Ma, C., Long, G., Shi, Y., & Xie, Y. (2018). Preparation of cleaner one-part geopolymer by investigating different types of commercial sodium metasilicate in China. *Journal of Cleaner Production*, *201*, 636-647. https://doi.org/https://doi.org/10.1016/j.jclepro.2018.08.060

Mack, V., Salehfard, R., & Korayem, A. (2023). Comparative study of the effects of key factors on concrete-to-concrete bond strength. *Civil Engineering Infrastructures Journal*. https://doi.org/10.22059/CEIJ.2023.353447.1903

Marques, B., António, J., Almeida, J., Tadeu, A., de Brito, J., Dias, S., Pedro, F., & Sena, J. D. (2020). Vibro-acoustic behaviour of polymer-based composite materials produced with rice husk and recycled rubber granules. *Construction and Building Materials*, *264*, 120221. https://doi.org/https://doi.org/10.1016/j.conbuildmat.2020.120221

Migunthanna, J., Rajeev, P., & Sanjayan, J. (2021). Investigation of waste clay brick as partial replacement of geopolymer binders for rigid pavement application. *Construction and Building Materials*, *305*. https://doi.org/10.1016/j.conbuildmat.2021.124787

Mohammadi, I., Khabbaz, H., & Vessalas, K. (2014). In-depth assessment of Crumb Rubber Concrete (CRC) prepared by water-soaking treatment method for rigid pavements. *Construction and Building Materials*, *71*, 456-471. https://doi.org/https://doi.org/10.1016/j.conbuildmat.2014.08.085

Mohammed, B. S., Haruna, S., Wahab, M. M. A., Liew, M. S., & Haruna, A. (2019). Mechanical and microstructural properties of high calcium fly ash one-part geopolymer cement made with granular activator. *Heliyon*, *5*(9), e02255. https://doi.org/10.1016/j.heliyon.2019.e02255

Mohd Tahir, M. F., Abdullah, M. M. A. B., Abd Rahim, S. Z., Mohd Hasan, M. R., Saafi, M., Putra Jaya, R., & Mohamed, R. (2022). Potential of industrial By-Products based geopolymer for rigid concrete pavement application. *Construction and Building Materials*, *344*. https://doi.org/10.1016/j.conbuildmat.2022.128190

Narasimhamurthy, G. T., Hanumanthappa, P. M., & Mattur, N. C. (2026). Development and characterisation of an optimum one-part geopolymer concrete mix with high mechanical strength. *Progress in Engineering Science*, *3*(3), 100323. https://doi.org/https://doi.org/10.1016/j.pes.2026.100323

Nascimento, F. A. C., Guimarães, A. C. R., & Castro, C. D. (2021). Comparative study on permanent deformation in asphalt mixtures from indirect tensile strength testing and laboratory wheel tracking. *Construction and Building Materials*, *305*, 124736. https://doi.org/https://doi.org/10.1016/j.conbuildmat.2021.124736

Neville, A. (1995). Properties of concrete (vol. 4): Longman london.

New Straits, T. (2025, 2025/10/10). 2026 Budget: RM2.5 billion allocated for federal road maintenance. *New Straits Times*. https://www.nst.com.my/news/nation/2025/10/1291936/2026-budget-rm25-billion-allocated-federal-road-maintenance

Nurdeen Mohamed, A., Younis Omran, Y., Abdualhamid Mohamed, A., & Lamen Saleh, S. (2024). Influence of Surface Roughness on Durability of New-Old Concrete Interface. *Advances in Technology Innovation*, *9*(2), 143-155. https://doi.org/10.46604/aiti.2024.13533

Obaidi, H., Gomez-Meijide, B., & Garcia, A. (2017). A fast pothole repair method using asphalt tiles and induction heating. *Construction and Building Materials*, *131*, 592-599. https://doi.org/https://doi.org/10.1016/j.conbuildmat.2016.11.099

Oliveira, L. B., de Azevedo, A. R. G., Marvila, M. T., Pereira, E. C., Fediuk, R., & Vieira, C. M. F. (2022). Durability of geopolymers with industrial waste. *Case Studies in Construction Materials*, *16*. https://doi.org/10.1016/j.cscm.2021.e00839

Opiso, E. M., Tabelin, C. B., Maestre, C. V., Aseniero, J. P. J., Park, I., & Villacorte-Tabelin, M. (2021). Synthesis and characterization of coal fly ash and palm oil fuel ash modified artisanal and small-scale gold mine (ASGM) tailings based geopolymer using sugar mill lime sludge as Ca-based activator. *Heliyon*, *7*(4), e06654. https://doi.org/10.1016/j.heliyon.2021.e06654

Orhan, T. Y., Karakoç, M. B., & Özcan, A. (2023). Durability characteristics of slag based geopolymer concrete modified with crumb rubber. *Construction and Building Materials*, *404*. https://doi.org/10.1016/j.conbuildmat.2023.132851

Osman, A. Y., & Irshidat, M. R. (2023). Development of sustainable geopolymer composites for repair application: Workability and setting time evaluation. *Materials Today: Proceedings*. https://doi.org/https://doi.org/10.1016/j.matpr.2023.03.683

Pacheco-Torgal, F., Castro-Gomes, J. P., & Jalali, S. (2008). Adhesion characterization of tungsten mine waste geopolymeric binder. Influence of OPC concrete substrate surface treatment. *Construction and Building Materials*, *22*(3), 154-161. https://doi.org/https://doi.org/10.1016/j.conbuildmat.2006.10.005

Papa, E., Medri, V., Amari, S., Manaud, J., Benito, P., Vaccari, A., & Landi, E. (2017). Zeolite-geopolymer composite materials: Production and characterization. *Journal of Cleaner Production*, *171*. https://doi.org/10.1016/j.jclepro.2017.09.270

Patel, Gupta, N., Chouhan, R. K., & Mudgal, M. (2022). Structural Behavior of Fly Ash–Based Geopolymer for Roller-Compacted Concrete Pavement. *Journal of Materials in Civil Engineering*, *34*(11), 04022300. https://doi.org/doi:10.1061/(ASCE)MT.1943-5533.0004438

Phummiphan, I., Horpibulsuk, S., Rachan, R., Arulrajah, A., Shen, S.-L., & Chindaprasirt, P. (2018). High calcium fly ash geopolymer stabilized lateritic soil and granulated blast furnace slag blends as a pavement base material. *Journal of Hazardous Materials*, *341*, 257-267. https://doi.org/https://doi.org/10.1016/j.jhazmat.2017.07.067

Pompo, D. (2021). World production and consumption of ceramic tiles. https://www.ctasc.com

Prasad, B., Anand, N., Arumairaj, P. D., Jose Francis, A., Samuel Aaron, S., Ram Gandla, S., & Abhilash, P. (2023). Influence of engineering fibers on fresh and mechanical properties of geopolymer concrete. *Materials Today: Proceedings*.

https://doi.org/https://doi.org/10.1016/j.matpr.2023.04.467

Provis, J., & Deventer, J. (2014). *Alkali Activated Materials: State-of-the-Art Report, RILEM TC 224-AAM*. https://doi.org/10.1007/978-94-007-7672-2

Pundienė, I., Pranckevičienė, J., Zhu, C., & Kligys, M. (2021). The role of temperature and activator solution molarity on the viscosity and hard structure formation of geopolymer pastes. *Construction and Building Materials*, *272*, 121661. https://doi.org/https://doi.org/10.1016/j.conbuildmat.2020.121661

Qin, Y., Qu, C., Ma, C., & Zhou, L. (2022). One-Part Alkali-Activated Materials: State of the Art and Perspectives. *Polymers (Basel)*, *14*(22). https://doi.org/10.3390/polym14225046

Rajagopal, M. R., Ganta, J., & Pamu, Y. (2024). Enhancing the Strength and the Environmental Performance of Concrete with Pre-Treated Crumb Rubber and Micro-Silica. *Recycling*, *9*(3). https://doi.org/10.3390/recycling9030032

Raut, A. N., Adamu, M., Singh, R. J., Ibrahim, Y. E., Murmu, A. L., Ahmed, O. S., & Janga, S. (2024). Investigating crumb rubber-modified geopolymer composites derived from steel slag for enhanced thermal performance. *Engineering Science and Technology, an International Journal*, *59*. https://doi.org/10.1016/j.jestch.2024.101880

Rawat, R., & Pasla, D. (2024). Assessment of mechanical and durability properties of FA-GGBS based lightweight geopolymer concrete. *Construction and Building Materials*, *426*, 135984. https://doi.org/https://doi.org/10.1016/j.conbuildmat.2024.135984

Ren, J., Sun, H., Li, Q., Li, Z., Ling, L., Zhang, X., Wang, Y., & Xing, F. (2021). Experimental comparisons between one-part and normal (two-part) alkali-activated slag binders. *Construction and Building Materials*, *309*. https://doi.org/10.1016/j.conbuildmat.2021.125177

Santos, I. D. S. D., Bao, S., & Huang, M. (2023). Mechanical and microstructural properties analysis of one-part geopolymer based on burnt coal cinder replaced by metakaolin. *Journal of Building Engineering*, *76*. https://doi.org/10.1016/j.jobe.2023.107265

Shah, S. N., Beddu, S., Yap, S. P., Putra, A., Othman, M. N., Yuen, C. W., & Mo, K. H. (2024). Physical, strength and acoustic properties of lightweight cement composite with preplaced chemically-treated crumb rubber. *Case Studies in Construction Materials*, *20*. https://doi.org/10.1016/j.cscm.2023.e02821

Shao, R., Li, J., Xu, S., Yu, Z., & Wu, C. (2025). Sustainable design of rubberised geopolymer-based ultra-high performance concrete using waste tyres: Mechanical, microstructural, and environmental evaluation. *Construction and Building Materials*, *502*, 144477. https://doi.org/https://doi.org/10.1016/j.conbuildmat.2025.144477

Siddika, A., Mamun, M. A. A., Alyousef, R., Amran, Y. H. M., Aslani, F., & Alabduljabbar, H. (2019). Properties and utilizations of waste tire rubber in concrete: A review. *Construction and Building Materials*, *224*, 711-731. https://doi.org/https://doi.org/10.1016/j.conbuildmat.2019.07.108

Singh, B., Ishwarya, G., Gupta, M., & Bhattacharyya, S. K. (2015). Geopolymer concrete: A review of some recent developments. *Construction and Building Materials*, *85*, 78-90. https://doi.org/https://doi.org/10.1016/j.conbuildmat.2015.03.036

Singh, N. B., & Middendorf, B. (2020). Geopolymers as an alternative to Portland cement: An overview. *Construction and Building Materials*, *237*. https://doi.org/10.1016/j.conbuildmat.2019.117455

Tahir, M. F., Abdullah, M. M. A. B., Mohd Hasan, M. R., & Zailani, W. W. (2019). *Optimization of fly ash based geopolymer mix design for rigid pavement application* (Vol. 2129). https://doi.org/10.1063/1.5118152

Tahir, M. F. M., Abdullah, M. M. A. B., Rahim, S. Z. A., Mohd Hasan, M. R., Sandu, A. V., Vizureanu, P., Ghazali, C. M. R., & Kadir, A. A. (2022). Mechanical and Durability Analysis of Fly Ash Based Geopolymer with Various Compositions for Rigid Pavement Applications. *Materials*, *15*(10), 3458. https://www.mdpi.com/1996-1944/15/10/3458

Tayeh, B. A., Abu Bakar, B. H., Megat Johari, M. A., & Voo, Y. L. (2012). Mechanical and permeability properties of the interface between normal concrete substrate and ultra high performance fiber concrete overlay. *Construction and Building Materials*, *36*, 538-548. https://doi.org/10.1016/j.conbuildmat.2012.06.013

Thakare, A. A., Gupta, T., Deewan, R., & Chaudhary, S. (2022). Micro and macro-structural properties of waste tyre rubber fibre-reinforced bacterial self-healing mortar. *Construction and Building Materials*, *322*, 126459. https://doi.org/https://doi.org/10.1016/j.conbuildmat.2022.126459

Thameem Ansari, M., Sakthieswaran, N., & Ganesh Babu, O. (2021). Experimental study of an eco-friendly concrete by inbuilt with treated crumb rubber. *Materials*

Today: Proceedings, *37*, 1028-1031. https://doi.org/10.1016/j.matpr.2020.06.287

Thao, Magee, B., & Woodward, D. (2020). A Preliminary Characterisation of Innovative Semi-Flexible Composite Pavement Comprising Geopolymer Grout and Reclaimed Asphalt Planings. *Materials*, *13*(16), 3644. https://www.mdpi.com/1996-1944/13/16/3644

Thomas, B. S., Kumar, S., Mehra, P., Gupta, R. C., Joseph, M., & Csetenyi, L. J. (2016). Abrasion resistance of sustainable green concrete containing waste tire rubber particles. *Construction and Building Materials*, *124*, 906-909. https://doi.org/https://doi.org/10.1016/j.conbuildmat.2016.07.110

Wang, T., Yu, M., Lin, H., Li, D., & Li, L.-y. (2024). Experimental investigation of mechanical properties of GGBS-FA-SF blended geopolymer concrete at elevated temperatures. *Fire Safety Journal*, *146*, 104156. https://doi.org/https://doi.org/10.1016/j.firesaf.2024.104156

Wang, Y.-S., Peng, K.-D., Alrefaei, Y., & Dai, J.-G. (2021). The bond between geopolymer repair mortars and OPC concrete substrate: Strength and microscopic interactions. *Cement and Concrete Composites*, *119*, 103991. https://doi.org/https://doi.org/10.1016/j.cemconcomp.2021.103991

Wei, J., Chen, K., Yu, H., Wang, S., Zhang, S., & Pan, C. (2024). Analyzing the compressive strength of one-part geopolymers using experiment and machine learning approaches. *Journal of Building Engineering*, *98*, 111429. https://doi.org/https://doi.org/10.1016/j.jobe.2024.111429

Wongsa, A., Sata, V., Nematollahi, B., Sanjayan, J., & Chindaprasirt, P. (2018). Mechanical and thermal properties of lightweight geopolymer mortar incorporating crumb rubber. *Journal of Cleaner Production*, *195*, 1069-1080. https://doi.org/https://doi.org/10.1016/j.jclepro.2018.06.003

Xiang, Q., Alae, M., Xu, L., & Xiao, F. (2024). Visco-plastic deformation characteristics of accelerated-aging asphalt mixture containing reclaimed asphalt pavement regenerated with crumb rubber based on Hamburg Wheel-Track test. *Journal of Cleaner Production*, *469*. https://doi.org/10.1016/j.jclepro.2024.143264

Xiao, Z., Pramanik, A., Basak, A. K., Prakash, C., & Shankar, S. (2022). Material recovery and recycling of waste tyres-A review. *Cleaner Materials*, *5*, 100115. https://doi.org/https://doi.org/10.1016/j.clema.2022.100115

Xie, J., Li, J., Lu, Z., Li, Z., Fang, C., Huang, L., & Li, L. (2019). Combination effects of rubber and silica fume on the fracture behaviour of steel-fibre recycled aggregate concrete. *Construction and Building Materials*, *203*, 164-173. https://doi.org/https://doi.org/10.1016/j.conbuildmat.2019.01.094

Xu, L., Yao, Y., Li, Y., Su, J., & Wu, Y. (2023). Review of the Interfacial Bonding Properties between Ultrahigh-Performance Concrete and Normal Concrete. *Applied Sciences*, *13*(11), 6697. https://www.mdpi.com/2076-3417/13/11/6697

Xu, Y., Jiang, Y., Xue, J., Tong, X., & Cheng, Y. (2020). High-Performance Semi-Flexible Pavement Coating Material with the Microscopic Interface Optimization. *Coatings*, *10*(3), 268. https://www.mdpi.com/2079-6412/10/3/268

Yan, J., Zhu, Z., Liu, R., Chen, M., Shao, C., Zhang, C., & Li, X. (2024). A multi-perspective study on the influence of physical and chemical properties of 5 types of fly ash on the performance of high-volume blended fly ash cementitious slurry. *Construction and Building Materials*, *411*, 134301. https://doi.org/https://doi.org/10.1016/j.conbuildmat.2023.134301

Yildirim, G., Ashour, A., Ozcelikci, E., Gunal, M. F., & Ozel, B. F. (2022). Development of Geopolymer Binders with Mixed Construction and Demolition Waste-Based Materials. *Engineering Proceedings*, *17*(1), 4. https://www.mdpi.com/2673-4591/17/1/4

Yousefi Oderji, S., Chen, B., Ahmad, M. R., & Shah, S. F. A. (2019). Fresh and hardened properties of one-part fly ash-based geopolymer binders cured at room temperature: Effect of slag and alkali activators. *Journal of Cleaner Production*, *225*, 1-10. https://doi.org/https://doi.org/10.1016/j.jclepro.2019.03.290

Zakeremamreza, A., Kianifar, M. E., Chibuisi, C., Ahmadi, E., & Salami, M. R. (2023). A high-performance rubberised alkali-activated mortar for repair of RC beams. *Construction and Building Materials*, *400*. https://doi.org/10.1016/j.conbuildmat.2023.132610

Zhang, H., Zhong, Q., Liu, T., & Lv, W. (2022). Preparation and characterization of waterborne unsaturated polyester resin interface binder for pothole repair. *Construction and Building Materials*, *342*, 127848. https://doi.org/https://doi.org/10.1016/j.conbuildmat.2022.127848

Zhang, K., Xu, H., Kong, X.-x., Zhang, C.-y., Lu, H.-f., & He, D. (2023). Study on the influence mechanism of micro-mechanical properties of heterogeneous

geopolymer gels. *Journal of Building Engineering*, *76*, 107164. https://doi.org/https://doi.org/10.1016/j.jobe.2023.107164

Zhang, M., Zhao, Y., & Chen, B. (2024). Efflorescence mitigation in fly ash/slag-based geopolymers: The role of precursor composition and proportions, and admixtures. *Construction and Building Materials*, *438*. https://doi.org/10.1016/j.conbuildmat.2024.137216

Zhang, Y., & Wu, D. Q. (2020). General applications of the semi-rigid pavement in South East Asia. *International Journal of Pavement Research and Technology*, *13*(3), 296-302. https://doi.org/10.1007/s42947-020-0114-1

Zhang, Z., Zhou, Z., Zhu, H., Duan, P., Fang, Y., & Jiang, Z. (2024). Mechanisms of CLDH seeding on hydration kinetics of slag-based geopolymer: Towards aluminosilicate cement phase engineering. *Composites Part B: Engineering*, *271*, 111157. https://doi.org/https://doi.org/10.1016/j.compositesb.2023.111157

Zhao, J., Li, J., Liu, W., & Xie, J. (2026). Effect of precursor and activator on macro and micro properties of fly ash and GGBS based one-part geopolymer. *Construction and Building Materials*, *513*, 145360. https://doi.org/https://doi.org/10.1016/j.conbuildmat.2026.145360

Zhao, J., Xie, J., Wu, J., Zhao, C., & Zhang, B. (2023). Workability, compressive strength, and microstructures of one-part rubberized geopolymer mortar. *Journal of Building Engineering*, *68*, 106088. https://doi.org/https://doi.org/10.1016/j.jobe.2023.106088

Zhao, L., & Tan, Y. (2011). A summary of cold patch material for asphalt pavements. Advanced Materials Research,

Zhao, Q., Ma, C., Huang, B., & Lu, X. (2023). Development of alkali activated cementitious material from sewage sludge ash: Two-part and one-part geopolymer. *Journal of Cleaner Production*, *384*, 135547. https://doi.org/https://doi.org/10.1016/j.jclepro.2022.135547

AUTHOR'S PROFILE



Mohd Najmudin Helmi bin Abu Bakar obtained a Bachelor of Engineering (Hons.) in Civil Engineering in 2023 from Universiti Teknologi MARA (UiTM), Shah Alam, Malaysia, and is currently pursuing his Doctor of Philosophy (PhD) in Civil Engineering at Universiti Teknologi MARA (UiTM), Shah Alam. His research focuses on the development of one-part geopolymer-based semi-rigid repair materials for pavement rehabilitation, with particular emphasis on industrial by-products (GGBS, fly ash, and waste concrete tailings), treated crumb rubber modification, and the influence of substrate surface roughness on interfacial bonding and rutting resistance. His work involves experimental investigations on fresh properties, mechanical performance, durability-related indicators, microstructural and phase characterisation (XRF, XRD, SEM), and interface behaviour to support field-relevant repair performance under repeated loading. His research outcomes aim to contribute towards sustainable and high-performance repair solutions for infrastructure maintenance.

LIST OF PUBLICATION:

Abu Bakara, M. N. H., Zailania, W. W. A., Apandia, N. M., Memona, N. A., Ismaila, S., Aznia, M. L. H. M., & Kotingc, S. (2025). Effect of Treated Crumb Rubber on Mechanical Properties of GGBS-WCT Based Rubberised Geopolymer Concrete. Jurnal Kejuruteraan, 37(6), 2749-2755.

Abu Bakar, M. N. H., Zailani, W. W. A., Apandi, N. M., Abdul Mutalif, M. S., Abdul Majid, A. M., Sinarta, I. N., & Agustin, N. K. A. (2024). Physico-Mechanical

Properties of GGBS based Geopolymer Mortar for Semi-Rigid Binder: Impact of Crumb Rubber Replacement. *Jurnal Kejuruteraan*, *36*(6), 2693-2700. https://doi.org/10.17576/jkukm-2024-36(6)-38

Abu Bakara, M. N. H., Ahmad Zailani, W. W., Zuljar, Z. K., Mohd Apandi, N., Beddu, S., & Agustini, N. K. A. (2023). Effect of high calcium precursor (HCP) content on bonding strength of geopolymer concrete exposed at different curing temperatures. *Scientific Research Journal*, *20*(2), 39-52.

Abu Bakara, M. N. H., Kudus, S. A., Mustaffa, N. K., Jamadin, A., Abbas, H. A., Hassan, R., & Kamaruddin, N. (2023). Effect of Rice-Husk as Replacement Cement on Mechanical Properties Concrete. *Journal of Mechanical Engineering*, *20*(2), 91-104.